

**Molecular Analysis of Thyroid Hormone  
Receptor  $\beta$  and Peroxisome Proliferator-  
Activated Receptor  $\gamma$  Action**

**MAURA AGOSTINI**

A thesis submitted in partial fulfillment of the requirements of the University of  
Hertfordshire for the degree of Doctor of Philosophy

The programme of research was carried out in the Department of Life Sciences, Faculty  
of Health and Human Sciences, University of Hertfordshire

in collaboration with the

Department of Medicine, University of Cambridge

May 2007

*For Rashieda and all the patients  
without whose kind cooperation none of this work would have been possible*

## ABSTRACT

The nuclear receptor superfamily comprises a group of ligand-activated transcription factors that regulate the expression of target genes. They play a central role in diverse physiological pathways, and are therefore extremely important in the aetiology of various human disorders and as pharmaceutical therapeutic targets. This thesis describes molecular analyses of the thyroid hormone receptor (TR) and the peroxisome proliferator-activated receptor gamma (PPAR $\gamma$ ), in disorders of thyroid hormone and insulin action respectively.

The syndrome of Resistance to Thyroid Hormone (RTH), characterized by reduced tissue responsiveness to circulating thyroid hormones, is associated with diverse mutations in the ligand-binding domain of the thyroid hormone  $\beta$  receptor, localizing to three clusters around the hormone binding cavity. The first part of this thesis describes three novel RTH mutations (S314C, S314F, S314Y), due to different amino acid substitutions in the same codon, occurring in six separate families. Characterization of these mutant receptors showed marked differences in their functional impairment. In the second part of the thesis I report detailed functional studies of natural and synthetic receptor agonists with loss-of-function PPAR $\gamma$  mutants (P467L; V290M), previously identified in patients with severe insulin resistance, type 2 diabetes mellitus and hypertension. Both PPAR $\gamma$  mutants act as dominant negative inhibitors of wild type receptor (WT) action because of their failure to fully dissociate from corepressors. My results provide evidence that tyrosine-based rather than thiazolidinedione PPAR $\gamma$  agonists, may represent a more rational therapeutic approach to restoring mutant receptor function and ameliorating insulin resistance in our patients. Then, in an unrelated kindred a different, digenic mechanism of insulin resistance, with a combination of loss-of-function mutations in PPAR $\gamma$  and PPP1R3 (muscle-specific subunit of protein-phosphatase 1 mediating glycogen synthesis) is described. Functional characterisation of these mutant proteins provides unique insights into the complex interplay between this nuclear receptor and a second metabolic signalling pathway. Finally, three novel heterozygous mutations, in the ligand and DNA binding domains of PPAR $\gamma$ , identified in three unrelated subjects with partial lipodystrophy, severe insulin resistance, dyslipidaemia and hypertension are described. Their functional characterization suggests that they inhibit WT action via a novel, non DNA-binding interference mechanism.

## ACKNOWLEDGEMENTS

Firstly I would like to express my gratitude to Professor Krish Chatterjee for giving me the opportunity to work in his lab, his invaluable advice and guidance throughout this project, his enduring patience in “repeating again” when I do not understand, but most of all for believing in me.

The patience and support of Dr Ralph Rapley must also be acknowledged.

I would like to thank current and past colleagues who have passed through the laboratory since 1997 when I arrived, for their scientific input, but more importantly for being excellent friends of the “*mad Italian woman*” (me!!). Among them a special thank you to Dr Mark Gurnell, who firstly taught me the basic techniques of molecular biology, for his encouragement and support throughout these studies. From the earlier days Dr Trevor Collinwood, Dr Rory Clifton-Bligh, Dr Maria Adams, Dr John Wentworth, Dr Sumit Bhattacharyya, Dr Jayashree Gopal, Dr Soome Park, Emily Wood and Dr Paul Brown should also be mentioned. More recently it has been a great pleasure to work with Dr Aaron Smith, Dr Erik Schoenmakers whose expert contributions are acknowledged in the text, Dr Catherine Mitchell, Christine Riches, Abdella Habib, Teresa Wallman and Suzanne Diston. I am deeply grateful to Odelia Rajanayagam for having been wonderfully patient and kind in providing technical help and support, but more importantly for being my special friend. I am also indebted to Erik and Odelia for proofreading this thesis.

It has been great to work in the CIMR, thank you to all the colleagues who have shared their expertise with me. Among them I am enormously grateful to Dr Giles Yeo for his ever-cheerful help; it has been great fun sharing with him the excitement of our first “move” into the Affimetrix world. Among the various collaborators I would like to acknowledge Dr John Schwabe for all the structural modelling except Figure 6.7c for which I must thank my friend Dr Pietro Roversi.

Thanks also to Dr David Savage, Dr Ines Barroso and Dr Gudrun Ihrke.

During the course of these studies I have been privileged to spend sometime abroad in the laboratory of Prof Laszlo Nagy working together with Dr Istvan Sztamari at the University of Debrecen (Hungary) and more recently in the laboratory of Prof David Marais working with Dr Dirk Blom at the University of Cape Town (SA).

Thank you also to James Fincham and his colleagues for their IT assistance.

Finally, above all my profoundest thanks to my friends and family for their unfailing support and encouragement throughout these studies.

## ABBREVIATIONS

$\alpha\alpha$	amino acids
ACS	acylCoA synthase
AF	activation domain
aP2	adipocyte protein 2
ATP	adenosine triphosphate
BMI	body mass index
bp	base pair
CBP	CREB binding protein
CD36	fatty acid translocase
C/EBP	CCAAT enhancer binding proteins
CNS	central nervous system
CREB	Cyclic AMP Response Element Binding Protein
CTE	carboxy terminal extension
DAX1	dosage-specific sex reversal-adrenal hypoplasia congenita critical region on the X chromosome 1
DBD	DNA-binding domain
DHR38	Drosophila hormone receptor 38
DIOs	deiodinases
DNA	deoxyribonucleic acid
cDNA	complementary DNA
DMSO	Dimethylsulfoxide
dNTP	deoxyribonucleotide
DRIP	VDR-interacting protein
DR	direct repeat
DTT	dithiothreitol
EDTA	di-sodium ethylenediaminetetraacetate dihydrate
EGTA	ethyleneglycol-bis-(beta-aminoethylether)-N, N, N', N'-tetraacetic acid
EMSA	electromobility shift assay
ER	estrogen receptor
ERAP	ER-associated proteins
FABP4	fatty acid binding protein 4
FAM	6-carboxy-fluorescein
FATP-1	fatty acid transporter protein-1
FCS	foetal calf serum
FFA	free fatty acids
FS	frameshift
GFP	green fluorescent protein
GyK	glycerol kinase
GRTH	generalized resistance to thyroid hormone
GS	glycogen synthase
GST	glutathione S-transferase
H	$\alpha$ -helix
HAT	Histone Acetyl Transferase
HDAC	Histone Deacetylases
HDL	high density lipoproteins
HEPES	N-(2-hydroxyethyl)piperazine-N'-(2-ethanesulfonic)
HMDM	human monocyte-derived macrophages
HREs	hormone response elements
ID	interaction domain

IDC	immature dendritic cells
IL	interleukin
IPTG	isopropylthio- $\beta$ -D-galactosidase
Ka	affinity constant
kb	kilobase
kD	kiloDaltons
KI	knock-in
KO	knock-out
LBD	ligand-binding domain
LDL	low density lipoproteins
LcoR	ligand-dependent corepressor
LPL	lipoprotein lipase
LRH1	liver receptor homologous protein 1
MAP	mitogen activated protein
MR	mineralcorticoid receptor
Mw	molecular weigh
NCoR	nuclear receptor corepressor
NEFA	non-esterified fatty acids
NLS	nuclear localization signal
NMR	nuclear magnetic resonance
NURR1	nuclear receptor related 1
oligo-dT	oligodeoxythymidylic acid
PAGE	polyacrylamide gel electrophoresis
PAX8	paired homeobox protein 8
PBS	phosphate-buffered saline
pCAF	p300/CBP-associated factor
PCOS	polycystic ovarian syndrome
PCR	polymerase chain reaction
PDIP1	PPAR $\gamma$ -DBD-interacting protein 1
PEG	polyethylene glycol
PEPCK	phosphoenol pyruvate carboxykinase
PGC-1	PPAR $\gamma$ coactivator 1
PLRS	PPAR $\gamma$ ligand resistance syndrome
PPAR $\gamma$	peroxisome proliferator-activated receptor gamma
PPP1R3	muscle-specific subunit of protein-phosphatase 1
PR	progesterone receptor
PRTH	pituitary resistance to thyroid hormone
PXR	pregnane X receptor
RIP 140	receptor interacting protein of 140 kDa
RNA	Ribonucleic acid
mRNA	messenger RNA
RAR	retinoic acid receptor
RTH	resistance to thyroid hormone
RT-PCR	reverse transcription polymerase chain reaction
RXR	retinoid X receptor
SDS	sodium dodecyl sulphate
SHP	short heterodimeric partner
SMRT	silencing mediator for retinoic acid and thyroid hormone receptors
SRC	steroid receptor coactivator
SUN-COR	Small Ubiquitous Nuclear Corepressor
T3	triiodothyronine
T4	thyroxine

TBL1	transducin beta-like protein 1
TBLR1	transducin beta-like protein 1-related protein
TE	Tris/EDTA buffer
TEMED	N, N, N', N'-tetramethylenediamine
TG	Triglyceride
TH	thyroid hormones
TIF	transcriptional intermediary factor
TNF $\alpha$	tumour necrosis factor- $\alpha$
TR	thyroid hormone receptor
TRAP	thyroid receptor accessory protein
TRE	thyroid hormone response element
TRH	thyrotropin-releasing hormone
Tris	tris(hydroxymethyl)aminomethane
TSH	thyroid-stimulating hormone
T2DM	type 2 diabetes mellitus
TZD	Thiazolidinedione
VDR	vitamin D receptor
v/v	volume/volume
WAT	white adipose tissue
WT	wild type
w/v	weight/volume
w/w	weight/weight
X-GAL	5'-bromo-4-chloro-3-indolyl- $\beta$ -D-galactosidase

## TABLE OF CONTENTS

<b>CHAPTER 1 General Introduction</b>	<b>1</b>
<b>1.1 The nuclear receptor superfamily</b>	<b>1</b>
1.1.1 A general overview	1
1.1.2 Receptor structure and domains	4
1.1.2.1 <i>The N-terminal (A/B) domains</i>	4
1.1.2.2 <i>The DNA-binding (C) domain</i>	5
1.1.2.3 <i>The hinge (D) domain</i>	6
1.1.2.4 <i>The C-terminal ligand binding (E, F) domain</i>	7
1.1.3 Transcriptional regulation by nuclear receptors	9
1.1.3.1 <i>Basal transcription</i>	9
1.1.3.2 <i>Coactivator families</i>	10
1.1.3.2.1 <i>The p160 family</i>	11
1.1.3.2.2 <i>CBP/300</i>	11
1.1.3.2.3 <i>The TRAP/DRIP complex</i>	12
1.1.3.2.4 <i>Other coactivators</i>	12
1.1.3.3 <i>Active repression by nuclear receptors</i>	13
1.1.3.4 <i>Nuclear receptor corepressors</i>	14
1.1.3.5 <i>Negative transcriptional regulation</i>	16
<b>1.2 Thyroid hormones, their receptors and the syndrome of Resistance to Thyroid Hormone</b>	<b>19</b>
1.2.1 Thyroid hormones	19
1.2.2 Thyroid hormone receptors	20
1.2.3 Resistance to Thyroid Hormone	21
1.2.3.1 <i>Clinical Features</i>	21
1.2.3.2 <i>Molecular genetics of RTH</i>	21
1.2.3.3 <i>Animal Model of RTH</i>	24
<b>1.3 Peroxisome proliferator-activated receptor gamma (PPAR<math>\gamma</math>)</b>	<b>27</b>
1.3.1 General overview of PPARs	27
1.3.2 PPAR $\gamma$ gene, mRNA and protein	28
1.3.3 Transcriptional activity of PPAR $\gamma$	29
1.3.4 Natural and synthetic ligands of PPAR $\gamma$	30
1.3.5 PPAR $\gamma$ and adipogenesis	32
1.3.6 PPAR $\gamma$ , insulin resistance and diabetes	33



1.3.7 Other diverse roles of PPAR $\gamma$	38
<b>CHAPTER 2 Material and Methods</b>	<b>57</b>
<b>2.1 Chemicals</b>	<b>57</b>
<b>2.2 Buffers</b>	<b>57</b>
<b>2.3 Nucleic acid preparation and analysis</b>	<b>58</b>
2.3.1 <i>Oligonucleotides</i>	58
2.3.2 <i>DNA</i>	58
2.3.2.1 <i>Extraction of genomic DNA from peripheral blood leukocytes</i>	58
2.3.2.2 <i>Plasmid DNA</i>	58
2.3.2.3 <i>Ethanol precipitation of DNA</i>	59
2.3.2.4 <i>PEG precipitation of nucleic acid</i>	59
2.3.3 <i>RNA</i>	
2.3.3.1 <i>RNA extraction from Immature Dendritic Cells</i>	59
2.3.4 <i>Nucleic acid quantification</i>	60
2.3.5 <i>Radio-labelling of nucleic acids</i>	60
2.3.6 <i>Enzymatic modification of DNA</i>	61
2.3.6.1 <i>Restriction enzyme digestion</i>	61
2.3.6.2 <i>Dephosphorilation</i>	61
2.3.6.3 <i>Agarose gel electrophoresis</i>	61
2.3.6.4 <i>Agarose gel extraction</i>	61
2.3.6.5 <i>DNA ligation</i>	62
2.3.7 <i>Polymerase chain reaction (PCR)</i>	62
2.3.8 <i>DNA sequencing</i>	63
2.3.9 <i>Site-directed mutagenesis</i>	63
2.3.10 <i>Reverse transcription-PCR</i>	63
<b>2.4 Protein preparation and analysis</b>	<b>64</b>
2.4.1 <i>In vitro translation</i>	64
2.4.2 <i>Polyacrylamide gel electrophoresis (SDS-PAGE)</i>	65
2.4.3 <i>Electrophoretic mobility shift assay (EMSA)</i>	66
2.4.4 <i>Ligand binding assays</i>	66
2.4.4.1 <i>TR<math>\beta</math></i>	66
2.4.4.2 <i>PPAR<math>\gamma</math></i>	66

2.4.5	<i>GST protein synthesis</i>	67
2.4.6	<i>Pulldown assays</i>	67
<b>2.5</b>	<b>Bacterial cell culture</b>	<b>67</b>
2.5.1	<i>Media</i>	68
2.5.2	<i>Preparation of competent cells</i>	68
2.5.3	<i>Transformation of competent cells</i>	69
2.5.4	<i>Glycerol stock</i>	69
<b>2.6</b>	<b>Cell culture</b>	<b>69</b>
2.6.1	<i>Routine cell culture and maintenance of cell lines</i>	69
2.6.2	<i>Transient transfection assays</i>	70
2.6.3	<i>Luciferase and <math>\beta</math>-Galactosidase assays</i>	71
2.6.4	<i>Isolation and culture of Immature Dendritic Cells from peripheral blood</i>	71
<b>CHAPTER 3</b>	<b>Three Novel Mutations at Serine 314 in the Thyroid Hormone <math>\beta</math> Receptor Differentially Impair Ligand Binding in the Syndrome of Resistance to Thyroid Hormone</b>	<b>73</b>
<b>3.1</b>	<b>Introduction</b>	<b>73</b>
<b>3.2</b>	<b>Methods</b>	<b>75</b>
3.2.1	<i>Clinical and genetic analyses</i>	75
3.2.2	<i>Plasmid constructs</i>	75
3.2.3	<i>Hormone and DNA binding assays</i>	75
3.2.4	<i>Cell culture and transient transfection assays</i>	76
<b>3.3</b>	<b>Results</b>	<b>77</b>
3.3.1	<i>Clinical and genetic analyses</i>	77
3.3.2	<i>Hormone and DNA binding</i>	77
3.3.3	<i>Functional activity and dominant negative inhibition</i>	78
<b>3.4</b>	<b>Discussion</b>	<b>87</b>

<b>CHAPTER 4 Tyrosine Agonists Reverse the Molecular Defects Associated with Dominant Negative Mutations in Human PPAR<math>\gamma</math></b>	<b>91</b>
<b>4.1 Introduction</b>	<b>91</b>
<b>4.2 Methods</b>	<b>94</b>
4.2.1 <i>Plasmid constructs</i>	94
4.2.2 <i>Protein-protein interaction assays</i>	94
4.2.3 <i>Ligand binding assays</i>	95
4.2.4 <i>Transfection assays</i>	95
4.2.5 <i>aP2 assays in Peripheral Blood Mononuclear Cells (PBMCs)</i>	95
<b>4.3 Results</b>	<b>97</b>
4.3.1 <i>Transcriptional activation</i>	97
4.3.2 <i>Hormone binding assay and coactivator recruitment</i>	98
4.3.3 <i>Basal repression and corepressor recruitment</i>	98
4.3.4 <i>Dominant negative activity</i>	99
4.3.5 <i>aP2 expression in primary human monocytes harbouring dominant negative PPAR<math>\gamma</math></i>	100
<b>4.4 Discussion</b>	<b>113</b>
<b>CHAPTER 5 Digenic Inheritance of Severe Insulin Resistance in a Human Pedigree</b>	<b>121</b>
<b>5.1 Introduction</b>	<b>121</b>
<b>5.2 Methods</b>	<b>123</b>
5.2.1 <i>Clinical studies</i>	123
5.2.2 <i>Screening of PPAR<math>\gamma</math> gene</i>	123
5.2.3 <i>Screening of PPP1R3A gene</i>	124
5.2.4 <i>Plasmid and constructs</i>	124
5.2.5 <i>DNA binding assays</i>	125
5.2.6 <i>Transactivation assays</i>	125

5.2.7	<i>Immunoprecipitation and Western blot analysis</i>	125
5.2.8	<i>Immunofluorescence Microscopy</i>	126
<b>5.3</b>	<b>Results</b>	<b>127</b>
5.3.1	<i>Clinical and genetic analyses</i>	127
5.3.2	<i>DNA binding of PPAR<math>\gamma</math> FS</i>	128
5.3.3	<i>Functional activity and dominant negative activity of PPAR<math>\gamma</math> FS</i>	129
5.3.4	<i>Characterization of the PPAR3A mutant</i>	129
<b>5.4</b>	<b>Discussion</b>	<b>138</b>
<b>CHAPTER 6</b>	<b>A Novel Class of Human PPAR<math>\gamma</math> Mutations Causes Lipodystrophic Insulin Resistance by Dominant Negative Inhibition via a Non-DNA Binding, Interference Mechanism</b>	<b>142</b>
<b>6.1</b>	<b>Introduction</b>	<b>142</b>
<b>6.2</b>	<b>Material and Methods</b>	<b>145</b>
6.2.1	<i>Clinical studies</i>	145
6.2.2	<i>Screening for PPARG and PPP1R3A mutations</i>	145
6.2.3	<i>Plasmids and constructs</i>	145
6.2.4	<i>DNA binding assay</i>	146
6.2.5	<i>Transfection assay</i>	146
6.2.6	<i>Cellular localisation of EGFP-PPAR<math>\gamma</math> fusion</i>	147
6.2.7	<i>Peripheral blood monocyte purification and IDC culture</i>	147
6.2.8	<i>Quantitative real-time PCR analysis of gene expression</i>	148
6.2.9	<i>RFLP analysis of PPAR<math>\gamma</math> transcripts</i>	148
6.2.10	<i>Immunoprecipitation and Western blot analysis</i>	149
6.2.11	<i>Adenoviral PPAR<math>\gamma</math> construction and expression</i>	149
<b>6.3</b>	<b>Results</b>	<b>150</b>
6.3.1	<i>Screening of PPARG and PPP1R3A genes</i>	150
6.3.2	<i>Clinical results</i>	151

6.3.3 <i>Novel PPAR<math>\gamma</math> mutants are non DNA-binding, with complete loss-of-function</i>	151
6.3.4 <i>Novel PPAR<math>\gamma</math> mutants translocate to the nucleus and interact with RXR</i>	153
6.3.5 <i>Novel PPAR<math>\gamma</math> mutants inhibit WT receptor action</i>	154
<b>6.4 Discussion</b>	<b>179</b>
<b>CHAPTER 7 Concluding Discussion</b>	<b>185</b>
<b>REFERENCES</b>	<b>197</b>
<b>APPENDIX Publications and conferences attended</b>	<b>228</b>

## LIST OF FIGURES

### *Chapter 1*

<b>Figure 1.1</b>	Nuclear receptor superfamily	44
<b>Figure 1.2</b>	Schematic representation of a nuclear receptor	45
<b>Figure 1.3</b>	DNA binding by nuclear receptors	46
<b>Figure 1.4</b>	Schematic representation of three distinct conformational states adopted by the ligand-binding domain of the estrogen receptor	47
<b>Figure 1.5</b>	Schematic representation of the domain structure of steroid receptor coactivator 1, a member of the p160 family of coactivators	48
<b>Figure 1.6</b>	Schematic representation of transcriptional regulation by TR	49
<b>Figure 1.7</b>	The hypothalamic-pituitary-thyroid axis	50
<b>Figure 1.8</b>	Schematic representation of amino acid homologies among human TR isoforms	51
<b>Figure 1.9</b>	TR $\beta$ mutations in the syndrome of resistance to thyroid hormone (RTH) cluster within three regions (I, II and III) of the ligand-binding domain	52
<b>Figure 1.10</b>	Schematic model of dominant negative inhibition by TR $\beta$ mutants in RTH	53
<b>Figure 1.11</b>	Comparison of the human PPARs	54
<b>Figure 1.12</b>	Human PPAR $\gamma$ isoforms	55
<b>Figure 1.13</b>	PPAR $\gamma$ target genes and adipocyte metabolism	56

### *Chapter 3*

<b>Figure 3.1</b>	Electropherograms showing sequences corresponding to wild type receptor and S314 hTR $\beta$ mutations	82
<b>Figure 3.2</b>	Differential dissociation of TR $\beta$ homodimers in response to T3 on the F2 everted repeat TRE from the chicken lysozyme gene	83
<b>Figure 3.3</b>	T3-dependent transcriptional activation of a thyroid response element containing reporter gene (MAL-TKLUC) by wild type (WT) and mutant (S314C, S314F, S314Y) thyroid hormone receptors	84
<b>Figure 3.4</b>	Dominant negative inhibition of wild type (WT) receptor activity by mutant receptors	85

<b>Figure 3.5</b>	Circulating Free T4 (FT4) levels in individuals harbouring each of the three codon 314 mutations	86
<b>Figure 3.6</b>	The crystal structure of human TR $\beta$ is shown, with Ser314 located in the periphery of the ligand-binding cavity	90
<b>Chapter 4</b>		
<b>Figure 4.1</b>	A panel of putative endogenous ligands fail to transactivate mutant PPAR $\gamma$	102
<b>Figure 4.2</b>	Synthetic PPAR $\gamma$ agonists	103
<b>Figure 4.3</b>	Binding of thiazolidinedione ( <sup>3</sup> H-rosiglitazone) and tyrosine agonist ( <sup>3</sup> H-farglitazar) radioligands to GST-PPAR $\gamma$ ligand-binding domain (LBD) chimaeras	104
<b>Figure 4.4</b>	Coactivator recruitment to mutant PPAR $\gamma$ is greater with tyrosine agonist (farglitazar) than thiazolidinedione (rosiglitazone)	105
<b>Figure 4.5</b>	PPAR $\gamma$ mutants repress basal transcription	106
<b>Figure 4.6</b>	WT and mutant PPAR $\gamma$ interact with the ID1 domain of SMRT	107
<b>Figure 4.7</b>	Farglitazar is more effective than rosiglitazone in promoting corepressor dissociation from mutant PPAR $\gamma$	108
<b>Figure 4.8</b>	Tyrosine agonist (farglitazar) reverses dominant negative inhibition by PPAR $\gamma$ mutants more effectively than putative natural ligand (15d-PGJ2) or thiazolidinedione (rosiglitazone)	109
<b>Figure 4.9</b>	Basal transcriptional repression by the P467L natural mutant is reversed, but constitutive activity of WT PPAR $\gamma$ is not affected by the addition of an L318A mutation	110
<b>Figure 4.10</b>	Introduction of the L318A mutation significantly attenuates the dominant-negative activity of the P467L PPAR $\gamma$ mutant through abolition of its interaction with corepressor	111
<b>Figure 4.11</b>	The tyrosine agonist (farglitazar) enhances target gene (aP2) expression in P467L mutant receptor containing peripheral blood mononuclear cells (PBMCs) more effectively than thiazolidinedione (rosiglitazone)	112
<b>Figure 4.12</b>	Crystallographic modelling showing how the tyrosine agonist (farglitazar) may preferentially stabilise helix 12 in mutant PPAR $\gamma$	118
<b>Figure 4.13</b>	An alignment of amino acid sequences corresponding to the corepressor interaction interface in PPAR $\alpha$ in the three PPAR subtypes	119

<b>Figure 4.14</b>	A molecular model showing the interface between peptide from SMRT (white) and PPAR $\gamma$ (green) with the location of the V290M mutation also depicted (purple)	120
--------------------	--	-----

### *Chapter 5*

<b>Figure 5.1</b>	Identification of Novel Mutations in PPAR $\gamma$ and PPP1R3A in two families with severe insulin resistance	133
<b>Figure 5.2</b>	Mutant PPAR $\gamma$ mutants fails to bind to DNA heterodimerically with their partner RXR	134
<b>Figure 5.3</b>	The FS PPAR $\gamma$ mutants are transcriptionally inactive in the context of both the $\gamma$ 1 and $\gamma$ 2 isoforms	135
<b>Figure 5.4</b>	The FS PPAR $\gamma$ mutants do not exhibit dominant-negative activity when co-expressed with their WT counterparts	136
<b>Figure 5.5</b>	Characterisation of the PPP1R3A FS (Fsh) mutant	137

### *Chapter 6*

<b>Figure 6.1</b>	Identification of novel mutations in PPAR $\gamma$ gene in subjects with partial lipodystrophy and insulin resistance	160
<b>Figure 6.2</b>	Subject 1 (S1), a 43-year-old female was heterozygous for a cysteine-114-arginine (C114R) PPAR $\gamma$ mutation	161
<b>Figure 6.3</b>	Subject 2 (S2), a 45-year-old female was heterozygous for a cysteine-131-tyrosine (C131Y) PPAR $\gamma$ mutation	162
<b>Figure 6.4</b>	Subject 3 (S3), a 38-year-old female, heterozygous for an argine-357-stop (R357X) mutation, presented with oligomenorrhoea and hirsutism following menarche aged 11yrs	163
<b>Figure 6.5</b>	T1-weighted MRI images at the level of the gluteal fat pad in a lean healthy female (WT, top panel on the left) and in the R357X, C114R and C131Y probands	164
<b>Figure 6.6</b>	Fasting plasma insulin concentrations versus body mass index (BMI, kg/m <sup>2</sup> ) showing that probands (S1-S3) exhibit marked hyperinsulinaemia when compared with normal subjects	165
<b>Figure 6.7</b>	Schematic representation of the structural and functional organization of PPAR $\gamma$ showing the amino-terminal (A/B), DNA binding (DBD) and ligand binding (LBD) domains	166
<b>Figure 6.8</b>	The PPAR $\gamma$ mutant receptors are transcriptionally inactive	167
<b>Figure 6.9</b>	Novel PPAR $\gamma$ mutants are unable to bind to DNA	168



<b>Figure 6.10</b>	Chimaeric fusion proteins consisting of the VP16 activation domain linked to the amino-terminus of full-length PPAR $\gamma$ 1 (WT or mutants) were co-expressed in 293EBNA cells with a PPARE-containing reporter gene [(PPARE) <sub>3</sub> TKLUC]	169
<b>Figure 6.11</b>	C114R, C131Y and R357X PPAR $\gamma$ mutants translocate to the nucleus whereas the FS PPAR $\gamma$ mutant remains cytoplasmic	170
<b>Figure 6.12</b>	Interaction between VP16-WT or mutant PPAR $\gamma$ fusions and Gal4-RXR $\alpha$ chimeras	171
<b>Figure 6.13</b>	Dominant negative inhibition of wild type receptor activity by mutant receptors	172
<b>Figure 6.14</b>	Comparison of aP2 (FABP4) expression in cells from a normal control subject (WT) and patients carrying the R357X or C114R PPAR $\gamma$ mutations	173
<b>Figure 6.15</b>	Levels of aP2 (FABP4) and PPAR $\gamma$ gene expression in cells from normal controls and individuals carrying mutation in PPAR $\gamma$	174
<b>Figure 6.16</b>	Relative expression of several PPAR $\gamma$ target genes (5 down-regulated and 5 up-regulated right panel) in WT and receptor mutation-containing (FS, C114R, R357X) IDCs, quantified by real-time quantitative qPCR using Taqman Low Density Arrays (TLDA)	175
<b>Figure 6.17</b>	RT-PCR with cDNA amplification confirms the presence of both the mutant and wild type mRNA transcripts in the R357X patient	176
<b>Figure 6.18</b>	R357X mutant PPAR $\gamma$ is expressed in peripheral blood monocyte derived immature dendritic cells (IDCs)	177
<b>Figure 6.19</b>	Adenoviral expression of C114R mutant PPAR $\gamma$ inhibits rosiglitazone-induced preadipocyte differentiation	178
<b>Figure 6.20</b>	Proposed model of transcriptional interference by naturally occurring PPAR $\gamma$ R357X, C114R and C131Y mutants	184

## *Chapter 7*

<b>Figure 7.1</b>	R397C and F360L human PPAR $\gamma$ 1 mutants exhibit dominant negative activity when coexpressed with their wild type receptor (WT) counterpart	194
<b>Figure 7.2</b>	Mutations in human PPAR $\gamma$ causing either receptor insufficiency or gain-of-function	195
<b>Figure 7.3</b>	Schematic representation of the pathogenesis of insulin resistance in subjects with PPAR $\gamma$ mutations	196

## LIST OF TABLES

<b>Table 1.1</b>	Human nuclear receptors	41
<b>Table 1.2</b>	Examples of diseases associated with altered nuclear receptor function	42
<b>Table 1.3</b>	Recognized Clinical Features of RTH	43
<b>Table 3.1</b>	Primers used to amplify and sequence coding exons 7-10 of human TR $\beta$ 1	80
<b>Table 3.2</b>	Biochemical and genetic data from 6 RTH families	81
<b>Table 5.1</b>	Primers used to amplify and sequence coding exons of the human PPAR $\gamma$ gene, including exon B encoding the unique N-terminal region of the PPAR $\gamma$ 2 isoform	130
<b>Table 5.2</b>	Clinical and biochemical characteristics of mutant allele carriers	131
<b>Table 5.3</b>	Distribution of leptin concentrations among individuals in the population-based MRC Ely cohort study stratified by sex and BMI.	132
<b>Table 6.1</b>	Sequences of primers used to amplify and sequence the coding region of the <i>PPP1R3A</i> gene (exons 1-4)	157
<b>Table 6.2</b>	Sequences of primers and probes used to amplify and quantitate gene expression in immature dendritic cells by qPCR	158
<b>Table 6.3</b>	Clinical, biochemical and body composition data from index cases harbouring the 3 novel PPAR $\gamma$ mutations	159
<b>Table 7.1</b>	Changes in clinical, biochemical and body composition parameters in the subject carrying the FS mutation (Subject vi in Figure 5.1) between 2002 when he was first studied and later in 2006	193

## *Chapter 1*

### **GENERAL INTRODUCTION**

#### **1.1 *The nuclear receptor superfamily***

##### **1.1.1 A general overview**

The development of a complex endocrine system is one of the most striking features of multicellular organism evolution, and allows the organism to coordinate its reaction to the environment, to regulate its development, and to maintain homeostasis in the face of external challenges. Among the numerous proteins involved in these complex processes, the nuclear receptor superfamily is a key player involved in a diverse array of functions from embryonic development to metamorphosis and from regulation of homeostasis to the control of metabolism. Members of this receptor family act as ligand-inducible transcription factors, thus providing a direct link between signaling pathway that control these processes and transcriptional responses of individual target genes. Many members of the nuclear receptor superfamily mediate the actions of known hormones including steroids, retinoids, thyroid hormones and vitamin D<sub>3</sub>. These hormones are important regulators of development, cell differentiation and organ physiology but it is only relatively recently that we have begun to understand the molecular basis for their actions. In the 1960s, Tata and colleagues observed an increase of RNA and protein synthesis after the administration of triiodothyronine (T<sub>3</sub>) in hypothyroid rats. These effects were blocked by the addition of actinomycin D, an inhibitor of gene transcription (Tata, 1963; Tata and Widnell, 1966). These observations suggested that thyroid hormone action is mediated, at least in part, through mechanisms involving the transcriptional regulation of T<sub>3</sub>-responsive genes. Development of radiolabeled ligands allowed the identification of protein binding for several hormones within the nuclear compartment, supporting the hypothesis that specific intracellular receptors mediate the transcriptional effects of these lipophilic molecules (Oppenheimer *et al.*, 1974; Sibley and Tomkins, 1974; Samuels *et al.*, 1976).

The cloning of the steroid receptors was an essential prerequisite for ultimately understanding the molecular basis of their actions. The glucocorticoid and estrogen receptors were the first RNA polymerase II-dependent transcription factors to be cloned (Hollenberg *et al.*, 1985; Miesfeld *et al.*, 1986; Green *et al.*, 1986). Following this, several groups reported the cloning of the receptors for progesterone (PR) (Conneely *et al.*, 1986), thyroid hormone (TR) (Sap *et al.*, 1986; Weinberger *et al.*, 1986) and all-*trans* retinoic acid (RAR) (Petkovich *et al.*, 1987). By 1990, a total of 15 highly homologous proteins had been identified, comprising a superfamily of nuclear receptors (Mangelsdorf, 1995). To date, there are more than 150 different members of the protein superfamily spanning a large diversity of species from the fly *Drosophila melanogaster* (with 21 genes) (Adams *et al.*, 2000) and the nematode *Caenorhabditis elegans* (with unexpectedly 270 genes) (Sluder *et al.*, 1999) to humans (with 48 genes) (Robinson-Rechavi *et al.*, 2001) but not from yeast, suggesting that this family of proteins evolved at the metazoan stage. A large number of nuclear receptors have been identified by virtue of their sequence homology with known receptors, but have been designated “orphan receptors” as no cognate ligand has yet been identified. A list of classical and orphan human receptors and their corresponding ligands is shown in Table 1.1.

On the basis of sequence alignment and phylogenetic tree construction the superfamily has been grouped into 6 subfamilies (Laudet, 1997). The diversity of nuclear receptors appears to have been generated mainly by two waves of gene duplication during evolution. The first occurred very early during metazoan evolution and resulted in the 6 subfamilies, while the second wave of gene duplication, which led to diversification within each group of receptors was contemporaneous to the diversification of early vertebrates (Laudet, 1997). It has been suggested that the ancestor of all nuclear receptors was likely to be an orphan transcription factor whose activity was regulated by conformational changes driven by events such as phosphorylation or protein-protein interaction which then evolved to acquire the ability to bind a ligand (Escriva *et al.*, 1997). However, the possibility that the ancestral receptor was ligand-dependent and that mutations changed its ligand-binding specificity or led to loss of ligand binding during evolution cannot be excluded.

Based on knowledge of their ligands and functions nuclear receptors can now be divided into three categories: i) the classical endocrine receptors; ii) the “adopted” orphan receptors; iii) the remaining orphan receptors as shown in Figure 1.1 (Chawla *et al.*, 2001; Berkenstam and Gustafsson, 2005). The endocrine receptors, whose ligands were known before the receptors were identified, consist of two groups: the classic nuclear steroid hormone receptors and the non-steroid hormone receptors. Steroid hormones are synthesized mainly in endocrine organs that are regulated by negative-feedback control and reach their target tissues (where they bind to their receptor with high affinity) through the circulation. Non-steroid hormones are derived from dietary lipids (vitamin A or cholesterol) or require exogenous elements for their synthesis (sunshine for vitamin D or iodine for thyroid hormone) and regulate endocrine or lipid-sensing pathways (Chawla *et al.*, 2001). Unlike the steroid hormone receptors, which are mainly cytoplasmic and bind to DNA as homodimers only after ligand binding, the non-steroid receptors localize to the nucleus even in absence of their ligands and often function as heterodimers with the retinoic X receptor (RXR). The adopted orphan receptors, whose ligands have been identified after the gene was cloned, also function as heterodimers with RXR and bind their ligands with low affinity. These receptors are considered lipid sensors and maintain nutrient lipid homeostasis by regulating genes involved in lipid metabolism, storage, transport and elimination. The final group of orphan receptors contains proteins whose ligands have not yet been identified. It is not known whether all orphan receptors have the potential to bind natural or synthetic ligands or whether they are “true” orphans that do not possess a ligand-binding pocket and might be regulated through alteration of their expression or by covalent modification or by interaction with other proteins (Gronemeyer *et al.*, 2004). The latter may particularly be the case for the NURR1 and DHR38 orphan receptors, whose crystal structures revealed the absence of a discernible ligand-binding cavity (Baker *et al.*, 2003; Wang *et al.*, 2003).

One in ten of the most commonly prescribed drugs act via nuclear receptors, attesting to their importance as therapeutic targets to combat disorders that have abnormal nuclear receptor signalling as a key pathological determinant (Table 1.2). Therefore characterization of the roles of nuclear receptors in normal physiology and abnormal disease processes is one of the major goals of biomedical research.

Over the last decade, our understanding of regulation of gene expression by nuclear receptors has grown greatly, with the knowledge that not only is the interaction of receptors with DNA necessary to elicit a transcriptional response, but also that many cofactors (coactivators and corepressors) are involved in transmitting receptor signalling to the basal transcriptional machinery. Moreover, a very recent study with expression profiling of all 49 mouse nuclear receptors mRNAs in a large variety of tissues, revealed the existence of a hierarchical transcriptional circuitry that extends beyond individual tissues to form a mega-network governing physiology on a whole organism scale (Bookout *et al.*, 2006). Furthermore, crystal structures of the ligand-binding domains (LBDs) of many nuclear receptors have been solved, providing an understanding of the structural basis of receptor action.

### **1.1.2 Receptor structure and domains**

The nuclear receptors share similar properties, including the ability to recognise and bind to specific DNA sequences usually located in the promoter regions of target genes and to interact in a co-operative fashion (dimerise) with each other or with other members of the family.

On the basis of primary amino acid sequence homologies, it has been possible to identify distinct functional domains, which are highly conserved amongst family members: a variable amino-terminal region (A/B) containing a ligand-independent transcriptional activation function (AF-1); a conserved central region (C) which is the DNA-binding domain (DBD); a linker region (D), followed by E/F domains that mediate ligand binding. The carboxy-terminal domain of many receptors also includes a strong, ligand-dependent, transcriptional activation function (AF-2) (Figure 1.2).

#### **1.1.2.1 *The N-terminal (A/B) domain***

The A/B domains of receptors are the most variable both in size, (ranging from 23 amino acids in the vitamin D receptor [VDR] to 602 amino acids in the mineralocorticoid [MR]) and sequence. Alternative splicing and differential promoter usage mediates the variability of these domains. No structural information is yet available for the A/B domains, and their functional role is not fully elucidated.

They may contain a constitutive transcriptional activation function (AF-1), whose mechanism and functional significance is relatively poorly understood. For some receptors (e.g. ER), a co-operative interaction between the AF-1 and AF-2 functions, perhaps mediated by bridging of cofactors between the N- and C-terminal domains, has been proposed (Kraus *et al.*, 1995).

Phosphorylation of key residues within the A/B domain of some receptors, e.g., by protein kinase A in RAR (Rochette-Egly *et al.*, 1995) or MAP kinase in peroxisome proliferator-activated receptor gamma (PPAR $\gamma$ ) (Adams *et al.*, 1997), may also play an important role in the regulation of AF-1 activity and could represent an important point of integration between cell surface and nuclear receptor signalling pathways.

#### **1.1.2.2 The DNA-binding (C) domain**

Together with the ligand-binding domain, the DNA-binding domain represents the most highly conserved region among different members of the nuclear receptor family, with the exception of two divergent members (dosage-specific sex reversal-adrenal hypoplasia congenita critical region on the X chromosome 1 [DAX1] and short heterodimeric partner [SHP]), suggesting that these domains mediate a common receptor function. The hallmark of most nuclear receptors is their ability to bind to specific regulatory DNA sequences termed hormone response elements (HREs), which are usually located within the promoter regions of target genes.

HREs consist of a 6 bp core recognition motif derived from the archetypal AGGTCA sequence, termed a “half-site”, which is: a) a part of an extended single motif preceded by a 5'-flanking A/T-rich sequence that binds nuclear receptors which interact as monomers; b) duplicated to form an inverted palindrome which bind steroid receptor homodimers; c) duplicated to form an everted palindrome in some special cases; d) duplicated to form direct repeats which bind nuclear receptors that heterodimerise with RXR (RXR itself and some orphan nuclear receptors can also bind such direct repeats as homodimers) (Figure 1.3a). The length of nucleotide sequence, which forms a “spacer region” between the half sites, is an important determinant of the specificity of hormonal responses.

The C domain of receptors consists of two zinc-finger motifs each containing four highly conserved cysteine molecules co-ordinating binding of a zinc atom. Together

with additional amino acid sequences in the hinge (D) domain which represent a C-terminal extension (CTE) of the DBD, the whole motif mediates monomeric DNA binding (Figure 1.3b). Nuclear magnetic resonance and crystallographic studies have provided insights into the mechanism by which NRs bind to DNA. Residues which are critical in mediating response element recognition are located at the distal end of the first zinc finger in a region termed the "P box"; other residues within the second finger form the so called "D box" which is involved in dimerization. The core of the DBD consists of two amphipathic  $\alpha$ -helices packed at right angles: the first helix which encompasses the 'P' box is orientated towards the major groove of DNA and makes direct contact with the core hexanucleotide response element; the second  $\alpha$ -helix is located at the carboxy-terminal end of the second zinc finger and supports the first helix. The NMR and crystal structures of RXR $\alpha$  and TR have identified an additional  $\alpha$ -helix located within the CTE, which makes contact with bases in the minor groove of DNA to provide further stability (Rastinejad *et al.*, 1995; Kumar and Thompson, 1998). This third  $\alpha$ -helix functions not only in the context of receptor homodimers (e.g., RXR) but also mediates interaction of receptors (e.g., RAR-RXR, TR-RXR) in heterodimers.

### **1.1.2.3 The hinge (D) domain**

This region situated between the DBD and the more distal ligand-binding domain is poorly conserved among the different receptors. It acts as a hinge between the DBD and the LBD, allowing rotation of the DBD. In the last few years interest in studying the hinge region has increased, as it appears to be more than a simple flexible connector and mediates important receptor functions. It contains the Nuclear Localization Signal (NLS), a peptide motif required for nuclear pore recognition and also residues whose mutation abolishes interaction with cofactors which are necessary for transcriptional regulation, e.g. the Nuclear CoRepressor protein, NCoR (Horlein *et al.*, 1995). Recently a region has been identified in the hinge domain of the liver receptor homologous protein 1 (LRH-1), which represses the activity of the receptor. This repressive activity can be abolished by mutations within the hinge domain (Xu *et al.*, 2003).



#### 1.1.2.4 The C-terminal ligand-binding (E, F) domain

The C-terminal domain of nuclear receptors is the second most conserved region and approximately 250 amino acids long. It is a multifunctional domain, which in addition to the binding of ligand, mediates homo- and heterodimerization, interaction with heat shock proteins, and contains a strong ligand-dependent transcription activation function (AF-2).

Elucidation of the crystal structures of several receptors either in the absence (apo-) or in presence (holo-) of ligand has dramatically enhanced our understanding of how nuclear receptor ligands exert their effects at the molecular level. These structures have revealed that the hallmark of nuclear receptors is a common fold conserved between ligand-binding domains, consisting of 12  $\alpha$ -helices (H1-H12) and one conserved  $\beta$  turn arranged as a "triple-layered sandwich". These form a central hydrophobic cavity, the ligand-binding pocket, into which the ligand can be accommodated. However some variations have been observed; for example in RAR $\gamma$  helix 2 (H2) has not been reported (Renaud *et al.*, 1995), while an additional short helix (H2') is present in PPAR $\gamma$  (Nolte *et al.*, 1998). The ligand-binding pockets of receptors are variable both in size, from 0Å (NURR1) to 1400Å (PPAR) and shape, in keeping with the structural diversity of their ligands. For example the large pocket seen in PPARs has a distinct, three-arm Y-shape, allowing it to bind numerous fatty acids and fatty acid derivatives with low affinity, while that of PXR has an elliptical shape which allows it to bind to the cholesterol lowering drug SR12813 in three different conformations and to larger ligands such as hyperforin and the antibiotic rifampicin, the largest known ligand for any nuclear receptor. Beside its size and the shape, the hydrophobic/hydrophilic nature of the surface of the pocket also plays a role in determining ligand-binding specificity (Li *et al.*, 2003).

Helix 12, at the C-terminal end of the ligand-binding domain, corresponds to the region which mediates hormone-dependent transcriptional activation or AF-2 activity. Thus, the AF-2 domain in most receptors adopts an amphipathic  $\alpha$ -helical conformation encompassing a highly conserved peptide motif  $\Phi\Phi X E \Phi\Phi$  (where  $\Phi$  = hydrophobic, X = any, E = glutamic acid residues), which is directly involved in interaction with transcriptional coactivators (Barrettino *et al.*, 1994; Gronemeyer and Laudet, 1995). Comparison of the apo-RXR $\alpha$  structure with that of RAR $\gamma$  in the

presence of all-*trans* retinoic acid led to the “mouse trap” model for nuclear receptor activation in which H12 undergoes a dramatic conformational change in response to ligand. Rather than protruding into solution as observed in the apo- RXR $\alpha$  structure (Bourguet *et al.*, 1995), in liganded RAR $\gamma$  H12 folds back against the core LBD thereby “closing” the ligand-binding pocket (Renaud *et al.*, 1995). Moreover the transconformation of H12 upon binding of ligand together with other additional structural changes (e.g. the bending of H3) generates a hydrophobic cleft on the surface of the receptor which facilitates the binding of coactivators. In an extension of this model, it has been demonstrated that binding of the antagonists raloxifene or dihydroxytamoxifen to the estrogen receptor (ER) results in a different position of H12, which is rotated and shifted with respect to its position when bound to the full agonist estrogen (Brzozowski *et al.*, 1997). As a consequence, H12 fails to reconstitute the hydrophobic surface, thus precluding coactivator binding (Figure 1.4).

However, some variations from this common structural organization are worthy of note: for example, in both unliganded PPAR $\gamma$  and PXR structures, H12 is packed against the body of the receptor in a position which is very similar to that seen in the holo-structures (Nolte *et al.*, 1998; Uppenberg *et al.*, 1998; Watkins *et al.*, 2001). It has been suggested that this position, which appears permissive for coactivator interaction, may account for the constitutive transcriptional activity of these receptors that is observed *in vivo*. Recently Kallenberger and colleagues have used fluorescence anisotropy to directly assess the mobility of H12 in PPAR $\gamma$ . They observed that H12 is significantly more mobile than the main body of the protein. Upon ligand binding H12 shows reduced mobility, accounting for its role as a molecular switch (Kallenberger *et al.*, 2003).

As described previously, other regions within the LBD mediate important functions. For example in TR, it was first proposed that a series of nine heptads repeats of hydrophobic residues (analogous to a leucine-zipper motif) mediated dimerization (Forman *et al.*, 1990). The observation that a leucine to arginine mutation (L428R) in the ninth heptad reduces heterodimer formation supported this model (Au-Fliegner *et al.*, 1993). However, crystal structures of RXR $\alpha$  and TR $\alpha$  have shown that, in addition to the ninth heptad contained within H11, other residues in helices 8, 9 and 10 are also involved in dimerization (Bourguet *et al.*, 1995; Wagner *et al.*,

1995). The first structure of a nuclear receptor LBD heterodimer to be reported, namely RAR $\alpha$ -RXR $\alpha$ , revealed that the heterodimerization interface mainly involves residues from H10, H9, loop 8-9 and H7 (Bourguet *et al.*, 2000). In addition, the crystal structure of the liganded PPAR $\gamma$ /RXR $\alpha$  heterodimer has also been described showing that the heterodimer interface is composed of conserved motifs within H10 of PPAR $\gamma$  and RXR $\alpha$  with additional charge interactions from residues in helices 7 and 9 (Gampe *et al.*, 2000).

With nuclear receptors heterodimers, some such as PPAR-RXR and LXR-RXR, are permissive for transcriptional activation when RXR is occupied by its cognate ligand, whereas others such as RAR-RXR and TR-RXR, are not (Mangelsdorf and Evans, 1995).

### **1.1.3 Transcriptional regulation by nuclear receptors**

#### **1.1.3.1 Basal transcription**

Nuclear receptors constitute a family of transcription factors that regulate gene expression in a ligand-dependent manner. According to an initial simple model of action, it was proposed that nuclear receptors interacted directly with components of the basal transcription machinery which includes a number of transcription factors such as TFIIA, TFIIB, TFIID and RNA polymerase II (Baniahmad *et al.*, 1993). Subsequently, biochemical approaches demonstrated that, for efficient transcriptional regulation, nuclear receptors require the recruitment of intermediary proteins or coregulators.

In general, unliganded or antagonist-bound receptors are either transcriptionally inert or actively promote transcriptional repression by interacting with a corepressor complex. Conversely agonist-bound receptors promote transcriptional activation by interaction with a coactivator complex.

It is also recognized that alterations of chromatin structure play an important role in gene expression, as chromatinized transcription units are repressed when compared to naked DNA (Wu, 1997; Wade and Wolffe, 1999). Two general classes of chromatin remodeling factors have been identified: 1) ATP-dependent nucleosome remodeling complexes, which use the energy derived from ATP hydrolysis to

catalyze nucleosome mobilization, and 2) factors that contain histone acetyltransferase or deacetylase activity.

There is evidence that increased acetylation of key lysine residues in nucleosomal histone tails correlates with transcriptional activation, whereas their hypoacetylation is associated with transcriptional repression (Pazin and Kadonaga, 1997). It has been suggested that acetylation causes unfolding of nucleosomes which makes the DNA more accessible to the transcription machinery, whereas hypoacetylation enhances chromatin condensation and transcriptional repression. Finally, the nucleosomal core can also be modified by phosphorylation, methylation and ADP-ribosylation, although the role of histone modifications other than acetylation is less well understood.

### **1.1.3.2 Coactivator families**

Coactivators represent a group of proteins that serve to enhance the ability of nuclear receptors to activate transcription via their associated enzymatic activities which include histone acetyltransferases, methyltransferases, ubiquitin ligases or as agents that integrate signaling via kinase-signaling pathways (Lonard and O'Malley, 2005). The earliest indications of the existence of a family of nuclear receptor transcriptional coactivators stemmed from observations of a phenomenon known as transcriptional interference or "squenching". This can be classically seen in transient transfection assays in which ligand-dependent transcriptional activation by one nuclear receptor can be attenuated by the presence of a second nuclear receptor, suggesting that the latter is in some way able to compete for a common entity, which is utilized by both receptors. Mutational analysis has shown that the receptor AF-2 domain which consists of a short conserved  $\alpha$ -helical (H12) sequence usually at the C terminus of the LBD, is involved in this interference. Moreover crystal structures of several nuclear receptor LBDs have shown that AF-2 plays a key role in facilitating coactivator recruitment and transactivation in response to hormone binding.

Initial biochemical studies performed with ER led to the identification of several proteins of a molecular mass of between 160 and 140kD, which only associated with the receptor in the presence of estradiol, and they were designated as ER-associated

proteins (ERAP) 160 (p160), ERAP 140 (p140) and receptor-interacting protein 140 (RIP 140) (Halachmi *et al.*, 1994; Cavailles *et al.*, 1995) respectively. Subsequently, different groups have cloned many similar proteins and to date a large number of factors that interact with nuclear receptors has been characterized. Many of these proteins appear to function as components of large multiprotein complexes.

#### 1.1.3.2.1 *The p160 family*

This family of proteins referred to as SRC-1/NCoA1, SRC-2/TIF2/GRIP1/NCoA2 and SRC-3/AIB-1/pCIP/ACTR/TRAM1/RAC3/NCoA3 consists of three members which share a common domain structure and exhibit sequence similarity of approximately 40% (Figure 1.5) (McKenna *et al.*, 1999; Aranda and Pascual, 2001). Investigation of the nuclear receptor interaction domain of the p160 protein family led to the identification of a specific LXXLL motif (where L is Leucine and X is any amino acid), and one or more of these motifs are present in all members. The LXXLL motif has been found to be necessary for interactions with nuclear receptors (Heery *et al.*, 1997; Torchia *et al.*, 1997). Recently, structures of several receptor LBDs complexed to parts of the p160 receptor interaction domain have been solved, revealing that these motifs form short  $\alpha$ -helices, which interact with a hydrophobic groove on the surface of the nuclear receptor LBD. For example, in PPAR $\gamma$ , the LXXLL coactivator helix is held in a "charge clamp" formed by a conserved lysine in H3 and a conserved glutamic acid in the C-terminal AF-2 helix (Nolte *et al.*, 1998). Several investigators have demonstrated the existence of intrinsic Histone Acetyl Transferase (HAT) activity within the C-terminal region of various members of the p160 family, including SRC-1 (Spencer *et al.*, 1997) and ACTR (Chen *et al.*, 1997).

#### 1.1.3.2.2 *CBP/p300*

The conserved C-terminal transcriptional activation (AF-2) domain of receptors also mediates interaction with either the cointegrator CREB binding protein (CBP), and the p300/CBP-associated factor (pCAF). The CREB (Cyclic AMP Response Element Binding Protein) Binding Protein (CBP) (Chakravarti *et al.*, 1996) and its homologue p300 (Shikama *et al.*, 1997) are large conserved proteins that serve essential coactivator roles for many different transcription factors, functioning in part

as a molecular scaffold but also by acetylating diverse substrates. In fact CBP/p300 not only directly binds to nuclear receptors via its amino-terminal region, but also associates with the p160 family of coactivators through a different domain in its C-terminus (Chen *et al.*, 1997; Spencer *et al.*, 1997; Korzus *et al.*, 1998). CBP/p300 together with pCAF are coactivators with potent HAT activity and they can also acetylate other (non-histone) transcriptional proteins, thereby regulating their activity (Chen *et al.*, 1999). Deletion or mutation of the HAT domain in CBP results in loss of function for many transcription factors, revealing the importance of this activity.

#### 1.1.3.2.3 *The TRAP/DRIP complex*

Recently, a multiprotein complex called TRAP or DRIP that interacts with thyroid hormone (Fondell *et al.*, 1996) and vitamin D receptors (Rachez *et al.*, 1999) respectively in a ligand-dependent manner has been identified. Both complexes, which consist of more than a dozen polypeptides ranging in size from 70 to 230 kD, are recruited to the AF-2 region in nuclear receptors via LXXLL interaction motifs. Unlike the other previously described coactivators, the TRAP/DRIP complex does not possess intrinsic histone acetyl transferase activity, but is able to interact directly with both nuclear receptors and the basal transcription machinery (Yuan *et al.*, 1998; Rachez *et al.*, 1999).

#### 1.1.3.2.4 *Other coactivators*

In addition to the aforementioned families, many other proteins have been shown to enhance transactivation by nuclear receptors. Some of them exhibit relative preference for a subset of nuclear receptors such as ARA70 (androgen receptor activator-70), which specifically enhances the activity of the androgen receptor in a ligand-dependent manner through its AF-2 domain (Yeh and Chang, 1996). Another interesting example is SRA (steroid receptor RNA activator) which activates the AF-1 function of steroid hormone receptors and interacts with SRC-1 (Lanz *et al.*, 1999). Recent studies suggest that cell-specific coactivators may also play critical roles in gene-specific transcriptional activation. One example is represented by PGC-1 (PPAR $\gamma$  coactivator 1) which is expressed specifically in brown fat and skeletal muscle and which enhances transactivation by TR and PPAR $\gamma$  on genes such as the uncoupling protein-1 (UCP-1). Exposure to low temperatures dramatically increases

PGC-1 mRNA expression and this has been suggested to be a key mechanism in the regulation of adaptive thermogenesis (Puigserver *et al.*, 1998).

Taken together, these observations indicate an increasingly complex model for transcriptional regulation and the current challenge is to understand how so many different proteins cooperate in gene activation. Kinetically, transcription may be viewed as a multistep process, in which the binding of receptors to their DNA-binding sites is followed by derepression and then by transcriptional initiation. In this model, it is proposed that chromatin remodeling complexes and complexes containing HAT activity are initially recruited to the promoter to relieve the repression imposed by the highly condensed state of chromatin and to facilitate the recruitment of additional coactivators. The combinatorial action of proteins finally leads to the assembly of the RNA polymerase II-containing transcription complex and the initiation of transcription (Figure 1.6).

### **1.1.3.3 Active repression by nuclear receptors**

In addition to the ligand-dependent transcriptional activation described previously, it has been observed that selected members of the nuclear receptor superfamily, including TR and RAR, repress basal transcription in the absence of ligand. Bahniahmad and colleagues first demonstrated the existence of active silencing domains in TR and showed that fusion of these domains to the heterologous DBD of the yeast Gal4 protein transferred repressor activity (Bahniahmad *et al.*, 1992). Subsequently, with the observation that the unliganded TR LBD could interact with TFIIB (Bahniahmad *et al.*, 1993), it was suggested that the receptor might inhibit the formation of the pre-initiation complex, by sequestering TFIIB and therefore acting directly as a repressor (Fondell *et al.*, 1993). However, following the identification of intermediary factors acting as repressors, this notion is less favoured and the current model assumes that unliganded receptors which mediate silencing activity are associated with such corepressors.

#### 1.1.3.4 Nuclear receptor corepressors

Biochemical studies led to the identification of a 270kD protein associated with unliganded TR and RAR named Nuclear CoRepressor or NCoR (Horlein *et al.*, 1995). At the same time the 168kD Silencing Mediator for Retinoid and Thyroid hormone receptors, (SMRT) was isolated through yeast two-hybrid screening of a human lymphocyte cDNA library (Chen and Evans, 1995). Although NCoR and SMRT are not identical, they are related both structurally and functionally and appear to be the products of a gene duplication event that occurred prior to the vertebrate evolutionary diversification. However, they exhibit distinct molecular and biological properties (Goodson *et al.*, 2005). Mutational analysis of TR $\beta$  led to the identification of an interaction domain for NCoR (called the COR box) located in the hinge region ( $\alpha$  203-230) with additional contributions to this interaction from the N-terminal portion of the LBD ( $\alpha$  230-260). Sequence comparison of this region in TR and RAR with that of other nuclear receptors which do not interact with corepressors indicated that the COR box is a conserved region. However, other residues that are also important in mediating transcriptional repression have been identified in the distal part of the receptor LBD (Zhang *et al.*, 1997). Moreover, corepressors appear to bind receptor dimers but not monomers on DNA (Zamir *et al.*, 1997). Mapping studies have revealed that NCoR and SMRT share two receptor interaction domains (ID-1 and ID-2) in the C-terminal region, and three independent repressor domains that can actively repress a heterologous DNA-binding domain located principally in the N-terminal and central region of SMRT and NCoR (Privalsky, 2004). Interestingly, more recently it has been shown that NCoR has an additional third ID located N-terminal of the two conserved IDs, that seems to be responsible for preferentially binding to TR (Webb *et al.*, 2000; Makowski *et al.*, 2003). Analogous to coactivators, each interaction domain contains sequences corresponding to a consensus LXXI/HIXXXI/L (where L = leucine, I = isoleucine, H = histidine and X = any amino acid) motif, which are also predicted to adopt an amphipathic  $\alpha$ -helical conformation (Hu and Lazar, 1999; Nagy *et al.*, 1999; Perissi *et al.*, 1999). However, compared with the LXXLL coactivator motif, the corepressor consensus motif represents an amino-terminally extended helix, which appears to mediate effective binding to the unliganded receptor. Moreover, this



observation suggests that the LXXI/HIXXXI/L motif in NCoR and SMRT and the LXXLL motif in coactivators may utilize overlapping sites on the receptor LBD for interaction, with an inability of the larger corepressor helix to fit within a "charge clamp". The recent co-crystallisation of antagonist-bound PPAR $\alpha$  with a peptide from the SMRT corepressor fulfils this prediction with the AF-2 helix in the receptor being displaced to accommodate the larger corepressor peptide (Xu *et al.*, 2002).

Further insight into the potential mechanism of transcriptional repression by nuclear receptors came from the discovery of mammalian homologs of the yeast Sin3 protein (Ayer *et al.*, 1995; Schreiber-Agus *et al.*, 1995) and the subsequent observation that these proteins interact with NCoR and SMRT (Nagy *et al.*, 1997; Alland *et al.*, 1997; Heinzel *et al.*, 1997). In turn, these proteins are components of a larger corepressor complex that also contain Histone Deacetylases (HDAC1/HDAC2), suggesting a model for repression in which histone deacetylation and subsequent chromatin condensation results in reduced access of the transcription machinery to the gene promoter (Heinzel *et al.*, 1997; Alland *et al.*, 1997). Since then several independent groups have reported the existence of multiple SMRT and NCoR complexes in which many component factors, including histone deacetylases, TBL-1, TBLR-1, GPS-2 and a number of other modulatory and effector proteins are recruited through docking surfaces (repression domains) located principally in the N-terminal and central regions of SMRT and N-CoR (Jepsen and Rosenfield, 2002; Privalsky, 2004), although the precise composition and the relationship of these complexes remain to be determined. However, it is noteworthy that SMRT and NCoR not only serve as factors which recruit these complexes, but also play a role in the activation of the enzymatic mechanism of their associated histone deacetylase HDAC3 (Guenther *et al.*, 2001; Codina *et al.*, 2005). Moreover, it is now clear that the functions of both SMRT and NCoR are further diversified through alternative mRNA splicing, yielding a series of corepressor protein variants that participate in distinctive transcription factor partnerships and display distinguishable repression properties which can be modulated in different cell types and to different developmental stages ( Goodson *et al.*, 2005).

In addition to NCoR and SMRT other corepressor proteins have been identified which interact directly with nuclear receptors and repress their transcriptional activity. For example the Small Ubiquitous Nuclear Corepressor (SUN-COR), which

shows no homology to NCoR and SMRT, interacts directly with TR and RevErb. The observation that SUN-COR interacts with NCoR and SMRT suggested that it may function as an additional component of a larger corepressor complex involved in transcriptional repression (Zamir *et al.*, 1997). Alien is another corepressor unrelated to SMRT and NCoR which was first identified in *Drosophila*. It is a very highly conserved protein among different species which interacts with a number of nuclear receptors, including TR, VDR and the ecdysone receptor. Its function has been well established for the orphan receptor Dax-1 (dosage-sensitive sex reversal adrenal hypoplasia critical region on the X chromosome, gene 1), where mutations which impair its binding to Alien seems to play an important role in the pathogenesis of adrenal hypoplasia congenita (Altincicek *et al.*, 2000). Hairless is another TR associated corepressor which can recruit HDACs independently from NCoR or SMRT and which has been shown to play an important role in mediating the effects of TH on brain development (Potter *et al.*, 2001).

#### **1.1.3.5 Negative transcriptional regulation**

There is also evidence to suggest that corepressors can participate in ligand-dependent transcriptional inhibition by nuclear receptors. One of the best characterized examples of this alternative form of transcriptional regulation is the feedback loop through which T<sub>3</sub> impairs transcription of the TRH, TSH $\alpha$  and TSH $\beta$  genes, thereby suppressing the production of hypothalamic TRH and pituitary TSH. In general, it has been observed that when bound to negative hormone response elements (HREs) in these gene promoters, the unliganded receptor increases basal levels of transcription, and that addition of ligand initially reverses this stimulation and then mediates active repression of transcription (Wondisford *et al.*, 1993; Hollenberg *et al.*, 1995). Unlike their positive counterparts, the mechanism by which negative HREs act are poorly understood but their location frequently in the vicinity of the TATA box, may suggest interference with the basal transcription complex. Tagami and colleagues proposed a model in which corepressors mediate basal activation of the TSH $\alpha$  and TRH promoters by unliganded TRs, since overexpression of NCoR and SMRT unexpectedly enhanced the basal activity of these promoters (Tagami *et al.*, 1997). In another study, it has been demonstrated

that T3 induces recruitment of HDAC2 and TR to a negative response element in the TSH $\beta$  promoter (Sasaki *et al.*, 1999). As yet, it is not possible to reconcile all these observations into a satisfying, unifying mechanism. One possibility is that the corepressor/HDAC complex mediates different responses in positive versus negative hormone response element contexts. Several lines of evidence indicate that coactivators may also play a role in ligand-dependent repression or negative transcriptional regulation: mutations in TR $\beta$  which disrupt its interaction with coactivators are associated with impaired negative regulation by TR *in vivo* (Collingwood *et al.*, 1997; Collingwood *et al.*, 1998); experiments in our own laboratory (R. Clifton-Bligh unpublished data) and by others (Tagami *et al.*, 1999) suggest that hormone-dependent repression by TR involves coactivator recruitment; targeted disruption of the SRC-1 coactivator gene in mice results in impaired negative feedback regulation of TRH and TSH genes by thyroid hormones (Weiss *et al.*, 1999).

In addition to the ligand-dependent repression through negative regulatory elements described above, recent studies have identified a novel mechanism of transrepression, by which NRs can inhibit transcription without direct, sequence-specific binding to DNA. Many NRs have been suggested to exert inhibitory effects on inflammatory response genes through direct interactions with the nuclear factor  $\kappa$ B (NF- $\kappa$ B) and activator protein 1 (AP-1) transcription factors (Pascual and Glass, 2006). Recently, ligand-dependent sumoylation of PPAR $\gamma$ , which prevents exchange of corepressor for coactivators, has been proposed as a novel mechanism through which PPAR $\gamma$  represses the transcriptional activation of inflammatory genes in mouse macrophages (Pascual *et al.*, 2005). Finally, cofactors containing an intrinsic repression function can be recruited by NRs in a ligand-dependent manner although their role in negative regulation remains to be elucidated. Examples of such cofactors are the receptor interacting protein of 140 kDa (RIP140) and the ligand-dependent corepressor (LCoR). RIP140 was initially reported as a coactivator, but subsequent studies showed that it is a widely expressed corepressor for nuclear receptors which controls energy homeostasis by regulating the expression of metabolic gene networks in adipose tissue and muscle (Parker *et al.*, 2006). LCoR was identified in a screen for proteins that interacted with the estrogen receptor  $\alpha$  (ER $\alpha$ ) LBD in an estradiol-dependent manner (Fernandes *et al.*, 2003). Despite their very limited

homology, LCoR and RIP140 share a similar mechanism of action. Both interact with a number of receptors in the presence of agonist but not antagonist, and recruit similar cofactors including HDACs. Finally, the orphan receptor short heterodimer partner (SHP) which interacts and inhibits the action of several NRs, mediates most of its repressive effect through recruitment of HDACs (Gobinet *et al.*, 2005).

## ***1.2 Thyroid hormones, their receptors and the syndrome of Resistance to Thyroid Hormone***

### **1.2.1 Thyroid hormones**

Thyroid hormones (TH) are essential for the regulation of a diverse array of physiological processes including growth, myocardial contractility, differentiation of the nervous system and metabolic rate. Disorders of the thyroid gland are among the most common endocrine maladies, thus the study of TH action has important biological and medical implications. Thyroxine (T4) and, to a lesser extent, 3,5,3'-triiodothyronine (T3), which is the biologically active hormone, are synthesized in the thyroid gland and secreted into the bloodstream under the control of hypothalamic thyrotropin-releasing hormone (TRH) and pituitary thyroid-stimulating hormone (TSH). In turn, T3 and T4 regulate TRH and TSH production as part of a negative feedback loop ensuring remarkable stability of serum thyroid hormones levels (Figure 1.7).

The primary effects of thyroid hormones on physiological processes are mediated through a nuclear thyroid hormone receptor (TR), which is intimately associated with chromatin and binds TH with high affinity and specificity. In addition to the receptor it is recognized that thyroid hormone action in tissue is modulated by other factors: for example, recently the monocarboxylate transporter 8 (MCT8), a membrane transporter, has been shown to be critical for T3 delivery to the human central nervous system (CNS) (Friesema *et al.*, 2004; Dumitrescu *et al.*, 2004). While T4 is produced entirely by the thyroid, T3 is mainly produced in the periphery through the deiodination of T4. Three types of deiodinases (DIOs), which are selenoenzymes that catalyze iodothyronine deiodination, have been described: the type I deiodinase (DIO 1) is widely distributed and is responsible for the generation of most T3 in peripheral tissues; DIO 2 generates T3 in the CNS and is involved in hypothalamic-pituitary negative feedback; the type 3 (DIO 3) deiodinase mediates TH catabolism (Bianco *et al.*, 2002). Recently a mutation in the human SECISBP2 gene, which encodes a common regulator that mediates selenium incorporation into proteins including the deiodinases, has been reported in association with low or normal circulating levels of T3 but elevated T4 levels, highlighting the importance of selenoproteins in thyroid feedback regulation (Dumitrescu *et al.*, 2005).

### 1.2.2 Thyroid hormone receptors

In 1986, two groups independently identified the *c-erb A* protein as a high-affinity receptor for thyroid hormone (Sap *et al.*, 1986; Weinberger *et al.*, 1986). This protein represents a cellular homologue of *v-erb A*, an avian retroviral oncogene, which shares significant similarity with other members of the nuclear receptor superfamily. Subsequent studies demonstrated that there are two different subtypes of the thyroid hormone receptor, TR $\alpha$  and TR $\beta$ , which are highly homologous in their ligand-binding and DNA-binding domains, but exhibit sequence divergence in the amino-terminal regions (Figure 1.8). These subtypes are encoded by two different genes on human chromosomes 17 (TR $\alpha$ ) and 3 (TR $\beta$ ) (Dayton *et al.*, 1984; Weinberger *et al.*, 1986). Alternate splicing of each gene generates several isoforms: TR $\alpha$ 1 and TR $\alpha$ 2 are derived from the  $\alpha$  gene, and TR $\beta$ 1 and TR $\beta$ 2 from the  $\beta$  gene (Benbrook and Pfahl, 1987; Thompson *et al.*, 1987; Hodin *et al.*, 1989). In contrast to the other isoforms, TR $\alpha$ 2 or *c-erb A* $\alpha$ 2 does not bind TH and has been suggested that it may act as a negative modulator of thyroid hormone action (Lazar, 1993). Interestingly, another novel TR $\alpha$  variant, TR $\alpha$ - $\Delta$ E6), which has been recently described in mouse, (Casas *et al.*, 2006) has been postulated to have a similar functional role. The phenotypic analysis of numerous TR knock-out animal models has revealed that the relative expression of the two TR isoforms varies from tissue to tissue and also temporally during development. TR $\alpha$ 1 is widely expressed from an early stage of development being predominantly found in the central nervous system (CNS), myocardium and skeletal muscle, and appears to be crucial for postnatal development, whereas expression of TR $\beta$  is highly restricted until later in embryogenesis and is mainly involved in control of TH synthesis, hepatic metabolism, and development of retinal and auditory functions (Flamant & Samurat, 2003). Of the two TR $\beta$  isoforms, TR $\beta$ 1 is found in almost all tissues but is most abundant in liver and kidney, whereas TR $\beta$ 2 is expressed in the anterior pituitary and specific areas of the hypothalamus, in addition to the developing brain and inner ear. Recently two other isoforms (TR $\beta$ 3 and TR $\Delta$  $\beta$ 3) have also been described, although their role and tissue distribution in humans remains to be defined (Williams, 2000). Like other nuclear receptors, TRs have a modular structure comprising six regions

(A–F) and three functional domains (Amino-terminal, DBD and LBD) as described in Section 1.1.2.

### **1.2.3 Resistance to Thyroid Hormone**

#### **1.2.3.1 *Clinical Features***

The syndrome of resistance to thyroid hormone (RTH), which has an estimated population prevalence of 1:50000 live births, is an uncommon rather than rare disorder, and is characterized by reduced responsiveness of target tissues to circulating TH. The biochemical hallmark of RTH is elevated levels of circulating free thyroid hormones (FT4 and FT3) associated with non-suppressed pituitary TSH secretion. RTH was first described in 1967 by Refetoff and colleagues in two siblings from a consanguineous marriage, who exhibited the classical hormonal profile described above (Refetoff *et al.*, 1967). Since both central and peripheral tissues appeared to be equally affected, the disorder was named generalized resistance to thyroid hormone (GRTH). In 1975, a young woman with the same biochemical signature of GRTH but with peripheral signs and symptoms of hyperthyroidism was described as a case of "selective" pituitary resistance to thyroid hormone (PRTH) (Gershengorn and Weintraub, 1975). Thus RTH, which occurs at any age and with no sex preference, can present with a wide range of different clinical features (Table 1.3) which vary both between different families with the disorder and amongst affected individuals within a single family.

Depending on the degree of associated peripheral thyrotoxic symptoms, the phenotype is either GRTH, which may be relatively asymptomatic except for the presence of goiter, or PRTH in which some features of hyperthyroidism are present (Chatterjee, 1997).

#### **1.2.3.2 *Molecular genetics of RTH***

In the majority of cases, RTH is familial and dominantly inherited. In 1988 Usala and colleagues first demonstrated linkage between the TR $\beta$  locus on chromosome 3 and RTH by restriction fragment length polymorphism analysis. Since then many

groups have reported that affected individuals are heterozygous for mutations in the TR $\beta$  gene. Interestingly, all the mutations cluster within the hormone-binding domain and are located in three "hot spot" regions ( $\alpha\alpha$  234-282, 310-353 and 426-461; Figure 1.9) (Collingwood *et al.*, 1998), with receptor regions involved in DNA binding, dimerization and corepressor interaction being devoid of natural mutations. This is in contrast to other nuclear receptor disorders (e.g. androgen resistance) in which mutations have been identified throughout all domains of the androgen receptor (Quigley *et al.*, 1995). Consistent with these observations, a recent study has shown that knock-in of a heterozygous mutation in the murine TR $\beta$  DBD which abolishes DNA binding, does not result in a RTH phenotype (Shibusawa *et al.*, 2003). Most patients have missense mutations due to single codon substitutions, although in frame codon deletions, frameshift mutations, and truncations due to premature stop codons have also been identified. Functional studies of the mutant receptors typically show negligible or reduced T3-binding and an impaired ability to activate or repress target gene transcription in a hormone dependent manner (Refetoff *et al.*, 1993). Interestingly, affected individuals from the very first family with recessively inherited RTH were shown to be homozygous for a complete deletion of both alleles of the TR $\beta$  receptor gene, while heterozygous family members harboring a deletion of one TR $\beta$  allele were completely normal with no evidence of thyroid dysfunction. This observation suggested that receptor haploinsufficiency is not a mechanism for this disorder. Therefore, it has been proposed that the mutant receptors in dominantly inherited RTH are not simply functionally impaired, but also capable of inhibiting wild-type receptor action (Sakurai *et al.*, 1990; Chatterjee *et al.*, 1991). Indeed, *in vitro* experiments have shown that the function of wild-type receptor is markedly inhibited by mutant receptors, a phenomenon known as dominant negative activity. The degree of dominant negative inhibition exerted by mutant TR depends in part on the level of mutant receptor expression. Genetic evidence supporting this notion has been provided by two rare cases of RTH. The first patient who was homozygous for dominant negative mutations in both TR $\beta$  alleles had severe RTH and mental retardation, whereas his parents who had mutations in only one TR $\beta$  allele had milder RTH (Ono *et al.*, 1991). Recently a second patient who was found to be either homozygous or hemizygous for a TR $\beta$  mutation exhibited a particularly severe



clinical phenotype with hypermetabolism, severe mental retardation and hearing loss while the only clinical manifestation of RTH in his heterozygous mother was a simple goiter (Frank-Raue *et al.*, 2004). One model to explain the molecular mechanism for dominant negative inhibition proposes that mutant receptor-RXR heterodimer complexes directly compete with their wild type counterparts for binding to TREs in target gene promoters (Figure 1.10). This model is supported by the observation that dominant negative action of RTH TR $\beta$  mutants is abolished by artificial mutations which disrupt their DNA binding or dimerisation with RXR (Collingwood *et al.*, 1994). A further attribute which is preserved in RTH TR $\beta$  mutants is their ability to silence basal gene transcription via corepressor recruitment. Indeed some RTH TR $\beta$  mutants show enhanced corepressor binding and disruption of such interaction by introduction of additional mutations abolishes their dominant negative activity (Yoh *et al.*, 1997). As a corollary to these findings, natural mutations occurring within TR $\beta$  domains which are essential for these key functions (DNA binding, dimerization, corepressor interaction) might be predicted to be clinically and biochemically silent, due to their inability to exert a dominant negative effect. Interestingly the functional characterization of a RTH TR $\beta$  mutant, unusually located outside the three mutation clusters, showed that it was selectively impaired for corepressor release and negative regulation of the TRH and TSH $\alpha$  genes, suggesting that this may be the minimum receptor abnormality required to produce an RTH phenotype (Clifton-Bligh *et al.*, 1998). To date over 100 different defects, including point mutations, in-frame deletions and frame-shift insertion have been reported in RTH patients from over 300 families. In general, analyses show that both GRTH and PRTH are associated with mutations in the TR $\beta$  gene indicating that the two disorders represent phenotypic variants of a single genetic entity.

It is of note that in a small but significant number of cases (10-15%) with clinical and biochemical features indistinguishable from those of subjects with RTH harbouring TR $\beta$  mutations, no receptor mutations have been identified. These cases are often referred to as “non-TR $\beta$  RTH”. Linkage analysis has excluded the TR $\beta$  and TR $\alpha$  genes as a cause of the disorder in several kindreds (Weiss *et al.*, 1996; Pohlenz *et al.*, 1999). These findings suggest the possibility that mutations in other proteins involved in TR signalling or dysregulation of their production might be involved in the non-TR $\beta$  RTH cases. Although some knock-out mouse models seem to support

this notion, in spite of extensive linkage studies and direct sequence analyses of several cofactor genes (SRC-1, SRC-3, SMRT) no post-receptor defects have been described in RTH patients to date (Refetoff *et al.*, 2004). However very recently a case of mosaicism for the R338W TR $\beta$  mutation in some cell lineages has been reported, including germline but not fibroblasts in a RTH patient (Mamasiri *et al.*, 2006). This suggests that the possibility of mosaicism should be considered and DNA from several different tissues examined in so-called “non-TR $\beta$  RTH” cases.

### **1.2.3.3 Animal Model of RTH**

The generation of various receptor knock-out (KO) mice has provided a great opportunity to understand the physiological roles of individual TR isoforms and demonstrate a critical function for TR $\beta$  in regulation of the pituitary-thyroid axis. Homozygous TR $\beta$  gene deletion (TR $\beta$  KO) mice in which both the TR $\beta$ 1 and TR $\beta$ 2 isoforms are absent, showed an increase in circulating thyroid hormone levels and an inappropriately elevated TSH, recapitulating the clinical features exhibited by recessively inherited cases of RTH (Forrest *et al.*, 1996). In addition to the hormonal disorder, the TR $\beta$  KO mice showed impaired auditory function indicating that the deaf-mutism in recessive human RTH is also likely to be related to a defect in TR $\beta$ , rather than a deletion of a contiguous gene. TR $\beta$ 2 null mice, with preserved expression of the TR $\alpha$  and TR $\beta$ 1 isoforms, exhibited a similar biochemical phenotype to that of TR $\beta$  KO, consistent with the fact that TR $\beta$ 2 plays a central role in the regulation of the hypothalamic-pituitary-thyroid axis (Abel *et al.*, 1999). In contrast mice with deletion of the TR $\alpha$ 1 isoform had low or normal serum TH, a decreased heart rate and lower body temperature with a phenotype quite dissimilar to RTH (Wikstrom *et al.*, 1998). To investigate the properties of mutant TR $\beta$ s in RTH *in vivo*, several groups have generated transgenic mice in which dominant negative TR $\beta$  mutants have been over-expressed either ubiquitously (Wong *et al.*, 1997) or selectively in tissues (Hayashi *et al.*, 1998; Abel *et al.*, 1999) and these models have provided valuable insights into mutant receptor function and pathophysiological mechanisms which mediate RTH (Reviewed in Yen, 2003 and Cheng, 2005). For example, selective targeting of a RTH TR $\beta$  mutant ( $\Delta$ 337T) to the pituitary using a tissue-specific promoter (Abel *et al.*, 1999), generated transgenic mice with elevated

TSH but only marginally raised T4 levels, suggesting that the additional dominant negative effect of mutant receptors on the hypothalamic TRH gene is required to elevate TH levels in patients with RTH. In contrast, ubiquitous transgenic mutant TR $\beta$  expression resulted in an animal model with more generalized tissue resistance (Wong *et al.*, 1997). These mice exhibited decreased body weight and a behavioural phenotype characterized by hyperactivity, which are recognized features of the human syndrome. However, in these animal models the expression of the mutant receptor transgene is not controlled by the TR $\beta$  gene promoter and as consequence the pattern of mutant receptor expression or the resulting phenotype might not correspond with that of human RTH.

Recently this issue has been addressed by the generation of two different knock-in (KI) mice models in which either a frame-shift mutation involving 14 carboxy-terminal amino acids (TR $\beta$  PV) (Kaneshige *et al.*, 2000) or an in-frame deletion of a threonine residue ( $\Delta$ 337T) (Hashimoto *et al.*, 2001) were introduced into the endogenous TR $\beta$  gene locus. Both of these mutations have been identified in human RTH and the mutant receptors exhibit markedly impaired transcriptional activation and potent dominant negative activity *in vitro*. Over the last few years the phenotypes of TR $\beta$  PV and  $\Delta$ 337T KI mice have been extensively characterized and they are clearly reminiscent of the human RTH phenotype.  $\Delta$ 337T KI mice showed higher levels of TH and TSH in comparison to the TR $\beta$  KO mice, supporting the notion that dominant negative inhibition by the mutant receptor antagonizes residual TR $\alpha$ 1 activity in the hypothalamic-pituitary-thyroid axis. Both heterozygous and homozygous  $\Delta$ 337T mice exhibited abnormalities of vestibulomotor function, which correlated with a general reduction in cerebellar size and in the area of the Purkinje cell layer (Hashimoto *et al.*, 2001). Consistent with phenotypes of RTH patients, TR $\beta$  PV KI mice also showed growth retardation (Kaneshige *et al.*, 2000), abnormal regulation of serum cholesterol (Kamiya *et al.*, 2003), hearing defects (Griffith *et al.*, 2002) and a thyrotoxic skeletal phenotype (O'Shea *et al.*, 2003). Homozygous mice had markedly raised levels of serum thyroid hormone and TSH and a much more severely pathological phenotype. Interestingly, homozygous mice had an increased incidence of thyroid cancer suggesting that dominant-negative activity by mutant TR might contribute to oncogenesis in this tissue (Suzuky *et al.*, 2002). The TR $\beta$  PV KI animal model has provided insights into the molecular basis for dominant negative

activity *in vivo*, confirming that mutant receptor homodimers and heterodimers compete with wild type TR $\beta$  for binding to target gene TREs. The interplay of receptor isoform predominance (e.g. TR $\beta$ 1 in liver, TR $\alpha$ 1 in heart), together with the promoter context of target gene TREs can influence the degree of dominant negative inhibition observed in different tissues (Cheng, 2005). Interestingly, crossing TR $\beta$  PV mice with SRC-1 knock-out animals enhanced the degree of resistance in the hypothalamic-pituitary-thyroid axis in heterozygous TR $\beta$  PV mice, providing evidence that coactivator ‘availability’ can also modulate mutant TR $\beta$  action *in vivo* (Kamiya *et al.*, 2003). To confirm this hypothesis, very recently another study of TR $\beta$ PV mice deficient in SRC-3 has been reported (Ying *et al.*, 2005). However, the profiles of tissue-dependent modulation of phenotype caused by the lack of SRC-1 versus SRC-3 in TR $\beta$ PV mice are not identical, suggesting that in addition to regulating nuclear receptor-dependent signalling, SRCs could also function independent of the nuclear receptor-signalling pathway. In fact, the lack of SRC-3 reduces the growth of both the pituitary and thyroid in TR $\beta$  PV mice, therefore lessening the dysregulation of the pituitary-thyroid axis, although growth impairment was worsened by the reduction of signalling via the IGF/P13K/AKT/mTOR pathway which has recently been reported to mediate cell growth and proliferation (Torres-Arzayus *et al.*, 2004).

### 1.3 Peroxisome proliferator-activated receptor gamma (PPAR $\gamma$ )

#### 1.3.1 General overview of PPARs

Peroxisome proliferator-activated receptors (PPARs) form an important subgroup of the nuclear receptor superfamily. The name PPAR originates from the initial cloning of a receptor subtype which was shown to be activated by various xenobiotic compounds (e.g. clofibrate) which induce proliferation of peroxisomes in the liver of rodents. This protein was called peroxisome proliferator-activated receptor, now known as PPAR $\alpha$  (Issemann and Green, 1990). Since then PPARs have been extensively investigated and evolved from uncharacterized orphan receptors to the most studied nuclear receptors. There are three PPAR subtypes which are products of distinct genes and they are designated PPAR $\alpha$ , PPAR $\delta$  (also called  $\beta$ , NUC-1 or FAAR) and PPAR $\gamma$ . The three PPARs subtypes are very similar in their DBDs, sharing approximately 90% amino acid identity, but are more divergent in their LBDs (Figure 1.11a). As members of the nuclear receptor family, they exhibit the canonical domain structure and bind to specific DNA elements called PPAR response elements (PPAREs) in the 5' flanking region of target genes as obligate heterodimers with the retinoid X receptor (RXR) (Figure 1.11b). Indeed, PPARs cannot bind DNA as monomers or homodimers but depend strictly on RXR as a binding partner. Interestingly, PPAR:RXR heterodimers are "permissive" in that they can be activated synergistically when occupied by ligands for either PPAR or RXR. Functional PPAREs are tandem repeats of an AGGNCA half-site separated by one nucleotide designated a direct repeat + 1 (DR-1) motif. Nucleotide sequences located immediately upstream of the first half-site confer polarity to the bound heterodimer such that PPAR $\gamma$  interacts with the 5' hexamer within the DR-1 element, whereas RXR occupies the downstream site (Juge-Aubry *et al.*, 1997; Di Rienzo *et al.*, 1997). Interestingly, this arrangement represents a reversal of polarity compared with VDR:RXR and TR:RXR heterodimers, where RXR occupies the upstream core hexamer of the direct repeat.

The three PPARs exhibit different expression patterns: PPAR $\alpha$  is most highly expressed in liver, kidney, heart and muscle; PPAR $\gamma$  is most abundant in fat cells, large intestine and cells of the monocyte lineage; PPAR $\delta$  is expressed in nearly all

tissues, with highest expression in skin, brain and adipose tissue (Braissant *et al.*, 1996). These differences in tissue distribution suggested that the different PPARs are not simply functionally interchangeable but likely to mediate distinct biological actions. Several studies have established an essential role for PPAR $\gamma$  in both adipocyte differentiation and function, while PPAR $\alpha$  is known to play an important role in fat catabolism in the liver. PPAR $\alpha$  ligands have been shown to induce expression of genes involved in fatty acid uptake and  $\beta$ -oxidation (Desvergne and Wahli, 1999). PPAR $\delta$  is less well characterized, but increasing evidence suggests it plays a role in the control of fatty acid oxidation adipose tissue and skeletal muscle with PPAR $\delta$  agonists improving plasma lipid profiles (Wang *et al.*, 2003; Evans *et al.*, 2004). In a very recent study Hummasti and Tontonoz used retroviral expression vectors to ectopically express each of the three PPAR isotypes in NIH-3T3 cells, measuring changes in gene expression in the presence of selective receptor agonists. The results of microarray analyses revealed many target genes common to all three receptors, but also unique targets for each receptor (Hummasti and Tontonoz, 2006). In the same study the investigators demonstrated that the differing biological activity of the PPARs not only results from their distinct expression patterns, but also stems from intrinsic differences localized to the N-terminal region of each receptor as demonstrated by analysis of chimeric constructs. For example, the amino-terminal domain of PPAR $\gamma$  confers the ability to promote adipogenesis on the DBD and LBD of PPAR $\delta$ , whereas the amino-terminal region of PPAR $\delta$  fused to the DBD and LBD of PPAR $\gamma$  mediates upregulation of fatty acid oxidation genes in differentiated adipocytes (Hummasti and Tontonoz, 2006).

### **1.3.2 PPAR $\gamma$ gene, mRNA and protein**

PPAR $\gamma$  is the most extensively studied of the three PPAR subtypes to date. The gene has been cloned from a number of species including salmon, mice, hamster, frogs, pigs, rhesus monkeys and human and shows a high level of conservation, which may reflect the pivotal role that this receptor plays in regulating glucose and lipid homeostasis which is an essential function in many species. The human PPAR $\gamma$  gene contains nine exons which extend over more than 100 kb of genomic DNA and has been mapped to chromosome 3p25 (Greene *et al.*, 1995). Four different receptor

isoforms have been identified as products of differential promoter usage. PPAR $\gamma$ 1, PPAR $\gamma$ 3 and PPAR $\gamma$ 4 mRNAs differ in their 5' untranslated regions but encode the same protein, whilst the PPAR $\gamma$ 2 mRNA generates a protein which contains an additional 28 amino acids at its amino-terminus (encoded by an additional exon B) (Figure 1.12). Analyses of the tissue distribution of receptor isoforms reveals some differences: PPAR $\gamma$ 1 is most widely expressed in adipose tissue, large and small intestine, haemopoietic cells, kidney, liver and skeletal muscle (Fajas *et al.*, 1997), whereas the PPAR $\gamma$ 2 and PPAR $\gamma$ 3 isoforms have a more restricted distribution. Thus, PPAR $\gamma$ 3 is found in adipose tissue, macrophages and colon and PPAR $\gamma$ 2 is expressed only in adipose tissue where it constitutes approximately 20% of the total PPAR $\gamma$  mRNA (Auboeuf *et al.*, 1997). PPAR $\gamma$ 4 has been described more recently and its tissue distribution is still to be defined (Sundvold and Lien, 2001). Moreover, the relative importance of these different receptor isoforms remains to be further elucidated.

### 1.3.3 Transcriptional activity of PPAR $\gamma$

PPAR $\gamma$ -mediated transactivation results from the binding of PPAR $\gamma$ :RXR heterodimers to a PPARE in the promoter region of target genes, and ligand activation of this complex. Binding of ligands to PPAR $\gamma$  causes a conformational change with exposure of new interfaces at the protein surface which mediate recruitment of transcriptional coactivators, including members of the p160/SRC family, the mediator complex via (also known as PBP, TRAP220, and DRIP205) and histone acetyltransferases CBP and p300 (McKenna and O'Malley, 2002). PGC-1 is another PPAR $\gamma$  coactivator, which plays an important role in metabolic regulation (Puigserver and Spiegelman, 2003). Interestingly, unlike most coactivators, which contain specific LXXLL peptide motifs mediating binding to the AF2 domain in the LBD of nuclear receptors, PGC-1 also binds PPAR $\gamma$  in a ligand-independent manner to a region that overlaps the DNA binding and hinge region (Puigserver *et al.*, 1998). Moreover it also plays critical roles in gene-specific transcriptional activation, being for example a potent coactivator on the uncoupling protein-1 gene, but not the aP2 gene. In the absence of ligand PPAR $\gamma$  can bind to corepressors (NCoR and SMRT), which repress target gene expression until ligand triggers their release and

recruitment of coactivators. Recently, Guan and colleagues have shown that corepressors control the transcriptional activity of PPAR $\gamma$  selectively on different target genes (Guan *et al.*, 2005). Thus, whilst many PPAR $\gamma$  genes are induced (e.g. aP2) during adipogenesis, others such as glycerol kinase (GyK) are expressed at low basal level and are dramatically up-regulated only following treatment with TZDs. Unlike the aP2 promoter, where PPAR $\gamma$  is constitutively associated with coactivators even in the absence of ligand, the receptor is bound to corepressors on the GyK promoter such that basal gene transcription is very low. Treatment of cells with ligand induces GyK expression by two different mechanisms: (i) corepressor release and coactivator recruitment as a consequence of receptor conformational change (ii) additional destabilization of corepressor binding to receptor as consequence of cellular upregulation of PGC-1, which specifically binds to PPAR $\gamma$  on the GyK promoter (Guan *et al.*, 2005).

In addition, post-transcriptional modification can also modulate the activity of both PPAR $\gamma$  isoforms. For example phosphorylation of serine 112 in the amino-terminal region of PPAR $\gamma$ 2 reduces its transcriptional activity (Adams *et al.*, 1997) and promotes receptor sumoylation at lysine 107, which further lowers its ability to act as transcriptional activator (Yamashita *et al.*, 2004).

Finally, there is also evidence to suggest that PPAR $\gamma$  may exert negative transcriptional regulatory effects when not bound directly to promoter DNA by interference with other transcriptional pathways (e.g. NF-kB, AP-1), and such transrepression (Pascual *et al.*, 2005) mechanisms have already been described earlier in section 1.1.3.5 of this introduction.

### **1.3.4 Natural and synthetic ligands of PPAR $\gamma$**

As part of the nuclear receptor family, PPAR $\gamma$  is a sensor of changes in levels of lipophilic ligands and responds by modifying gene transcription, but the precise nature of its endogenous ligand(s) remains to be defined. To date a variety of natural ligands have been reported including long-chain polyunsaturated fatty acids, arachidonic acid metabolites derived from the cyclooxygenase and lipoxygenase pathway (such as 15-deoxy  $\Delta^{12,14}$  prostaglandin J<sub>2</sub> [15d-PGJ<sub>2</sub>] and 15-hydroxyeicosatetraenoic [15-HETE]), fatty acid derived components of oxidized low



density lipoproteins (OxLDL) (e.g. 9-hydroxyoctadecadienoic acid [9-HODE] and 13-HODE) (Willson *et al.*, 2000). However, most of these ligands bind with lower affinity compared with the affinity of well-established ligands for other nuclear receptors. The cyclopentone prostaglandin 15d-PGJ<sub>2</sub> was suggested to be the most potent endogenous ligand for PPAR $\gamma$  and is commonly used as the prototype for naturally-occurring PPAR $\gamma$  agonists (Forman *et al.*, 1995). However, doubt as to whether this is a true PPAR $\gamma$  ligand *in vivo* was recently raised when it was shown to be produced at extremely low levels during adipocyte differentiation *in vitro* and when PPAR $\gamma$  activity is high in humans (Bell-Parikh *et al.*, 2003). Recently another higher-affinity, lipophilic, PPAR $\gamma$ -specific ligand has been shown to be generated endogenously in the early stages of murine 3T3-L1 preadipocytes differentiation (Tzamei *et al.*, 2004), but further investigation is required to define the exact nature of this molecule(s) and to determine its biological relevance. Overall, despite intensive research, whether PPAR $\gamma$  has a unique, highly affinity natural ligand or whether it operates as a physiological lipid sensor (activated by exposure to a variety of weakly activating fatty acids and eicosanoids) still remains to be answered. Several synthetic compounds have been recognized as high affinity PPAR $\gamma$  ligands. The anti-diabetic thiazolidinedione (TZD) class of drugs which includes troglitazone, rosiglitazone and pioglitazone has been shown to act via PPAR $\gamma$ , as have several more recently identified compounds e.g. tyrosine-based agonists. However, although these PPAR $\gamma$  “full agonists” improve insulin resistance, they paradoxically cause weight gain, through a combination of increased adipogenesis and enhanced fat storage, and possibly fluid retention. In an attempt to separate the beneficial effects (e.g. improvement in insulin sensitivity) from the less desirable side effects (e.g. increased adipogenesis) of TZDs, several biotechnology and pharmaceutical companies have sought to develop new classes of drugs with better therapeutic properties. The term “SPPARMs” has been coined to denote compounds which can selectively modulate PPAR $\gamma$  function, often by virtue of differentially regulating target genes, as consequence of differential binding of coregulators and dissociation of corepressors. An example of a selective PPAR $\gamma$  modulator or SPPARM is N-(9-fluorenylmethyloxycarbonyl) F-MOC-L-leucine, which selectively improves insulin sensitivity but without promoting weight gain in mice (Rocchi *et al.*, 2001). Interestingly, when activated by F-MOC-L-leucine, PPAR

recruits the coactivator SRC-1, whereas TZD agonists induce association of PPAR $\gamma$  with transcriptional intermediary factor 2 (TIF-2). Such differential cofactor recruitment could explain differential *in vivo* biological effects of these agents. TIF-2 is an important determinant of adipogenesis and can inhibit adaptive thermogenesis and lipid oxidation as demonstrated by the fact that mice lacking TIF-2 exhibit reduced weight gain despite increased caloric intake, hyperactive brown adipose tissue and increased adaptive thermogenesis (Picard *et al.*, 2002). Another partial agonist is MCC555 which also induces a different pattern of coactivator recruitment, with a diminished ability to recruit SRC-1 when compared to rosiglitazone (Reginato *et al.*, 1998). The discovery of such compounds has prompted widespread screening of libraries of both structurally-related and chemically distinct molecules with the subsequent identification of an array of potential SPPARMs: PAT5a, an unsaturated TZD with partial agonist activity, is a potent antidiabetic agent with only weak adipogenic activity (Misra *et al.*, 2003); similar properties have been reported for the novel non-TZD selective PPAR $\gamma$  modulators nTZDpa (Berger *et al.*, 2003) and KR-62980 (Kim *et al.*, 2006); a panel of N-benzyl-indole selective PPAR $\gamma$  modulators, with partial agonist activity *in vitro*, exhibited potent glucose-lowering activity in db/db mice, but attenuated increases in heart weight and brown adipose tissue when compared with full agonist (Liu *et al.*, 2005). Although the potential role of these new classes of drugs in the treatment of insulin resistance is promising, their molecular mechanism needs to be fully characterized.

Finally, it is also worth noting that several “herbal” antidiabetic remedies (such as *Punica granatum* flower (PGF), mulberry, Korean red ginseng and banaba) have been shown to enhance PPAR $\gamma$  activity (Huang *et al.*, 2005; Park *et al.*, 2005).

### **1.3.5 PPAR $\gamma$ and adipogenesis**

Adipose tissue is composed principally of adipocytes, which store energy in the form of triglyceride and release it as free fatty acids. Together with skeletal muscle, adipose tissue is the main regulator of energy balance in the body. Excessive accumulation of adipose tissue results in obesity whereas its absence is associated with lipodystrophic syndromes. There are several lines of evidence to indicate that PPAR $\gamma$  plays a crucial role in adipocyte formation and function (Tontonoz *et al.*,

1994; Hu *et al.*, 1995). During adipocyte differentiation, the expression of numerous genes involved in lipid storage and control of metabolism including adipocyte P2 (aP2) (Tontonoz *et al.*, 1994), acyl-CoA synthase (Schoonjans *et al.*, 1995), phosphoenol pyruvate carboxykinase (PEPCK) (Tontonoz *et al.*, 1995), fatty acid transporter (FATP-1) (Martin *et al.*, 1997) and lipoprotein lipase (LPL) (Schoonjans *et al.*, 1996) are regulated by PPAR $\gamma$ . Furthermore, adipose mass is reduced in PPAR $\gamma$  knock-out (KO) mice, with homozygous null animals being completely devoid of adipose tissue and heterozygous null mice exhibiting decreased adipose tissue mass (Kubota *et al.*, 1999; Miles *et al.*, 2000). In addition to PPAR $\gamma$ , other transcription factors such as the CCAAT enhancer binding proteins (C/EBPs), ADD-1/SREBP and several secreted factors also regulate the complex process of adipogenesis (Fajas *et al.*, 2001). However, recently Rosen and colleagues showed that rather than being an equal codirector of the adipocyte differentiation program, PPAR $\gamma$  plays a leading role in the adipogenic transcriptional hierarchy (Rosen *et al.*, 2002). In order to determine which receptor isoform (PPAR $\gamma$ 2 or PPAR $\gamma$ 1) is the master regulator of adipocyte differentiation, Ren and colleagues retrovirally expressed either PPAR $\gamma$ 1 or PPAR $\gamma$ 2 in receptor null preadipocytes. Despite a comparable expression level of both proteins, only PPAR $\gamma$ 2 was able to mediate adipogenesis, suggesting that it is the most important isoform in adipogenesis (Ren *et al.*, 2002). On the other hand using a similar experimental paradigm, another group obtained contrasting results, which suggested that the adipogenesis could be mediated by either PPAR $\gamma$ 1 or PPAR $\gamma$ 2 (Mueller *et al.*, 2002). However, they found that the pro-adipogenic activity of PPAR $\gamma$ 2 was greater than that of PPAR $\gamma$ 1. The notion that PPAR $\gamma$ 2 is the master regulator of adipocyte differentiation is also supported by the phenotype of partial lipodystrophy in mice with selective disruption of PPAR $\gamma$ 2 and by the failure of preadipocytes isolated from these mice to differentiate *in vitro* (Zhang *et al.*, 2004).

### **1.3.6 PPAR $\gamma$ , insulin resistance and diabetes**

Type 2 diabetes is characterized by resistance of peripheral tissues, including skeletal muscle, fat and liver to the action of insulin. The thiazolidinediones (TZDs) represent a novel class of anti-diabetic agents that are capable of lowering circulating

glucose levels without enhancing pancreatic insulin secretion. The discovery that TZDs are high affinity agonists for PPAR $\gamma$ , suggested a role for this receptor in controlling insulin sensitivity and prompted us to screen the human gene in a cohort of subjects with severe insulin resistance in collaboration with Professor Steve O’Rahilly (University of Cambridge), leading to the identification of two heterozygous missense mutations (P467L and V290M) in the ligand-binding domain of PPAR $\gamma$  (Barroso *et al.*, 1999). P467L and V290M were found in three subjects with extreme insulin resistance, type 2 diabetes and early-onset hypertension from two unrelated families. Functional characterization of these mutant receptors revealed that, in addition to being functionally impaired, when co-expressed with equal amounts of the wild type receptor, the mutants inhibited wild type PPAR $\gamma$  action in a dominant negative manner, consistent with heterozygosity for PPAR $\gamma$  mutations in affected subjects, and dominant inheritance of the disorder in one family (Barroso *et al.*, 1999). These data provided the first genetic evidence that PPAR $\gamma$  is critical for the control of tissue insulin sensitivity in humans. Following this two other groups have identified other loss-of-function mutations in the ligand-binding domain of human PPAR $\gamma$  (Agarwal and Garg, 2002; Hegele *et al.*, 2002). Together, these reports describe eight subjects with similar features, and have helped to define the clinical phenotype of the PPAR $\gamma$  ligand resistance syndrome (PLRS) (Gurnell *et al.*, 2003; Semple *et al.*, 2006). Virtually all affected patients were severely insulin resistant and exhibited a stereotyped form of partial lipodystrophy, with loss of subcutaneous fat from the limbs and gluteal region but relative preservation of both subcutaneous and visceral abdominal depots. The observation that two children with the P467L mutation were also hyperinsulinaemic, suggests that insulin resistance is a very early feature of this condition (Savage *et al.*, 2003), and adult consequences of this include polycystic ovarian syndrome (PCOS) and acanthosis nigricans. Additional features of PLRS include a propensity to develop early-onset diabetes, dyslipidaemia, fatty liver and hypertension.

Recently, an animal model equivalent to human P467L mutation (P465L) has been independently generated by two groups (Tsai *et al.*, 2004; Gray *et al.*, 2006). The heterozygous mice have normal total adipose tissue weight, but exhibit reduced intra-abdominal fat mass and increased extra-abdominal subcutaneous fat compared to wild type animals, i.e. altered body fat distribution, but in a manner which is

different from that observed in human subjects. Surprisingly, unlike their human counterparts, the mice were also insulin sensitive. Interestingly, hypertension was the only phenotypic abnormality observed in P465L mice which was in common with human P467L subjects. These findings initially raised concerns about the validity of rodent models in exploring the consequences of loss-of-function mutation in human PPAR $\gamma$ . However, Gray and colleagues have generated P465L mutant mice on a hyperphagic, leptin deficient (*ob/ob*) backgrounds and this grossly exacerbated the insulin resistance and metabolic disturbances associated with leptin deficiency, despite a reduction in excess whole body fat mass and adipocyte abnormalities (Gray *et al.*, 2006), recapitulating the clinical phenotype observed in human subjects.

Following the identification of these earlier mutations in the ligand-binding domain of PPAR $\gamma$ , we have described a different, digenic mechanism of insulin resistance in an unrelated kindred with a combination of heterozygous, loss-of-function mutations in *PPARG* and *PPP1R3* (muscle-specific protein-phosphatase 1 regulatory subunit, involved in glycogen synthesis) (Savage *et al.*, 2002; Chapter 5). Recently, other PPAR $\gamma$  mutations have been identified in patients with similar clinical features and they will be discussed in more detail in Chapters 6 of this thesis (Agostini *et al.*, 2006; Al-Shali *et al.*, 2004; Gordon *et al.*, 2006; Francis *et al.*, 2006; Hegele *et al.*, 2006).

In addition to these mutations, a different type of genetic defect which may affect the function of PPAR $\gamma$  in adipogenesis has been described. A Proline to Glutamine substitution at codon 115 (P115Q) has been described in four markedly obese subjects (Ristow *et al.*, 1998). This heterozygous mutation, which disrupts mitogen-activated protein kinase-dependent phosphorylation of the receptor at an adjacent residue (serine 112) (Adams *et al.*, 1997), results in a constitutively active receptor which enhances adipocyte differentiation thus promoting obesity. Recently, a mutant mouse model in which PPAR $\gamma$  phosphorylation is abolished analogous to the human mutation has been described. Interestingly, in contrast to the human subjects harbouring the P115Q mutation, these mice were not obese, but were protected against insulin resistance in the context of diet-induced obesity (Rangwala *et al.*, 2003).

In population studies, a much more common PPAR $\gamma$  genetic variant is a polymorphism replacing Proline with Alanine at codon 12 (Pro12Ala) in the amino-terminal domain of PPAR $\gamma$ 2, with an allelic frequency ranging between 2% and 23% in different ethnic groups (Deeb *et al.*, 1998; Masugi *et al.*, 2000). This amino acid variant has been associated with increased protection against the development of type 2 diabetes and insulin resistance (Deeb *et al.*, 1998; Altshuler *et al.*, 2000) and, more recently, a decreased incidence of cardiac disease (Ridker *et al.*, 2003). However, its effect on body mass index (BMI) remains unclear, being variably associated with either increased (Beamer *et al.*, 1998) or decreased weight (Deeb *et al.*, 1998). A further paradox is that heterozygous PPAR $\gamma$  null mice are protected from developing insulin resistance relative to wild type controls when they are challenged with a high fat diet and develop normally otherwise, with no apparent metabolic defect (Kubota *et al.*, 1999; Miles *et al.*, 2000). Despite the knowledge that TZDs act via PPAR $\gamma$  and that natural human PPAR $\gamma$  mutations are associated with severe insulin resistance, the mechanisms by which PPAR $\gamma$  controls insulin action *in vivo* remain unclear and the target tissue(s) where TZDs act remain to be defined. One line of evidence favours receptor action in adipose tissue, where PPAR $\gamma$  is predominantly expressed. In keeping with this, mice lacking adipose tissue have been shown to be refractory to the antidiabetic effects of TZDs (Chao *et al.*, 2000). PPAR $\gamma$  activation in adipocytes increases levels of GLUT4, the insulin-stimulated glucose transporter (Young *et al.*, 1995; Wu *et al.*, 1998) and may have direct effects on other genes important for glucose homeostasis. To explain the insulin-sensitizing effects of TZDs it has also been hypothesised that PPAR $\gamma$  activation in adipose tissue exerts whole body effects on free fatty acid (FFA) flux, promoting their uptake/trapping in fat rather than in muscle and liver, where such excess fatty acid delivery is believed to cause insulin resistance via a “lipotoxic” mechanism and simultaneously decreasing FFA release by lipolysis from adipose tissue, thus enhancing insulin sensitivity by a reduction in circulating FFA. This has become known as the “lipid steal” hypothesis and has recently been supported by observations made in rodents (Ye *et al.*, 2004). Consistent with this, PPAR $\gamma$  ligands enhance the expression level of several genes involved in hydrolysis of plasma TGs (lipoprotein lipase, LPL) (Desvergne and Wahli, 1999), fatty acid uptake and esterification (fatty acid translocase, CD36; fatty acid transport protein, FATP;

acylCoA synthase, ACS) (Desvergne and Wahli, 1999), lipogenesis and TG synthesis (phosphoenolpyruvate carboxykinase, PEPCK; glycerol kinase, GyK) (Tontonoz *et al.*, 1995; Guan *et al.*, 2002) (Figure 1.13). TZDs also induce changes in adipose tissue morphology and typically higher number of smaller adipocytes are seen in TZD-treated rodents (Okuno *et al.*, 1998). In addition there is now a general consensus that adipose tissue should not be simply considered a reservoir for energy storage but also as a true endocrine organ, which secretes a diverse series of hormones, collectively referred to as adipokines (Ahima and Flier, 2000). These adipokines (e.g. leptin, adiponectin, tumour necrosis factor- $\alpha$  [TNF $\alpha$ ], interleukin-6 [IL-6], resistin) are capable of exerting profound effects on whole-body insulin sensitivity, allowing a cross talk between adipose tissue, skeletal muscle and liver in the regulation of glucose homeostasis. Leptin, which is the best established of these adipokines, is positively correlated to adipose tissue mass and acts as suppressor of appetite in humans (Farooqi *et al.*, 1999). Leptin administration to lipodystrophic, leptin-deficient humans markedly improves insulin sensitivity (Oral *et al.*, 2002). Moreover transplantation of normal, but not leptin-deficient white adipose tissue (WAT) into totally lipodystrophic mice also improves insulin sensitivity (Colombo *et al.*, 2002) suggesting that this hormone may have some direct role in regulating insulin action. Adiponectin is one of the most abundant plasma proteins in humans whose levels (in contrast to leptin) are inversely related to the total WAT mass. TZDs increase adiponectin gene expression, suggesting that this adipokine may represent a critical link between PPAR $\gamma$  activation and insulin sensitization (Maeda *et al.*, 2001). In keeping with this, circulating levels of adiponectin in three individuals harbouring loss of function mutations in PPAR $\gamma$  were markedly lower than in normal controls or severely insulin resistant subjects with normal PPAR $\gamma$  (Combs *et al.*, 2002). Recently, these observations were confirmed in five additional patients with PPAR $\gamma$  mutations, but direct evidence for insulin sensitization by adiponectin is still awaited (Semple *et al.*, 2006). Resistin, a small secreted protein, enhances systemic insulin resistance and there is evidence that TZDs inhibit production of this factor (Steppan *et al.*, 2001) but in humans this peptide may be mainly monocyte-derived rather than secreted from adipose tissue as in the rodent. PPAR $\gamma$  agonists also reduce the expression of 11 $\beta$ -hydroxysteroid dehydrogenase type 1 (11 $\beta$ -HSD1), which mediates the production of active cortisol

from inactive cortisone in liver and fat, thus facilitating cortisol-induced adipocyte differentiation (Berger *et al.*, 2001). Alternatively, PPAR $\gamma$  may act directly on skeletal muscle, where it is also expressed, albeit at much lower levels than in adipocytes. TZDs enhance PPAR $\gamma$  expression in muscle (Park *et al.*, 1998) and their action *in vivo* includes promote glucose uptake into human skeletal muscle (Inzucchi *et al.*, 1998). In addition TZD have also been shown to decrease blood glucose and improve insulin sensitivity in transgenic mice lacking adipose tissue (Burant *et al.*, 1997). However two different studies of mice with muscle-specific PPAR $\gamma$  deletion showed discordant effects on insulin sensitivity. One study reported modest whole-body insulin resistance and normal glucose disposal into muscle (Norris *et al.*, 2003), whilst the second reported progressive and severe insulin resistance as consequence of markedly impaired muscle glucose uptake in response to insulin (Hevener *et al.*, 2003), and these differences may reflect the age or genetic background of animals studied.

### **1.3.7 Other diverse roles of PPAR $\gamma$**

It is now recognized that PPAR $\gamma$  may play an important role in diverse biological processes. As already described PPAR $\gamma$  plays an important role in adipocyte differentiation and lipid metabolism; the receptor also has a role in macrophage function and in neoplasia (Lehrke and Lazar, 2005; Savage, 2005; Semple *et al.*, 2006).

Initially, PPAR $\gamma$  was reported to induce expression of CD36, a cellular scavenger receptor for atherogenic LDL and therefore increase lipid uptake and storage, and ultimately drive conversion of the macrophage into an atherogenic foam cell (Tontonoz *et al.*, 1997). In keeping with this it was found to be expressed at a relatively high level in human atherosclerotic plaque macrophages in addition to being expressed in blood monocytes and induced during macrophage differentiation (Ricote *et al.*, 1998). However, despite these observations however, TZD treatment has been shown to be vasoprotective and capable of reducing atherosclerosis in mouse models, through activation of lipid efflux pathways in macrophages that prevent lipid accumulation (Chawla *et al.*, 2001; Chinetti *et al.*, 2001). Moreover PPAR $\gamma$  has also been shown to have anti-inflammatory action in macrophages where



receptor activation inhibits the production of pro-inflammatory cytokines such as IL-6 and TNF- $\alpha$  (Ricote *et al.*, 1998). Evidence that PPAR $\gamma$  may play a role in the control of blood pressure is provided by the observation that patients with dominant negative mutations in PPAR $\gamma$  exhibit severe early-onset hypertension (Barroso *et al.*, 1999) and that mice with the homologous P465L mutation, are significantly hypertensive despite normal insulin sensitivity, suggesting that hypertension is not a consequence of insulin resistance (Tsai *et al.*, 2004). In addition, TZDs treatment lowers blood pressure in diabetic patients (Ogihara *et al.*, 1995) and in a range of animal models of hypertension (Pershadsingh *et al.*, 1993; Walker *et al.*, 1999). Since PPAR $\gamma$  is expressed in vascular endothelial cells (Libby *et al.*, 1999; Iijima *et al.*, 1998), receptor agonists may exert their effects by regulating the production of factors which control vascular tone, promoting release of the vasodilator C-type natriuretic peptide (Doi *et al.*, 1998) or inhibiting release of the vasoconstrictor endothelin (Satoh *et al.*, 1999). Likewise it has been reported that PPAR $\gamma$  agonists block calcium channel activity in vascular smooth muscle cells (Nakamura *et al.*, 1998).

The interest in studying the effects of PPAR $\gamma$  on neoplastic processes originated from the observation that TZDs promote cell cycle arrest in logarithmically growing NIH-3T3 fibroblasts and in malignantly transformed adipogenic HIB-1B cells (Altiok *et al.*, 1997). Subsequently it was shown that activation of PPAR $\gamma$  by pioglitazone blocked the cell cycle and caused differentiation of human liposarcoma cells (Tontonoz *et al.*, 1997) and troglitazone has been successfully used to induce adipogenesis in cases of advanced liposarcoma in man (Demetri *et al.*, 1999). In addition, TZDs have been shown to arrest cell growth and to reduce secretion of the tumor marker prostate-specific antigen (PSA) from cultured prostate cell lines, and an encouraging response to TZD treatment has been observed in metastatic prostate cancer (Mueller *et al.*, 2000). Moreover, PPAR $\gamma$  expression has been demonstrated in human breast and colon tumours and in corresponding cell lines and studies in these cellular contexts have shown a significant antiproliferative effect of PPAR $\gamma$  agonists (Elstner *et al.*, 1998; Sarraf *et al.*, 1998). However, contrary to these results, a recent study showed that enhanced PPAR $\gamma$  signalling in mice constitutively expressing high levels PPAR $\gamma$  in their breast tissue exacerbates mammary gland tumor development of breast cancer (Saez *et al.*, 2004). In addition, somatic, loss-of-

function mutations in PPAR $\gamma$  have been described in human colon cancer tumours (Sarraf *et al.*, 1999); contradictory observations show an increase in polyp size and frequency in a mouse model of colonic cancer following treatment with PPAR $\gamma$  agonists (Lefebvre *et al.*, 1998; Saez *et al.*, 1998). These findings indicate that further studies are needed to elucidate the role of PPAR $\gamma$  in the pathophysiology of cancer. Finally, a somatic chromosomal translocation involving the *PAX8* and *PPARG* genes has been documented in approximately 20% of human follicular thyroid carcinoma, resulting in the expression of a chimaeric fusion protein consisting of Pax-8 lacking its C-terminal activation domain linked to full length PPAR $\gamma$ 1. This chimaeric protein exerts a dominant negative inhibitory effect on the transcriptional activity of wild type PPAR $\gamma$  (Kroll *et al.*, 2000). The exact molecular mechanism of action of the PAX8-PPAR $\gamma$  oncogene in thyroid cells remains to be elucidated.

Names	Abbreviation	Nomenclature	Ligand
Thyroid hormone receptor	TR $\alpha$	NR1A1	Thyroid hormone (T3)
	TR $\beta$	NR1A2	Thyroid hormone (T3)
Retinoic acid receptor	RAR $\alpha$	NR1B1	Retinoic acid
	RAR $\beta$	NR1B2	Retinoic acid
	RAR $\gamma$	NR1B3	Retinoic acid
Peroxisome proliferator activated receptor	PPAR $\alpha$	NR1C1	Fatty acids, Leukotriene B4, Fibrates
	PPAR $\beta$	NR1C2	Fatty acids
	PPAR $\gamma$	NR1C3	Fatty acids, TZDs, prostaglandin J <sub>2</sub>
Rev ErbA	RevErb $\alpha$	NR1D1	Unknown
	RevErb $\beta$	NR1D2	Unknown
Retinoic Acid-related orphan receptor	ROR $\alpha$	NR1F1	Cholesterol, cholesteryl sulphate
	ROR $\beta$	NR1F2	Retinoic acid
	ROR $\gamma$	NR1F3	Unknown
Liver X receptor	LXR $\alpha$	NR1H3	Oxysterols, T0901317, GW3965
	LXR $\beta$	NR1H2	Oxysterols, T0901317, GW3965
Farnesoid X receptor	FXR $\alpha$	NR1H4	Bile acids, Fexaramine
	FXR $\beta$ *	NR1H5	Lanosterol
Vitamin D receptor	VDR	NR1I1	1-25(OH) <sub>2</sub> vitamin D3, lithocholic ac
Pregnane X receptor	PXR	NR1I2	Xenobiotics, PCN, hyperforin
Constitutive androstane Receptor	CAR	NR1I3	Xenobiotics, phenobarbital
Human nuclear factor 4	HNF-4 $\alpha$	NR2A1	Unknown
	HNF-4 $\beta$	NR2A2	Unknown
Retinoid X receptor	RXR $\alpha$	NR2B1	9- <i>cis</i> -Retinoic acid
	RXR $\beta$	NR2B2	9- <i>cis</i> -Retinoic acid
	RXR $\gamma$	NR2B3	9- <i>cis</i> -Retinoic acid
Testis receptor	TR2	NR2C1	Unknown
	TR4	NR2C2	Unknown
Tailless	TLL	NR2E2	Unknown
Photoreceptor-specific Nuclear receptor	PNR	NR2E3	Unknown
Chicken ovalbumin upstream promoter Transcription factor	COUP-TFI	NR2F1	Unknown
	COUP-TFII	NR2F2	Unknown
ErbA2-related gene-2	EAR2	NR2F6	Unknown
Estrogen receptor	ER $\alpha$	NR3A1	Estradiol-17b, tamoxifen, raloxifene
	ER $\beta$	NR3A2	Estradiol-17b, various synthetic compounds
Estrogen-related receptor	ERR $\alpha$	NR3B1	Unknown
	ERR $\beta$	NR3B2	DES, 4-OH tamoxifen
	ERR $\gamma$	NR3B3	DES, 4-OH tamoxifen
Glucocorticoid receptor	GR	NR3C1	Cortisol, dexamethasone, RU486
Mineralcorticoid receptor	MR	NR3C2	Aldosterone, spironolactone
Progesterone receptor	PR	NR3C3	Progesterone, medroxyprogesterone Acetate, RU486
Androgen receptor	AR	NR3C4	Testosterone, flutamide
NGF-induced factor B	NGFI-B	NR4A1	Unknown
Nur related factor 1	NURR1	NR4A2	Unknown
Neuron-derived orphan receptor 1	NOR1	NR4A3	Unknown
Steroidogenic factor 1	SF1	NR5A1	Oxysterols
Liver receptor homologous protein 1	LRH1	NR5A2	Oxysterols
Germ cell nuclear factor	GCNF	NR6A1	Unknown
DSS-ACH critical region on the Chromosome, gene 1	DAX-1	NROB1	Unknown
Short heterodimeric partner	SHP	NROB2	Unknown

**Table 1.1** Human nuclear receptors (adapted from Germain *et al.*, 2006). \*FXR $\beta$  is a pseudogene in humans and does not encode a functional receptor. TZDs, thiazolidinediones; DES, diethylstilbestrol; DSS-ACH, dosage-sensitive sex reversal-adrenal hypoplasia congenital; NGF, nerve growth factor 1; PCN, pregnenolone 16 $\alpha$ -carbonitrile.

<i>NUCLEAR RECEPTORS</i>	<i>ASSOCIATED DISEASES</i>
Androgen Receptor (AR)	Androgen Resistance, Kennedy's Syndrome, Prostate cancer
DAX1	Adrenal hypoplasia congenita
Estrogen Receptor (ER)	Breast cancer, osteoporosis Alzheimer's disease
Nuclear Receptor related-1 (NURR1)	Parkinson's disease
Photoreceptor-specific Nuclear Receptor (PNR)	Enhanced S cone syndrome
Peroxisome Proliferator Activated Receptor (PPAR $\gamma$ )	Type 2 diabetes, obesity, atherosclerosis, cancer
RAR, RXR	APML, acne, psoriasis, hepatocarcinoma, melanoma
Steroidogenic factor 1	Gonadal and adrenal dysgenesis
Thyroid Hormone Receptor (TR $\beta$ )	Resistance to thyroid hormone
Vitamin D Receptor (VDR)	Vitamin D resistant Rickets
HNF4 $\alpha$	MODY (Maturity-onset diabetes of the young)

**Table 1.2** Examples of diseases associated with altered nuclear receptor function.

APML, acute promyelocytic leukaemia.

---

Elevated serum free thyroid hormones
Normal TSH with enhanced bioactivity
Goitre
Growth retardation, short stature
Low body mass index in childhood
Attention-deficit hyperactivity disorder, low IQ
Tachycardia, atrial fibrillation, heart failure
Hearing loss
Ear, nose, and throat infections
Osteopenia

---

**Table 1.3** Recognized Clinical Features of RTH

	<b>Endocrine Receptors</b>	<b>Adopted Orphan Receptors</b>	<b>Orphan Receptors</b>
<b>Ligands:</b>	High-affinity Hormones	Low-affinity dietary or other lipids	Unknown
	ER $\alpha, \beta$ PR AR GR MR  RAR $\alpha, \beta, \gamma$ TR $\alpha, \beta$ VDR EcR	RXR $\alpha, \beta$ PPAR $\alpha, \beta, \gamma$ LXR $\alpha, \beta$ FXR PXR/SXR CAR	SF-1 LRH-1 DAX-1 SHP TLX PNR NGFI-B $\alpha, \beta, \gamma$ ROR $\alpha, \beta, \gamma$ ERR $\alpha, \beta, \gamma$ RVR $\alpha, \beta, \gamma$ GCNF TR 2,4 HNF-4 COUP-TF $\alpha, \beta, \gamma$

**Figure 1.1** Nuclear receptor superfamily. Nuclear receptors are grouped according to the source and type of their ligand. All 48 human receptors and the insect ecdysone receptor (EcR), which is the only non vertebrate nuclear receptor with a known ligand, are shown. Figure adapted from Chawla *et al.*, 2001.

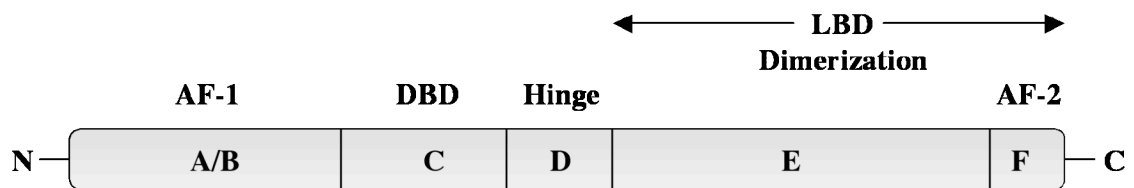


**Figure 1.2** Schematic representation of a nuclear receptor. The variably sized N-terminal region (A/B) in many receptors contains a ligand-independent transcription activation function (AF-1). The conserved DNA-binding domain (DBD), or region C, mediates recognition of specific regulatory DNA sequences usually located in target gene promoters. Domain D, a flexible hinge region, connects the DBD to the E/F region which contains the ligand binding domain (LBD) as well as a dimerization interface and a ligand-dependent transactivation function (AF-2), that localizes to the extreme C-terminal portion of the LBD.

**Figure 1.3** DNA binding by nuclear receptors **a.** Nuclear receptors can bind DNA as monomers, homodimers and heterodimers with RXR to specific binding sites (response elements) composed of one or two half-core motifs (generally AGGTCA) represented by the arrow, which can be arranged as inverted, everted or direct repeats. N denotes any nucleotide and variable number of these (N) constitute a “spacer” found in some response elements. **b.** Schematic representation of the DNA-binding domain of the thyroid hormone receptor. Key amino acids within this domain include two groups of cysteine residues which each coordinate a single zinc atom to form two ‘zinc-finger’ DNA binding motifs. Residues within the P box aid in the discrimination of the response element, whilst those in the D box contribute to the formation of a dimerisation interface. A sequence (underlined) within the C-terminal extension of the DBD mediates nuclear localisation.

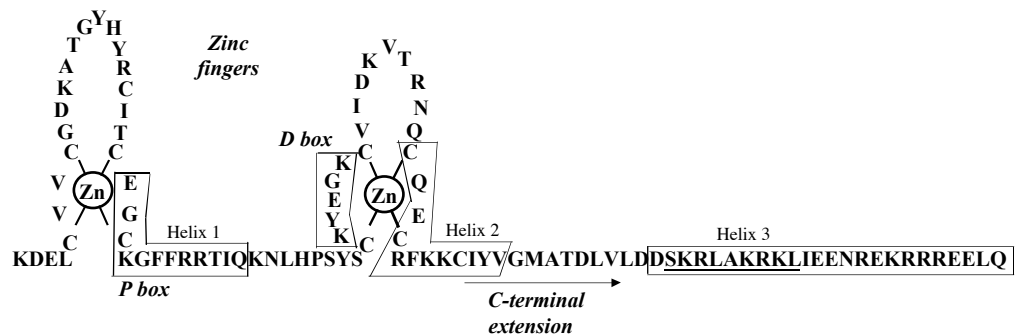


a.



Response element	Schematic sequence	NR mode of binding	Examples
Single half- site		Monomer	RevErb NGF-IB
Palindromic repeat:			
-Inverted repeat	(N) <sub>n</sub>	<div style="display: flex; align-items: center;"> <div style="font-size: 3em; margin-right: 10px;">{</div> <div style="margin-right: 10px;">Homodimer</div> <div style="margin-right: 10px;">TR (n=0)</div> </div> <div style="margin-top: 10px;"> <div style="font-size: 3em; margin-right: 10px;">{</div> <div style="margin-right: 10px;">Heterodimer</div> <div style="margin-right: 10px;">RXR-RAR (n=0)</div> </div>	
-Everted repeat	(N) <sub>n</sub>	<div style="display: flex; align-items: center;"> <div style="font-size: 3em; margin-right: 10px;">{</div> <div style="margin-right: 10px;">Homodimer</div> <div style="margin-right: 10px;">TR (n=6)</div> </div> <div style="margin-top: 10px;"> <div style="font-size: 3em; margin-right: 10px;">{</div> <div style="margin-right: 10px;">Heterodimer</div> <div style="margin-right: 10px;">RXR-TR (n=6)</div> <div style="margin-right: 10px;">RXR-RAR (n=8)</div> <div style="margin-right: 10px;">RXR-VDR (n=9)</div> </div>	
-Direct repeat	(N) <sub>n</sub>	<div style="display: flex; align-items: center;"> <div style="font-size: 3em; margin-right: 10px;">{</div> <div style="margin-right: 10px;">Homodimer</div> <div style="margin-right: 10px;">RXR (n=1)</div> </div> <div style="margin-top: 10px;"> <div style="font-size: 3em; margin-right: 10px;">{</div> <div style="margin-right: 10px;">Heterodimer</div> <div style="margin-right: 10px;">PPAR-RXR (n=1)</div> <div style="margin-right: 10px;">RXR-RAR (n=1, 2 or 5)</div> <div style="margin-right: 10px;">RXR-VDR (n=3)</div> <div style="margin-right: 10px;">RXR-TR (n=4)</div> </div>	

b.



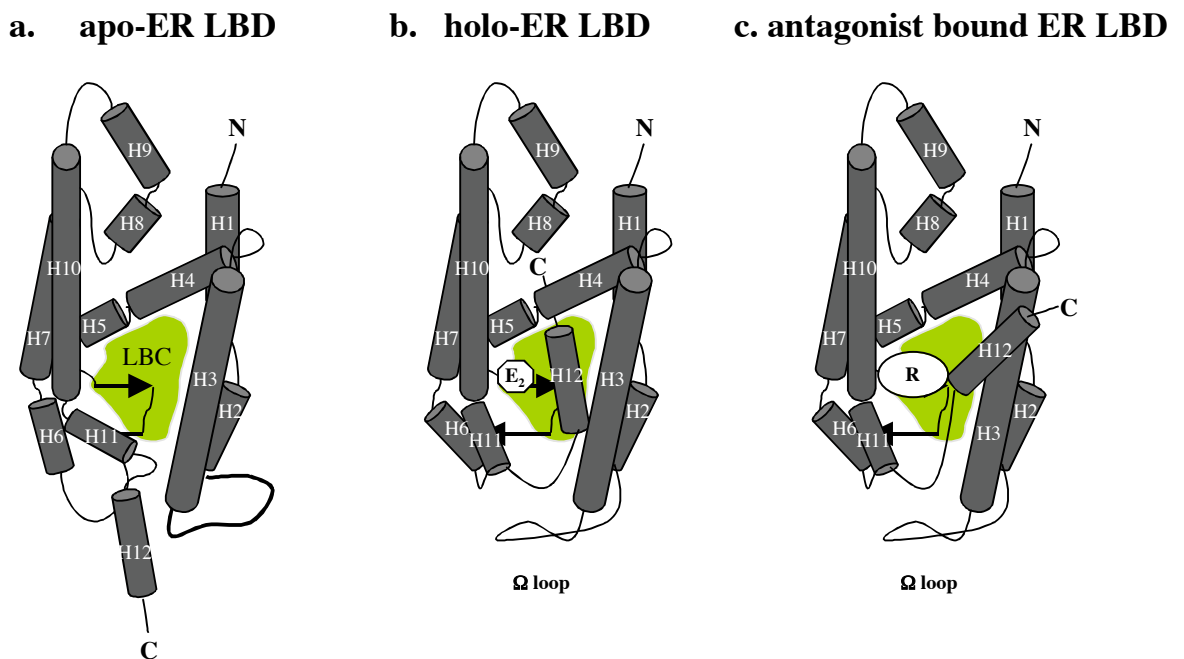


**Figure 1.4** Schematic representations of three distinct conformational states adopted by the ligand-binding domain (LBD) of the estrogen receptor (ER). 12  $\alpha$ -helices (H1-12 - shown as cylinders) and a single  $\beta$ -turn (shown by the arrow) form a triple layered structure enclosing a hydrophobic ligand-binding cavity (LBC). **a.** apo-ER modelled on the apo-RXR $\alpha$  structure. **b.** holo-ER demonstrating realignment of H11, H12 and the  $\Omega$  loop between H2 and H3 upon binding of oestradiol ( $E_2$ ). **c.** Raloxifene (antagonist - R) binding induces an alternate receptor conformation from that seen in the holo-receptor such that H12 no longer reconstitutes the coactivator binding cleft with helices 3 and 4. Adapted from Moras and Gronemeyer, 1998.

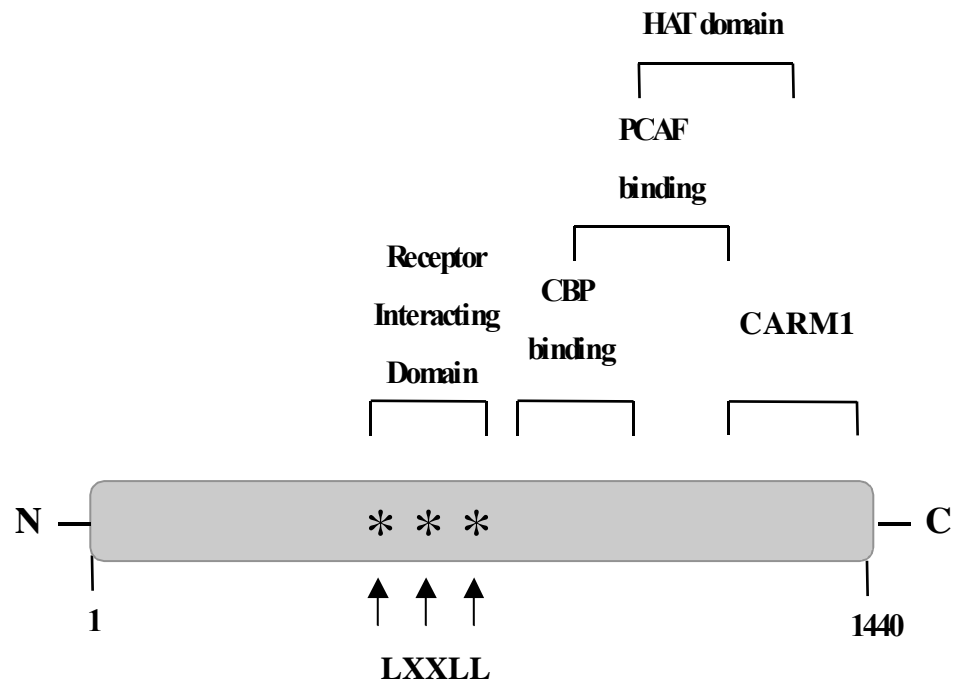
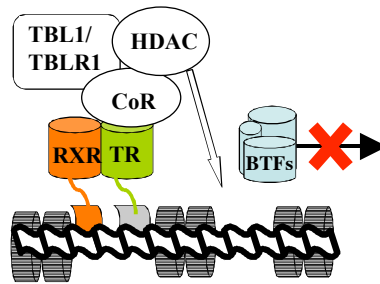


**Figure 1.5** Schematic representation of the domain structure of steroid receptor coactivator 1 (SRC-1), a member of the p160 family of coactivators. The receptor interaction domain contains three LXXLL motifs each denoted by an asterisk. The brackets denote functional regions mediating histone acetyltransferase (HAT) activity and interaction with CBP, PCAF and the arginine methyltransferase CARM1.

## -T3 Basal Repression



## + T3 Transcriptional Activation

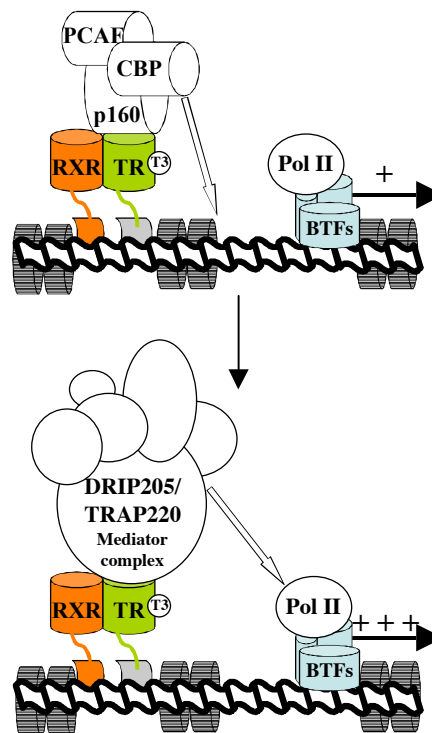


**Figure 1.6** Schematic representation of transcriptional regulation by TR. In the absence of ligand, TR recruits a protein complex consisting of corepressors (e.g. NcoR or SMART) which function as a platform for the further binding of exchange factors (TBL1/TBLR1) and histone deacetylase (HDAC) protein, which remodels chromatin into a condensed conformation, rendering the DNA promoter less accessible to the basal transcription factors machinery (BTFs). Binding of T<sub>3</sub> facilitates dissociation of the corepressor complex and recruitment of a protein complex (e.g. SRC-1, PCAF and CBP) with histone acetylase activity (HAT) which transforms chromatin into an open conformation. Exchange of the HAT complex for a DRIP/TRAP mediator complex, leads to interaction with the basal transcriptional machinery including RNA polymerase II (Pol II), increasing gene transcription.

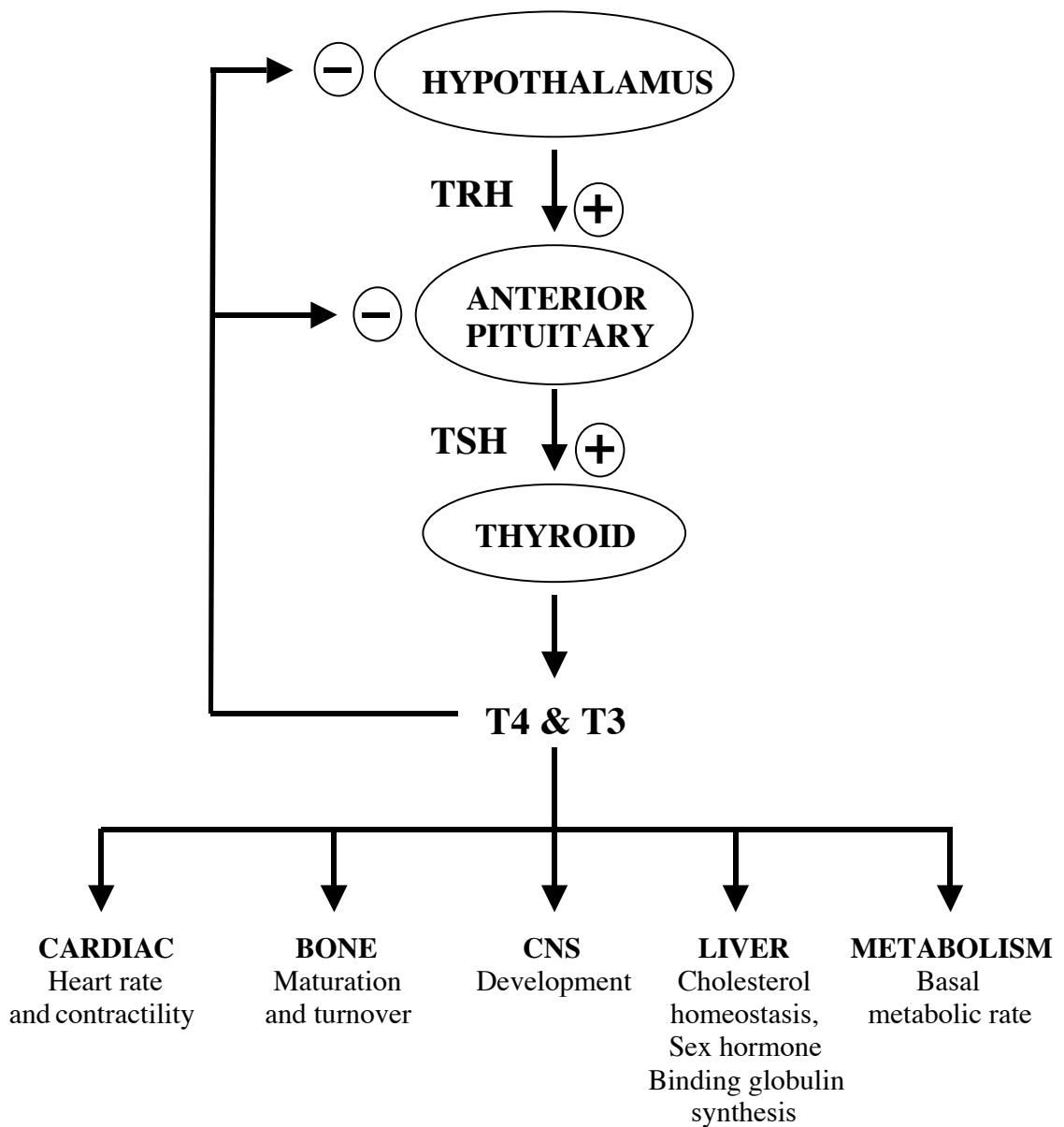


**Figure 1.7** The hypothalamic-pituitary-thyroid axis. TRH promotes release of TSH which in turn induces the secretion of T3 and T4. Negative feedback regulation by T3/T4 exerts control at both hypothalamic and pituitary levels. Some of the effects of thyroid hormones on peripheral target tissues are shown.

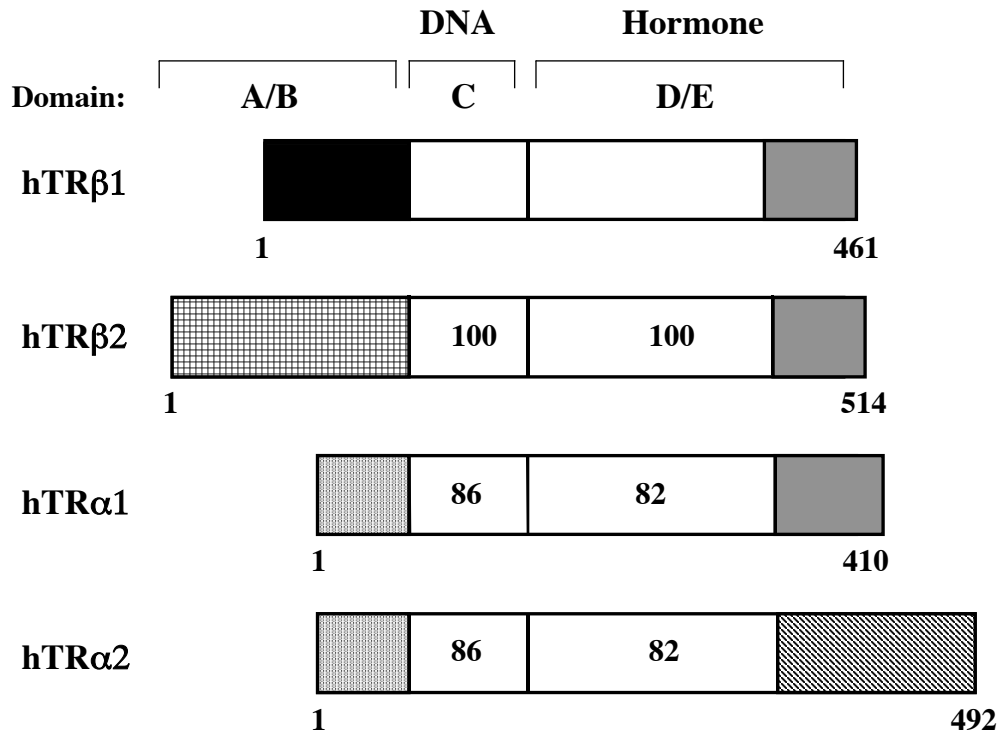


**Figure 1.8** Schematic comparison of amino acid homologies among human TR isoforms. The length of receptors is indicated and the percent amino acid homology with TRβ1 is included in the receptor diagrams.



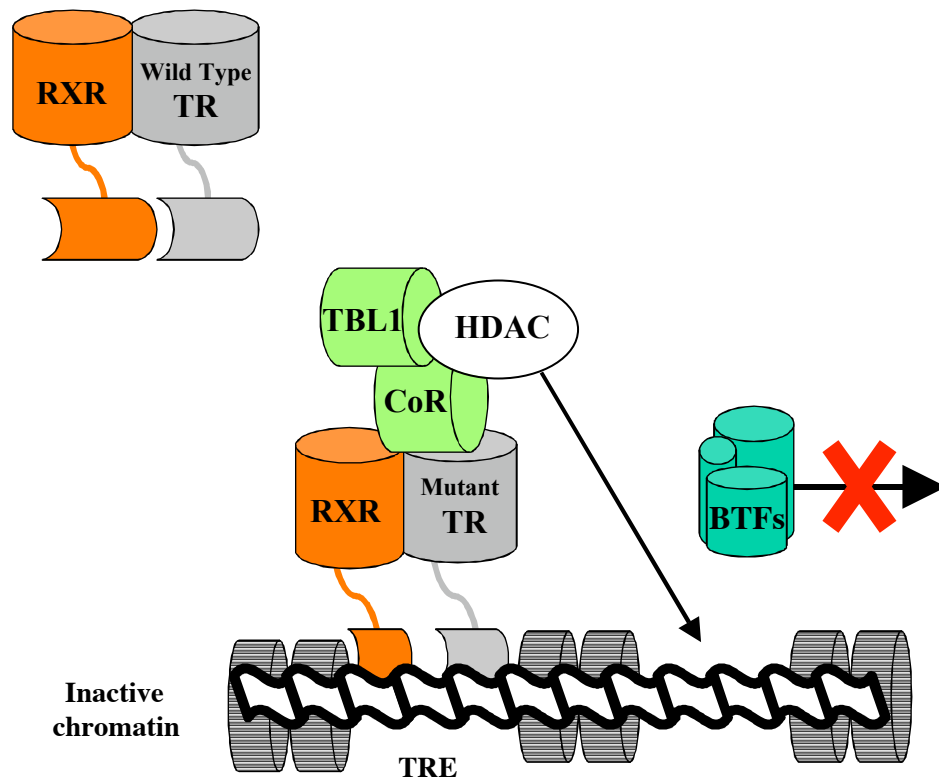


**Figure 1.10** Schematic model of dominant negative inhibition by TR $\beta$  mutants in RTH. Mutant TR-RXR heterodimers compete with their wild type counterparts at binding sites (TREs) within target gene promoters, with failure to release the corepressor complex leading to transcriptional silencing. BTFs, basal transcription factors.



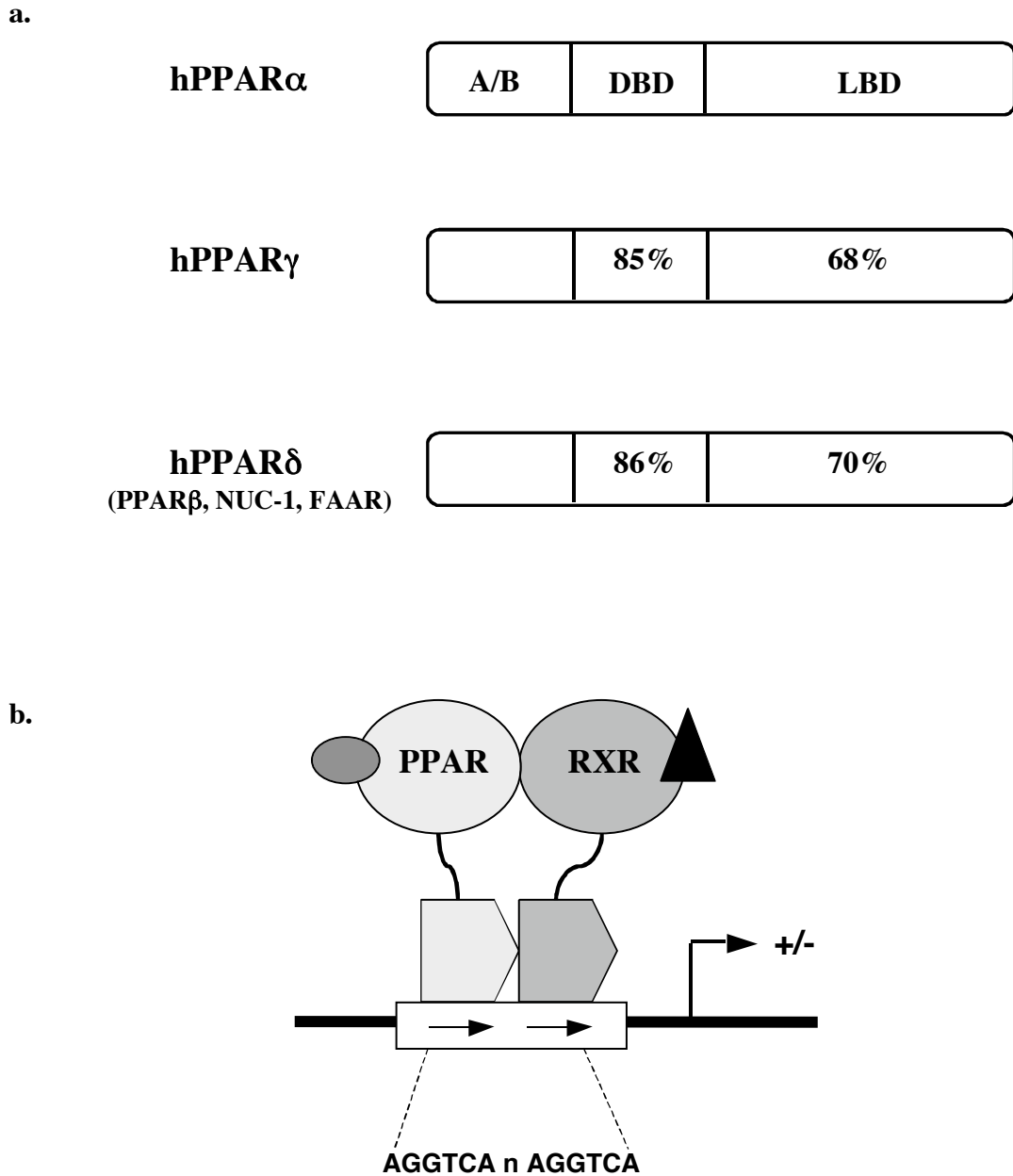


**Figure 1.11 a.** Comparison of the human PPARs. The A/B, DNA binding (DBD) and ligand-binding (LBD) domains are indicated. Numbers represent percent amino acid identity with PPAR $\alpha$ . **b.** The PPARs bind as a heterodimer with RXR to specific tandem repeat regulatory DNA sequences separated by one nucleotide (DR-1 response element). The PPAR/RXR heterodimer can be synergistically activated by ligands for PPAR and RXR.

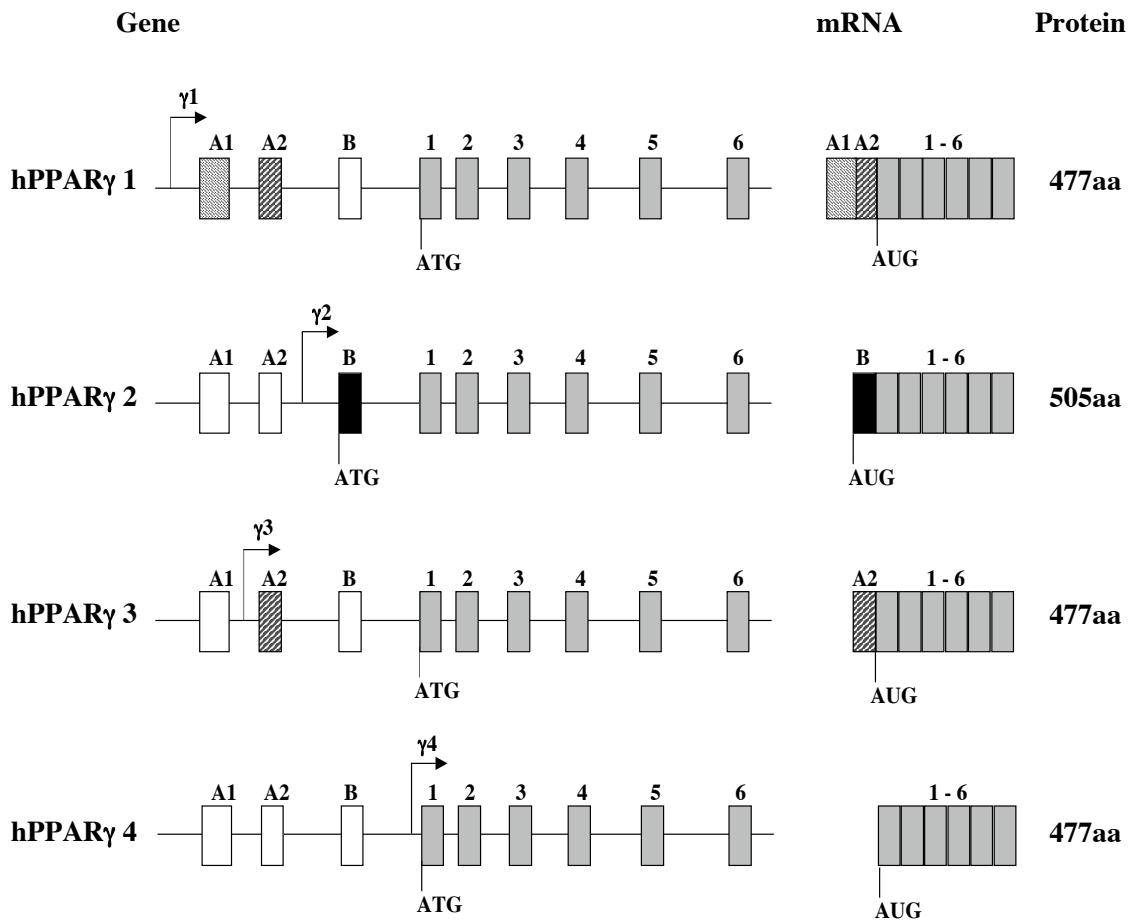


**Figure 1.12** Human PPAR $\gamma$  isoforms. The organization of the hPPAR $\gamma$  gene and the four mRNAs that differ at their 5'-end as a consequence of differential promoter usage and alternative splicing are shown. Exons 1-6 are common to all three transcripts, exon B encodes an unique amino-terminal region (28 amino acids) that is specific to the PPAR $\gamma$ 2 isoform and A1 and A2 encode differing 5'-untranslated regions. The length of predicted protein products is also indicated.

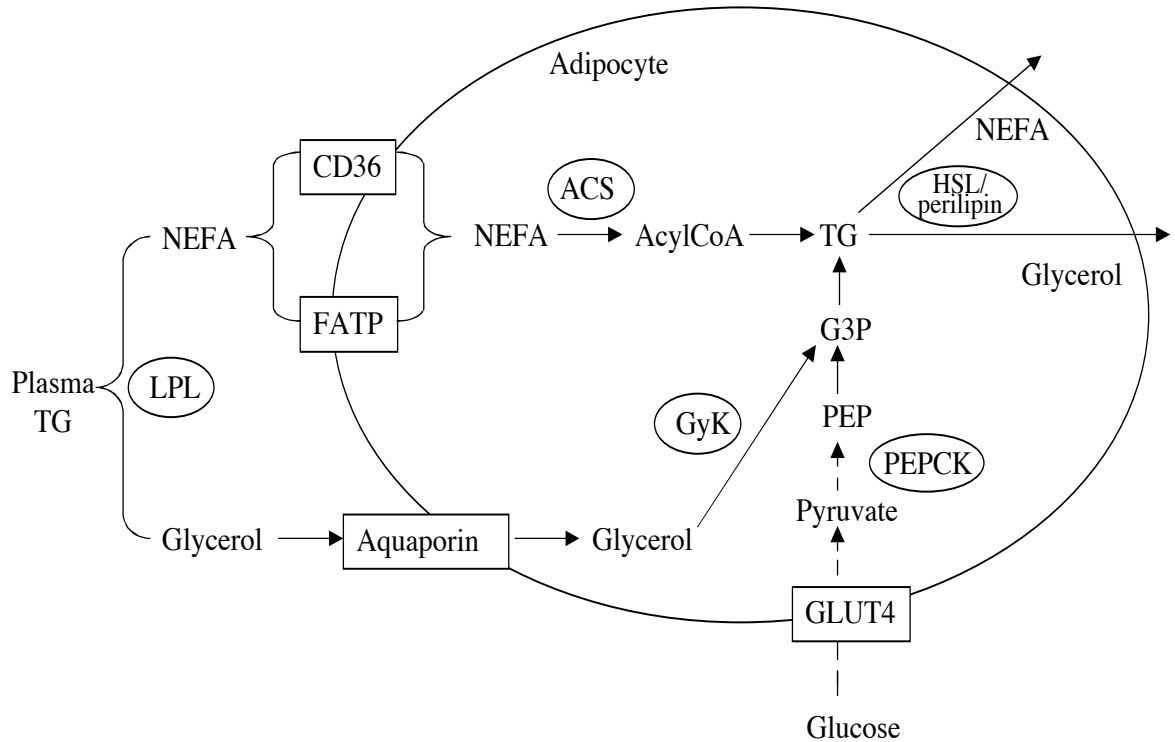


**Figure 1.13** PPAR $\gamma$  target genes and adipocyte metabolism. PPAR $\gamma$  regulates adipocyte metabolism by inducing expression of several genes which are boxed or circled. Plasma triglycerides (TG) are hydrolysed by lipoprotein lipase (LPL) to non-esterified fatty acids (NEFA) and glycerol. Fatty acid transport protein (FATP) and fatty acid translocase (CD36) facilitate uptake of NEFA, whilst aquaporin channels facilitates glycerol transport. Within the adipocyte NEFAs are esterified into TG via the action of acylCoA synthase (ACS), while glycerol is converted into glycerol-3-phosphate (G3P) by glycerol kinase (GyK). In addition G3P can be also generated through glyceroneogenesis mediated by phosphoenolpyruvate carboxykinase (PEPCK). Dashed lines indicate several intermediate steps; PEP, phosphoenol pyruvate. PPAR $\gamma$  can also influence lipolysis by inducing the expression of perilipin, which is an important determinant of hormone-sensitive lipase (HSL) activity.

## Chapter 2

### MATERIAL AND METHODS

#### 2.1 Chemicals

Unless otherwise specified, all chemicals were obtained from Sigma. Specific exceptions included reagents supplied by BDH laboratories (agarose, chloroform, acetic acid, hydrochloric acid, Triton X-100, propan-2-ol/isopropanol and ethylenediaminetetraacetic acid-EDTA), Difco (tryptone, yeast extract and bacto-agar), Fisher Scientific (NaOH, glycerol, methanol), Pharmacia (glutathione sepharose G50) and Bio-Rad (Acrylamide).

#### 2.2 Buffers

The following commonly used buffers were prepared according to standard recipes (Sambrook *et al.*, 1989)

TE 10mM Tris HCl pH 8.0, 1mM EDTA pH 8.0

TBE 45mM Tris-borate, 1mM EDTA pH 8.0

PBS 137mM NaCl, 2.7mM KCl, 10mM Na<sub>2</sub>HPO<sub>4</sub>, 1.7mM KH<sub>2</sub>PO<sub>4</sub>

STE 0.1mM NaCl, 10mM Tris HCL pH 8.0, 1mM EDTA pH 8.0

PIC Phenol: isoamylalcohol: chloroform – 25 : 1 : 24

IC isoamylalcohol: chloroform – 1 : 24

5x agarose gel loading buffer: 0.25% w/v bromophenol blue, 0.25% w/v xylene cyanol, 30% v/v glycerol in deionised H<sub>2</sub>O

2x SDS gel loading buffer: 125mM Tris HCl pH 6.8, 4% w/v SDS, 20% v/v glycerol, 10% v/v 2-mercaptoethanol

## **2.3 Nucleic acid preparation and analysis**

### **2.3.1 Oligonucleotides**

Oligonucleotide primers were synthesized by Sigma Genosys, usually at 0.05  $\mu$ M synthesis scale and without modification. Notable exceptions were those oligonucleotides used in site-directed mutagenesis, which were subjected to polyacrylamide gel electrophoresis (PAGE) purification.

### **2.3.2 DNA**

#### *2.3.2.1 Extraction of genomic DNA from peripheral blood leukocytes*

Genomic DNA was prepared using the QIAamp blood extraction kit (Qiagen). The initial sucrose lysis step was performed using the following buffer:

Lysis buffer : 10mM Tris HCl pH8.0, 320 mM sucrose, 5mM MgCl<sub>2</sub>, 1% v/v Triton-X-100

Usually 2-5 ml of blood sample was mixed with 30-50ml of lysis buffer, rotary mixed for 5 minutes and then leukocytes were recovered by centrifugation at 2,400rpm for 5 minutes, and resuspended in 200 $\mu$ l of sterile PBS. DNA was then extracted according to the manufacturer's instructions.

#### *2.3.2.2 Plasmid DNA*

3 ml of Luria Bertani (LB) ampicillin (amp) cultures were inoculated with single bacterial colonies from LB amp plates and incubated overnight in an orbital shaker at 37°C. These cultures were then used either directly for miniprep preparation or for further inoculation of megaprep cultures. All plasmid preparations were performed using Qiagen kits according to the manufacturer's instructions. Typical yields were: minipreps up to 50 $\mu$ g and megapreps up to 2mg.

#### 2.3.2.3 *Ethanol precipitation of DNA*

This technique was used to purify and concentrate DNA. Two and a half volumes of 100% ethanol and 1/10 volume 3M NaOAc or 1M KOAc were added to the sample, mixed and placed on dry ice for at least 20 minutes. The mixture was then centrifuged at 13,000rpm for 15 minutes and 50-300µl of 70% ethanol was added to the pelleted DNA to wash off co-precipitated salts. The sample was re-centrifuged at 13,000rpm for 3-5 minutes, the supernatant decanted and the tubes placed at room temperature with lids open until residual ethanol had evaporated. All DNA preparations were then dissolved in an appropriate amount of distilled sterile water or TE.

#### 2.3.2.4 *PEG precipitation of nucleic acid*

This technique was used to purify DNA and to remove unincorporated bases and primers following PCR reactions. The aqueous phase of the PCR sample was transferred to a 1.5ml centrifuge tube, one volume of PEG solution (26.2% w/w polyethylene glycol MW 8000, 0.6M KOAc, 6.6mM MgCl<sub>2</sub>) was added, vortexed and placed at room temperature (RT) for 15 minutes. It was then centrifuged for 15 minutes at 13,000rpm, the supernatant aspirated and the pellet was washed and resuspended as described in section 2.3.2.3.

### **2.3.3 RNA**

#### 2.3.3.1 *RNA extraction from Immature Dendritic Cells*

Total RNA from immature dendritic cells (IDC) was extracted with TRIZOL Reagent (Invitrogen Life Technologies). This reagent is a mono-phasic solution of phenol, which allows separation of RNA from other cellular constituents, and guanidine isothiocyanate, a ribonuclease inhibitor. To prevent RNase contamination, before proceeding to extract RNA, pipettes gloves and bench were cleaned with RNAzap detergent and all the procedures were carried out using sterile, disposable plastic ware and pipettes reserved for RNA work.

IDC cells were collected into RNase free eppendorf tubes by centrifugation and lysed in 1 ml of TRIZOL by repetitive pipetting. The homogenized samples were incubated for 5 minutes at RT to permit the complete dissociation of nucleoprotein

complexes and then 200  $\mu$ l of chloroform was added. The samples were shaken vigorously for 15 seconds and incubated at RT for 10 minutes and then centrifuged at 14,000rpm for 15 minutes at 4<sup>o</sup>C. The (upper) aqueous phase was then transferred into a clean tube and a similar volume of isopropyl alcohol was added and mixed well to precipitate the RNA. Following incubation for 10 minutes at RT the RNA was centrifuged at 14,000rpm for 10 minutes at 4<sup>o</sup>C and the supernatant removed. The RNA pellet was then washed once with 1 ml of 75% ethanol and centrifuged again at 14,000rpm for 5 minutes. At the end of the procedure the RNA was left to air-dry for not more than 10 minutes and dissolved in nuclease free water, incubated for 10 minutes at 60<sup>o</sup>C and stored at -70<sup>o</sup>C.

#### **2.3.4 Nucleic acid quantification**

All nucleic acid preparations were quantitated by measurement of their absorbance at 260nm ( $A_{260}$ ) and purity calculated as  $A_{260} / A_{280}$  ratio with 1.8 representing the desired purity for DNA. The UV-160A spectrophotometer (Shimadzu, Japan) or the Genequant II DNA/RNA calculator (Pharmacia, UK) were used to measure the absorbances and nucleic acid concentrations calculated according to the following formula:

$$\text{concentration (ng/}\mu\text{l)} = \text{dilution factor} \times A_{260} \times \text{OD value}$$

OD values are 50 for double stranded DNA, 40 for RNA and between 30 to 40 for oligonucleotides (exact OD values for oligonucleotides were provided by Sigma Genosys, UK).

#### **2.3.5 Radio-labelling of nucleic acids**

<sup>32</sup>P-labelled probes used in electrophoretic mobility shift assay (EMSA) were generated using annealed, semi-overlapping oligonucleotide duplexes (0.3  $\mu$ M) which were filled in using the Klenow fragment of DNA polymerase I (Roche Diagnostics) in the presence of 5 $\mu$ l  $\alpha$ -<sup>32</sup>PdCTP (1000 $\mu$ Ci/ $\mu$ l; Amersham) and 70  $\mu$ M unlabelled dATP, dGTP and dTTP. To remove unincorporated nucleotides and

random hexamer-labelled probes the resultant probes were purified using a Sephadex G-50 column according to a standard protocol (Sambrook *et al.*, 1989).

### **2.3.6 Enzymatic modification of DNA**

#### *2.3.6.1 Restriction enzyme digestion*

Restriction enzymes were obtained from either New England Biolabs (USA) or Roche Diagnostics (Germany). Reaction conditions varied according to the supplier's instructions, but typically involved incubation at 37°C for 60 minutes followed by heat inactivation at 65°C for 15 minutes.

#### *2.3.6.2 Dephosphorylation*

To prevent the re-ligation of compatible ends of digested vectors, shrimp alkaline phosphatase (Roche Diagnostics, Germany) was used to catalyse the hydrolysis of the 5' phosphate group. Following dephosphorylation for 1 hour at 37°C, the alkaline phosphatase was inactivated by heating to 65°C for 15 minutes.

#### *2.3.6.3 Agarose gel electrophoresis*

Agarose gels of 1% and 2% w/v were prepared in 1x TBE buffer containing 0.5mg/ml ethidium bromide and used to separate large (500-7000bp) and small (100-1000bp) DNA fragments respectively. The samples (mixed in loading dye) were loaded onto the gel and electrophoresed at 130V for 30-90 minutes in 500ml of 1x TBE. To estimate the size of nucleic acid fragments, standard size markers were also included. Images were obtained using an Eagle-eye II or Biorad gel imager.

#### *2.3.6.4 Agarose gel extraction*

This technique was used to isolate DNA fragments following restriction digestion. The plasmid DNA insert and backbone vectors were separated by agarose gel electrophoresis, visualized using an UV light source and cut from the gel using a clean razor blade. The fragments were then purified using a commercial Kit (QIAquick kit, Qiagen, UK) according to the manufacturer's instructions and resuspended in dH<sub>2</sub>O or TE.



### 2.3.6.5 DNA ligation

DNA ligation was carried out using the Roche Diagnostics T4 standard ligation (requiring overnight incubation at 16°C) or rapid ligation (5-10 minutes at room temperature) kits. Ligations were performed with a 3:1 molar ratio of insert to vector for fragments with complementary overhangs as recommended in the manufacturer's instructions.

### 2.3.7 Polymerase chain reaction (PCR)

All reactions were mixed on ice and performed in an Omnigene (Hybaid, UK) or Geneamp (Perkin Elmer, UK) thermal cycler. The volumes of reaction were between 10 and 50µl with the following concentrations of constituent parts:

dNTPs (A, G, C, T)	0.2mM each
10x reaction buffer	1x
primers (supplied by Sigma Genosys, UK)	0.2µM
MgCl <sub>2</sub>	1.5-2.5mM
template DNA	variable (typically 1µg)
<i>Taq</i> polymerase	0.2-0.5µl
dH <sub>2</sub> O	to final reaction volume

Cycle parameters were set using the following guidelines:

denaturation temperature: 92-94°C

denaturation time: 15 seconds for templates < 500bp, 30 seconds if larger

annealing temperature: 2°C below lowest T<sub>m</sub> of primers.

annealing time: 30 seconds

polymerase temperature: 72°C

polymerase time: 30 seconds per kb DNA to be amplified.

Cycles: 30-35.

### **2.3.8 DNA sequencing**

DNA sequencing was performed using the Perkin Elmer (USA) dye-terminator kit and an ABI Avant 3100 automated sequence analyser. This kit consists of a pre-mixed solution containing dye-labelled dideoxynucleotides, sequencing buffer, *Taq* polymerase and magnesium. Typically 1 $\mu$ g of DNA was mixed with 4 $\mu$ l of sequencing mix and 1 $\mu$ l of the appropriate primer (5-10 $\mu$ M) in a final volume of 10 $\mu$ l. Either miniprep, maxiprep or PCR products were used as template; the latter were purified by PEG precipitation as outlined in section 2.3.2.4 prior to use. Cycle sequencing was performed at 94 $^{\circ}$ C for 30 seconds, 60 $^{\circ}$ C for 2 minutes and 72 $^{\circ}$ C for 30 seconds, with a final extension step at 72 $^{\circ}$ C for 5 minutes. The products were ethanol-precipitated and resuspended in 10 $\mu$ l of Hi-Di<sup>TM</sup> Formamide (Applied Biosystem). Samples were denatured by heating to 95 $^{\circ}$ C for 2 minutes and placed on ice prior to loading. Details of apparatus and solutions required for sequencing using the ABI 3100 can be found in their respective operation manuals.

### **2.3.9 Site-directed mutagenesis**

Site-directed mutagenesis was performed using the Stratagene "Quik-change<sup>TM</sup>" Kit according to the manufacturer's instructions. In brief, the basic procedure involves annealing of complementary primers (containing the desired mutation) to the wild type plasmid DNA. Following replication of both strands using PfuTurbo DNA polymerase, the parental strands were digested with Dpn I demethylation enzyme. The newly synthesised strands, each containing a "nick" at the 5' end of the oligonucleotide primer sequence, were transformed into XL-1 blue *Escherichia Coli* (*E. Coli*) with subsequent repair of the "nicked" strands by the supercompetent cells. Mini-prepping of DNA, followed by direct sequencing, identified colonies containing the desired mutations, which were then used to prepare megapreps.

### **2.3.10 Reverse transcription-PCR**

Reverse transcription was performed using the SuperScript<sup>TM</sup> II Reverse Transcriptase (Invitrogen). The following component were added to 20 $\mu$ l final

volume and mixed gently:

RNA 100ng/ $\mu$ l	4 $\mu$ l
5X SSII buffer	4 $\mu$ l
100 mM DTT	2 $\mu$ l
2.5 mM DNTs	4 $\mu$ l
100 mM specific primer	0.06 $\mu$ l
SuperScript™ Enzyme	0.1 $\mu$ l
RNAse free water	5.84 $\mu$ l

The reaction was incubated at 42°C for 30 minutes followed by 10 minutes at 72°C.

## 2.4 Protein preparation and analysis

### 2.4.1 *In vitro* translation

A TNT coupled reticulocyte lysate kit (Promega, UK) was used to synthesize "cold" and "hot" (<sup>35</sup>S-labelled) TR $\beta$ 1, RXR $\alpha$ , PPAR $\gamma$  and CBP proteins from their corresponding expression vectors. A typical 50 $\mu$ l reaction contained:

TNT lysate	25 $\mu$ l
TNT buffer	2 $\mu$ l
RNasin	1 $\mu$ l
Amino acid minus methionine mix	1 $\mu$ l
<sup>35</sup> S-methionine (or 'cold' methionine containing mix)	4 $\mu$ l
T7 RNA polymerase	1 $\mu$ l
Plasmid DNA	1 $\mu$ l
Nuclease-free dH <sub>2</sub> O to a final volume of	50 $\mu$ l

Reactions were incubated at 30°C for 90 minutes and the integrity of products checked by running 2-4 $\mu$ l of the translation (in duplicate) on an SDS gel followed by autoradiography with storage at -70°C.

#### **2.4.2 Polyacrylamide gel electrophoresis (SDS-PAGE)**

Proteins were analyzed under denaturing conditions by electrophoresis through an SDS-polyacrylamide gel, whose components are detailed below.

##### *Stacking gel:*

30% acrylamide	0.67ml
0.5M Tris pH 6.8	1.25ml
10% sodium dodecyl sulphate (SDS)	50 $\mu$ l
dH <sub>2</sub> O	3ml
10% ammonium persulfate (APS)	25 $\mu$ l
(N,N,N',N') tetramethylethylenediamine (TEMED)	2.5 $\mu$ l

##### *Separating gel:*

30% acrylamide	3.33ml
1.5M Tris pH 8.8	2.5ml
10% SDS	100 $\mu$ l
dH <sub>2</sub> O	4ml
10% APS	50 $\mu$ l
TEMED	5 $\mu$ l

Protein samples were mixed with an equal volume of loading buffer (1.25M Tris (pH 6.8), 2.5% SDS, 20% w/w glycerol, 10% w/w  $\beta$ -mercaptoethanol, 0.1% w/w bromophenol blue), denatured and electrophoresed at 30mA for 60 minutes using a SE 250 Duel Gel II apparatus (Hoefer Scientific, Germany). The stacking layer was excised and the separating gel stained for 20 minutes using Coomassie blue, prior to gentle washing in fixing solution (10% w/v glacial acetic acid, 20% w/v methanol) for 15 minutes. Thereafter the gel was placed on 3mm Whatman paper and dried under vacuum at 80°C for 45 minutes. Gels containing <sup>35</sup>S-labelled proteins were placed in an X-ray cassette and the film exposed overnight.

### **2.4.3 Electrophoretic mobility shift assay (EMSA)**

This technique was useful to examine the ability of nuclear receptors to bind to DNA and, in the case of TR and PPAR, to heterodimerise with RXR. Approximately 1nM labelled oligonucleotide probe (see section 2.3.4) was incubated for 20 minutes at room temperature with *in vitro* translated receptor protein in shift buffer (20mM HEPES pH 7.8, 50mM KCl, 10% glycerol, 2mM DTT). The reactions were loaded onto a 5-6% native polyacrylamide gel measuring 0.1 x 14 x 14 cm, which had been pre-run at 300V for 30 minutes in a gel electrophoretic apparatus cooled to 0-5°C (Biorad). Electrophoresis was usually performed for 90 minutes at 300V and subsequently the gel was fixed, dried and exposed as outlined in section 2.4.2.

### **2.4.4 Ligand binding assays**

#### **2.4.4.1 TR $\beta$**

The ligand binding affinities of *in vitro* translated wild type and mutant receptor proteins were determined using a previously described filter binding assay (Adams *et al.*, 1994). In brief each receptor was incubated with 0.02nM <sup>125</sup>I-T3 in binding buffer (20mM Tris pH 8, 50mM KCl, 1mM MgCl<sub>2</sub>, 10% glycerol, 5mM DTT) in the presence of increasing amounts of unlabelled cold competing T3 (0-1 $\mu$ M). Following 2 hours of incubation at 30°C, bound T3 was separated from unbound T3 by passage through a filter membrane (Millipore HA filters, 0.45 $\mu$ m) under vacuum followed by three washes with 2ml of ice-cold binding buffer. Filters were then transferred into LP3 tubes and counted in a  $\gamma$ -counter. The binding affinity constants (K<sub>a</sub>'s) were calculated using Scatchard analyses from three separate experiments, each carried out in duplicate.

#### **2.4.4.2 PPAR $\gamma$**

The abilities of wild type and mutant PPAR $\gamma$  proteins to bind to [<sup>3</sup>H]-rosiglitazone and [<sup>3</sup>H]-farglitazar were determined using a modification of the previously described filter binding assay (Adams *et al.*, 1994). GST-PPAR $\gamma$  LBD fusion proteins were incubated with approximately 1nM of tritiated ligand in binding buffer (50mM HEPES pH 7.9, 100mM KCl, 2mM DTT, 10% glycerol). Following 45

minutes incubation at 25<sup>0</sup>C, an excess of competing cold ligand (BRL49653 or GI262570) was added and the reaction was incubated for a further 2 hours. Bound ligand was separated from free ligand as outlined in section 2.4.4.1 by passage through filters, which were pre-incubated with BSA (1%) and Tween (1%) to reduce non-specific binding with the [<sup>3</sup>H]-farglitazar compound.

#### **2.4.5 GST protein synthesis**

Glutathione S-transferase (GST) fusion proteins were prepared as previously described (Adams *et al.*, 1997) with minor modifications. *E. Coli* were grown for 3 hours at 37<sup>0</sup>C prior to induction with 0.4mM isopropylthio- $\beta$ -D-galactosidase (IPTG) at 30<sup>0</sup>C for a further 2 hours. Following purification, the proteins, bound to glutathione-sepharose beads, were quantified by SDS gel and aliquoted at -70<sup>0</sup>C.

#### **2.4.6 Pulldown assays**

This technique was employed to investigate receptor-coactivator interactions. GST-PPAR $\gamma$  ligand binding domain (LBD) (see section 2.4.5) in binding buffer (40mM HEPES pH 7.8, 100mM KCL, 5mM MgCl<sub>2</sub>, 0.2 mM EDTA, 1% Nonidet P-40, 10% glycerol, 2mM DTT) were mixed with 5 $\mu$ l of <sup>35</sup>S-labelled *in vitro* translated CBP, together with ligand or vehicle, and incubated at 4<sup>0</sup>C for 2 hours. Following three washing steps with NETN buffer (20mM Tris pH 8.0, 100mM NaCl, 1mM EDTA, 0.5% Nonidet P-40), bound CBP was determined by SDS-PAGE. Coomassie staining was used to verify equal protein loading, followed by fixation and exposure by autoradiography.

#### **2.5 Bacterial cell culture**

Routine bacterial cell culture was carried out according to standard protocols (Sambrook *et al.*, 1989).

### 2.5.1 Media

LB broth	10g/l bacto-tryptone, 5g/l bacto-yeast extract, 10g/l NaCl; adjusted to pH 7.4 with NaOH
LB agar	as above but with the addition of 16g/l of bacto-agar
LB + Amp	As for LB broth or LB agar but containing 50µg/ml of ampicillin
Minimal media	7.5g agarose in 450ml dH <sub>2</sub> O, autoclaved and cooled to <50°C. Then add: 50ml 10x M9 salts solution (60g/l Na <sub>2</sub> HPO <sub>4</sub> , 10g/l NH <sub>4</sub> Cl, 5g/l NaCl) 0.5ml 1M MgSO <sub>4</sub> 50µl 1M CaCl <sub>2</sub> 2.5ml thiamine (2.5mg/ml) 5ml glucose (20% w/v)

### 2.5.2 Preparation of competent cells

DH5α *E. Coli* were rendered competent using standard techniques (Sambrook *et al.*, 1989) and the following buffers:

RF1	100mM RbCl, 50mM MnCl <sub>2</sub> , 30mM K acetate pH 7.5, 10mM CaCl <sub>2</sub> , 15% v/v glycerol, adjusted to pH 5.8 with glacial acetic acid and filter sterilised (store at 4°C)
RF2	100mM MOPS pH 6.8, 10mM RbCl, 75 mM CaCl <sub>2</sub> , 15% v/v glycerol, adjusted to pH 6.8 with NaOH and filter sterilised (store at 4°C)

Briefly, a glycerol stock of the *E. coli* DH5 $\alpha$  strain was streaked out onto minimal medium plates. Following growth for 4-5 days, a single colony was inoculated into 10ml of LB broth and cultured over night at 37 $^{\circ}$ C in a shaking incubator. On the following day 1ml of culture was used to inoculate 200ml of LB media and then grown until the OD<sub>595</sub> was between 0.3 and 0.5. Bacteria were pelleted by centrifuging the broth at 2000rpm for 10 minutes and then resuspended in 50ml of ice-cold RF1 buffer and incubated in ice for 20 minutes. The suspensions were re-centrifuged as before and resuspended in 25ml of ice-cold RF2 buffer. Aliquots of 200 $\mu$ l were frozen in dry ice and then stored at -70 $^{\circ}$ C. Alternatively, competent XL-1 or XL-2 blue *E.Coli* strains were purchased from Stratagene.

### ***2.5.3 Transformation of competent cells***

Aliquots of competent cells were thawed on ice. 2-5 $\mu$ l of ligation product or 1-2 $\mu$ l of plasmid DNA were then added, gently mixed by pipetting and the mixture incubated on ice for 10 minutes. Thereafter cells were heat shocked at 42 $^{\circ}$ C for 45 seconds and returned to ice for 2 minutes. Cells were rescued by the addition of 500 $\mu$ l of LB media and incubated at 37 $^{\circ}$ C for 30-60 minutes before plating on LB Amp plates. The plates were then incubated at 37 $^{\circ}$ C over night.

### ***2.5.4 Glycerol stock***

Glycerol stocks of *E. Coli* containing key plasmids were generated by adding 0.15ml of the appropriate LB culture to 0.85ml of sterile glycerol with subsequent storage at -70 $^{\circ}$ C.

## **2.6 Cell culture**

### ***2.6.1 Routine cell culture and maintenance of cell lines***

All mammalian cell culture work was carried out in a laminar airflow cabinet (Gelaire BSB4, Airflow) to maintain a sterile environment. Monolayer cultures of human cells were cultured in 10cm dishes and maintained in 10ml medium at 37 $^{\circ}$ C



in humidified air supplemented with 5% CO<sub>2</sub> (IR 1500 automatic CO<sub>2</sub> incubator, Flow Laboratories).

JEG3 cells (derived from a human choriocarcinoma) and 293EBNA cells (derived from human kidney fibroblasts) were obtained from either the European Collection of Animal Cell Culture (ECACC) or the American Tissue and Cell Culture (ATCC). JEG3 cells were grown in Optimem supplemented with 2% fetal calf serum (FCS) and 1% penicillin/streptomycin/fungizone (PSF). 293EBNA cells were grown in Dulbecco's modified Eagle medium (DMEM), supplemented with 10% FCS and 1% PSF. To study the effects of ligands on transcriptional regulation, FCS was depleted of steroid hormones by mixing with Dowex ion exchange resin (AG-1-X8) for 24 hours.

Optmem, DMEM, FCS and PSF were all obtained from GIBCO-BRL.

### **2.6.2 *Transient transfection assays***

Introduction of plasmid DNA into cultured JEG3 and 293EBNA cells was performed using the calcium phosphate transfection method as described in Sambrook *et al.*, 1989. In brief, calcium phosphate-DNA co-precipitates were prepared by slowly mixing 2M CaCl<sub>2</sub> solution with the mammalian expression vector DNAs in HEPES-buffered saline (HBS: 140mM NaCl, 5mM KCl, 0.75mM Na<sub>2</sub>HPO<sub>4</sub>·2H<sub>2</sub>O, 6mM dextrose, 25mM HEPES, pH 7.05). The mixture was left at room temperature for 45 minutes prior to use. 50µl of the appropriate suspension was then added to the appropriate wells of a 24-well tissue culture plate (containing cells grown to 60-70% confluency) with 500µl of fresh medium. Cells were incubated with the calcium phosphate-DNA precipitates for 4-6 hours before replacement with fresh medium, prior to harvesting 36-40 hours later. At this point cells were then lysed, and reporter gene assays subsequently performed as described in the following section.

### **2.6.3 Luciferase and $\beta$ -Galactosidase assays**

At completion of the transfection, the medium was aspirated and the cells were washed once with 500 $\mu$ l PBS then lysed in 200  $\mu$ L of gly-gly buffer (containing 25mM glycine-glycine pH 7.8, 15mM MgSO<sub>4</sub>, 4mM EGTA) with 1mM DTT and 1% Triton X-100 at RT for 10 minutes. Cell lysates were removed to a 1.5ml eppendorf tube and centrifuged briefly to pellet cell debris. 100 $\mu$ l of supernatant was assayed for luciferase activity by the addition of 300 $\mu$ l assay buffer (gly-gly buffer with 16.5mM KH<sub>2</sub>PO<sub>4</sub>, 2.2mM ATP and 0.1mM DTT) in a 5ml LP3 tube and immediately transferred to a luminometer (Autolumat LB 953, Berthold) to measure light emission over 10 seconds following addition of 100 $\mu$ l of luciferin solution (gly-gly buffer with 0.2mM luciferin and 10 mM DTT).

$\beta$ -galactosidase activity in 20 $\mu$ l cell lysate was determined by the addition of 150 $\mu$ l reaction buffer (63mM Na<sub>2</sub>HPO<sub>4</sub>.2H<sub>2</sub>O, 14mM NaH<sub>2</sub>PO<sub>4</sub>.2H<sub>2</sub>O, 1mM MgCl<sub>2</sub>, 14mM  $\beta$ -mercaptoethanol, and 0.9% *o*-nitrophenyl- $\beta$ -D-galactopyranoside (ONPG) in a flat-bottomed microtitre plate. After incubating at 37<sup>o</sup>C for 5-30 minutes, the relative activity in each reaction was determined by measuring absorbance at 415nm in a microtitre plate reader (Molecular Devices).

### **2.6.4 Isolation and culture of Immature Dendritic Cells from peripheral blood**

Anticoagulant-treated blood was diluted 1:1 with PBS and layered very carefully on the Ficoll-Paque Plus (Amersham Biosciences), which provides a sterile ready to use Ficoll-sodium diatrizoate solution of the proper density, viscosity and osmotic pressure for use in a simple and rapid lymphocyte isolation procedure (10ml of Ficoll / 20ml of diluted blood). Following 30 minutes centrifugation at 2,500rpm without brake, lymphocytes at the interface between the plasma and the Ficoll-Paque Plus were recovered and transferred in a clean tube, washed with PBS in 45ml final volume and centrifuged at 1,500rpm for 10 minutes. The supernatant was then removed and the cells were suspended with 25ml of PBS by gently drawing them in and out of a Pasteur pipette and centrifuged again at 1,500rpm for 10 minutes. This wash step to remove platelets and any excess of Ficoll-Paque Plus was repeated twice.

Following the last wash step, cells were suspended in 10 ml of PBS and run through a pre-separation filter (Miltenyi Biotec) to remove cell aggregates, centrifuged again at 1,500rpm for 10 minutes. The pellet cells were then incubated with the magnetic labeling mix [100 $\mu$ l of MACS CD14 MicroBeads (Miltenyi Biotec) and 400 $\mu$ l buffer A (PBS, 0.5% BSA and 2mM EDTA)] at 4°C x 20 minutes.

The labeling mix was washed with Buffer A until 10ml final volume and centrifuged at 1500rpm for 10 minutes. The supernatant was removed and the cells resuspended with 5ml of Buffer A and applied onto LS Columns (Miltenyi Biotec) in a high-gradient magnetic field to retain the labeled cells. The flowthrough consists mainly of lymphocytes, because CD14 positive monocytes are retained on the column being linked to the antibody-coated beads. After washing twice to remove the unlabeled cells, LS Columnn were removed from the separator and placed in a new tube and positively selected cell fraction was finally eluted. Monocytes were resuspended into 6-well culture plates at a density of  $1.5 \times 10^6$  cell/ml and cultured in RPMI 1640 supplemented with 10% FBS containing 800U/ml GM-CSF (Leucomax) and 500U/ml IL-4 (Peprotech), to induce differentiation into immature dendritic cells, for 24 hours with vehicle (DMSO) or 1 $\mu$ M Rosiglitazone.

## Chapter 3

### THREE NOVEL MUTATIONS AT SERINE 314 IN THE THYROID HORMONE $\beta$ RECEPTOR DIFFERENTIALLY IMPAIR LIGAND BINDING IN THE SYNDROME OF RESISTANCE TO THYROID HORMONE

#### 3.1 Introduction

Recognition that the syndrome of Resistance to Thyroid Hormone (RTH) is linked to the thyroid hormone  $\beta$  receptor (TR $\beta$ ) gene locus (Usala *et al.*, 1988) has led to the identification of an increasing number of natural mutations whose functional characterization has provided important insights into structure-function relationships in this receptor. RTH is characterized by elevated serum free thyroid hormones (FT4 and FT3) in the presence of unsuppressed thyrotropin (TSH) levels, reflecting resistance to the normal negative feedback mechanisms within the hypothalamus and pituitary (Refetoff *et al.*, 1993). The degree of resistance within peripheral tissues determines whether thyrotoxic clinical features are associated with the condition (Beck-Peccoz and Chatterjee, 1994). An autosomal dominant mode of inheritance, in conjunction with the recognition that receptor mutants are functionally impaired, has led to the proposal that these abnormal proteins are able to inhibit the function of their wild type (WT) counterparts in a dominant negative manner (Sakurai *et al.*, 1990; Chatterjee *et al.*, 1991). Such dominant negative inhibition requires the preservation of DNA binding and heterodimerization functions in mutant receptors (Collingwood *et al.*, 1994; Nagaya *et al.*, 1992; Nagaya and Jameson, 1993), consonant with the observation that no RTH mutants have hitherto been reported in the DNA binding or dimerization domains of TR $\beta$ . In fact the majority of natural mutations cluster around the ligand-binding pocket (Clifton-Bligh *et al.*, 1998) and impair hormone binding.

This chapter describes the molecular characterization of three novel single nucleotide substitutions in TR $\beta$  associated with RTH, which result in different missense mutations at residue 314 (S314C, S314F, S314Y). Examination of the crystal structure of TR $\beta$  suggests that Ser 314 plays a structural role in ligand

binding. Functional characterization of the natural mutants permits understanding as to how the different amino acid substitutions at this position affect receptor function. Although all the mutations affected ligand binding, there were significant differences in the extent of the alteration with corresponding variation in their transcriptional and dominant negative properties.

## **3.2 Methods**

### **3.2.1 Clinical and genetic analyses**

All studies were approved by the local research ethic committees (REC ref: 98/154), and informed consent was provided by each affected and control subject for all investigations. Serum free T4 (FT4) and free T3 (FT3) levels were measured with a Delfia fluoroimmunoassay (Wallac, Milton Keynes, UK). TSH levels were determined with a sensitive 'second generation' assay (Delfia, Wallac, Milton Keynes, UK). The coefficient of variation was less than 10% in all instances.

Genomic DNA was extracted from peripheral blood leukocytes using standard techniques. Exons 7-10 of TR $\beta$ 1 from each index case were amplified by PCR using intronic primers (Table 3.1) and sequenced as previously described (Chapter 2; Adams *et al.*, 1994). Each mutation was verified in three independent PCR reactions, and other family members were screened for the presence of the identified mutation.

### **3.2.2 Plasmid constructs**

Receptor mutations were generated by site directed mutagenesis of wild type (WT) human TR $\beta$ 1 cDNA and confirmed by direct sequencing (Chapter 2). Both wild type and mutant receptors were subcloned into pGEM7z and the eukaryotic expression vector RSV (containing the Rous sarcoma virus enhancer and promoter) for *in vitro* and transfection studies respectively. For functional assays, a reporter gene containing a direct repeat thyroid response element (TRE) spaced by four nucleotides (DR+4) from the malic enzyme gene upstream of the thymidine kinase promoter and luciferase (MAL-TKLUC) was cotransfected with receptor expression vectors and a  $\beta$ -galactosidase reference plasmid (Bos- $\beta$ -gal)(chapter 2).

### **3.2.3 Hormone and DNA binding assays**

Receptor proteins were synthesized by coupled transcription and translation (TNT, Promega, Southampton, UK). T3 binding affinities were determined using a modification of a filter assay, and binding affinity constants ( $K_a$ 's) calculated using

Scatchard analyses from three separate experiments on independently generated protein samples (Chapter 2).

Receptor binding to DNA was assessed by electrophoretic mobility shift assays using *in vitro* translated receptors quantitated by SDS-PAGE analysis and a <sup>32</sup>P-labelled oligonucleotide duplex corresponding to an everted repeat (F2) TRE from the chicken lysozyme gene. TR exhibits both homodimeric and heterodimeric (with the retinoid X receptor, RXR) binding to this TRE, with dissociation of the homodimer on addition of ligand. Details of the oligonucleotide duplex sequences and reaction conditions have been described previously (Collingwood *et al.*, 1994).

#### **3.2.4 Cell culture and transient transfection assays**

JEG-3 (human choriocarcinoma) cells were grown in Optimem containing 2% (vol/vol) fetal calf serum and 1% (vol/vol) penicillin, streptomycin and fungizone (GIBCO BRL, Paisley, Scotland). 18 hours prior to transfection the medium was changed to Optimem with 2% AG-1-X8 resin-stripped fetal calf serum. Twenty-four well plates of cells were transfected by a 5 hours exposure to calcium phosphate containing the reporter plasmid MAL-TKLUC (500ng), TR $\beta$ 1 expression vectors (50ng) and the internal control plasmid Bos- $\beta$ -gal (200ng). After a further 36 hours, cells were lysed and extracts assayed for luciferase and  $\beta$ -galactosidase activity using standard methods (Chapter 2).

### 3.3 Results

#### 3.3.1 *Clinical and genetic analyses*

The clinical features and biochemistry in six families with RTH are shown in Table 3.2. All patients exhibited thyroid function tests characteristic of RTH - namely elevated serum free T4 and free T3 with an inappropriately normal TSH. Whilst index cases presented with goitre or thyrotoxic symptoms, most affected family members were asymptomatic and detected by screening. One patient (IV), first presented with Graves' disease, but subsequent thyroid function tests in remission were consistent with RTH. Direct sequencing of exons 7-10 of TR $\beta$ 1 of index cases showed that each individual was heterozygous for a single nucleotide substitution at codon 314 in exon 9. A single nucleotide change in the wild type sequence TCC (serine), corresponding to a missense mutation, was noted in each family: cases I, II, III TTC substitution (phenylalanine)-S314F; cases IV and V TAC substitution (tyrosine)-S314Y; case VI TGC substitution (cysteine)-S314C (Figure 3.1). There was complete concordance between the presence of a receptor defect and the abnormal biochemistry associated with RTH, suggesting that these receptor abnormalities were highly likely to be causative.

#### 3.3.2 *Hormone and DNA binding*

All natural mutations in TR $\beta$  cluster in the ligand-binding domain and consequently the majority exhibit reduced hormone binding. Accordingly, each mutation was introduced into the WT TR $\beta$ 1 cDNA and *in vitro* synthesised proteins assayed for binding of <sup>125</sup>I-T3. As expected from their location within the ligand-binding domain, mutant receptors demonstrated impaired binding compared with wild type receptor. Scatchard analyses indicated that their ligand affinities were reduced with a marked difference in the magnitude of the abnormality between mutations. Thus, in comparison to a wild type K<sub>a</sub> (+/-SEM) of 0.68 x 10<sup>10</sup> M<sup>-1</sup> (0.11), the S314C mutant bound ligand with a slightly reduced affinity (K<sub>a</sub> = 0.48 x 10<sup>10</sup> M<sup>-1</sup> (0.07)). In contrast, with the S314F and S314Y mutant receptor proteins, no specific radiolabelled T3 binding was detected, suggesting a profound ligand binding defect.



Previous studies have shown that TR is able to bind DNA both as a homodimer and heterodimer with RXR and that homodimeric complexes dissociate following the binding of ligand (Yen *et al.*, 1992). Accordingly both homo and heterodimeric binding of WT and mutant receptors were examined using an everted repeat TRE configuration, to test the hypothesis that mutant receptor homodimer dissociation would be variably altered depending on the degree of impairment in hormone binding. In the absence of ligand, WT receptor formed homo and heterodimer complexes and following the addition of (100nM) T3 the homodimer complex dissociated readily (Figure 3.2). In comparison, the addition of 100nM T3 resulted in a differential displacement of homodimer between mutants, with a rank order of WT>S314C>S314F>S314Y.

### **3.3.3 Functional activity and dominant negative inhibition**

To evaluate their transcriptional properties, expression vectors encoding WT or mutant receptors were cotransfected with a reporter gene (MAL-TKLUC) containing a direct repeat TRE configuration. In comparison with WT receptor, S314Y was transcriptionally inactive even at the highest concentration of T3 (1000nM), whilst S314F produced detectable activity (10-15% of the maximal wild type response) only at 100 and 1000nM T3. In marked contrast, although impaired relative to WT at the lower concentrations of ligand (0.1 and 1.0nM), the S314C mutant exhibited a right-shifted activation profile attaining a maximal transcriptional response comparable to WT at 100nM T3 (Figure 3.3).

Consonant with its dominant mode of inheritance, it has been suggested that the mutant receptors in RTH inhibit the action of their wild type counterparts in a dominant negative manner (Sakurai *et al.*, 1990; Chatterjee *et al.*, 1991). The dominant negative potency of each RTH mutant was therefore examined in transient transfection analyses using the same TRE. Either WT receptor alone or equal amounts of WT and mutant receptor were cotransfected with MAL-TKLUC, and transcriptional activity was assayed at either low (1nM) or high (1000nM) T3 concentrations. At 1nM T3, coexpressed S314F or S314Y mutants reduced transactivation by WT receptor comparably (WT alone 100%; WT + S314F or WT + S314Y 45%) whereas cotransfected S314C mutant was less inhibitory (WT 100%;

WT + S314C 68%). At the higher T3 concentration, dominant negative inhibition by the S314C mutant was more readily reversible with 80% transactivation of WT alone, whereas the S314F and S314Y continued to exert significant inhibitory effects (transactivation 60% of WT alone) (Figure 3.4).

In view of the marked differences in ligand binding affinity, transactivation and dominant negative activity of the S314 mutants *in vitro*, we sought to determine whether this might be reflected in the degree of resistance to thyroid hormone action *in vivo*. A previous study has suggested that the magnitude of elevation of circulating free T4 (reflecting the degree of resistance within the pituitary-thyroid axis) may correlate with the degree of impairment in hormone binding affinities of mutant receptor protein *in vitro* (Weiss *et al.*, 1993). A comparison was therefore made between the circulating free T4 levels in individuals harboring the three different codon 314 mutations (Figure 3.5). Interestingly, those with the S314Y or F mutations exhibited higher FT4 levels on average than patients with the S314C mutation, with a trend which, although not significant, suggested a correlation between the degree of resistance and the extent of mutant receptor dysfunction.

---

<b>Primer</b>	<b>Sequence</b>
Exon 7 Forward	5' - TGT AAA ACG ACG GCC AGT CAG TGC TCC CAC TCC TGA GGC - 3'
Exon 7 Reverse	5' - GAT TCT AGA AAT TGA GGT AGA AAA CAC TGG - 3''
Exon 8 Forward	5' - TGT AAA ACG ACG GCC AGT GTTCAG AAG ATG ATT TTC TGC - 3'
Exon 8 Reverse	5' - GAT CTG CAG ACC CAG TAT TCC TGG AAA CTG - 3'
Exon 9 Forward	5' - TGT AAA ACG ACG GCC AGT ACA GAA GGT TAT TCC TAT TGC - 3'
Exon 9 Reverse	5' - GAT CTG CAG GCT CTT TGG ATG CCC ACT AAC - 3'
Exon 10 Forward	5' - TGT AAA ACG ACG GCC AGT AGG CCT GGA ATT GGA CAA AGC - 3'
Exon 10 Reverse	5' - GGA ATT ATG AGA ATG AAT TCA GTC AGT - 3'

---

**Table 3.1** Primers used to amplify and sequence coding exons 7-10 of human TR $\beta$ 1.

Case <sup>o</sup>	Age/Sex	Clinical Features <sup>x</sup>	FT4 9.0-20 pmol/L	FT3 <sup>+</sup> 3.0-7.5 pmol/L	TSH 0.4-4.0 mU/L	Nucleotide change	Codon change <sup>s</sup>
I	35/F	Goitre, thyrotoxic	24	6.4 <sup>@</sup>	2.3	1226 TCC to TTC	S314F
I.I f	69/M	Asymptomatic	21	4.7 <sup>#</sup>	2.6	"	S314F
I.II b	31/M	Asymptomatic	28	9.5	5.1	"	S314F
I.III s	28/F	Asymptomatic	24	8.5	2.1	"	S314F
I.IV b	33/M	Asymptomatic	36	12	0.9	"	S314F
II	37/M	Goitre	37	11	0.6	1226 TCC to TTC	S314F
II.I so	5/M	Goitre, Otitis media	38	15	3.0	"	S314F
III	51/M	Asymptomatic	41	13	1.0	1226 TCC to TTC	S314F
IV#	47/F	AITD	28	13	1.5	1226 TCC to TAC	S314Y
IV.I so	29/M	Asymptomatic	34	17	1.9	"	S314Y
IV.II b	48/M	Asymptomatic	23	9.4	1.2	"	S314Y
IV.III n	10/F	Failure to thrive, ADHD	55	16	2.3	"	S314Y
V*	51/F	Goitre	30	11	6.1	1226 TCC to TAC	S314Y
V.I so	13/M	Asymptomatic	48	17	1.1	"	S314Y
VI	26/F	Goitre, anxiety, palpitations	24	9	1.5	1226 TCC to TGC	S314C
VI.I b	40/M	Goitre, anxiety, palpitations	25	11	1.3	"	S314C
VI.II m	63/F	Goitre, anxiety, palpitations	25	9	0.9	"	S314C

**Table 3.2** Biochemical and genetic data from 6 RTH families

<sup>o</sup> index case and affected relatives: f=father; m=mother; d=daughter; so=son; s=sister; b=brother; n=niece

\* Subtotal thyroidectomy; no thyroid hormone replacement therapy; #Thyroid function tests when AITD in remission

<sup>x</sup> ADHD = attention deficit hyperactivity disorder; AITD = autoimmune thyroid disease

<sup>s</sup> Codon nomenclature based on a predicted protein sequence of 1-461 residues (Sakurai *et al.*, 1990)

<sup>+</sup> <sup>@</sup> = Free T3 on other occasions = 10.7; 8.0; 8.3.

<sup>#</sup> = Free T3 on another occasion = 9.

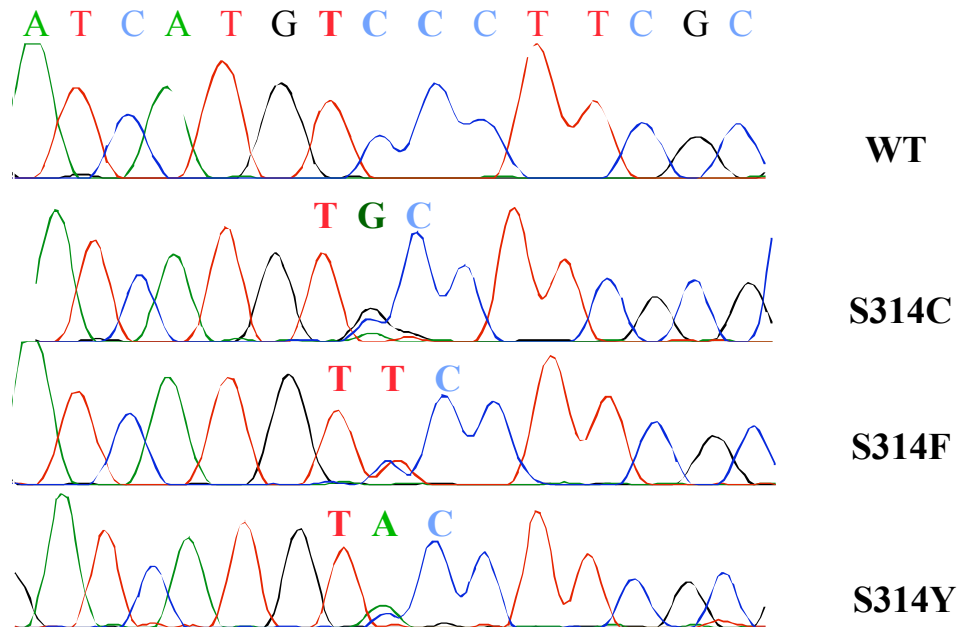


**Figure 3.1** Electropherograms showing sequences corresponding to wild type receptor and S314 hTR $\beta$  mutations. Partial sequence of exon 9 from an unaffected individual and three index cases are shown. A single nucleotide substitution in the wild type sequence at codon 314 changes TCC (serine) to TGC (cysteine), or TTC (phenylalanine) or TAC (tyrosine) respectively.

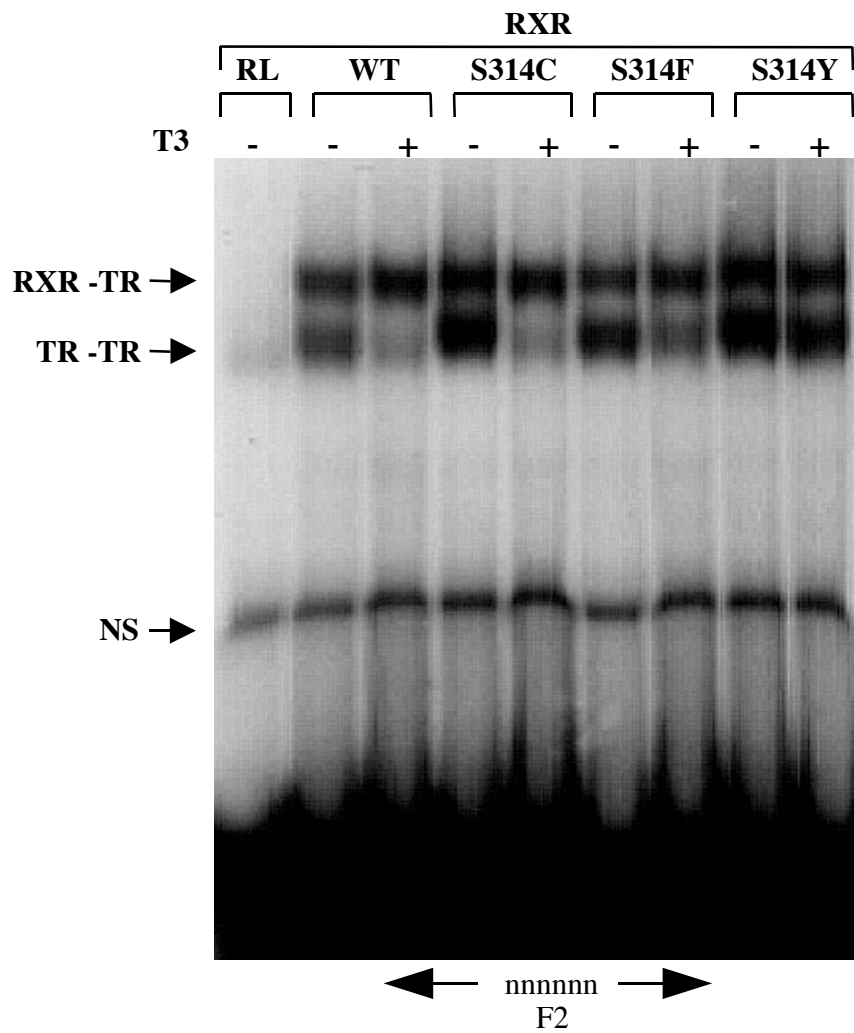


**Figure 3.2** Differential dissociation of TR $\beta$  homodimers in response to T3 on the F2 everted repeat TRE from the chicken lysozyme gene. Using an electrophoretic mobility supershift assay, *in vitro* translated TR $\beta$  (wild type - WT, or mutants - S314C, S314F, S314Y) and RXR were coincubated with the F2 TRE in the absence or presence of T3 (100nM). Complexes were resolved by PAGE. The location of homodimer (TR-TR) and heterodimer (RXR-TR) complexes is indicated. RL, reticulocytes lysate; NS, non specific complex

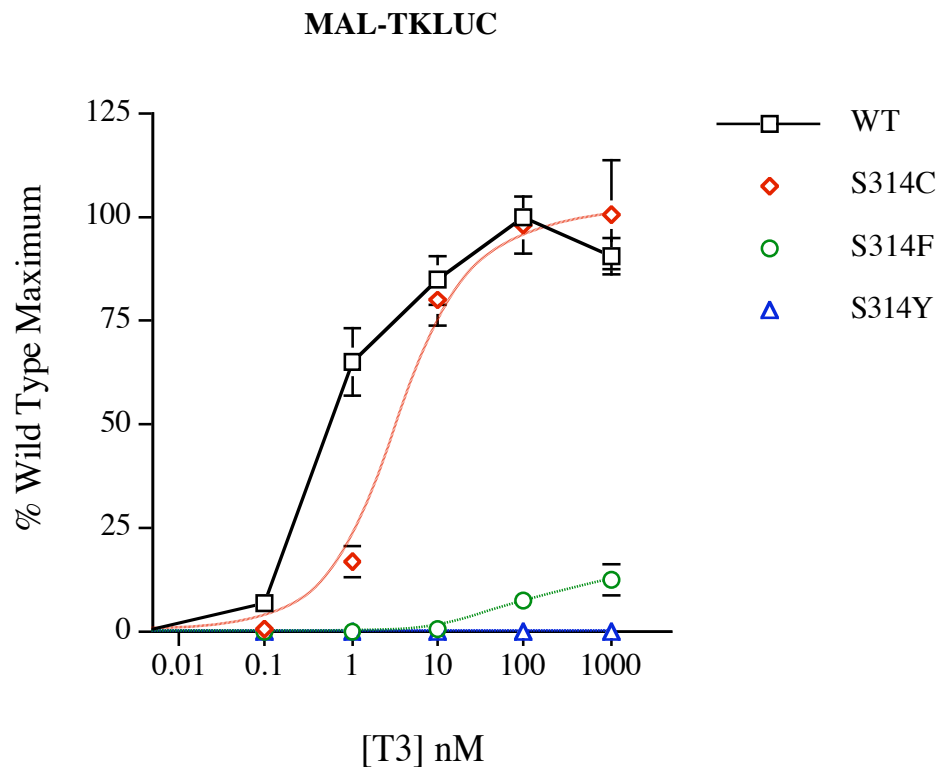


**Figure 3.3** T3-dependent transcriptional activation of a thyroid response element containing reporter gene (MAL-TKLUC) by wild type (WT) and mutant (S314C, S314F, S314Y) thyroid hormone receptors. JEG-3 cells were cotransfected with either 50ng WT or mutant TR $\beta$  expression vectors together with the reporter construct MAL-TKLUC (500ng) and an internal control plasmid (Bos- $\beta$ -gal, 200ng). Hormone dependent activation in response to increasing amounts of T3 was normalised against the internal control and expressed as a percentage of the maximum WT receptor response. Data shown represent the mean  $\pm$  s.e.m. of at least 3 experiments, each done in triplicate.

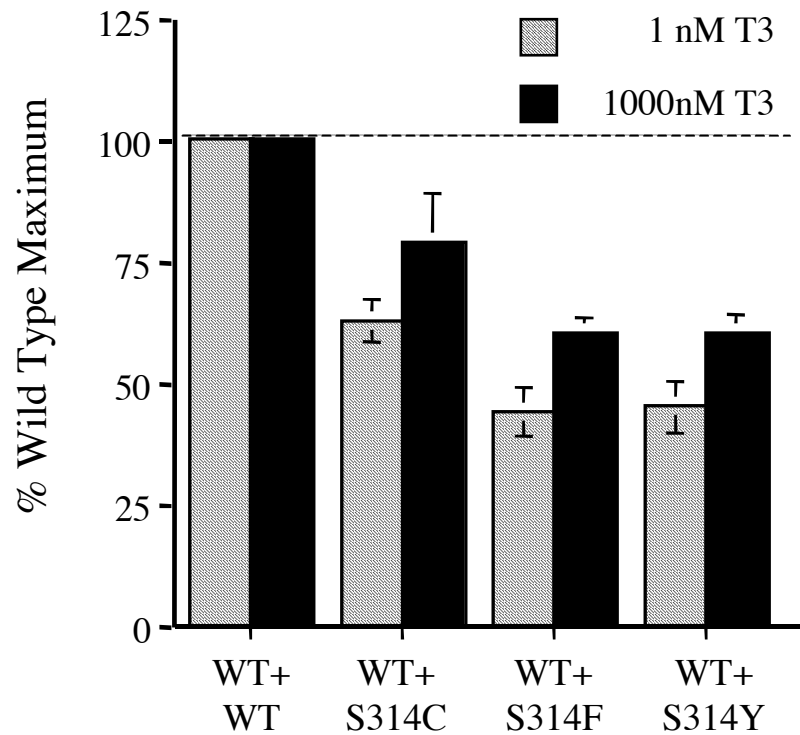


**Figure 3.4** Dominant negative inhibition of wild type (WT) receptor activity by mutant receptors. JEG-3 cells were cotransfected with 500ng of the reporter plasmid MAL-TKLUC, 200ng of the internal control Bos- $\beta$ -gal and either 100ng of WT expression vector alone or 50ng each of wild type and mutant receptor vectors. 50ng and 100ng of wild type receptor expression vector yield similar transcriptional responses. Corrected luciferase activity was measured after incubation with low (1nM) or high (1000nM) T3 concentrations and values expressed as a percentage of the maximal WT receptor response. Data shown represent the mean  $\pm$  s.e.m. of at least 3 experiments, each done in triplicate.



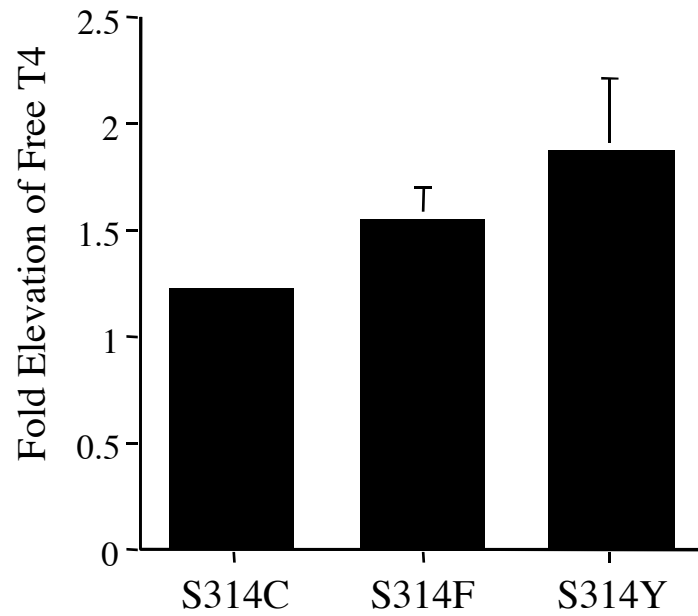


**Figure 3.5** Circulating Free T4 (FT4) levels in individuals harbouring each of the three codon 314 mutations. FT4 levels expressed as fold elevation relative to the upper limit of the normal reference range (denoted as 1.0) were calculated for all individuals shown in Table 3.2, except the index case in pedigree 5 in whom the pituitary-thyroid axis had been disrupted by previous thyroid surgery. For each mutation, values shown represent the mean  $\pm$  s.e.m.

### 3.4 Discussion

In this chapter I have compared the functional properties of three novel mutations (S314C, S314F, S314Y), due to different nucleotide substitutions in the same codon in the thyroid hormone receptor  $\beta$  gene (Figure 3.1), occurring in six kindreds with RTH.

All affected individuals exhibited characteristic biochemical features with elevated circulating free thyroid hormones and a non-suppressed TSH, in keeping with the notion that this disorder is characterised by resistance within the hypothalamic-pituitary-thyroid axis. Two of the mutations (S314F, S314Y) were identified in separate families with no apparent shared ancestry, suggesting that they had arisen independently in a mutation-prone GC rich region as has been documented previously in RTH (Weiss *et al.*, 1993). Most affected individuals were asymptomatic or noted to have a goitre, but in four cases thyrotoxic features were present. There was no clear correlation between clinical features and the underlying genetic defect, underscoring the variable clinical phenotype in this disorder (Beck-Peccoz and Chatterjee, 1994).

RTH also exhibits molecular heterogeneity, being associated with diverse mutations which all localize to the ligand-binding domain of the TR $\beta$  gene. On the basis of their transcriptional and hormone binding properties, it has been suggested that RTH mutants can be subdivided into three categories (Meier *et al.*, 1993): type I mutants exhibit reduced transactivation consistent with the degree of impairment in their ability to bind ligand; type II mutants show a disproportionate loss of transactivation relative to their altered ligand binding affinity; type III mutants exhibit negligible ligand binding and comparably impaired transactivation. In this study, the mutations that have been identified in codon 314 of TR $\beta$  exhibited divergent functional properties. The S314C substitution resulted in a moderate impairment in hormone binding. Consonant with this, it exhibited a Type I transactivation profile with functional impairment at lower T3 levels but full transactivation at higher T3 concentrations. In contrast, the S314F and S314Y substitutions resulted in a complete loss of ligand binding. These mutants showed Type III transcriptional responses with S314Y being unable to activate transcription and S314F achieving only 15% of the maximal WT response at 1000nM T3 (Figure 3.3).

All three codon 314 mutants are capable of inhibiting the transcriptional activity of wild type TR when they are coexpressed (Figure 3.4). This dominant negative effect has been observed previously with a large number of other RTH mutants and is in keeping with the dominant mode of inheritance of this disorder (Collingwood *et al.*, 1994; Collingwood *et al.*, 1998; Meier *et al.*, 1992). Gel mobility shift assays indicate that all three codon 314 mutants retain the ability to bind to DNA and heterodimerise with RXR (Figure 3.2). This observation supports previous hypotheses that DNA binding and heterodimerisation are functional properties which are critical for RTH mutants to exert dominant negative activity (Collingwood *et al.*, 1994; Nagaya *et al.*, 1992; Nagaya and Jameson, 1993). In addition to differences in transcriptional function, these studies also suggest that the three S314 mutants differ in dominant negative potency: the S314F and S314Y mutants inhibited WT receptor function more strongly (55%) than S314C (32%) (Figure 3.4); in addition, the inhibition by S314F/Y mutants was less readily reversible with higher T3 levels than S314C. It has been suggested that the ability of some RTH mutants to form TR homodimers which constitutively repress basal transcription, may contribute to their dominant negative inhibitory potency (Piedrafita *et al.*, 1995; Yen *et al.*, 1995; Kitajima *et al.*, 1995). In keeping with this hypothesis, it was noted that the weaker dominant negative mutant S314C formed TR homodimers which dissociated more readily with T3 whereas the more potent S314F and S314Y mutants formed homodimer complexes that were less T3 reversible (Figure 3.2). Interestingly, the extent of thyroid dysfunction *in vivo* appeared consistent with the magnitude of receptor dysfunction *in vitro* (Figure 3.5).

To investigate the potential reasons for the marked divergence in their functional properties, the effect of the different amino acid mutations in Ser 314 in human TR $\beta$  has been modelled in collaboration with Dr J.W.R. Schwabe (Laboratory of Molecular Biology, Cambridge, UK) (Wagner *et al.*, 1995). Figure 3.6a shows that the side-chain of Ser 314 plays a structural role in the periphery of the hydrophobic ligand binding cavity, consistent with the functional data indicating its importance in hormone binding. When viewed in greater detail (Figure 3.6b), it is evident that this serine is tightly packed in van der Waal's contact with the side-chains of Ile 353, Ile 431 and Leu 428, with the hydroxyl group of Ser 314 within hydrogen bonding distance of the carbonyls of Met 310 and Glu 311. Mutation of Ser 314 to a cysteine

would probably weaken these hydrogen bonds. However, since the side-chain volumes of serine and cysteine are so similar, few structural perturbations might be anticipated, explaining the relatively modest effect of this mutation on ligand binding. In contrast, when Ser 314 is replaced by a phenylalanine, the bulky aromatic side-chain of the latter clashes sterically with Ile 431, Met 310 and ligand (Figure 3.6c). Rotation of the sidechain of Met 310 to accommodate this, results in a clash with His 435 and Phe 459. It is likely that such steric effects would prove more deleterious and indeed, it is known that different substitutions of His 435 in TR $\beta$  markedly impair ligand binding (Sakurai *et al.*, 1990).

In conclusion, this chapter describes three novel mutations in TR $\beta$  in RTH due to distinct nucleotide substitutions at a single codon (314), which differentially impair receptor function. The data presented suggest that the degree of functional impairment *in vitro* correlates with the extent to which interaction of Ser 314 with T3 is disrupted and might also be related to the magnitude of thyroid dysfunction *in vivo*.

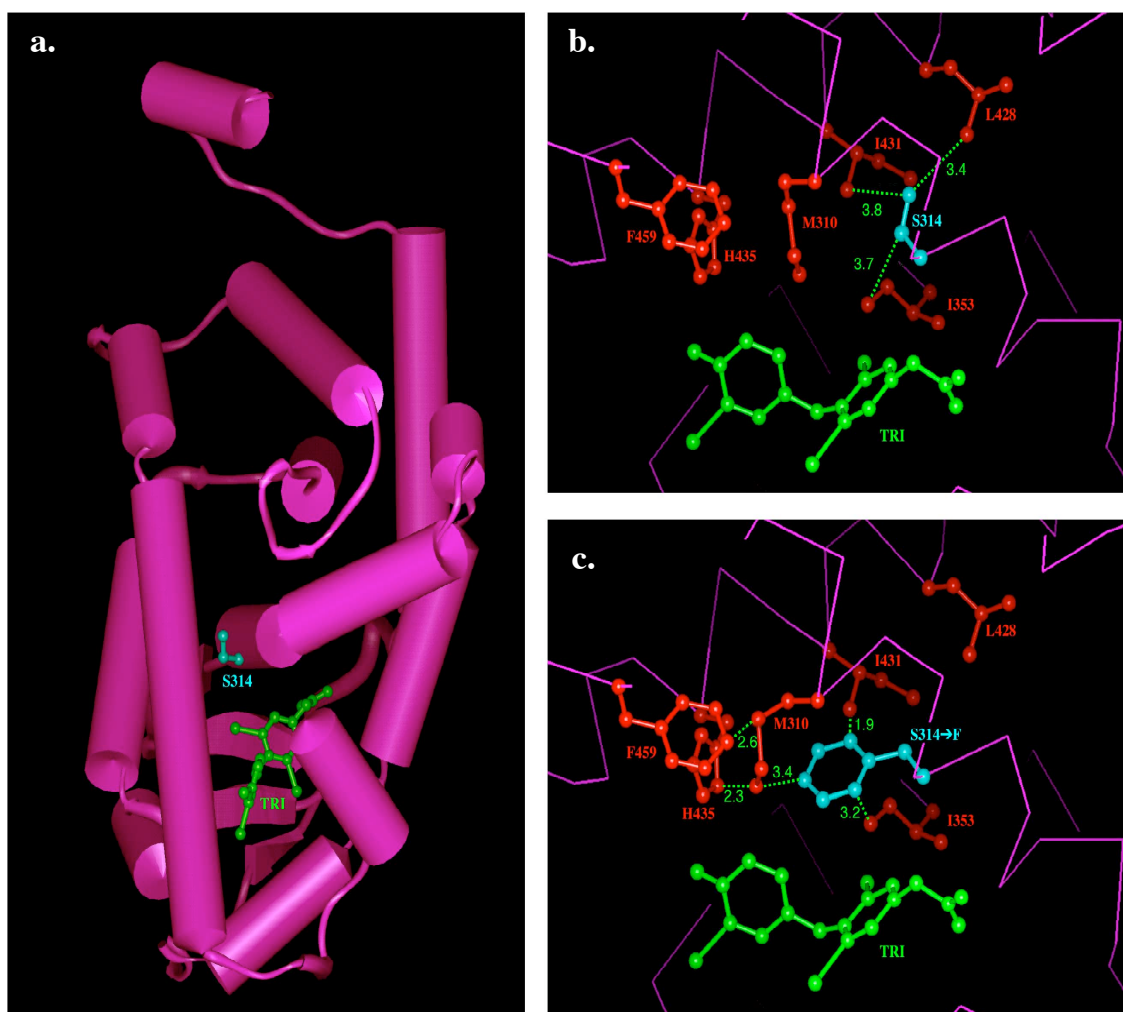


**Figure 3.6 a.** The crystal structure of human TR $\beta$  is shown, with Ser314 located in the periphery of the ligand-binding cavity. **b.** Enlarged view showing the residues in contact with Ser314. **c.** The mutation of Ser314 to Phe was modelled by replacing the side-chain and then selecting the most favourable rotamer conformation. The orientation for the phenylalanine shown here is the only one that did not clash badly with the peptide backbone. However, this orientation clashed with the side-chain of Met310 and Ile431. The orientation of Met310 could be adjusted to avoid the clash with the phenylalanine, but this caused it to clash with both Phe459 and His435. In conclusion the bulky aromatic side-chain cannot readily be accommodated without significant structural perturbations.

## Chapter 4

# TYROSINE AGONISTS REVERSE THE MOLECULAR DEFECTS ASSOCIATED WITH DOMINANT NEGATIVE MUTATIONS IN HUMAN PPAR $\gamma$ .

### 4.1 Introduction

Peroxisome proliferator-activated receptor  $\gamma$  (PPAR $\gamma$ ), a member of the nuclear receptor superfamily, was first characterized as a transcriptional regulator of adipocyte-specific gene expression (Tontonoz *et al.*, 1994a) and preadipocyte differentiation (Tontonoz *et al.*, 1994b). A number of unsaturated fatty acids (arachidonic, linoleic,  $\gamma$ -linolenic, eicosapentaenoic) activate PPAR $\gamma$  and may represent endogenous ligands for the receptor in this context (Kliwer *et al.*, 1997; Desvergne and Wahli, 1999). Eicosanoid derivatives of fatty acids can act as endogenous PPAR $\gamma$  activators in other biological contexts: in the macrophage, hydroxyoctadecadienoic acid (HODE) and hydroxyeicosatetraenoic acid (HETE), the 15-lipoxygenase products of arachidonic and linoleic acids, inhibit the production of inflammatory cytokines (Huang *et al.*, 1999) and promote the uptake and catabolism of oxidised LDL (Nagy *et al.*, 1998); 15-deoxy  $\Delta^{12,14}$  prostaglandin J<sub>2</sub> (15d-PGJ<sub>2</sub>), a terminal metabolite of prostaglandin D<sub>2</sub>, which binds PPAR $\gamma$  and promotes adipocyte differentiation, has been most widely studied as a putative naturally-occurring ligand (Forman *et al.*, 1995; Kliwer *et al.*, 1995).

The thiazolidinediones (TZDs) were synthesised as potentially hypolipidaemic derivatives of clofibrate, but then developed as antidiabetic agents on account of their unexpected insulin sensitising action *in vivo*. TZDs are high affinity PPAR $\gamma$  ligands (Lehmann *et al.*, 1995), with the rank order of their binding affinities mirroring antihyperglycaemic activity, suggesting a role for this receptor in mediating their antidiabetic action. Previously, we described two different mutations (P467L, V290M) in the ligand-binding domain (LBD) of human PPAR $\gamma$  (Barroso *et al.*, 1999) in two families, with affected individuals exhibiting severe insulin resistance, early onset type 2 diabetes mellitus and hypertension, providing direct evidence that

this receptor regulates human glucose homeostasis. In addition to being functionally impaired, the mutant receptors inhibit wild type PPAR $\gamma$  action in a dominant negative manner, consistent with heterozygosity for mutant PPAR $\gamma$  in affected subjects and dominant inheritance of the disorder in one family (Barroso *et al.*, 1999).

The syndrome of Resistance to Thyroid Hormone (RTH), a disorder characterised by elevated circulating thyroid hormones with tissue refractoriness to thyroid hormone action, is associated with similar dominant negative mutations in the human thyroid hormone  $\beta$  receptor (TR $\beta$ ) (Refetoff *et al.*, 1993). Here, functional studies have shown that higher concentrations of ligand can overcome dominant negative inhibition by many TR $\beta$  mutants *in vitro* (Collingwood *et al.*, 1994) and that the administration of supraphysiological doses of thyroid hormone can restore target tissue responsiveness *in vivo* (Hayashi *et al.*, 1995). By analogy, it was reasoned that the administration of a PPAR $\gamma$  agonist to enhance mutant receptor function and reverse dominant negative activity, might represent a rational approach to the treatment of the severe insulin resistance in our affected subjects. Three TZD PPAR $\gamma$  agonists have been developed for clinical use: troglitazone, the first insulin-sensitising antidiabetic agent to be licensed, was later withdrawn due to unpredictable and potentially fatal hepatotoxicity; however the newer agents, pioglitazone and rosiglitazone, offer comparable efficacy and appear to be devoid of this side-effect (Krentz *et al.*, 2000). Recently, high affinity, tyrosine-based, PPAR $\gamma$  agonists, eg. farglitazar (GI 262570), with potent glucose-lowering activity *in vivo* (Brown *et al.*, 1999) and proven antidiabetic efficacy in Type 2 diabetes patients (Fiedorek *et al.*, 2000), have been developed.

In this chapter the functional characterisation of dominant negative natural PPAR $\gamma$  mutants is reported. Consonant with the severe clinical phenotype, a range of putative natural ligands are unable to activate mutant PPAR $\gamma$ . The mutant receptors exhibit markedly impaired transcriptional responses with TZDs, but in contrast, tyrosine-based receptor agonists correct defects in ligand binding, corepressor release and coactivator recruitment, permitting transcriptional activation comparable to wild-type receptor. In comparison to the TZD rosiglitazone, the tyrosine agonist farglitazar completely reverses dominant negative inhibition by both mutant receptors *in vitro* and activates PPAR $\gamma$  target gene (adipocyte P2) expression in

P467L mutant peripheral blood mononuclear cells (PBMCs) more effectively. Crystallographic modelling reveals a structural basis for these observations: both mutations destabilise helix 12 (Kallenberger *et al.*, 2003), and, as in the recently elucidated PPAR $\alpha$ /silencing mediator of retinoid and thyroid receptors (SMRT) structure (Xu *et al.*, 2002) this may facilitate corepressor interaction; conversely, unlike rosiglitazone, the synthetic ligand farglitazar is able to make additional contacts within the receptor ligand-binding pocket, thereby providing additional stability to helix 12, which mediates transactivation. Tyrosine-based PPAR $\gamma$  agonists, rather than TZDs, may represent a more rational approach to restoring mutant receptor function *in vivo* and ameliorating insulin resistance in our patients.



## 4.2 Methods

### 4.2.1 Plasmid constructs

Full-length human PPAR $\gamma$ 1 cDNA was cloned by reverse transcription polymerase chain reaction from total human preadipocyte RNA and introduced into the pcDNA3 expression vector (Invitrogen, Groningen, Netherlands). The P467L and V290M mutants were generated by site-directed mutagenesis of the wild type (WT) receptor template as previously described (Chapter 2; Barroso *et al.*, 1999). DNA sequences encoding residues 173 - 475 of the WT and mutant PPAR $\gamma$  ligand-binding domains (LBDs) were cloned into pGEX4T (Amersham Pharmacia Biotech, Bucks, UK) and AASV (Tone *et al.*, 1994) to yield GST-PPAR $\gamma$  and VP16-PPAR $\gamma$  LBD fusions respectively. Gal4-SMRT consists of the 468 C-terminal amino acids of SMRT fused in-frame to the Gal4 DNA-binding domain (DBD) in pCMX (Chen and Evans, 1995). Gal4-ID1 (amino acids 2302-2352), Gal4-ID2 (amino acids 2131-2201) and Gal4-ID1+2 (amino acids 2131-2352) contain one or more of the nuclear receptor interaction domains of SMRT as reported previously (Nagy *et al.*, 1999). (PPARE)<sub>3</sub>TKLUC (Forman *et al.*, 1995) and UASTKLUC (Tone *et al.*, 1994) have been described previously.

### 4.2.2 Protein-protein interaction assays

Bacterially expressed GST fusion proteins were prepared according to standard protocols (Chapter 2; Barroso *et al.*, 1999). After purification, proteins bound to glutathione-Sepharose beads (Amersham Pharmacia Biotech, Bucks, UK) in binding buffer (40mM HEPES pH 7.8, 100mM KCl, 5mM MgCl<sub>2</sub>, 0.2 mM EDTA, 1% Nonidet P-40, 10% glycerol, 2mM DTT) were mixed with 5 $\mu$ l of <sup>35</sup>S-labelled *in vitro* translated CREB-binding protein (CBP) together with ligand or vehicle, and incubated at 4°C for 2 hours. Following washing with NETN buffer (20mM Tris pH 8.0, 100mM NaCl, 1mM EDTA, 0.5% Nonidet P-40), bound CBP was determined by SDS-PAGE. Comparable loading of the GST-PPAR $\gamma$  LBD fusion proteins was confirmed with Coomassie staining prior to autoradiography.

### **4.2.3 Ligand binding assays**

Hormone-binding assays were performed using bacterially expressed GST-PPAR $\gamma$  LBD fusion proteins and the PPAR $\gamma$  ligands [ $^3$ H]-rosiglitazone and [ $^3$ H]-farglitazar in a modification of a previously described filter binding assay (Chapter 2; Adams *et al.*, 1994). Filters were pre-incubated with BSA (1%) and Tween (1%) to reduce non-specific binding with the [ $^3$ H]-farglitazar compound. Again, addition of comparable amounts of PPAR $\gamma$  LBD fusion proteins was confirmed through Coomassie staining of aliquots subjected to SDS-PAGE. Results denote the mean  $\pm$  s.e.m. of experiments performed on three separate occasions.

### **4.2.4 Transfection assays**

Calcium phosphate-mediated transfection was performed in 24-well plates of 293EBNA cells. Each well was cotransfected with 50-100ng of receptor expression vector, 500ng of reporter construct, 100ng of the internal control plasmid Bos- $\beta$ -gal and, where indicated, 50-100ng of additional construct. Cells were harvested and assayed as outlined in Chapter 2. Results represent the mean  $\pm$  s.e.m. of at least three independent experiments, each performed in triplicate.

### **4.2.5 *aP2* assays in Peripheral Blood Mononuclear Cells (PBMCs)**

These experiments were performed by Dr D.B. Savage (Cambridge, UK) and accordingly the methods are outlined in brief. Blood was obtained from the index case harbouring the P467L PPAR $\gamma$  mutation (Barroso *et al.*, 1999) and peripheral blood mononuclear cells (PBMCs) were isolated by ficoll gradient centrifugation, washed in PBS and cultured in RPMI 1640 (Sigma-Aldrich, Dorset, UK) with 1% charcoal-stripped fetal bovine serum (FBS) in 6-well plates with  $3 \times 10^6$  cells/well. Following exposure to either rosiglitazone or farglitazar for 24 hours, RNA was isolated from cells using a commercial kit (Qiagen, West Sussex, UK) and reverse-transcribed to generate first-strand cDNA. This was serially diluted and analysed by quantitative PCR as described previously (Savage *et al.*, 2001). Results shown are the mean of two independent experiments in the individual carrying the P467L

mutation (a deterioration in her clinical condition precluded venesection for a third determination).

## 4.3 Results

### 4.3.1 *Transcriptional activation*

The transcriptional activities of wild type receptor and PPAR $\gamma$  mutants were assayed by cotransfection of receptor expression vectors together with a reporter gene (PPARE)<sub>3</sub>TKLUC containing three copies of the PPARE from the acyl-CoA oxidase gene linked to the thymidine kinase promoter and luciferase, in the absence or presence of an array of putative natural ligands (Figure 4.1). As has been previously described, WT PPAR $\gamma$  exhibited some constitutive basal transcriptional activity (Zamir *et al.*, 1997), but showed a further transcriptional response to unsaturated fatty acids (linoleic acid, arachidonic acid,  $\gamma$ -linolenic acid), 15d-PGJ<sub>2</sub> and eicosanoids (13-HODE, 15-HETE) which ranged from 50 to 80% of that obtained with a synthetic PPAR $\gamma$  agonist rosiglitazone. In contrast, the P467L and V290M mutants were completely unresponsive to all the natural ligands tested, despite their partial response to the synthetic receptor agonist.

To evaluate the potential therapeutic role of synthetic PPAR $\gamma$  agonists the transcriptional properties of the PPAR $\gamma$  mutants were examined with each of the TZDs licensed for clinical use. In comparison to WT PPAR $\gamma$ , the P467L and V290M mutant receptors were virtually unresponsive to both troglitazone (Figure 4.2c) and pioglitazone (Figure 4.2d) only achieving 40 to 50% of wild type receptor activity at the highest concentration (10 $\mu$ M) of ligand. Similarly, only 1 to 10 $\mu$ M rosiglitazone elicited partial transcriptional responses (50 to 75% of WT) from the mutant receptors (Figure 4.2e). Replacement of the 2,4-thiazolidinedione head group (Figure 4.2a) with tyrosine-based substituents has led to the development of a series of high affinity PPAR $\gamma$  agonists (Figure 4.2b). In marked contrast to the TZDs, these compounds showed greater activity with PPAR $\gamma$  mutants. GW1929 (Figure 4.2f) and GW7845 (Figure 4.2g) induced significant transcriptional activation by both P467L and V290M mutant receptors even at low concentrations (10 to 100nM) of ligand, enabling both mutants to achieve maximal responses comparable to WT receptor. Farglitazar, which is being developed for clinical use, showed the greatest activity, with the PPAR $\gamma$  mutants achieving >75% of wild type receptor activity at 10nM concentration of ligand (Figure 4.2h). Importantly, such greater potency of tyrosine

agonists compared to thiazolidinedione was more evident with PPAR $\gamma$  mutants than WT receptor. Thus, whereas farglitazar was 100 times more potent than rosiglitazone with WT PPAR $\gamma$  (WT activation with 100nM rosiglitazone (Figure 4.2e) versus 1nM farglitazar (Figure 4.2h), the tyrosine agonist was 1000 times more potent than rosiglitazone with the PPAR $\gamma$  mutants (P467L and V290M activation with 10,000nM rosiglitazone (Figure 4.2e) versus 10nM farglitazar (Figure 4.2h).

#### **4.3.2 Hormone binding assay and coactivator recruitment**

It has previously been shown that the impaired transcriptional function of the P467L PPAR $\gamma$  mutant reflects a combination of defects in binding to ligand and recruitment of coactivator (Barroso *et al.*, 1999). A comparison of these properties of the P467L and V290M receptor mutants was therefore made with TZD versus tyrosine-based PPAR $\gamma$  agonists. In ligand binding assays with bacterially expressed WT or mutant GST-PPAR $\gamma$  LBD fusion proteins and [<sup>3</sup>H]-rosiglitazone or [<sup>3</sup>H]-farglitazar, neither mutant receptor exhibited specific binding to the radiolabelled TZD, whereas both mutant proteins showed significant specific binding to the tyrosine agonist (Figure 4.3). In a protein-protein interaction assay, both rosiglitazone and farglitazar ligands mediated strong recruitment of <sup>35</sup>S-labelled coactivator CBP to wild type receptor. However, the P467L and V290M mutants showed negligible coactivator binding even at high concentrations (10 $\mu$ M) of thiazolidinedione, whereas a lower concentration (1 $\mu$ M) of tyrosine agonist promoted recruitment of CBP (Figure 4.4).

#### **4.3.3 Basal repression and corepressor recruitment**

Some members of the nuclear receptor family (e.g., TR and RAR) are able to silence basal gene transcription through ligand-independent interaction with specific corepressor proteins such as NCoR (Horlein *et al.*, 1995) and SMRT (Chen and Evans, 1995) with ligand binding promoting corepressor dissociation. The effects of P467L and V290M mutant receptors on basal gene transcription and their interaction with corepressor were therefore examined. In comparison to cells transfected with empty expression vector, WT PPAR $\gamma$  activated basal reporter gene activity (~5-fold); in striking contrast, both PPAR $\gamma$  mutants not only lacked such activation but

significantly repressed basal gene transcription (pcDNA3 = 1.0; P467L = 0.44; V290M = 0.53) (Figure 4.5), suggesting that they might interact aberrantly with corepressors *in vivo*. Several studies have identified domains (ID1 and ID2) within NCoR and SMRT that mediate interaction with nuclear receptors (Nagy *et al.*, 1999; Perissi *et al.*, 1999). To study the interaction between PPAR $\gamma$  mutants and corepressor, mammalian two-hybrid assays were performed, with cotransfection of fusions consisting of the ID1+2, ID2 or ID1 domains of SMRT linked to the DNA-binding domain of Gal4, together with VP16 linked to either WT, P467L or V290M PPAR $\gamma$  LBDs. In the absence of ligand, WT receptor and both PPAR $\gamma$  mutants were recruited comparably to Gal4-ID1+2, and additional experiments with individual ID domain fusions indicated that this interaction was mediated through the ID1 region (Figure 4.6). Next, the effect of thiazolidinedione versus tyrosine-based PPAR $\gamma$  agonists on receptor-corepressor interaction was investigated. With the addition of increasing concentrations (100 to 1000nM) of TZD ligand (rosiglitazone), both mutant receptors exhibited significantly attenuated and incomplete dissociation from a Gal4-ID1 corepressor fusion when compared to the WT receptor (Figure 4.7). However, the addition of tyrosine agonist (farglitazar) induced progressive and nearly complete dissociation of both mutant receptors from Gal4-ID1 similar to WT PPAR $\gamma$  (Figure 4.7).

#### **4.3.4 Dominant negative activity**

Previous studies indicate that inhibition of wild type receptor function by the P467L and V290M PPAR $\gamma$  mutants is a likely mechanism for impaired receptor action *in vivo* (Barroso *et al.*, 1999). A comparison of the relative efficacy of both natural and synthetic agonists in ameliorating such dominant negative inhibition by PPAR $\gamma$  mutants was made. Cells transfected with WT receptor plus an equal amount of either P467L or V290M PPAR $\gamma$  mutants were studied with increasing concentrations of natural (15d-PGJ<sub>2</sub>) or synthetic ligands (rosiglitazone or farglitazar). In keeping with their transcriptional activities with each ligand when tested alone, the P467L and V290M mutants exhibited significant dominant negative inhibition (30-35%) of wild type receptor function even at maximal concentrations of 15d-PGJ<sub>2</sub> (Figure 4.8). Moreover, both mutants exerted strong dominant negative activity at low

(10nM) concentrations of TZD and such inhibition was retained at higher (1 $\mu$ M) levels of ligand with the V290M mutant (Figure 4.8). In contrast, low (10nM) or high (1 $\mu$ M) concentrations of tyrosine agonist farglitazar completely reversed dominant negative inhibition by the PPAR $\gamma$  mutants (Figure 4.8).

Failure of ligand-dependent corepressor release has been shown to mediate dominant negative inhibition by natural TR $\beta$  mutants in RTH (Yoh *et al.*, 1997). We therefore sought to determine whether corepressor interaction is important for dominant negative activity of the natural PPAR $\gamma$  mutants. The crystal structure of a PPAR $\alpha$ -SMRT complex has recently been elucidated (Xu *et al.*, 2002) and residues in PPAR $\alpha$  that mediate binding to a polypeptide from SMRT are highly conserved in PPAR $\gamma$  (Fig 4.13). One of these conserved residues in PPAR $\gamma$  (Leu 318) was mutated to Alanine on either wild type or P467L mutant PPAR $\gamma$  backgrounds, with comparison of their transcriptional properties in the absence of ligand. The L318A receptor mutant showed comparable constitutive activity to WT PPAR $\gamma$ ; however, the P467L/L318A double mutation exhibited attenuated repression of basal transcription when compared with the P467L mutant (Figure 4.9: pcDNA3 = 1.0; P467L = 0.48; P467L/L318A = 0.85). Consistent with this, in a mammalian two-hybrid assay, the L318A mutation abolished interaction of the P467L mutant with the ID1 domain of SMRT corepressor (Figure 4.9, inset). Moreover, in comparison to the P467L mutation alone, the P467L/L318A double mutant exhibited almost negligible dominant negative inhibition of WT PPAR $\gamma$  activity (Figure 4.10).

#### ***4.3.5 aP2 expression in primary human monocytes harbouring dominant negative PPAR $\gamma$***

The adipocyte P2 (aP2) gene, a well-validated PPAR $\gamma$  target gene has previously been shown to be expressed and regulated by PPAR $\gamma$  ligands in peripheral blood mononuclear cells (PBMCs) (Pelton *et al.*, 1999). To determine whether the differences in mutant PPAR $\gamma$  responses to synthetic agonists observed *in vitro* might correlate with ligand-dependent responses in cells from our affected subjects, the ability of both rosiglitazone and farglitazar to induce aP2 expression in cultured PBMCs taken from the index case harbouring the P467L mutation (Barroso *et al.*, 1999) was examined. Rosiglitazone induced aP2 expression in patient PBMCs in a

dose dependent manner, but with farglitazar the dose response curve of the target gene activation was significantly left shifted (Figure 4.11). The magnitude of maximal aP2 target gene induction in response to either ligand was similar. The results suggest that the tyrosine agonist is a more potent activator of PPAR $\gamma$ -mediated transcription than its thiazolidinedione counterpart in primary cells from an affected subject.



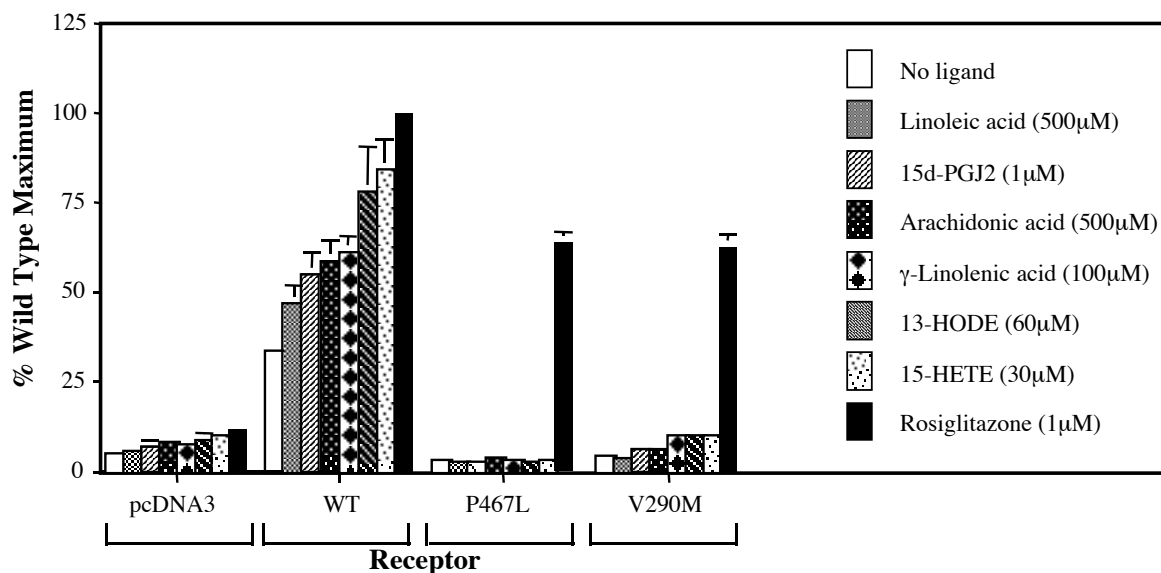


**Figure 4.1** A panel of putative endogenous ligands fail to transactivate mutant PPAR $\gamma$ . 24-well plates of 293EBNA cells were transfected with 500ng of (PPARE)<sub>3</sub>TKLUC reporter gene, 100ng of Bos- $\beta$ -gal control plasmid and 100ng of empty (pcDNA3) or different receptor expression vectors as shown. Transcriptional activity in response to a variety of endogenous ligands is shown. Results represent the mean  $\pm$  s.e.m. of at least 3 independent experiments, each performed in triplicate, and are expressed as a percentage of the maximal wild type observed response. 15 d-PGJ2 - 15 deoxy $\Delta^{12, 14}$  prostaglandin J2; 13-HODE–hydroxyoctadecadienoic acid; 15-HETE– hydroxyeicosatetraenoic acid.

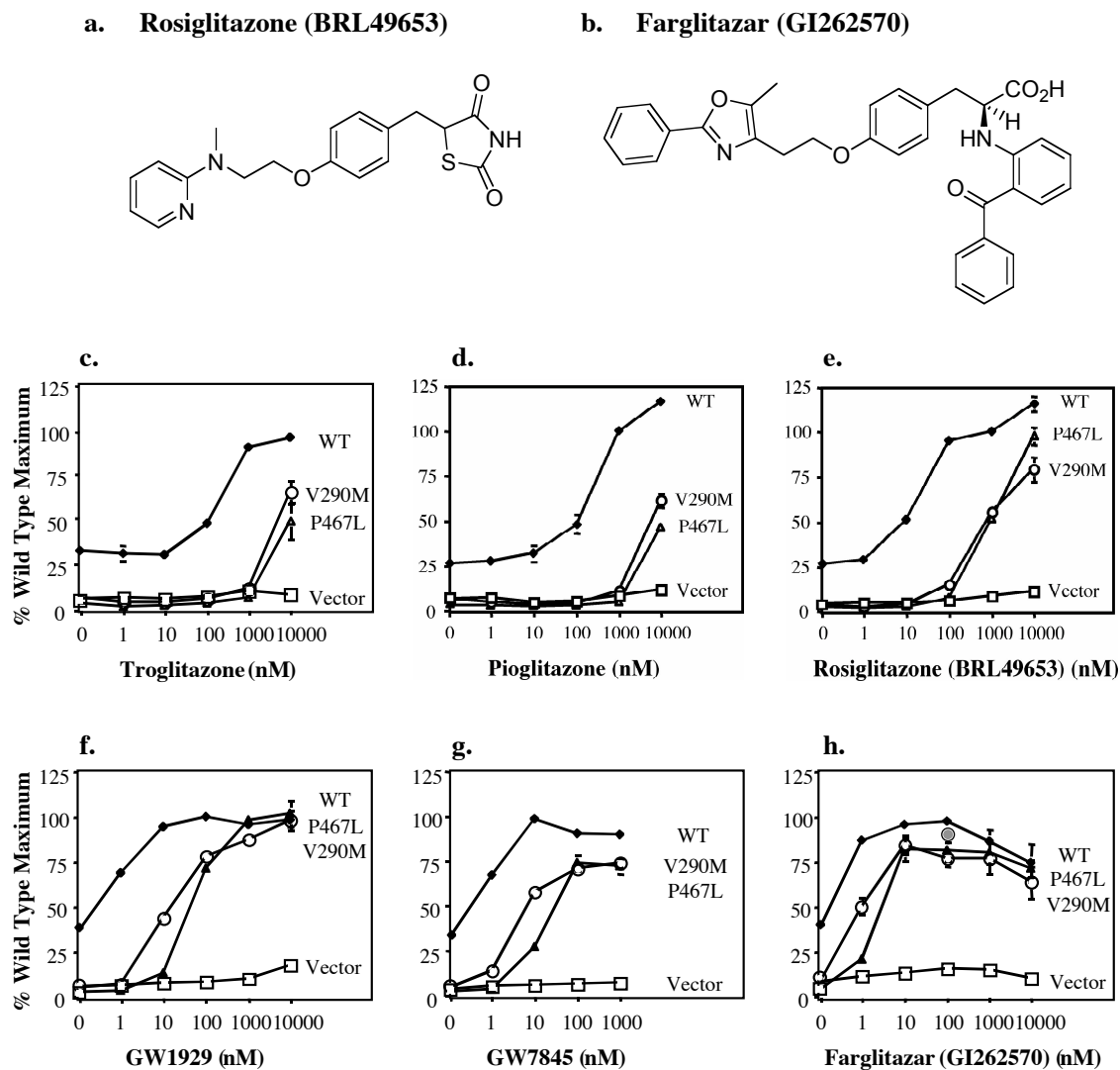


**Figure 4.2 a,b.** Synthetic PPAR $\gamma$  agonists. Comparison of the chemical structures of **a.** rosiglitazone (thiazolidinedione) and **b.** farglitazar (tyrosine agonist). **c-h.** Tyrosine-based but not thiazolidinedione receptor agonists restore the transcriptional activity of P467L and V290M PPAR $\gamma$  mutants. 24-well plates of 293EBNA cells were transfected as outlined in **Figure 4.1**. Transcriptional activity in response to ligand is shown for **c.** troglitazone **d.** pioglitazone **e.** rosiglitazone **f.** GW1929 **g.** GW7845 and **h.** farglitazar. Results (expressed as a percentage of the wild type maximum) denote the mean  $\pm$  s.e.m. of at least 3 independent experiments each performed in triplicate. The *gray circle* in **h.** denotes the transcriptional response of WT PPAR $\gamma$  to 100 nM rosiglitazone, indicating that it is the same magnitude as maximal receptor responses to farglitazar.

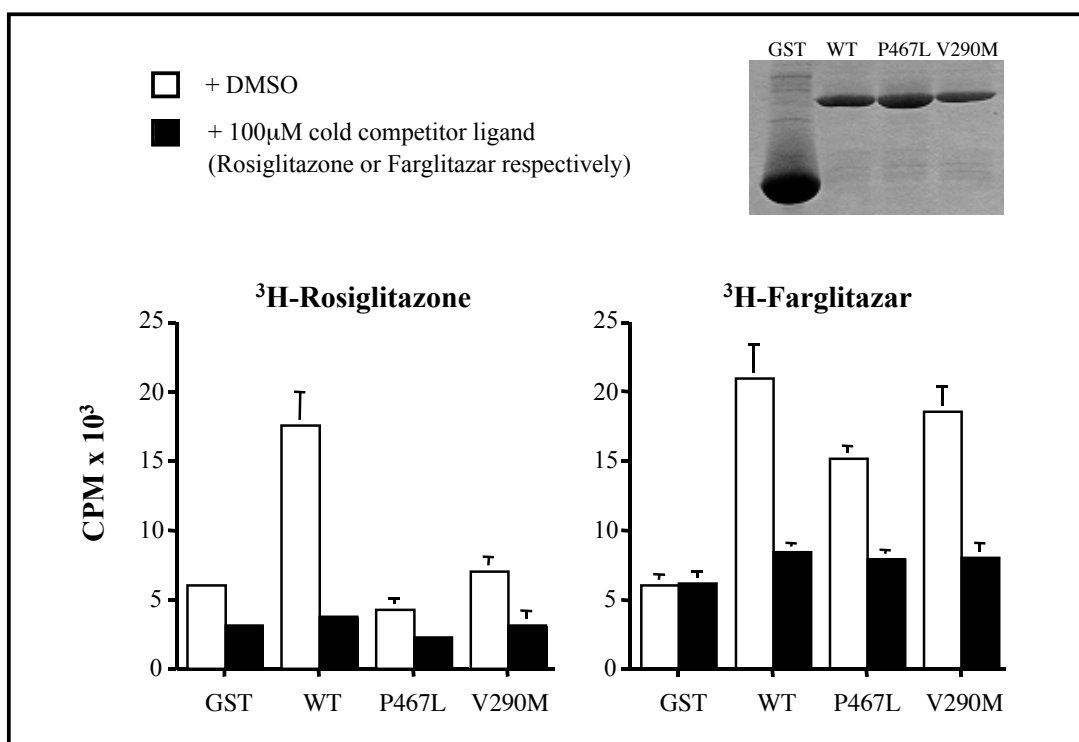


**Figure 4.3** Binding of thiazolidinedione (<sup>3</sup>H-rosiglitazone) and tyrosine agonist (<sup>3</sup>H-farglitazar) radioligands to GST-PPAR $\gamma$  ligand-binding domain (LBD) chimaeras. Bacterially expressed GST-PPAR $\gamma$  LBD fusion proteins were incubated with radioligand as indicated, in the absence or presence of 10μM cold competing ligand (rosiglitazone or farglitazar respectively). *Inset*: Coomassie-stained gel of proteins used in ligand binding assays confirming comparable expression of WT and mutant receptors, with GST present in excess. Results represent the mean  $\pm$  s.e.m. of 3 independent experiments each performed in duplicate.

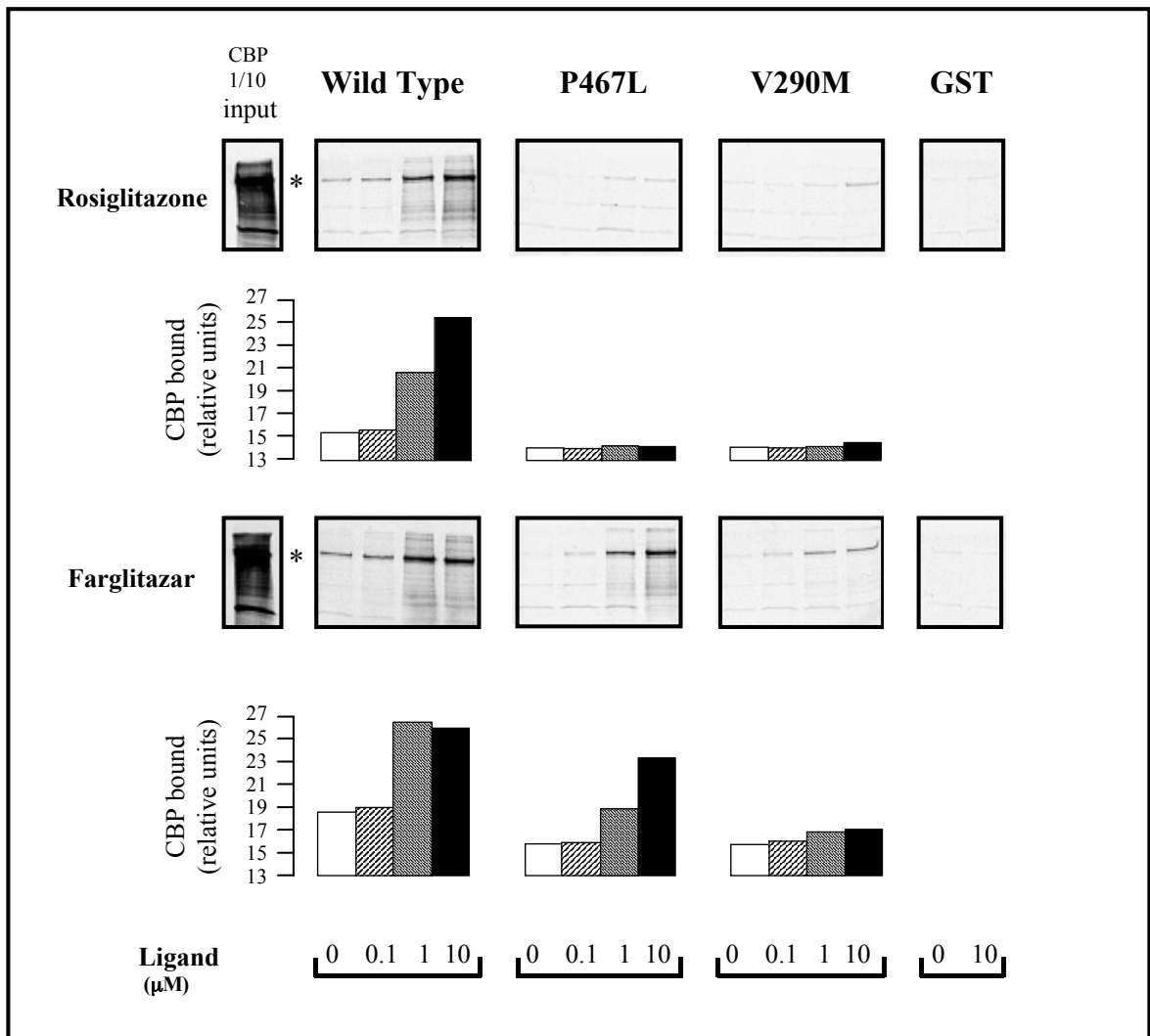


**Figure 4.4** Coactivator recruitment to mutant PPAR $\gamma$  is greater with tyrosine agonist (farglitazar) than thiazolidinedione (rosiglitazone). WT and mutant GST-PPAR $\gamma$  LBD fusion proteins (quantitated as in Figure 4.3) were tested for interaction with  $^{35}\text{S}$ -labelled *in vitro* translated CREB-binding protein (CBP) in the presence of increasing concentrations of ligand (rosiglitazone or farglitazar). Control assays were performed with GST alone. Histograms below each panel quantify the amount of CBP bound. An asterisk (\*) denotes the band corresponding to full-length CBP.

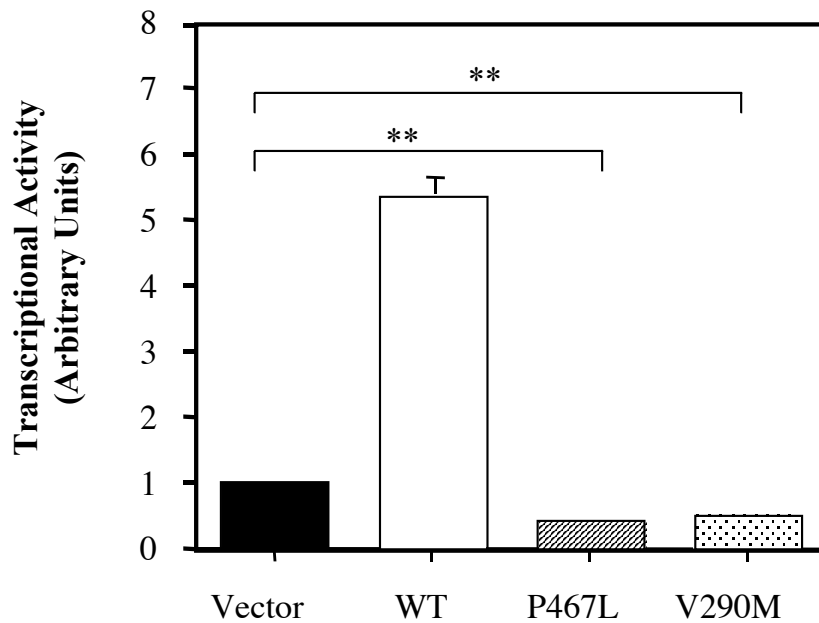


**Figure 4.5** PPAR $\gamma$  mutants repress basal transcription. **a.** Unlike their Wild Type (WT) counterpart, both the P467L and V290M mutants silence basal gene transcription. 293EBNA cells were transfected with 500ng reporter gene (PPARE) $_3$ TKLUC, 100ng Bos- $\beta$ -gal (internal control) and 100ng of receptor expression vectors (empty vector, WT, P467L or V290M). Results represent the mean  $\pm$  s.e.m. of 3 independent experiments each performed in triplicate.

\*\* ,  $P < 0.001$



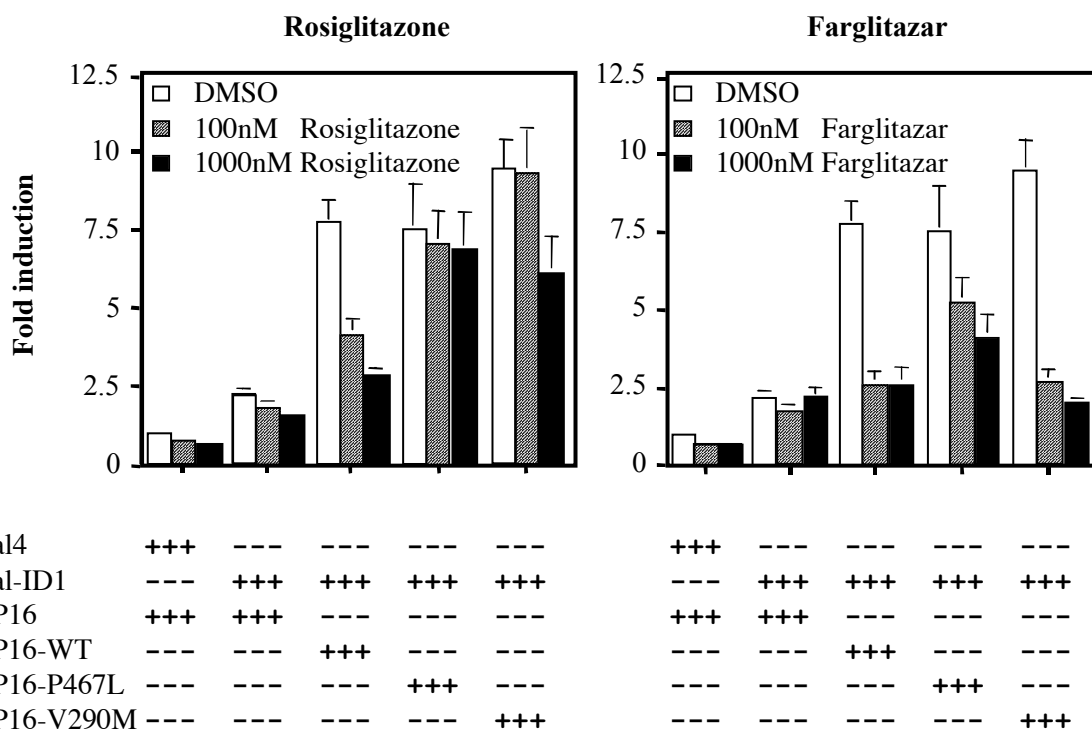


**Figure 4.7** Farglitazar is more effective than rosiglitazone in promoting corepressor dissociation from mutant PPAR $\gamma$ . 293EBNA cells were transfected with 500ng of the reporter construct UASTKLUC, 100ng of the internal control Bos- $\beta$ -gal, 50ng of expression vectors encoding the Gal4 DNA-binding domain (Gal4) alone or fused to the ID1 domains of SMRT, and 50ng of expression vector encoding VP16 alone or VP16 fused to the ligand-binding domain of WT PPAR $\gamma$  (WT), P467L PPAR $\gamma$  (P467L) or V290M PPAR $\gamma$  (V290M) and treated with vehicle (dimethylsulfoxide, DMSO), rosiglitazone or farglitazar. In all cases, results represent the mean  $\pm$  s.e.m. of 3 independent experiments each performed in triplicate.

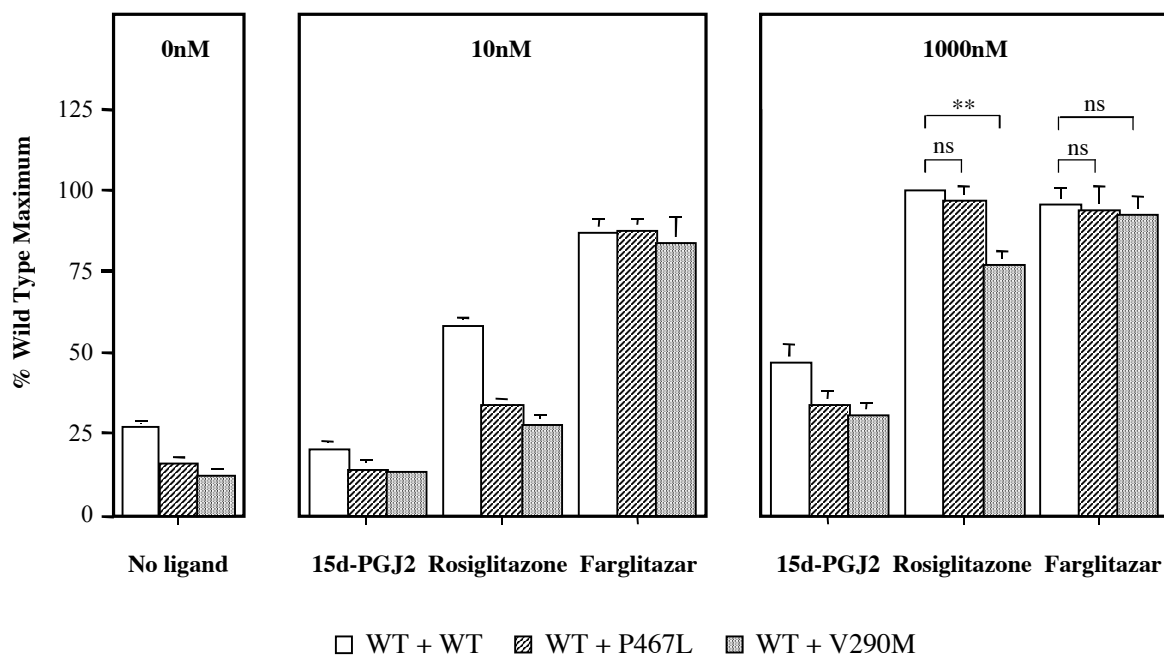


**Figure 4.8** Tyrosine agonist (farglitazar) reverses dominant negative inhibition by PPAR $\gamma$  mutants more effectively than putative natural ligand (15d-PGJ2) or thiazolidinedione (rosiglitazone). 293EBNA cells were transfected with 100ng of wild type (WT) receptor plus an equal amount of either WT or mutant (P467L; V290M) expression vector (with the same reporter gene and internal control constructs as described in figure 4.1), in the presence of increasing concentrations of ligand. The transcriptional responses mediated by either 100ng or 200ng of WT receptor were identical (data not shown). Results are expressed as a percentage of the wild type maximum response and represent the mean  $\pm$  s.e.m. of 3 independent experiments each performed in triplicate. \*\*,  $P < 0.001$ ; ns, not significant.



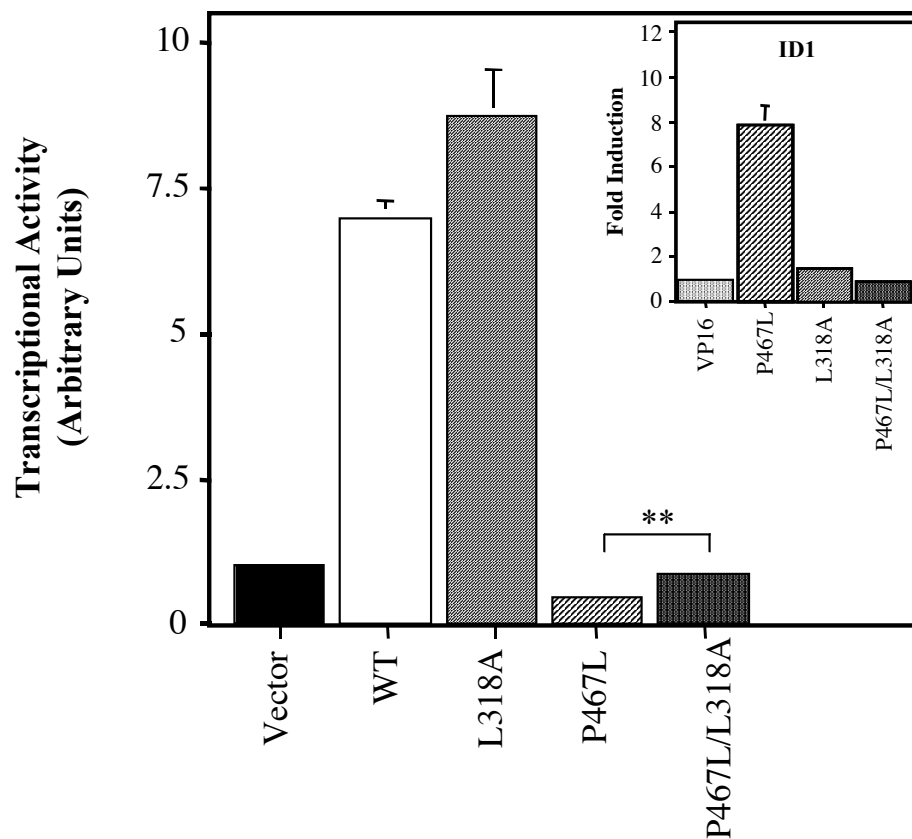


**Figure 4.9** Basal transcriptional repression by the P467L natural mutant is reversed, but constitutive activity of WT PPAR $\gamma$  is not affected by the addition of an L318A mutation. Inset, Interaction of P467L with the ID1 domain of SMRT in two hybrid assays is abolished after introduction of the L318A mutation. 293EBNA cells were transfected and results analyzed as in Figures 4.5 and 4.7. \*\*, P < 0001.

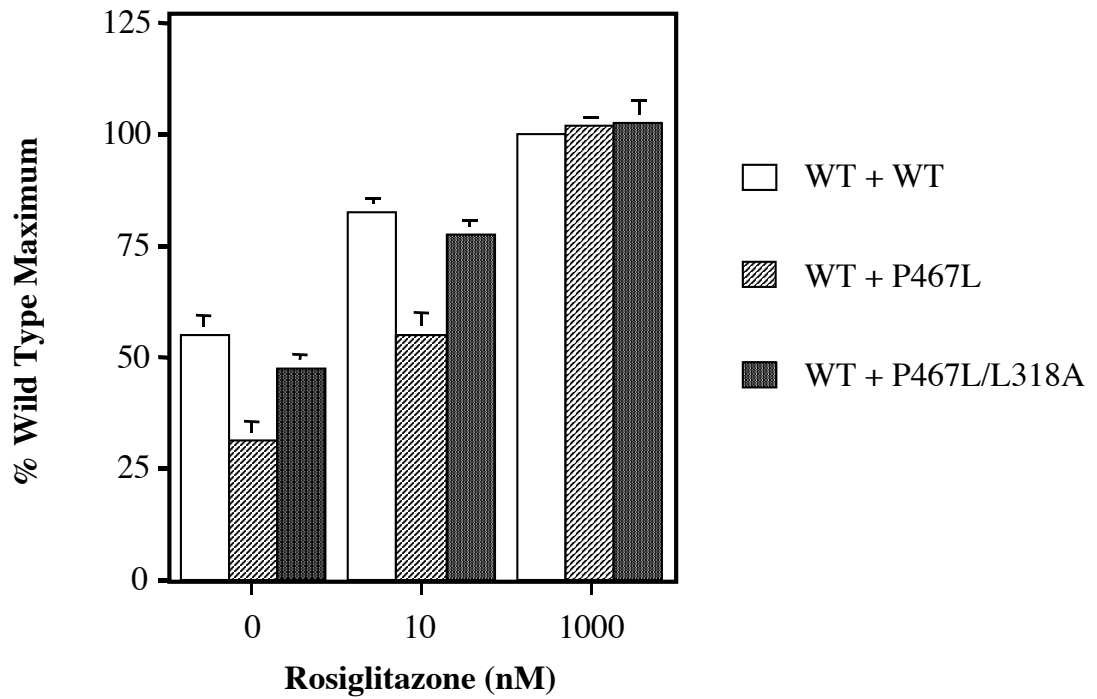


**Figure 4.10** Introduction of the L318A mutation significantly attenuates the dominant negative activity of the P467L PPAR $\gamma$  mutant through abolition of its interaction with corepressor. 293EBNA cells were transfected as in Figure 4.8 and treated with vehicle (dimethylsulfoxide, DMSO) or rosiglitazone.

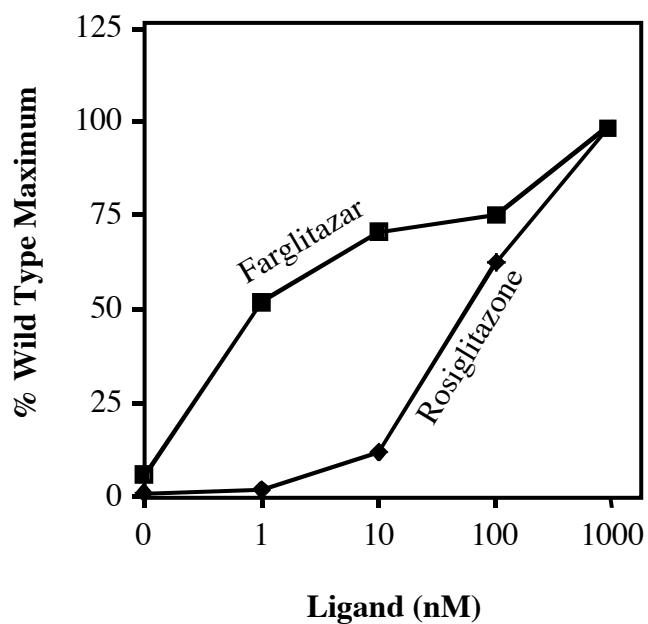


**Figure 4.11** The tyrosine agonist (farglitazar) enhances target gene (aP2) expression in P467L mutant receptor containing peripheral blood mononuclear cells (PBMCs) more effectively than thiazolidinedione (rosiglitazone). Following 24 hours exposure to increasing concentrations of rosiglitazone or farglitazar, aP2 gene expression in PBMCs was quantitated by RT-PCR. The results are expressed as a percentage of the maximum response and represent the mean of two (P467L) independent experiments. The s.e.m was less than 10% and has been omitted for clarity. The data shown in this figure has been kindly provided by Dr D. Savage (University of Cambridge).

#### 4.4 Discussion

We have previously described two different heterozygous, loss-of-function mutations (P467L, V290M) in the ligand-binding domain of human PPAR $\gamma$ . Affected individuals exhibited marked fasting hyperinsulinaemia and the skin lesion acanthosis nigricans signifying severe insulin resistance; importantly, subjects had developed complications secondary to insulin resistance, including characteristic dyslipidemia (elevated triglycerides, low high-density lipoprotein cholesterol), ovarian dysfunction and type 2 diabetes mellitus; they also showed early-onset hypertension unrelated to diabetic comorbidity (Barroso *et al.*, 1999). Whereas both receptor mutants were very functionally impaired and dominant negative inhibitors of wild type receptor action, they retained some transcriptional activity at highest concentrations of ligand (Barroso *et al.*, 1999). We therefore reasoned that if either higher levels of endogenous natural ligands or synthetic receptor agonists could overcome the functional defect and dominant negative inhibition by PPAR $\gamma$  mutants *in vitro*, they might be useful to treat the severe clinical phenotype when administered *in vivo*.

Despite being able to activate transcription via wild type PPAR $\gamma$ , even micromolar concentrations of putative endogenous ligands, including omega-3 ( $\gamma$ -linolenic) and omega-6 (linoleic, arachidonic) polyunsaturated fatty acids, eicosanoids (13-HODE, 15-HETE) and 15d-PGJ<sub>2</sub>, were unable to induce transcriptional activity from the mutant receptors (Figure 4.1). Furthermore, high levels of 15d-PGJ<sub>2</sub> were unable to reverse significant dominant negative inhibition of wild type receptor function by the P467L and V290M PPAR $\gamma$  mutants (Figure 4.8). Such unresponsiveness of mutant receptors to endogenous ligands correlates with the clinical findings of partial lipodystrophy in adults and significant insulin resistance even in two young children aged 4 and 7yrs with the P467L mutation (Savage *et al.*, 2003), which underscore the severity of the clinical phenotype. In addition, such unresponsiveness *in vitro* suggests that raising levels of endogenous PPAR $\gamma$  ligands in affected subjects is unlikely to be a successful therapeutic approach.

With thiazolidinedione PPAR $\gamma$  agonists, both the lower affinity (WT PPAR $\gamma$  EC<sub>50</sub>=500nM) agents troglitazone and pioglitazone and the more potent (WT PPAR $\gamma$  EC<sub>50</sub>=43nM) rosiglitazone, induced significant transcriptional activity with the

P467L and V290M mutants only at 10 $\mu$ M or 1 $\mu$ M concentrations of ligand (Figure 4.2c-e). A novel class of synthetic PPAR $\gamma$  ligands (GW1929, GW7845 and farglitazar), where N-tyrosine moieties have been substituted for the 2,4-thiazolidinedione head group, have been developed (Henke *et al.*, 1998) and are known to be high affinity ( $EC_{50}$ =0.3-6nM) agonists for wild type PPAR $\gamma$ . In marked contrast to TZDs, the tyrosine-based agonists proved capable of rescuing mutant PPAR $\gamma$  function even at low concentrations of ligand (1-10nM), eliciting a maximal transcriptional response comparable to WT receptor (Figure 4.2f-h). Furthermore, the greater potency of tyrosine versus thiazolidinedione agonist is more marked with the PPAR $\gamma$  mutants than wild type receptor, indicating that this class of ligand acts specifically to restore mutant receptor function.

Further comparisons of rosiglitazone versus farglitazar, indicated that the ability of the tyrosine agonist to correct deficits in ligand binding, coactivator recruitment and corepressor displacement mediated its enhancement of mutant receptor function (Figures 4.3, 4.4 and 4.7). To elucidate the molecular basis for the observed differences between the two classes of PPAR $\gamma$  ligand, the crystal structures of the PPAR $\gamma$ /RXR $\alpha$  heterodimer complexed with either rosiglitazone or farglitazar (Gampe *et al.*, 2000) were examined in collaboration with Dr J.W.R. Schwabe (Laboratory of Molecular Biology, Cambridge, UK). In keeping with other nuclear receptors, an amphipathic  $\alpha$ -helix (H12) at the receptor carboxy-terminus mediates important interactions with both ligand and coactivator (SRC-1) (Nolte *et al.*, 1998): in both crystal structures, Tyr473 makes contact with ligand, forming hydrogen bonds with either the 2,4-thiazolidinedione headgroup of rosiglitazone or the carboxylate headgroup of farglitazar; the side chain of Leu468 from the opposite side of H12 contributes to a hydrophobic cleft on the receptor surface which accommodates the coactivator peptide whereas Glu471 acts in concert with Lys 301 to form a “charge clamp” that stabilises interaction with coactivator. Pro467 forms the amino-terminal boundary of helix 12 and Val290 (within helix 3) packs against H12. It has been previously demonstrated, using fluorescence anisotropy, that mutation of either residue disrupts the position and orientation of helix 12, thereby compromising interactions with both ligand and coactivator (Kallenberger *et al.*, 2003). Comparison of the TZD versus tyrosine agonist-bound PPAR $\gamma$  structures reveals that farglitazar occupies more (~ 40% vs. 25%) of the ligand-binding pocket

with a 5-methyl-2-phenyloxazole tail and benzophenone head group, making additional hydrophobic interactions in the cavity, which probably account for its increased PPAR $\gamma$ -binding affinity, compared with rosiglitazone (Figure 4.12). Unlike a subset of nuclear receptors (including TR and RAR) which are capable of repressing basal transcription in the absence of ligand through recruitment of corepressor proteins such as NCoR (Horlein *et al.*, 1995) and SMRT (Chen and Evans, 1995), in transfection assays wild type PPAR $\gamma$  exhibits constitutive transcriptional activity (Figure 4.5) (Zamir *et al.*, 1997). Whether such activity represents receptor activation by endogenous PPAR $\gamma$  ligands or is an intrinsic property of unliganded PPAR $\gamma$ , with H12 being in an “active” conformation in the apo-receptor crystal structure (Nolte *et al.*, 1998) remains unclear. In contrast, both the P467L and V290M PPAR $\gamma$  mutants not only lack such constitutive activity but also act as potent transcriptional repressors in the absence of exogenous ligand (Figure 4.5). These properties are similar to those of artificial dominant negative human [L468A/E471A (Gurnell *et al.*, 2000)] and murine [L466A (Park *et al.*, 2003)] PPAR $\gamma$  mutants described previously. However, in a two-hybrid assay, both WT and natural PPAR $\gamma$  mutants recruited corepressors (Figure 4.6). To reconcile these apparently discordant observations, we suggest that corepressor is greatly over expressed relative to endogenous coactivators in the two-hybrid assay, probably promoting its interaction with WT PPAR $\gamma$  in a manner which is not relevant to its normal action in cells containing more physiological levels of each cofactor type. Evidence in favour of this notion is provided by our observation that the introduction of a mutation (L318A), which disrupts corepressor interaction with both WT PPAR $\gamma$  and the P467L mutant, has no discernible effect on the constitutive transcriptional activity of WT receptor, whereas it reverses transcriptional silencing and dominant negative inhibition by the P467L mutant (Figures 4.9 and 4.10).

The ability to silence basal gene transcription is also a characteristic of dominant negative inhibition by mutant nuclear receptors in other disorders e.g. thyroid hormone receptor  $\beta$  (TR  $\beta$ ) mutants in resistance to thyroid hormone (RTH) (Yoh *et al.*, 1997), the PML-RAR fusion protein in acute promyelocytic leukaemia (APML) (Lin *et al.*, 1998), and the oncogene *v-erbA* (Damm *et al.*, 1989). Furthermore, some TR $\beta$  mutants in RTH have been shown to interact aberrantly with corepressor, exhibiting failure to dissociate fully with ligand (Clifton-Bligh *et al.*, 1998; Safer *et*

*al.*, 1998), and corepressor dissociation from PLZF-RAR fusions in APL is refractory to retinoic acid treatment (Lin *et al.*, 1998; Grignani *et al.*, 1998; He *et al.*, 1998). In this context, both PPAR $\gamma$  mutants exhibited delayed and incomplete corepressor release in the presence of saturating levels (1 $\mu$ M) of rosiglitazone (Figure 4.7), whereas a moderate concentration (100nM) of farglitazar promoted near normal dissociation of corepressor (Figure 4.7). Furthermore, such failure of natural PPAR $\gamma$  mutants to release corepressor fully with TZD is analogous to the properties of the artificial helix 12 PPAR $\gamma$  mutants (L468A/E471A; L466A) described previously (Gurnell *et al.*, 2000; Park *et al.*, 2003).

Recently, the crystal structure of a ternary complex consisting of the PPAR $\alpha$  LBD bound to an antagonist and a polypeptide motif from the corepressor SMRT has been solved (Xu *et al.*, 2002). Notable features of this structure include 1) displacement of helix 12 such that it adopts a different position compared to its active conformation in the agonist-bound structure and 2) docking of a SMRT motif in a hydrophobic groove formed by helices 3, 4 and 5 of the receptor. The LBDs of PPAR $\gamma$  and PPAR $\alpha$  are similar (~71% homology) and an alignment of residues in helix 3 from the receptors (Figure 4.13) indicates striking homology, with 12 out of 14 amino acids mediating PPAR $\alpha$ -SMRT interaction being identical in PPAR $\gamma$ . These observations permit crystallographic modelling to provide insights into how the natural PPAR $\gamma$  mutations (P467L, V290M) facilitate interaction with corepressor. Both mutations destabilise helix 12, preventing it from adopting the agonist-bound conformation (Kallenberger *et al.*, 2003). By analogy with the altered conformation of helix 12 in the antagonist-bound PPAR $\alpha$ /SMRT structure, we suggest that such displacement of H12 favours corepressor recruitment. In addition, with the V290M mutation, an additional factor may stabilise corepressor binding. A crystallographic model of PPAR $\gamma$  complexed with SMRT (Figure 4.14) shows that the side chain of V290 is in contact with an isoleucine residue (I + 4) of the SMRT motif. However the interaction is relatively weak due to the distance (~4Å) between the isoleucine and valine residues and the fact that these hydrophobic side chains are partially solvent exposed. In contrast, when residue 290 is substituted by methionine, its extended side chain has improved van der Waals contacts, predicting stabilization of corepressor interaction.

Whereas both PPAR  $\gamma$  mutants inhibited wild type receptor function significantly at lower (10nM) concentrations of rosiglitazone (Figure 4.8), the same concentration of farglitazar fully relieved dominant negative inhibition by both mutant receptors (Figure 4.8). To determine whether differential responses of the mutant receptors to the two ligands *in vitro* might translate into differences in clinical efficacy *in vivo*, the abilities of both rosiglitazone and farglitazar to induce PPAR $\gamma$  target gene (aP2) expression in PBMCs from a patient with the P467L receptor mutation were compared. As anticipated, even at low concentrations (1 to 10nM), farglitazar evoked a greater target gene response from mutant PBMCs than was observed with rosiglitazone, indicating greater efficacy of the tyrosine agonist versus its TZD counterpart (Figure 4.11). Although peak plasma drug levels following oral administration of farglitazar (5mg) are slightly lower (300nM) (Sorbera *et al.*, 2001) than after 8mg of rosiglitazone (1 $\mu$ M) (Cox *et al.*, 2000), these studies indicate that they still exceed concentrations of agonist required to restore the function and abrogate dominant negative activity of mutant receptors *in vitro*. A trial of rosiglitazone therapy in a subject with the P467L mutation was more effective than in the subject with the V290M PPAR $\gamma$  mutation, mirroring the dominant negative properties of these mutant receptor *in vitro* (Savage *et al.*, 2003). Accordingly, the tyrosine-based PPAR $\gamma$  agonist may have greater potential efficacy *in vivo* and future clinical studies will determine whether it does represent a more rational therapeutic approach to treating the severe insulin resistance in our affected patients.



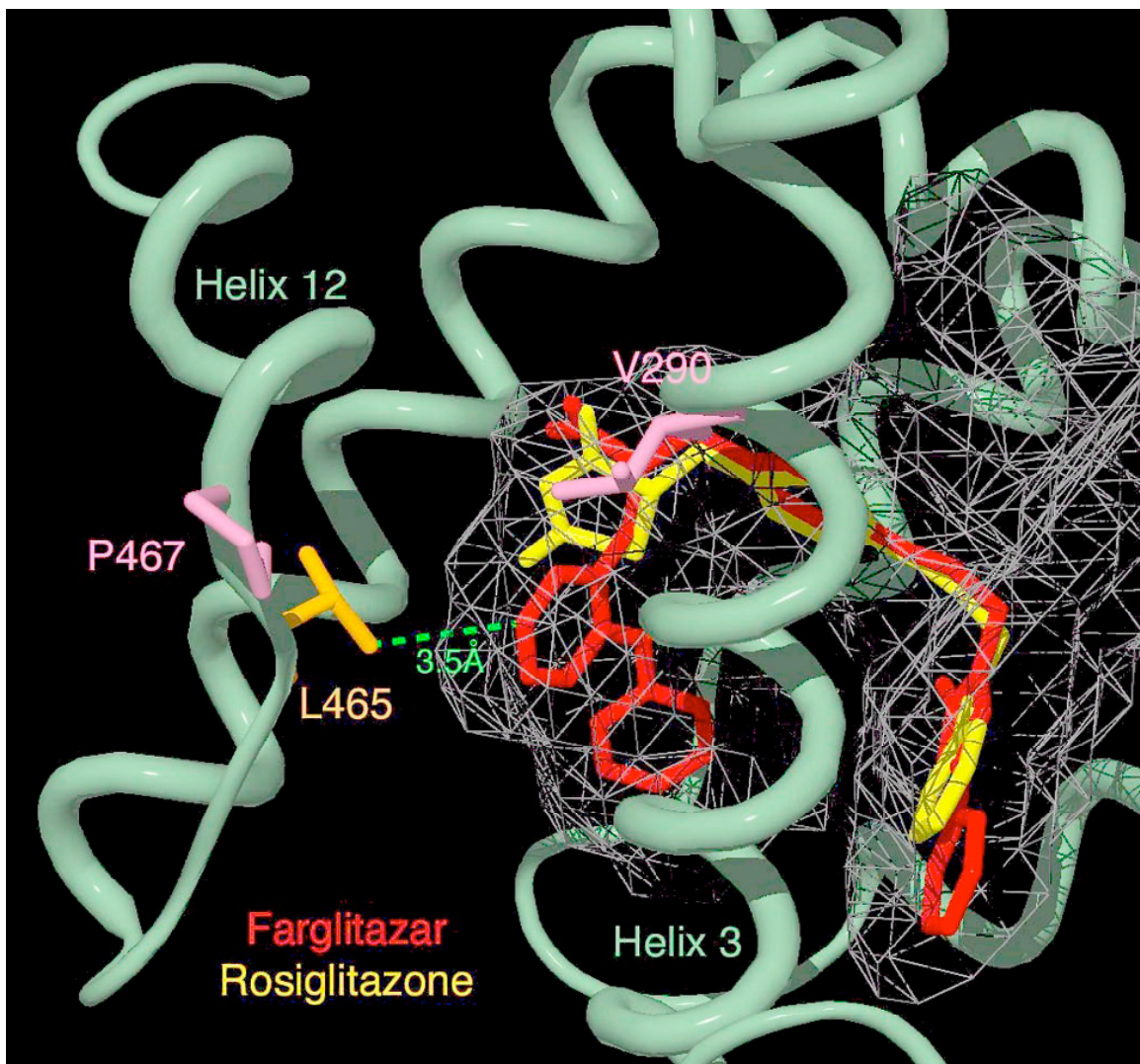


**Figure 4.12** Crystallographic modelling showing how the tyrosine agonist (farglitazar) may preferentially stabilise helix 12 in mutant PPAR $\gamma$ . Superimposition of PPAR $\gamma$  structures bound to either tyrosine (farglitazar) or thiazolidinedione (rosiglitazone) agonists showing part of the cavities (grey mesh) containing either ligand. On the helical backbone (green), the side chains (pink) of residues (P467, V290) mutated in our patients with severe insulin resistance are depicted. Both mutations are predicted to disrupt the orientation of helix 12 as described previously (Barroso *et al.*, 1999), thereby perturbing known important interactions of this helix with ligand [rosiglitazone (yellow) or farglitazar (red)] and coactivator. However, in the tyrosine agonist bound structure, the existence of an additional van der Waal's interaction between ligand and the side chain (orange) of a residue (L465) which precedes H12, may stabilise its position and preserve functional interactions.

<b>PPAR<math>\alpha</math></b>	<b>281</b>	V	E	T	V	T	E	L	T	E	F	A	K	A	I	P	G	F	A	N	L	D	L	N	D	Q	V	T	L	L	K	Y	G	V	Y	<b>314</b>
<b>PPAR<math>\gamma</math></b>	<b>290</b>	V	E	A	V	Q	E	I	T	E	Y	A	K	S	I	P	G	F	V	L	N	D	L	N	D	Q	V	T	L	<b>L</b>	K	Y	G	V	H	<b>323</b>
<b>PPAR<math>\delta</math></b>	<b>254</b>	V	E	T	V	R	E	L	T	E	F	A	K	S	I	P	S	F	S	S	L	F	L	N	D	Q	V	T	L	L	K	Y	G	V	H	<b>287</b>

**Figure 4.13** An alignment of amino acid sequences corresponding to the corepressor interaction interface in PPAR $\alpha$  in the three PPAR subtypes. Residues in PPAR $\alpha$  mediating contact with the peptide motif from SMRT are highlighted (\*) and boxes denote complete conservation of 12 out of 14 of these amino acids between the receptors. L318 in PPAR $\gamma$  is highlighted in bold.

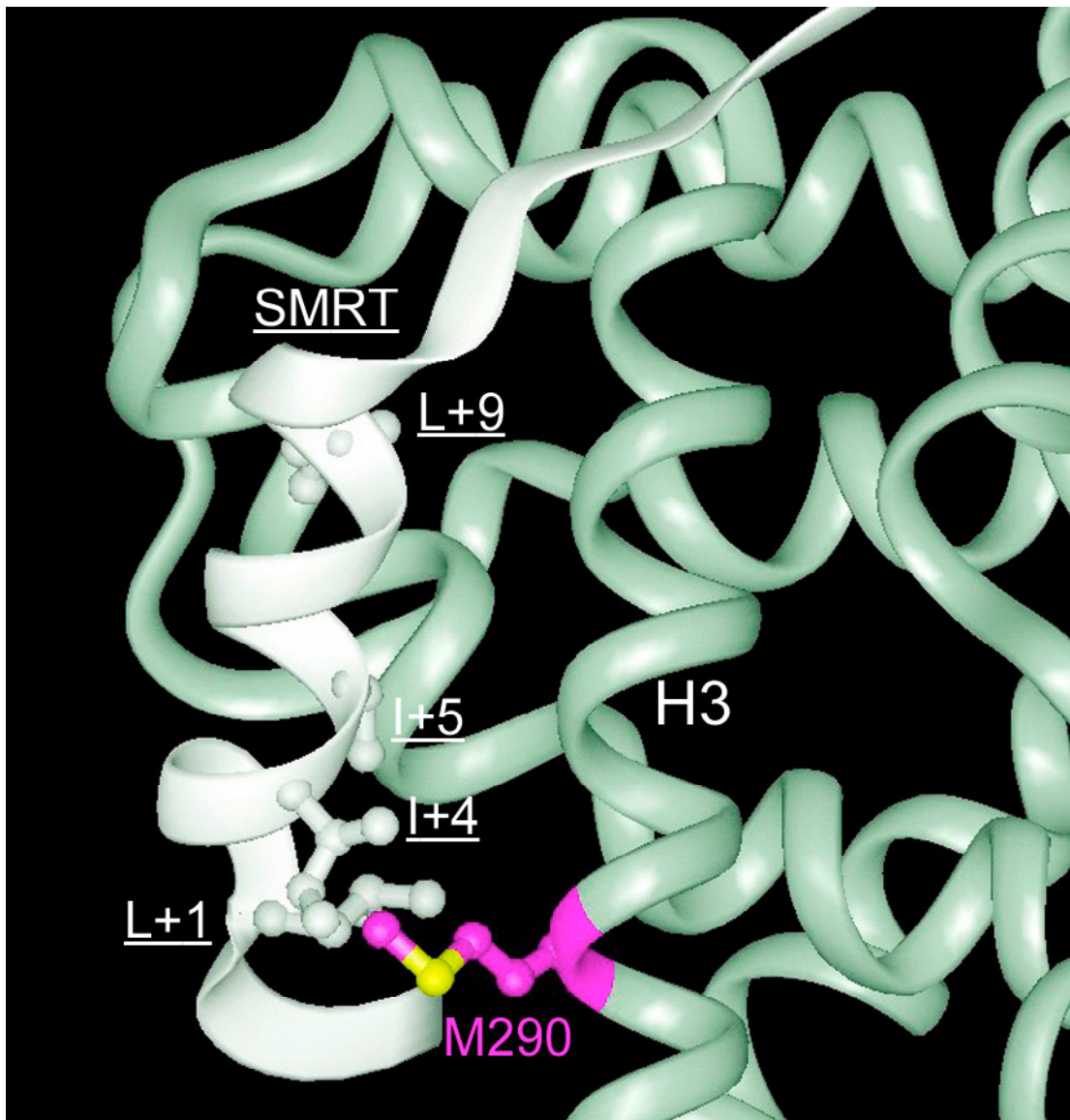


**Figure 4.14** A molecular model showing the interface between peptide from SMRT (white) and PPAR $\gamma$  (green) with the location of the V290M mutation also depicted (purple). The key SMRT residues that are predicted to form the interface (I+4, I+5, L+1, L+9) are numbered as reported in the PPAR $\alpha$ /SMRT crystal structure (Xu *et al.*, 2002).

## Chapter 5

# DIGENIC INHERITANCE OF SEVERE INSULIN RESISTANCE IN A HUMAN PEDIGREE

### 5.1 Introduction

Diabetes mellitus, defined as a state in which carbohydrate and lipid metabolism are improperly regulated by insulin, is a major public health problem.

There are an estimated 143 million people worldwide with the disorder representing an approximate five-fold increase over the last 10 years. It has been estimated that the number will probably double by the end of the current decade as a consequence of our shift towards a more sedentary lifestyle predisposing to obesity and insulin resistance (Harris *et al.*, 1998). The cost of caring for affected individuals is likely to be prohibitively high, even for the more financially “well-off” Western Economies. Although the aetiology of diabetes mellitus can be divided into a number of different categories, broadly speaking most patients are considered to be either type 1 or type 2 in origin.

Type 1 diabetes mellitus (T1DM) results from the autoimmune destruction of the insulin-producing  $\beta$  cells of the islets of Langerhans. Patients with this form are absolutely dependent on exogenous insulin. Type 2 diabetes mellitus (T2DM) is the most common form of the disorder and, in the majority of instances, is characterized by progressive resistance to the action of insulin in multiple tissues including skeletal muscle, liver and fat, followed by a gradual decrease in insulin secretion as a consequence of diminishing pancreatic  $\beta$ -cell function. However, even when insulin resistant individuals are able to secrete sufficient insulin to remain euglycemic, they are at increased risk of developing a cluster of abnormalities, which include hypertension, dyslipidemia and hypercoagulability, that have been brought together under the umbrella term “metabolic syndrome”. Although the value of diagnosing the presence of the metabolic or insulin resistance syndrome over and above paying due attention to individual cardiovascular risk factors is currently a matter of debate, if nothing else it emphasises that premature atherosclerosis and vascular

complications of insulin resistance and T2DM, are a major cause of excess morbidity and mortality. Accordingly improving insulin sensitivity is an important goal for those involved in the management of this condition.

It is clear that genetic factors significantly influence insulin sensitivity. For example relatives of type 2 diabetics are more likely to manifest insulin resistance, whilst offspring of type 2 diabetic parents are almost invariably resistant (Rewers and Hamman, 1995). Moreover studies in monozygotic twins reveal a high heritability of diabetes, with a 50%-75% estimate in the heritability of insulin resistance (Rewers and Hamman, 1995). The complexity of insulin signalling and the capacity of multiple factors to interfere with normal insulin action make the range of candidate genes for insulin resistance very large. Although the inherited susceptibility to insulin resistance is thought to involve the interplay of variants at multiple genetic loci, no clear examples of gene-gene interaction have as yet been reported.

This chapter describes a kindred in which five severely insulin resistant subjects (but none of their unaffected family members), were doubly heterozygous for frameshift/premature stop mutations in two unrelated genes, namely *PPAR $\gamma$* , a gene highly expressed in adipocytes, and *PPP1R3A*, which encodes the muscle-specific regulatory subunit of protein phosphatase-1. The finding that genetic defects in proteins primarily involved in either carbohydrate or lipid metabolism can combine to result in an extreme phenotype of insulin resistance provides a model for the type of gene-gene interaction that may underlie insulin resistance associated with commoner human metabolic disorders such as Type 2 diabetes.

## **5.2 Methods**

### **5.2.1 Clinical studies**

Family A, a pedigree with multiple affected members was identified through screening a cohort of subjects with severe insulin resistance (S.I.R.). The inclusion criteria for this cohort are extreme hyperinsulinaemia (fasting plasma insulin > 150pmol/l; or plasma insulin > 1000pmol/l at 2 hours post-glucose load; or daily insulin requirement of > 200U if lean, >300U if obese) but with a BMI < 37Kg/m<sup>2</sup> and the presence of the skin lesion acanthosis nigricans (S'O Rahilly, 2002).

Routine biochemical measurements were undertaken using standard commercially available assays in the Department of Clinical Biochemistry, Addenbrooke's Hospital, Cambridge. Measured total body fat was quantified by magnetic resonance imaging (MRI) as described previously (Thomas *et al.*, 1998) in the Department of Radiology, Addenbrooke's Hospital, Cambridge. Homeostatic model assessment was used to calculate insulin sensitivity (Matthews *et al.*, 1985). Intramyocellular lipid content (IMCL) was determined by Magnetic Resonance Spectroscopy (MRS) as described previously (Rico-Sanz *et al.*, 1999) and plasma leptin concentration was measured using an in-house two-site immunoassay.

### **5.2.2 Screening of *PPARG* gene**

Genomic DNA was extracted from peripheral blood using standard techniques as outlined in Chapter 2, section 2.3.2.1. All coding exons of *PPARG*, including exon B encoding the unique N-terminal of PPAR $\gamma$ 2, were PCR amplified with gene specific primers (Table 5.1). PCR cycle conditions were as follows: initial denaturation at 94°C for 3 minutes, then 34 cycles at 94°C for 30 seconds, 60°C for 30 seconds, 72°C for 1 minute, with a final extension at 72°C for 10 minutes. Following standard purification of the PCR products (Chapter 2, section 2.3.2.4) sequencing was performed using an ABI 310 PRISM automated sequencer as previously described (Chapter 2, section 2.3.7).

### **5.2.3 Screening of *PPP1R3A* gene**

This work was undertaken by Dr Ines Barroso, Incyte Genetics Ltd (Cambridge, UK).

In brief, genomic DNA from subjects was randomly pre-amplified in a primer extension pre-amplification (PEP) reaction (Zhang *et al.*, 1992). All coding exons and splice junctions of the human *PPP1R3A* gene were PCR amplified from PEP DNA with gene specific primers. PCR products were studied by single-stranded conformation polymorphism (SSCP) analysis and those exhibiting anomalous migration were sequenced directly to identify the nucleotide change (Thorpe *et al.*, 1999). Evidence for the presence of the *PPP1R3A* FS mutation was screened for in participants in two independent population-based case-control studies in East Anglia, UK. Diabetes was assumed to be of the type 2 form if its onset was after the age of 30 years and insulin therapy was not required during the first year following diagnosis. Controls were individually age- and gender-matched to each of the cases, but excluded if they had an HbA1c > 6.0%.

### **5.2.4 Plasmid and constructs**

Full-length human PPAR $\gamma$ 1 and PPAR $\gamma$ 2 cDNAs were cloned by reverse transcription polymerase chain reaction from total human preadipocyte RNA and introduced into the pcDNA3 expression vector (Invitrogen, Groningen, Netherlands) as XhoI/Xba I fragments. The PPAR $\gamma$  FS mutant was generated by site-directed mutagenesis of both wild type (WT) isoforms ( $\gamma$ 1 and  $\gamma$ 2) receptor templates as previously described (Chapter 2, section 2.3.8) and verified by direct sequencing. WT $\gamma$ 1, WT $\gamma$ 2, FS $\gamma$ 1 and FS $\gamma$ 2 expression vectors for *in vitro* transcription/translation were generated by cloning Xho I/Xba I fragments of corresponding pcDNA3 fusions into pGEM11Zf(+) (Promega). Comparable expression of the <sup>35</sup>S-labelled proteins was verified by coupled transcription and translation *in vitro* (TNT, Promega). (PPARE)<sub>3</sub>TKLUC (Forman *et al.*, 1995) and UASTKLUC (Tone *et al.*, 1994) have been described previously. The HA-tagged WT or PPP1R3Afs (Fsh) mutant expression vectors (pACCMV.pLpA-HA-PPP1R3) were kindly provided by P. Cohen (Rasmussen *et al.*, 2000).

### **5.2.5 DNA binding assays**

Receptor binding to DNA was assessed using electrophoretic mobility assays as described previously (Chapter 2, section 2.4.3) using <sup>35</sup>S-labelled in vitro translated receptors quantitated by SDS-PAGE analysis and a <sup>32</sup>P-labelled oligonucleotide duplex corresponding to the PPARE from the acyl-CoA oxidase gene (Zamir *et al.*, 1997).

### **5.2.6 Transactivation assays**

293EBNA cells were cultured in 24-well plates in DMEM containing 10% fetal bovine serum and changed to medium containing AG-1-X8 resin-stripped serum prior to transfection. Each well was cotransfected with 500ng of (PPARE)<sub>3</sub>TKLUC (Forman *et al.*, 1995) reporter construct together with 100ng of receptor expression vector (wild type, frameshift mutant or empty vector pcDNA3) using the calcium phosphate method (Chapter 2, section 2.6.2). The ligand was added 5 hours after transfection and cells were harvested 36 hours later. Luciferase values were normalised to β-galactosidase activity from the internal control plasmid Bos-β-gal as previously described (Collingwood *et al.*, 1994), and represent the mean ± s.e.m. of at least three independent experiments, each performed in triplicate.

### **5.2.7 Immunoprecipitation and Western blot analysis**

Expression levels of the PPP1R3A mutant were examined by Western blotting of CHO cell extracts. These experiments were performed by Dr David Savage (University of Cambridge). In brief, CHO cells were transiently transfected with epitope tagged PPP1R3A wild type (WT) or mutant (Fsh) expression vectors. Following immunoprecipitation of the whole-cell lysates with an antibody direct against the epitope tag, the proteins were separated, blotted and analyzed with an antibody targeted against the protein phosphatase 1 catalytic subunit (PP1C). To confirm the expected size of the proteins, western blotting of whole-cell lysates, using a sheep monoclonal N-terminal PPP1R3A antibody was performed.



### ***5.2.8 Immunofluorescence Microscopy***

This experiment was performed by Dr Gudrun Ihrke (Cambridge Institute for Medical Research, Cambridge). Cells were fixed in 3% paraformaldehyde/0.05% glutaraldehyde in 100 mM K-Hepes/3 mM MgCl<sub>2</sub> buffer (pH 7.5) for 15 minutes, treated with 0.5% borohydride/PBS for 10 minutes, and then blocked and permeabilised in 1% BSA/0.1% saponin for 20 minutes. When cells were permeabilised before fixation, they were incubated for 5 minutes in 0.05% saponin in 80 mM K-Pipes/5 mM EGTA/1 mM MgCl<sub>2</sub> (pH 6.8) at room temperature. Cells were labelled with a rat anti-HA antibody (Boehringer; 1:100) followed by Texas Red goat anti-rat (Molecular Probes; 1:200). Confocal images were collected using a Leica TCS SP system and processed using Adobe Photoshop software (Adobe Systems).

## 5.3 Results

### 5.3.1 Clinical and genetic analyses

As part of an ongoing programme of investigation into the aetiology of inherited syndromes of severe insulin resistance (S O’Rahilly, Cambridge) we identified a pedigree (Family A) with multiple affected members (Figure 5.1c). The grandparents (subjects Ii and Iii) had typical late-onset Type 2 diabetes with no clinical features of severe insulin resistance. However, three of their six children and two of their grandchildren had acanthosis nigricans, a dermatological marker of extreme insulin resistance. All five subjects with acanthosis nigricans had markedly elevated fasting plasma insulin levels, indicative of severe insulin resistance (Figure 5.1d). Mutational screening studies identified a heterozygous frameshift/premature stop mutation in the *PPAR $\gamma$*  gene [(A<sup>553</sup> $\Delta$ AAAT)fs.185(stop 186) – denoted hereafter as *PPAR $\gamma$*  FS] (Fig. 5.1a), which was present in the grandfather (Ii), all five severely insulin resistant relatives, and one other relative who was normo-insulinaemic (IIvi). Further candidate gene studies revealed that a heterozygous frameshift/premature stop mutation in the gene encoding the muscle-specific regulatory subunit of protein phosphatase-1 (*PPP1R3A*) [(C<sup>1984</sup> $\Delta$ AG)fs662(stop668) – denoted hereafter as *PPP1R3A* FS] (Figure 5.1b) was also present in this family. In this case the mutation was present in the grandmother (Iii), all five severely insulin resistant subjects and one other relative. Thus, all five severely insulin resistant subjects, and no other family members, were doubly heterozygous for frameshift mutations in the two unrelated genes. Fasting insulin levels in the singly heterozygous and wild-type family members were similar and within the range seen in the normal population (Figure 5.1d). In contrast, the double heterozygotes showed extreme hyperinsulinaemia (Figure 5.1d). In addition to hyperinsulinaemia and acanthosis nigricans, T2DM, hyperlipidaemia and hypertension were present in the double heterozygotes to a variable extent (Figure 5.1c and Table 5.2).

In light of these findings, all probands from our severe insulin resistance (SIR) cohort (n-129) were screened for mutations in *PPAR $\gamma$*  and *PPP1R3A*. Other than the two dominant negative (P467L and V290M) mutations in *PPAR $\gamma$*  previously reported (Barroso *et al.*, 1999), and the common Pro12Ala population polymorphism variant

(Deeb *et al.*, 1998), no other missense, nonsense or frameshift mutations were identified. However, one other unrelated subject had the same heterozygous frameshift mutation in *PPPIR3A* that was found in Family A. This subject (III, Family B) presented with acanthosis nigricans aged 20 years. At that age he had a body mass index of 36.5 kg/m<sup>2</sup> and a fasting plasma insulin of 437 pmol/L (N<80 pmol/L). He inherited the mutation from his moderately obese father (BMI 30 kg/m<sup>2</sup>) who also had marked hyperinsulinemia (fasting plasma insulin 178 pmol/L) (Figure 5.1e). The two other wild-type family members were clinically and biochemically normal. Of note, the proband subsequently lost 40 kg and reduced his BMI to 27 kg/m<sup>2</sup>. At that stage his fasting insulin level fell dramatically to 93 pmol/L. This observation is consistent with normal fasting insulin levels (31 pmol/L) in a lean 20-year-old male carrier of the *PPPIR3A* mutation in family A (Figure 5.1c, subject IIIii).

### **5.3.2 DNA binding of PPAR $\gamma$ FS**

PPAR $\gamma$  is a ligand-inducible transcription factor that regulates target gene transcription as a heterodimer with the retinoid X receptor (RXR). This heterodimeric complex can be activated synergistically by antidiabetic PPAR $\gamma$  agonists (e.g. thiazolidinediones) and RXR-specific ligands (Mukherjee *et al.*, 1997). PPAR $\gamma$  exhibits a modular structure consisting of a central DNA-binding domain, an amino-terminal activation domain, and a carboxy-terminal ligand-binding domain (Figure 5.1a). The frameshift premature stop mutation leads to a mutant receptor which is truncated within the second zinc finger of the DNA-binding domain – a region common to both the  $\gamma$ 1 and  $\gamma$ 2 isoforms of the receptor (Figure 5.1a), and which is critical in mediating receptor interaction with PPAR-specific response elements (PPAREs) in target gene promoters. Accordingly, the ability of the PPAR $\gamma$  mutants to bind DNA as heterodimers with RXR was examined in an electrophoretic mobility shift assay. Unlike their wild type (WT) counterparts, neither FS PPAR $\gamma$ 1 (FS $\gamma$ 1) nor FS PPAR $\gamma$ 2 (FS $\gamma$ 2) mutants formed heterodimeric complexes when coincubated with a radiolabelled probe encoding the acyl-CoA oxidase PPARE (Figure 5.2).

### **5.3.3 Functional activity and dominant negative activity of PPAR $\gamma$ FS**

Consistent with their inability to bind DNA in contrast to WT receptor, neither mutant mediated transactivation when cotransfected with a reporter gene containing a PPARE and increasing concentrations of the thiazolidinedione, rosiglitazone (Figure 5.3). Moreover, unlike the previously reported naturally occurring missense PPAR $\gamma$  mutants (P467L and V290M) (Barroso *et al.*, 1999), the truncated mutants did not exhibit dominant negative activity when co-expressed with WT receptor (Figure 5.4).

### **5.3.4 Characterization of the PPP1R3A mutant**

PPP1R3A is a skeletal- and cardiac muscle-specific regulatory subunit of protein phosphatase 1. The *PPP1R3A* FS mutation is predicted to truncate the protein prematurely (Figure 5.1b), resulting in the loss of its C-terminal sarcoplasmic reticulum-binding domain (Newgard *et al.*, 2000). When transiently expressed in CHO cells the frameshift mutant expression vector produced a detectable protein of the expected reduced size (approximately 83 kD) (Figure 5.5a). Furthermore, the truncated protein was capable of interacting with the catalytic subunit of PP1 (PP1C) with an efficiency similar to WT PPP1R3A (Figure 5.5b). However, confocal microscopy revealed strikingly different intracellular distributions of the WT and mutant PPP1R3A. A significant fraction of WT PPP1R3A localised, as expected, to intracellular membranes and was therefore resistant to release following saponin permeabilisation of cells, whereas mutant PPP1R3A was almost completely lost from cells following permeabilisation suggesting it is mislocalised intracellularly and probably cytosolic (Figure 5.5c).

Primer	Sequence
Exon B Forward	5' – ATA TCA GTG TGA ATTBACA GC – 3'
Exon B Reverse	5' – CCT GGA AGA CAA ACT ACA AG – 3'
Exon 1 Forward	5' – AGA TTG CTG TGT TCT CTA G – 3'
Exon 1 Reverse	5' – CCT AGT AGT CTG AAA AGT G – 3'
Exon 2 Forward	5' – CAT GGG ATA ATT ATC CTC TCA C – 3'
Exon 2 Reverse	5' – GGT TCT GCT GAA ATG AA – 3'
Exon 3 Forward	5' – TTC GTG CTT CCA TGT GTC – 3'
Exon 3 Reverse	5' – CTG GTC TGG CAG CTA TAA TG – 3'
Exon 4 Forward	5' – GCA CAG TGT GTG TTC AGA GC – 3'
Exon 4 Reverse	5' –CCA ATG AAG ACA GCA GAA G – 3'
Exon 5 Forward	5' –AGT TAG AAA TCT CCA AGT CAT CCC ACG – 3'
Exon 5 Reverse	5' – TCA TCC CAC CCT CTT TCA TAG AAG ATC – 3'
Exon 6 Forward	5' – TGA ACC CCC TGT TGT GTT TTC CAT ATG – 3'
Exon 6 Reverse	5' – AGG GAA ATG TTG GCA GTG GCT CAG GAC – 3'

**Table 5.1** Primers used to amplify and sequence coding exons of the human *PPARG* gene, including exon B encoding the unique N-terminal region of the PPAR $\gamma$ 2 isoform.

Fig. 5.1 reference	Family A					Family B						Reference values
	Doubly heterozygous subjects					PPAR $\gamma$ FS mutant heterozygotes		PPP1R3A FS mutant heterozygotes				
	IIii	IIiii	IIiv	IIIiii	IIIiv	Ii	IIvi	lii	IIIii	Ii		
Age	49	47	41	25	21	71	32	71	20	20	65	
Gender	F	F	F	F	F	M	M	F	M	M	M	
BMI (kg/m <sup>2</sup> )	26.8	26.0	28.0	31.4	29.0	24.2	25.8	32.9	18.9	36.5	30	
Blood pressure	190/ 110	140/ 80*	130/ 84	130/ 70	150/ 110	170/ 90*	125/ 90	170/ 105*	105/ 69	135/ 82*	172/ 93*	
Measure total body fat as percentage of predicted body fat	84.3	63.5	83.7	46.8	79.4	n/a	75.2	n/a	n/a	n/a	n/a	100%
Glucose	5.6	6.4	4.4	9.2‡	3.9	12‡	4.6	4.5	5.2	4.4	6.2	3.5 – 6.3 mmol/L
Insulin	195	359	197	411	346	61	46	56	31	437	178	< 80 pmol/L
% insulin sensitivity (HOMA) ¶	27	15	28	14	20	87	115	95	168	13	30	100%
Triglycerides	6.1	2.1†	3.4	34.6	10.1	6.6	1.5	1.1	0.7	1.5	2.4	Desirable < 2mmol/L
HDL	0.82	0.63	0.81	0.52	1.04	0.71	1.02	1.84	1.36	0.7	0.91	Desirable > .9mmol/L
NEFA	1442	202†	526	2532	867	1219	584	933	n/a	n/a	n/a	280 – 920 umol/L
Uric acid	0.31	0.24	0.23	0.23	0.28	0.35	0.31	0.23	0.32	0.17	0.44	0.15 – 0.35 mmol/L
Leptin	12.1	4.4	8.2	17.3	12.4	1.2	0.9	13.2	0.6	14.6	19.8	ug/L
IMCL/Creatine ratio (soleus muscle)	19.8	19.1	25.5	28.3	44.9	n/a	28.3	n/a	n/a	n/a	n/a	13.6 ± 6.6§

**Table 5.2** Clinical and biochemical characteristics of mutant allele carriers. All samples were obtained following an overnight fast. \*, Measurements undertaken on anti-hypertensive therapy; †, Measurements undertaken by lipid lowering therapy; ‡, Abnormalities detected at the time of screening; Body fat was quantified by magnetic resonance imaging (MRI) as described previously (Thomas *et al.*, 1998). Predicted body fat (Black *et al.*, 1983): for women = (1.48\*BMI (kg/m<sup>2</sup>)) – 7.00; for men = (1.281\*BMI (kg/m<sup>2</sup>)) – 10.13; ¶, HOMA (homeostasis model assessment) (Matthews *et al.*, 1985); § IMCL reference values represent mean and SD of measurements from 76 control subjects (unpublished observations EL Thomas and JD Bell). HDL, high-density lipoprotein; NEFA, non-esterified fatty acids; IMCL, intramyocellular lipid.

		Leptin concentrations (ng/ml)								
SEX	BMI (kg/m <sup>2</sup> )	n	mean	median	percentiles				min	max
					5	25	75	95		
Men	≤25	278	3.3	2.5	0.4	1.2	4.4	8.3	0.1	22.8
	25-30	375	5.9	4.7	1.5	3.0	7.5	13.0	0.5	26.3
	30-35	98	10.9	9.5	4.2	6.3	13.8	26.0	2.1	36.7
	>35	8	18.8	15.5	7.8	12.4	27.6	31.7	7.8	31.7
Women	≤25	535	10.6	8.9	2.4	5.4	13.9	24.4	0.2	45.8
	25-30	348	21.1	18.9	8.6	13.8	26.8	38.9	3.0	65.7
	30-35	126	34.6	32.3	14.9	25.4	43.6	60.2	8.1	79.1
	>35	60	58.0	52.4	22.7	43.6	70.4	113.6	11.9	137.4

**Table 5.3** Distribution of leptin concentrations among individuals in the population-based MRC Ely cohort study stratified by sex and BMI.

**Figure 5.1** Identification of Novel Mutations in *PPAR $\gamma$*  and *PPP1R3A* in two families with severe insulin resistance.

a, Heterozygous *PPAR $\gamma$*  frameshift / premature stop mutation [(A<sup>553</sup> $\Delta$ AAAT)fs.185(stop186)]. The frameshift leads to truncation of the receptor within the second zinc-finger of the DNA-binding domain (DBD) and is predicted to involve both  $\gamma$ 1 and  $\gamma$ 2 receptor isoforms. M, methionine; K, lysine; S, serine; X, Stop; LBD, ligand-binding domain.

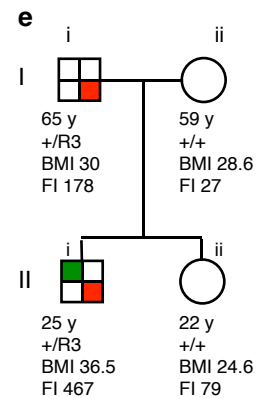
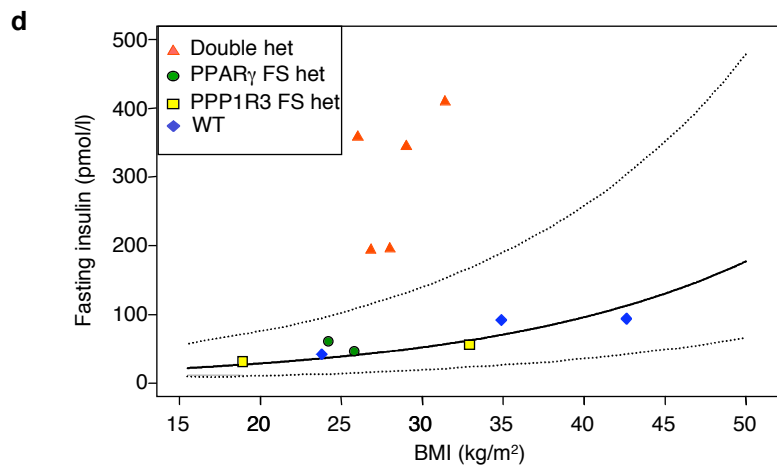
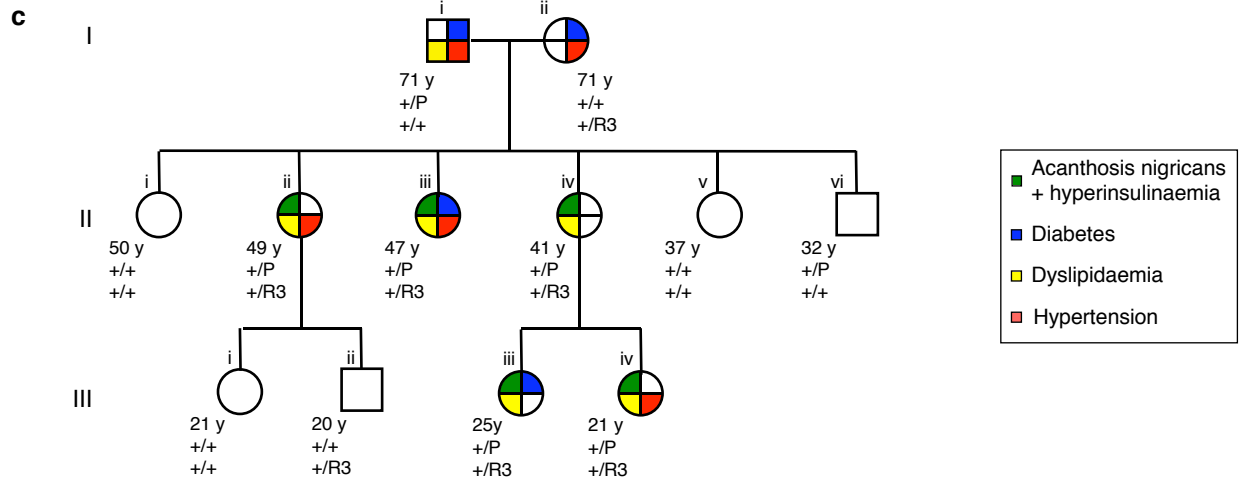
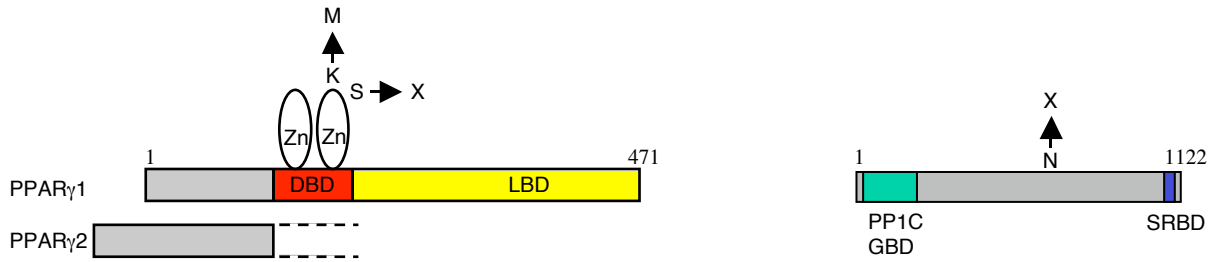
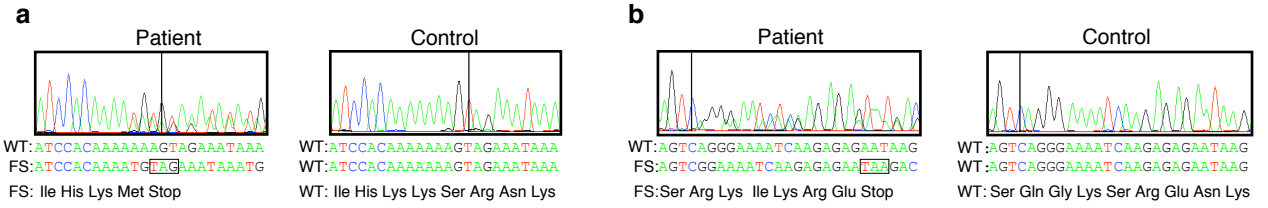
b, Heterozygous *PPP1R3A* frameshift mutation [(C<sup>1984</sup> $\Delta$ AG)fs.662(stop 668)]. The frameshift results in a premature Stop codon (X) at position 668 (N, asparagine) with predicted subsequent loss of the carboxyterminal putative sarcoplasmic reticulum-binding domain (SRBD) (Newgard *et al.*, 2000) but preservation of the aminoterminal PP1C/ GBD, PP1C- and glycogen binding domains.

c, Pedigree of Family A indicates complete concordance between features of severe insulin resistance and the presence of both mutations. The age and genotype (+, wild-type; P, *PPAR $\gamma$*  mutation; R3, *PPP1R3A* mutation) of members is indicated. Doubly heterozygous individuals were variably affected by additional features of metabolic syndrome. Dyslipidaemia is defined by triglycerides > 2mmol/L and high-density lipoprotein (HDL) < 1mmol/L.

d, Fasting plasma insulin concentrations plotted against body mass index [BMI (kg/m<sup>2</sup>)] in Family A. The solid line represents the log-linear regression line between fasting insulin and BMI in 1121 normal participants in the MRC Ely population-based cohort study. The 95% confidence intervals (broken lines) include 95% of individuals at any given BMI.

e, Pedigree of Family B which suggests that carriers of the *PPP1R3A* mutation develop fasting hyperinsulinaemia when obese. The age, BMI (kg/m<sup>2</sup>), fasting plasma insulin (FI in pmol/L) and genotype (+, wild-type; R3, *PPP1R3A* mutation) are indicated.





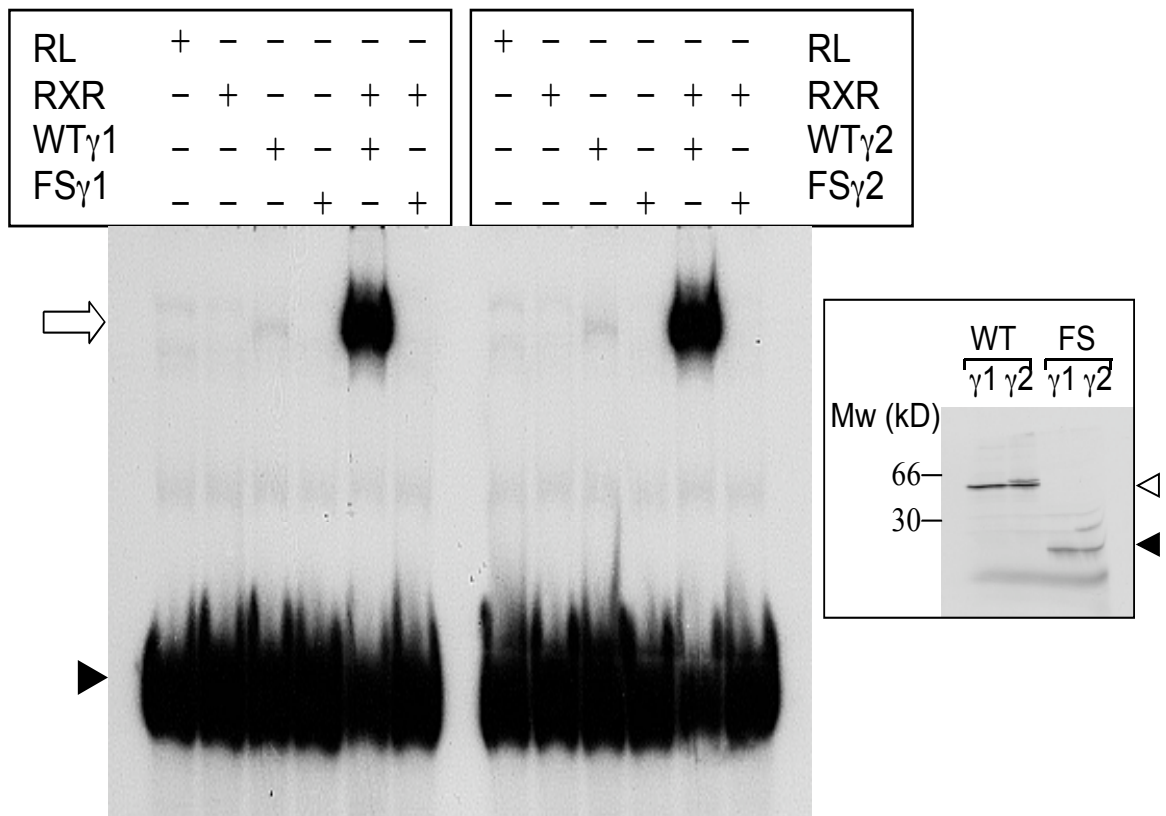


**Figure 5.2** Mutant PPAR $\gamma$  mutants fails to bind to DNA heterodimerically with their partner RXR. Using an electrophoretic mobility supershift assay, in vitro translated WT PPAR $\gamma$ 1 (WT $\gamma$ 1), WT PPAR $\gamma$ 2 (WT $\gamma$ 2), FS PPAR $\gamma$ 1 (FS $\gamma$ 1) or FS PPAR $\gamma$ 2 (FS $\gamma$ 2) and RXR were coincubated with oligonucleotide duplexes encoding the acyl-CoA oxidase PPARE. Complexes were resolved by PAGE. The open arrow indicates the location of the PPAR $\gamma$ -RXR heterodimer, whilst the solid arrowhead denotes free unbound probe. Inset,  $^{35}$ S-labelled in vitro translated WT and FS mutant PPAR $\gamma$ 1 and PPAR $\gamma$ 2 analysed by SDS-PAGE showing that wild type (open arrowhead) and truncated mutant (closed arrowhead) proteins are synthesised. RL, reticulocyte lysate; Mw, molecular weight.

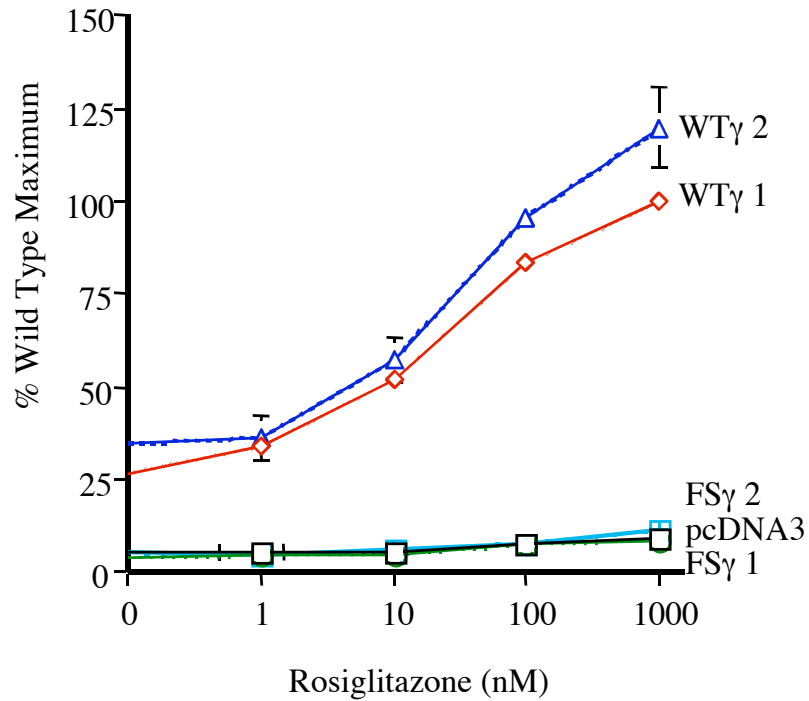


**Figure 5.3** The FS PPAR $\gamma$  mutants are transcriptionally inactive in the context of both the  $\gamma$ 1 and  $\gamma$ 2 isoforms. 293EBNA cells were transfected with WT $\gamma$ 1, WT $\gamma$ 2, FS $\gamma$ 1, FS $\gamma$ 2 or empty (pcDNA3) expression vectors (100ng) together with a reporter gene (PPARE)<sub>3</sub>TKLUC (500ng), in the presence of increasing concentrations of the thiazolidinedione (rosiglitazone). Results are expressed as a percentage of the maximum activation obtained with WT $\gamma$ 1 and represent the mean  $\pm$  s.e.m. of at least three independent experiments.

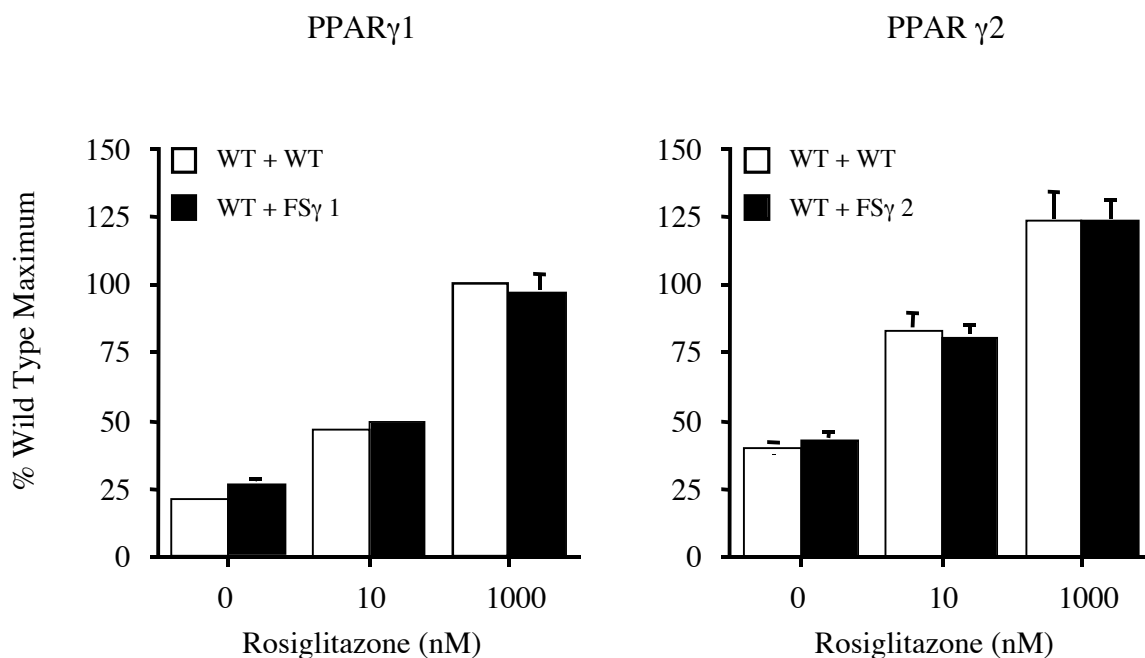


**Figure 5.4** The FS PPAR $\gamma$  mutants do not exhibit dominant negative activity when co-expressed with their WT counterparts. 293EBNA cells were transfected with 100ng of WT plus an equal amount of either WT or FS mutant expression vectors, together with the same reporter construct as in Figure 5.3. Results are expressed as a percentage of the maximum activation obtained with WT $\gamma$ 1. The transcriptional responses attained with either 100ng or 200ng of WT receptor are identical (data not shown).

**Figure 5.5** Characterisation of the PPP1R3A FS (Fsh) mutant.

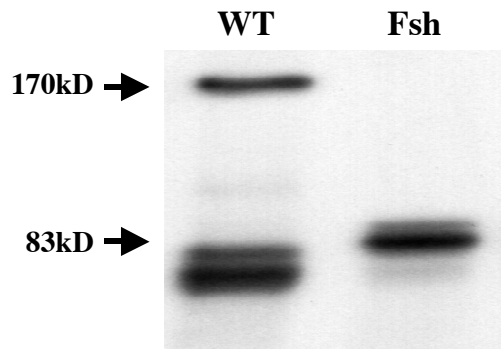
CHO cells were transiently transfected (Fugene) with HA-tagged wild type (WT) or PPP1R3A FS (Fsh) mutant expression vectors [pACCMV.pLpA-HA-PPP1R3 (Rasmussen *et al.*, 2000), gift from P. Cohen].

a, Western blotting of whole cell lysates using a sheep monoclonal N-terminal PPP1R3A antibody (gift from P. Cohen). Note that PPP1R3A undergoes rapid proteolysis (Tang *et al.*, 1991) and one of the proteolytic fragments is of similar size to the Fsh mutant.

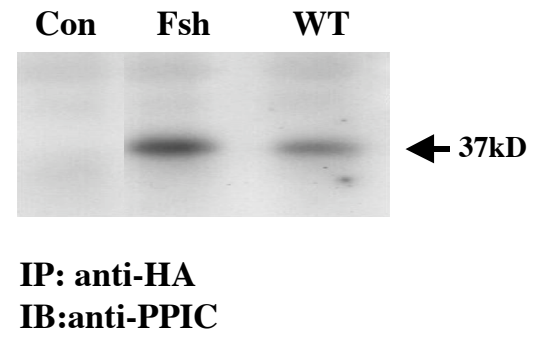
b, Whole cell lysates from non-transfected (Con) and transfected CHO cells were immunoprecipitated with an anti-HA antibody (Santa Cruz) and Western blotted with an anti-PP1C antibody (Santa Cruz), showing that interaction between wild type and mutant regulatory subunits with catalytic subunit is preserved.

c, Confocal microscopy of wild type (WT) and mutant (Fsh) PPP1R3A. Cells transiently transfected with HA-tagged versions of PPP1R3A were fixed either without (left panel) or with prior permeabilisation in saponin to release cytosolic PPP1R3A (right panel), then fixed and labelled with an anti-HA antibody. The loss of mutant Fsh protein in cells permeabilised with saponin prior to fixation indicates that the proteins are freely cytosolic whereas the WT protein is probably attached to intracellular membranes.

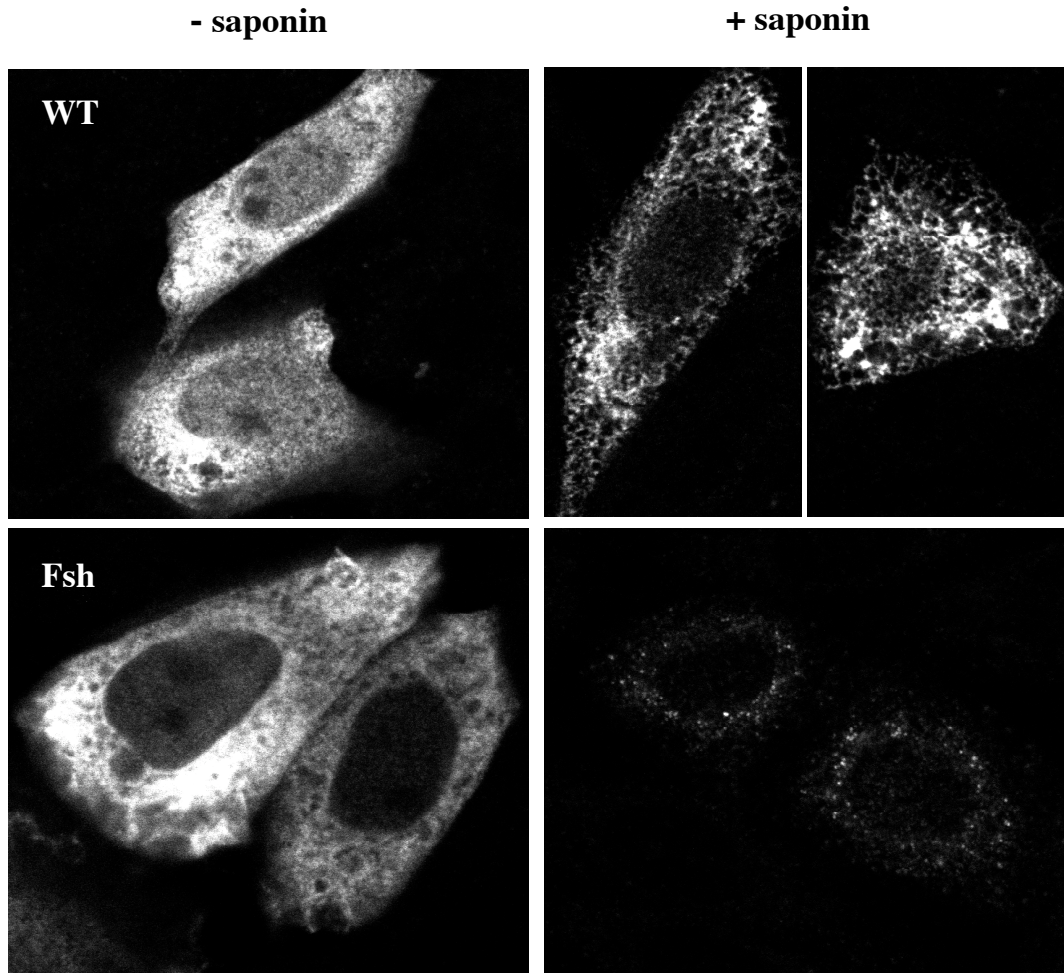
a.



b.



c.



## 5.4 Discussion

In this chapter I have described a family in which five members had acanthosis nigricans and severe hyperinsulinemia. Intriguingly, genetic screening revealed that all five subjects, but none of their unaffected relatives, were double heterozygotes for frameshift mutations in two unrelated genes, peroxisome proliferator activated receptor (*PPAR* $\gamma$ ) and the muscle-specific regulatory subunit of protein phosphatase 1 (*PPP1R3A*). The frameshift premature stop mutation in *PPAR* $\gamma$  generates a protein, which is unable to bind to DNA and is transcriptionally nonfunctional with no dominant negative activity. Is a loss of function mutation in a single allele of human *PPAR* $\gamma$  a plausible contributor to insulin resistance? *PPAR* $\gamma$  agonists clearly enhance insulin sensitivity (Olefsky, 2000) whilst humans with dominant negative mutations in *PPAR* $\gamma$  (Barroso *et al.*, 1999) and mice with severe *PPAR* $\gamma$  deficiency (Yamauchi *et al.*, 2001) are markedly insulin resistant. Surprisingly however, heterozygous *PPAR* $\gamma$  deficient mice appear to be more insulin sensitive than their wild-type littermates, particularly after high fat feeding (Kubota *et al.*, 1999; Miles *et al.*, 2000). While both of the subjects from Family A who only carry the *PPAR* $\gamma$  FS mutation have fasting insulin levels in the normal range, the co-existence of this mutation with the *PPP1R3A* frameshift mutation results in severe insulin resistance. These findings might appear to conflict with those in the heterozygous *PPAR* $\gamma$  null mice. There are several possible explanations for this apparent discrepancy. Firstly, the combination of a genetic defect in muscle glycogen synthesis with the haploid *PPAR* $\gamma$  state has not yet been specifically examined in mice. Secondly, while the particular *PPAR* $\gamma$  mutation found in Family A does not appear to have any dominant negative activity when tested in the assays shown, it is conceivable that it might have some properties that are distinct from a purely null allele *in vivo*. Finally, it is possible that species-specific differences in adipose tissue biochemistry (Bjorntorp and Sjostrom, 1978) may mean that quantitative decrements in *PPAR* $\gamma$  function have different metabolic implications for humans and rodents.

The mutation found in both Family A and Family B profoundly affects the structure of *PPP1R3A*, a key molecule in the regulation of glycogen metabolism. Insulin activates glycogen synthase (GS), the rate-limiting enzyme in glycogen synthesis, by promoting its dephosphorylation, via the inhibition of kinases (glycogen synthase

kinase-3 and protein kinase-A) and the activation of protein phosphatase-1 (PP1) (Newgard *et al.*, 2000). Insulin specifically activates discrete pools of PP1 in the vicinity of glycogen by facilitating binding of the PP1 catalytic subunit (PP1C) to glycogen targeting regulatory (PPP1R) subunits (Newgard *et al.*, 2000). The glycogen targeting subunit appears to serve as 'molecular scaffolds', bringing PP1C with its substrates glycogen synthase together in a macromolecular complex, and in the process significantly enhances PP1C activity (Newgard *et al.*, 2000).

Is the *PPP1R3A* FS mutation a plausible contributor to a state of insulin resistance? Mice rendered null for *PPP1R3A* have major defects in muscle glycogen synthesis although somewhat unexpectedly, the effects of insulin on this process are maintained in these animals (Suzuky *et al.*, 2001). The *PPP1R3A* FS mutation results in a major mislocalisation of the truncated protein within the cell and could have biological effects distinct from those resulting from a simple null allele. The truncated mutant *PPP1R3A* maintains its ability to interact with the catalytic subunit and may therefore be capable of actively interfering with the latter's normal function. While previous studies have demonstrated that intracellular localisation influences GS activity (Nielsen *et al.*, 2001), the precise functional consequences of the mislocalisation of *PPP1R3* are still to be determined.

As a result of 1) the *a priori* knowledge that both genes are intimately involved in insulin action 2) the fact that the mutations found result in truncated proteins with clear abnormalities in their function or localisation and 3) the observation that only the five doubly heterozygous members of family A and not the other seven members had unequivocal severe insulin resistance, it appears highly likely that the extreme insulin resistant phenotype seen in this family is the result of an interaction between the two mutations. Thus, familial extreme insulin resistance can now be added to the short list of human inherited conditions in which digenic inheritance has been described. These include some forms of retinitis pigmentosa (Goldberg and Molday, 1996) and junctional epidermolysis bullosa (JEB) (Floeth and Bruckner-Tuderman, 1999). It has been suggested that Bardet-Biedl syndrome (BBS) may be a complex trait requiring three mutant alleles in at least two genes to manifest the phenotype (Katsanis *et al.*, 2001).

While no previous human examples of digenic inheritance of human insulin resistance or Type 2 diabetes have been described, a number of experimental genetic manipulations in murine models have established the principle that such gene-gene



interaction might result in metabolic disorders. Thus Bruning and colleagues demonstrated that while mice heterozygous for insulin receptor or IRS-1 (insulin receptor substrate-1) knock-outs had minor metabolic abnormalities, doubly heterozygous animals were markedly insulin resistant and had a high incidence of diabetes (Bruning *et al.*, 1997). Similarly Terauchi and colleagues crossed insulin receptor substrate-1 (IRS-1) and glucokinase knock-out mice, and produced a digenic model of Type 2 diabetes (Terauchi *et al.*, 1997). How might the mutations in Family A interact to result in extreme insulin resistance? Of note, all previous well-documented examples of human digenic disease have involved direct protein-protein interactions between the two mutant gene products. Family A differs strikingly from this paradigm as, in their case, the genes concerned are predominantly expressed in different tissues, namely skeletal muscle and fat. Therefore, the interaction presumably occurs through a subtle amplifying effect of a metabolic derangement in one tissue on the other. Both skeletal muscle and adipose tissue are key players in insulin-stimulated nutrient storage and may communicate by as yet ill-defined mechanisms (Birnbaum, 2001). The development of muscle insulin resistance in fat-specific GLUT4 knock-out mice (Abel *et al.*, 2001) recently provided compelling *in vivo* evidence for such a dialogue between fat and muscle. As well as regulating fatty acid fluxes, adipocytes secrete several proteins ('adipokines') with potential endocrine effects, including leptin, TNF $\alpha$ , interleukin-6, resistin and adiponectin, all of which may alter insulin sensitivity (Steppan and Lazar, 2002). The precise mechanism by which loss of a single *PPAR* $\gamma$  allele might contribute to maladaptive metabolic cross talk awaits elucidation, but deficiency of such a key transcriptional regulator of adipocyte biology may well alter plasma fatty acid flux and/or adipokine concentrations. In this regard it is notable that plasma leptin levels were < 25<sup>th</sup> percentile of BMI and sex-matched controls in all doubly heterozygous subjects (Table 5.3). Additionally, the levels of intramyocellular lipid (IMCL) were elevated in the soleus muscle from doubly heterozygous subjects compared to controls (IMCL: creatine ratio 27.5 $\pm$ 10.5 vs. 13.6 $\pm$ 6.6,  $p < 0.05$ ). Levels of IMCL are highly correlated with whole body and muscle insulin sensitivity and are thought to reflect excessive delivery of non-esterified fatty acids from adipose stores to myocytes (Kelley and Goodpaster, 2001). It is tempting to hypothesise that, in family B who carry only the *PPP1R3A* mutation, the expanded fat mass of obesity acted as the

“second hit” by altering adipose tissue function. This notion is supported by the dramatic effect of weight loss on fasting hyperinsulinaemia in subject IIIi in Family B.

The *PPAR* $\gamma$  frameshift mutation was not detected in 1034 UK Europid subjects (517 diabetics and 517 controls) and is therefore likely to be “private” to the index pedigree. In contrast the *PPP1R3* frameshift mutation was found in two independent case-control studies in a total of 20/1029 UK Type 2 diabetics and 8/1033 normoglycaemic controls (weighted Mantel-Haenszel odds ratio 2.53 (95% confidence limits 1.06 – 6.70,  $p = 0.03$ .) suggesting that this mutation may also predispose to Type 2 diabetes in the general UK population. Given the rarity of this mutation further large multicentre population genetic studies will be required to robustly test this hypothesis.

These findings provide the most tangible evidence yet available that mutations which, when present alone, have, at most, subtle effects on different, metabolically relevant tissues can combine to result in extreme disturbances of human insulin action. Of note the two genes involved, *PPP1R3A* and *PPAR* $\gamma$  have their major roles in the regulation of carbohydrate and lipid metabolism respectively. There has been considerable debate about the relative roles of disturbances of carbohydrate or lipid metabolism as the ‘prime mover’ in the development of insulin resistance, the metabolic syndrome and Type 2 diabetes (McGarry, 1992). The illustration that a combination of modest primary defects in both processes can have such catastrophic consequences for insulin sensitivity emphasises the requirement for taking an integrated approach to the search for aetio-pathogenic pathways in common metabolic diseases such as Type 2 diabetes.

## Chapter 6

# A NOVEL CLASS OF HUMAN PPAR $\gamma$ MUTATIONS CAUSES LIPODYSTROPHIC INSULIN RESISTANCE BY DOMINANT NEGATIVE INHIBITION VIA A NON-DNA BINDING, INTERFERENCE MECHANISM

### 6.1 Introduction

The nuclear receptor PPAR $\gamma$  plays an important role in adipogenesis and glucose homeostasis. The presence of heterozygous loss-of-function mutations within the ligand-binding domain (LBD) of PPAR $\gamma$  in patients with insulin resistance provides direct genetic evidence of a link between PPAR $\gamma$  action and the regulation of mammalian glucose homeostasis (Barroso *et al.*, 1999; Agarwal and Garg, 2002; Hegele *et al.*, 2002). Originally we described three individuals, each heterozygous for one of two mutations (V290M, P467L), within the LBD of PPAR $\gamma$ , all of whom exhibited marked insulin resistance with early onset T2DM, together with numerous features of the metabolic syndrome including dyslipidaemia (high triglycerides, low levels of high density lipoprotein (HDL) cholesterol) and hypertension (Barroso *et al.*, 1999). Subsequent studies revealed each of the affected individuals to have a reduction of subcutaneous limb and buttock fat (Chatterjee, 2001; Savage *et al.*, 2003) i.e. a stereotyped pattern of partial lipodystrophy.

At a molecular level, both mutations retained DNA binding but were severely deficient in their ability to transactivate by virtue of attenuated ligand binding and failure to recruit transcriptional coactivators in response to synthetic (Barroso *et al.*, 1999) or putative natural ligands (Chapter 4; Agostini *et al.*, 2004). Moreover, they were able to recruit corepressors to silence transcription and to suppress the transcriptional activity of cotransfected wild type receptor through dominant negative inhibition in a manner analogous to that seen with naturally occurring thyroid hormone receptor  $\beta$  (TR $\beta$ ) mutants in the syndrome of resistance to thyroid hormone (RTH Refetoff *et al.*, 1993).

Subsequently two other groups have reported the presence of mutations in the LBD of PPAR $\gamma$  in patients with partial lipodystrophy and insulin resistance. Hegele and colleagues identified four heterozygotes for the PPAR $\gamma$ 2 F388L (F360L in PPAR $\gamma$ 1) mutation in a three-generation Canadian kindred (Hegele *et al.*, 2002). Agarwal and Garg found an R425C (R397C in PPAR $\gamma$ 1) PPAR $\gamma$ 2 mutation in a single patient who was ascertained based on a clinical diagnosis of partial lipodystrophy (Agarwal and Garg, 2002).

Previously, we have also identified a heterozygous frameshift premature stop codon mutation in the DNA-binding domain (DBD) of PPAR $\gamma$  in several individuals in a large UK kindred. This mutation (FS) yields a truncated protein lacking a significant proportion of the DBD and the entire LBD. FS PPAR $\gamma$  is unable to bind DNA, fails to regulate a PPAR $\gamma$  target gene and exhibits no discernible dominant negative activity. Significantly, only individuals who were doubly heterozygous for the FS mutant and an additional defect in an unrelated gene which encodes the muscle-specific regulatory subunit of protein phosphatase 1 (PPP1R3A), exhibited severe insulin resistance (Savage *et al.*, 2003 and chapter 5) suggesting that PPAR $\gamma$  haploinsufficiency alone is insufficient to bring about the full clinical phenotype. However, in contrast, Hegele and colleagues have reported that heterozygosity for a single base mutation in the PPAR $\gamma$ 4 gene promoter leading to reduced receptor expression and possible haploinsufficiency was associated with partial lipodystrophy and insulin resistance in two individuals from one family (Al-Shali *et al.*, 2004); more recently the same group has identified a frameshift mutation designated E138fs $\Delta$ AATG PPAR $\gamma$ 2 and predicted to truncate the receptor at the junction of the N-terminus and DBD in a single female subject with similar phenotype (Hegele *et al.*, 2006). However, it should be noted that the possibility of interaction with a second gene defect to produce the clinical phenotype was not excluded in either of these cases.

Taken together these findings have helped to refine our understanding of the clinical phenotype of the disorder associated with human PPAR $\gamma$  mutations, which includes as core features stereotyped partial lipodystrophy, involving the limbs and buttocks with relative sparing of the face and central abdominal adipose depots, insulin resistance, dyslipidaemia and hypertension. Non HIV-related, gluteal and limb partial lipodystrophy (PLD) is also largely associated with mutations in the LMNA

gene (lamin A/C) (Cao and Hegele, 2000; Shackleton *et al.*, 2000; Speckman *et al.*, 2000).

We therefore decided to continue screening for mutations in PPAR $\gamma$  in individuals exhibiting these clinical features focusing particularly on a subset of patients with partial lipodystrophy in whom sequencing of the LMNA gene had revealed no abnormalities.

This chapter will describe three novel heterozygous mutations, one in the LBD and two in the DBD of PPAR $\gamma$ , which we have identified in three unrelated subjects with partial lipodystrophy, severe insulin resistance, dyslipidaemia and hypertension. No associated defect in the *PPP1R3A* gene or other mutations in the coding or promoter regions of PPAR $\gamma$  were identified in these subjects. These novel PPAR $\gamma$  mutations are unable to bind to DNA and are transcriptionally inactive. However, in contrast to the previously described FS mutation, the novel mutant proteins retain the ability to translocate appropriately to the nucleus and exhibit dominant negative activity when co-expressed with wild type receptor in cotransfection assays.

*Ex vivo* evidence for such dominant negative inhibition is provided through the study of primary monocyte-derived immature dendritic cells from subjects harbouring the novel mutations, which are markedly refractory to stimulation with PPAR $\gamma$  agonist. These observations suggest that dominant negative inhibition is exerted by the new PPAR $\gamma$  mutants and occurs via a novel mechanism, possibly through competition for coactivators, thus interfering with transcriptional activation by their WT counterpart. Analogous heterozygous mutations, lacking DNA binding activity, in TR $\beta$  or VDR are not associated with a pathogenic phenotype, raising the possibility that the PPAR $\gamma$  signalling pathway mediating adipocyte differentiation or lipogenesis is uniquely sensitive to interference by depletion of critical cofactors or a cofactor complex.

## **6.2 Material and methods**

### **6.2.1 Clinical studies**

All studies were approved by the local research ethic committees (REC ref: 03/114), and informed consent was provided by each affected and control subject for all investigations. Case histories of each proband harboring the C114R, C131Y and R357X mutations are outlined in Figures 6.2, 6.3 and 6.4.

### **6.2.2 Screening for *PPAR* $\gamma$ and *PPP1R3A* mutations**

A cohort of patients with insulin resistance and partial lipodystrophy was screened for mutations in *PPARG* and *PPP1R3A* genes. Genomic DNA was extracted from peripheral blood leucocytes using a standard technique as described in Chapter 2, section 2.3.2.1. The coding regions of *PPP1R3A* (exons 1-4) and *PPAR* $\gamma$  (exons 1-6, exon B and the promoter region of *PPAR* $\gamma$ 4) genes were amplified using gene specific primers (Tables 5.1 and 6.1) and a protocol previously described (Chapter 2, section 2.3.8). Purified PCR products were subjected to automated sequencing using the Big Dye Terminator v3.1 Cycle Sequencing Kit (Applied Biosystem), with the same primers used for PCR amplification, and analysed using an ABI Prism 3100 sequencer (Chapter 2, section 2.3.9).

### **6.2.3 Plasmids and constructs**

Full-length human *PPAR* $\gamma$ 1 and *PPAR* $\gamma$ 2 cDNAs were cloned by reverse transcription polymerase chain reaction from total human preadipocyte RNA and introduced into the pcDNA3 expression vector (Invitrogen, Groningen, Netherlands) as XhoI/XbaI fragments. The *PPAR* $\gamma$  mutants were generated by site-directed mutagenesis of both wild type (WT) isoform ( $\gamma$ 1 and  $\gamma$ 2) receptor templates as previously described (Chapter 2, section 2.3.10) and verified by direct sequencing. The expression of <sup>35</sup>S-labelled proteins was verified by coupled transcription and translation *in vitro* (TNT, Promega). Fusion proteins of *PPAR* $\gamma$  and VP16 were generated by cloning full-length *PPAR* $\gamma$  cDNAs in to the KpnI/NheI site of pCMX-VP16-N (kind gift of R. Evans) resulting in an amino-terminal fusion of VP16 to

PPAR $\gamma$ . The full-length sequences of WT and PPAR $\gamma$ 1 mutants were inserted between the XmaI/BamHI site of pEGFP-C1 (Clontech) to produce expression vectors encoding for EGFP-tagged-WT or mutants PPAR $\gamma$ 1 proteins. Gal-4 RXR $\alpha$  (Collingwood *et al.*, 1994), (PPARE)<sub>3</sub>TKLUC (Forman *et al.*, 1995) and UASTKLUC constructs (Tone *et al.*, 1994) have been described previously. The haP2-LUC reporter gene consists of 5400 kb of human aP2 promoter sequence cloned upstream of luciferase and has been described previously (Rival *et al.*, 2004).

#### **6.2.4 DNA binding assay**

The ability of WT and mutant receptors to bind to DNA or heterodimerize with RXR was assessed in electrophoretic mobility shift assays as described previously (Chapter 2, section 2.4.3) using <sup>35</sup>S-labelled *in vitro* translated full-length PPAR $\gamma$  proteins quantitated by SDS-PAGE analysis and RXR $\alpha$  co-incubated with various <sup>32</sup>P-labelled oligonucleotide duplexes encoding the following native human (h) PPARE: aP2, adipocyte protein 2 or fatty acid binding protein 4 (FABP4) (h), which was identified by alignment of the human promoter sequence with the response element identified in the murine gene (Graves *et al.*, 1992); Adiponectin (h) (Iwaki *et al.*, 2003); ACoABP, acyl coenzyme A binding protein (h) (Helledie *et al.*, 2002); mCPT1, muscle carnitine palmitoyl transferase 1 (h) (Mascaro *et al.*, 1998); LXR $\alpha$ , liver X receptor  $\alpha$  (h) (Laffitte *et al.*, 2001); CAP1, cbl associated protein (h) (Baumann *et al.*, 2000); LPL, lipoprotein lipase (Schoonjans *et al.*, 1996); ACoAOx, acyl coenzyme A oxidase (h) (Varanasi *et al.*, 1996); ACoAOx (r) (Zamir *et al.*, 1997). The sequences of these native PPAREs are shown in Figure 6.9a.

#### **6.2.5 Transfection assays**

293EBNA cells were cultured in 24-well plates in DMEM containing 10% fetal bovine serum and changed to medium containing AG-1-X8 resin-stripped serum prior to transfection. Each well was cotransfected with 500ng of (PPARE)<sub>3</sub>TKLUC (Forman *et al.*, 1995) reporter construct together with 25-100ng of receptor expression vector (wild type, mutants or empty vector pcDNA3) using the calcium phosphate method (Chapter 2, section 2.6.2). Where appropriate, ligand was added 5

hours after transfection and cells were harvested 36 hours later. For mammalian-2-hybrid transfections each well was transfected with 50ng of VP16-PPAR $\gamma$  expression vectors and Gal-4 RXR $\alpha$  together with 500ng of UASTKLUC reporter.

3T3-L1 cells were transfected using the following conditions: for each well of a 24-well plate, a mixture of 50 $\mu$ l Optimem (GIBCO) and 1 $\mu$ l Lipofectamine2000 (Invitrogen) was, after 5 minutes incubation, added to a mixture of 66ng of receptor expression vector (wild type, mutants or empty vector pcDNA3), 265ng haP2-luc and 65ng Bos- $\beta$ -gal. Following 30 minutes incubation, this mixture was added to the cells cultured in 500 $\mu$ l DMEM containing 10% FCS without antibiotics. After 5 hours the medium was replaced by 0.5ml normal growth medium containing the appropriate ligand. The cells were harvested after 36 hours.

Luciferase values were normalised to  $\beta$ -galactosidase activity from the internal control plasmid Bos- $\beta$ -gal (65-100ng) as previously described (Collingwood *et al.*, 1994), and represent the mean  $\pm$  s.e.m. of at least three independent experiments, each performed in triplicate.

### **6.2.6 Cellular localisation of EGFP- PPAR $\gamma$ fusion**

This experiment was performed by my colleague Dr Erik Schoenmakers. In brief 293EBNA cells were grown in glass well slides (Nalgene Nunc International) to 30% confluence and then transfected using Lipofectamine2000 (Invitrogen) according to manufacturer's instructions with 1 $\mu$ g of expression vector encoding EGFP alone (GFP), or EGFP-wild type PPAR $\gamma$ 1 or EGFP-mutant PPAR $\gamma$ 1 fusion proteins for each well. After fixation using 4% paraformaldehyde and nuclear staining with 4,6-diamidino-2-phenylindole (DAPI), slides were mounted (Vectashield medium, Vector Laboratories) and fluorescence visualized by digital microscopy using a Nikon DXM1200 camera system.

### **6.2.7 Peripheral blood monocyte purification and IDC culture**

Monocytes were derived from peripheral blood from the index cases harbouring PPAR $\gamma$  mutations and from normal control subjects by Ficoll gradient centrifugation and immunomagnetic cell separation using anti-CD14-conjugated microbeads (VarioMACS; Miltenyi Biotec). Immature dendritic cells (IDCs) were prepared as



described previously (Sallusto and Lanzavecchia, 1994; Chapter 2, section 2.6.4). Briefly, monocytes were resuspended into 6-well culture plates at a density of  $1.5 \times 10^6$  cell/ml and cultured in RPMI 1640 supplemented with 10% FBS containing 800U/ml GM-CSF (Leucomax) and 500U/ml IL-4 (Peprotech) for 24 hours in the presence of vehicle (DMSO) or 1 $\mu$ M Rosiglitazone.

### **6.2.8 Quantitative real-time PCR analysis of gene expression**

Total RNA from IDCs was isolated using TRIZOL reagent (Invitrogen), and 100ng subjected to reverse transcription (performed at 42 $^{\circ}$ C for 30minutes) using the Superscript II reverse transcriptase kit (Invitrogen). Quantitative real-time PCR (qPCR) (ABI PRISM, Applied Biosystems), was carried out as follows: 40 cycles at 95 $^{\circ}$ C for 12 seconds and 60 $^{\circ}$ C for 40 seconds using Taqman assays. All qPCR reactions were performed in triplicate with one control reaction without RT enzyme. The comparative Ct method was used to quantify transcripts and normalize for expression levels of the 36B4 housekeeping gene, which did not vary with ligand treatment. The sequences of the primers and probes are showed in Table 6.2.

Taqman qPCR low density arrays (TLDA) were used to quantify the expression of multiple target genes in IDCs, according to the manufacturer's instructions. To obtain cDNA, RNA was reverse transcribed using the High Capacity cDNA Archive kit (Applied Biosystems). The following commercially available Taqman assays (Applied Biosystems) were used: ADRP/ADFP (Hs00605340\_m1), APOC1 (Hs00155790\_m1), CLDN1 (Hs00221623\_m1), aP2/FABP4 (Hs00609791\_m1), CLECSF5 (Hs00183780\_m1), CD1E (Hs00229421\_m1), MYO1B (Hs00362654\_m1), IL1R2 (Hs00174759\_m1), OAS1 (Hs00242943\_m1), p30 (Hs00396457\_m1), cyclophilinA/PPIA (Hs99999904\_m1). The comparative Ct method was used to quantify transcripts and normalize to cyclophilinA expression levels, which did not vary with ligand treatment. Thereafter, data were further normalized to the expression level of ligand-treated WT PPAR $\gamma$  cell samples. TLDA data analysis and normalization was carried out using GeneSpring 7.2 (Agilent).

### **6.2.9 RFLP analysis of PPAR $\gamma$ transcripts**

Following reverse transcription of RNA obtained from immature dendritic cells of

the patient carrying the R357X mutation and a normal control, as described in 6.2.8, 2 $\mu$ l of cDNAs were amplified by PCR using the PPAR-FOR and PPAR-REV primers shown in table 6.2. PCR conditions were initial denaturation for 3 minutes at 95°C followed by 30 cycles of 95°C denaturation for 1 minute, 55°C annealing for 1 minute and 72°C elongation for 1 minute. After column purification (QIAGEN), the PCR products were digested with Cac8I enzyme at 37°C for 2 hours and the digestion products analysed by electrophoresis on a 2% (w/v) agarose gel.

#### **6.2.10 Immunoprecipitation and Western blot analysis**

IDCs generated from 200ml of peripheral blood (from a normal control subject and the R357X patient) as described in paragraph 6.2.7, and 293EBNA cells transfected with WT or mutant PPAR $\gamma$ 1 constructs, were lysed in ice-cold RIPA buffer containing no SDS but with a mixture of protease inhibitors (Roche Molecular Biochemicals). Following centrifugation at 12,000g for 10 minutes at 4°C, cell supernatants were immunoprecipitated at 4°C over night with anti-human PPAR $\gamma$  common monoclonal mouse antibody (K8713 Perseus Proteomics) and protein A beads and separated by electrophoresis. For Western blot analysis, detection was performed with anti-PPAR $\gamma$  (H-100) rabbit antibody (Santa Cruz Biotechnology).

#### **6.2.11 Adenoviral PPAR $\gamma$ construction and expression**

This experiment was performed by my colleague Dr Erik Schoenmakers. Briefly recombinant type 5 adenoviruses (Ad5) expressing GFP alone, or GFP plus either wild type or C114R mutant PPAR $\gamma$ 1 were generated using the *AdEasy Vector System* (Quantum Biotechnologies, Montreal) and amplified and purified as previously described (Gurnell *et al.*, 2000). Chub-S7 human preadipocyte cells were cultured in 6-well plates and differentiation was induced as previously reported (Darimont *et al.*, 2003) in the presence of 100nM rosiglitazone. Cells were transduced with 2x10<sup>7</sup> pfu/well of recombinant virus one day prior to induction of differentiation and comparable infection efficiency was verified by fluorescence microscopy. Samples for qPCR were collected at day 0 (start of differentiation), day 3, day 5 and day 7. Fully differentiated Chub-S7 cells were fixed and stained with Oil Red O as described previously (Adams *et al.*, 1997).

## 6.3 Results

### 6.3.1 Screening of *PPARG* and *PPP1R3A* genes

All coding exons of PPAR $\gamma$  including exon B encoding the amino-terminal splice variant PPAR $\gamma$ 2 and the promoter region of PPAR $\gamma$ 4 were PCR amplified and direct sequenced in a cohort of 32 patients with insulin resistance and partial lipodystrophy. Three individuals were found to be heterozygous for different single nucleotide substitutions which are predicted to generate three novel missense receptor mutations: for consistency, the codon nomenclature of all PPAR $\gamma$  mutations described is in the  $\gamma$ 1 isoform context, based on a predicted protein sequence of 477 amino acids. Subject 1 (S1, the index case from kindred A) was found to be heterozygous for a single nucleotide substitution (T to C) resulting in a cysteine to arginine mutation at codon 114 (C114R) within the first zinc-finger in the DBD of the receptor (Figures 6.1 and 6.7); Subject 2 (S2, the index case from kindred B) also had a mutation in the DBD of the receptor - a single G to A nucleotide substitution resulting in cysteine to tyrosine transition at codon 131 (C131Y), again within the first zinc-finger of the DBD within the P box region (Figures 6.1 and 6.7). Her father and one of her two sisters were found to be heterozygous for the same mutation, while her unaffected mother and other sister were homozygous for the wild type receptor sequence; Subject 3 (S3, the index case from Kindred C) was heterozygous for a single nucleotide substitution (C to T) replacing Arginine with a premature stop codon at residue 357 (R357X) in the LBD of the receptor. Her similarly affected deceased mother was also found to harbor the R357X mutation (Figure 6.1 and 6.7). Other unaffected family members did not carry the mutation. No other nucleotide changes in PPAR $\gamma$  were found in the three subjects. All coding exons and splice junctions of *PPP1R3A* were sequenced in each index case and we identified no mutations or polymorphisms, thereby excluding the possibility of a second genetic defect at this locus as described previously (Savage *et al.*, 2002; Chapter 5). None of these mutations have been identified in sequencing *PPARG* in cohorts of normal subjects (122) or in insulin resistant subjects (93).

### **6.3.2 Clinical results**

The three probands were identified by screening a cohort of patients with unexplained insulin resistance and partial lipodystrophy. Clinical details together with the results of investigations undertaken on the index cases harbouring the different mutations are provided in Table 6.3 and Figures 6.2, 6.3 and 6.4 and confirm many of the features associated with the previously reported cases (Barroso *et al.*, 1999; Savage *et al.*, 2002; Hegele *et al.*, 2002; Agarwal and Garg, 2002). All subjects exhibited marked fasting hyperinsulinaemia with acanthosis nigricans in S3. On physical examination all of the probands had loss of subcutaneous fat from the gluteal region and a muscular appearance of the upper and lower extremities (Figures 6.2, 6.3 and 6.4). In addition, MRI of fat distribution revealed a consistent and remarkable paucity of subcutaneous limb and buttock fat (Figure 6.5). Marked dyslipidaemia (raised triglycerides, low HDL) with hepatic steatosis was a feature of all cases. S2 and S3 exhibited early onset hypertension unrelated to comorbidities. S3 had suffered recurrent bouts of pancreatitis.

### **6.3.3 Novel PPAR $\gamma$ mutants are non DNA binding, with complete loss-of-function**

When assayed by cotransfection with a PPARE-containing reporter gene [(PPARE)<sub>3</sub>TKLUC], the novel PPAR $\gamma$  mutants exhibited negligible transcriptional activity, lacking both the constitutive basal activity previously noted with WT PPAR $\gamma$  (Chapter 4; Agostini *et al.*, 2004; Zamir *et al.*, 1997) as well as any response to rosiglitazone, a potent thiazolidinedione receptor agonist (Figure 6.8). Such complete loss-of-function was reminiscent of the properties of the previously reported FS PPAR $\gamma$  mutant and might be anticipated in an analogous truncation mutant (R357X) not possessing the transactivation (AF-2) domain at the receptor carboxyterminus (Figure 6.7) (Zamir *et al.*, 1997, Wu *et al.*, 2003), but the lack of activity with the receptor DBD mutants (C114R and C131Y) prompted further investigation of their DNA binding properties.

PPAR $\gamma$  is a ligand-dependent transcription factor that regulates target gene transcription by binding to specific response elements as a heterodimer with retinoid X receptor (RXR). This complex has been shown to bind a DNA response element,

usually consisting of a direct repeat (DR1) of the consensus sequence (AGGTCA) separated by a single nucleotide, derived from PPAR-responsive target genes (Ijpenberg *et al.*, 1997); a recent study has suggested that the stringency of PPAR $\gamma$  binding to some response elements is relatively relaxed, and does not require complete integrity of its DNA binding domain (Temple *et al.*, 2005). Like all nuclear receptors PPAR $\gamma$  exhibits a modular structure consisting of a central DBD, which contains two zinc-fingers, an amino-terminal activation domain, and a carboxy-terminal LBD (Fig 6.7). The R357X premature stop mutation leads to a mutant receptor that is truncated between helices 6 and 7 of the LBD – a region common to both the  $\gamma$ 1 and  $\gamma$ 2 isoforms of the receptor (Figure 6.7). R357X protein lacks the carboxy terminal region containing the dimerization interface for RXR, and as consequence, we predicted that it would be unable to form a heterodimeric complex with RXR and therefore fail to bind DNA despite preservation of its DBD. The C114R and C131Y mutations are located in the DBD, which is common to both  $\gamma$ 1 and  $\gamma$ 2 isoforms of the receptor, and which is critical in mediating receptor interaction with PPAR-specific response elements (PPAREs) in target gene promoters (Figure 6.7). In particular the two mutated cysteine residues coordinate the zinc ion within the first zinc-finger. Accordingly, the ability of the PPAR $\gamma$  mutants to bind DNA as heterodimers with RXR was tested using a range of previously documented or predicted PPAREs from known target genes using an electrophoretic mobility shift assay (EMSA). As a control we also included the FS PPAR $\gamma$  mutant, which has previously been shown to lack DNA binding (Savage *et al.*, 2002; Chapter 5). Unlike the wild type (WT) receptor, both DBD and LBD truncation receptor mutants showed negligible heterodimeric binding on an array of PPAREs (Figure 6.9). However, it was still conceivable that the DBD (C114R, C131Y) mutants could be recruited indirectly to a PPARE by binding RXR via the known dimerisation interface within their intact LBD (Gampe *et al.*, 2000), or conversely, that the R357X LBD truncation mutants might bind a PPARE monomerically as has been documented for TR (Lazar *et al.*, 1991). To test this possibility, fusions of the VP16 activation domain linked to full-length PPAR $\gamma$  were coexpressed with (PPARE)<sub>3</sub>TKLUC and, in comparison to WT the mutant receptors showed no reporter gene activity, suggesting negligible recruitment to its response element

(Figure 6.10). Thus, like the FS receptor mutant, the novel DBD and LBD truncation PPAR $\gamma$  mutants lack DNA binding.

#### **6.3.4 Novel PPAR $\gamma$ mutants translocate to the nucleus and interact with RXR**

To function as transcription factor PPAR $\gamma$  interacts with transcriptional machinery within the nucleus, and therefore the inability of mutant receptors to bind DNA raised the question as to whether the novel mutations simply resulted in null alleles or whether they encoded proteins which could conceivably interfere with WT signalling. We speculated that if the latter possibility were to be the case, the mutant receptors would need to target normally to the nucleus. So to visualize the localization of receptor proteins in living cells, we generated fusion of green fluorescent protein (GFP) linked to WT and PPAR $\gamma$  mutants. Confocal microscopy showed that while GFP alone remained mainly in the cytoplasm the GFP-WT PPAR $\gamma$  fusion localized to the nucleus as expected (Figure 6.11). The GFP-mutant PPAR $\gamma$  proteins revealed differing distributions inside the cells: the R357X, C114R and C131Y GFP fusion proteins were able to translocate appropriately to the nucleus in a manner similar to the WT receptor, in keeping with preservation of the putative nuclear localization signal (NLS) located in the hinge region between the DNA and the ligand-binding domains; in contrast the GFP-FS truncation mutant, which lacks this targeting sequence, remained cytoplasmic like GFP (Figure 6.11). Having observed appropriate nuclear localisation, we next examined whether the PPAR $\gamma$  mutants might interact with RXR in a mammalian two-hybrid assay. Cotransfection of full-length wild type PPAR $\gamma$  protein fused to the activating domain of VP-16 with the expression vector GAL4-RXR $\alpha$  encoding the DBD of the yeast transcription factor GAL4 linked to the LBD of RXR $\alpha$  (residues 198-467), resulted in a marked induction of luciferase activity (Figure 6.12) as did the VP16-C114R and VP16-C131Y. Negligible induction was observed with VP16-R357X indicating markedly impaired heterodimeric interaction between this truncation mutant and RXR $\alpha$ . This result suggested that defective dimerisation was responsible for the impaired DNA binding properties observed with the R357X mutant in EMSA.

### 6.3.5 Novel PPAR $\gamma$ mutants inhibit WT receptor action

Having established that the novel PPAR $\gamma$  mutants could translocate to the nucleus and interact with RXR, we next sought to determine whether they might interfere with WT receptor signalling. Using the (PPARE)<sub>3</sub>TKLUC reporter gene, we investigated whether mutant receptors were able to inhibit wild type receptor action in a dominant negative manner. Mutant receptors R357X, C114R and C131Y were coexpressed at ratio of 1:1 & 2:1 with the WT receptor and reporter gene activities assayed at two ligand concentrations (10nM and 1000nM). Although mutant to wild type receptor ratios of 2:1 demonstrated the greatest dominant negative activity, these inhibitory effects were also apparent with equal ratios of transfected receptors (Figure 6.13a), unlike the FS PPAR $\gamma$  mutant previously described, which did not exhibit any dominant negative activity (Chapter 5, Figure 5.4).

The murine adipocyte P2 (*aP2*) gene is a classical target of PPAR $\gamma$  action (Tontonoz *et al.*, 1994; Guan *et al.*, 2005) and the human homologue (*FABP4*) is similarly responsive (Pelton *et al.*, 1999). Therefore we decided to assess the dominant negative activity of mutant receptors with the human *aP2/FABP4* gene promoter in 3T3-L1 adipocytes. Both the DBD and R357X LBD truncation PPAR $\gamma$  mutants inhibited WT PPAR $\gamma$  activation, whereas the FS mutant lacked such dominant negative inhibitory activity (Figure 6.13b).

The fatty acid binding protein 4 / adipocyte P2 (*FABP4* or *aP2*) gene, is also a well-validated PPAR $\gamma$  target gene in other tissues, having previously been shown to be expressed and regulated by PPAR $\gamma$  ligands in peripheral blood mononuclear cells (PBMCs) (Pelton *et al.*, 1999). Moreover, very recently it has been shown that PPAR $\gamma$  is promptly up-regulated and transcriptionally active in differentiating dendritic cells (DCs), with the highest levels of receptor expression and ligand responsiveness occurring within the first 24 hours of differentiation (Szatmari *et al.*, 2004). We therefore, decided to examine the expression levels of PPAR $\gamma$  and *aP2/FABP4* in IDCs generated from controls subjects and probands harbouring different PPAR $\gamma$  mutations to determine whether the dominant negative activity of PPAR $\gamma$  mutant observed *in vitro*, might be reflected also *ex vivo*. Compared with a normal control subject of similar age and sex, ligand-dependent induction of *aP2* expression in R357X and C114R containing IDCs was markedly impaired even at

the highest concentration of rosiglitazone tested (Figure 6.14). Importantly both WT and mutation-containing cells exhibited similar levels of PPAR $\gamma$  expression (data not shown). On at least three different occasions we examined aP2 induction in IDCs obtained from a number of subjects harbouring the C114R, C131Y, R357X and FS mutations in the absence and presence of ligand (1 $\mu$ M Rosiglitazone). In parallel we also examined the induction of aP2 in IDCs from 2 normal controls (one male and one female) and 2 comparably insulin resistant patients known not to harbour mutations in PPAR $\gamma$  (one male and one female). As shown in Figure 6.15a aP2 expression was consistently and significantly up regulated as a result of ligand treatment in all four controls, whereas such induction was markedly attenuated in C114R, C131Y and R357X patients. Interestingly, aP2 expression in FS mutation-containing cells was also up regulated in a similar manner to that observed in control IDCs. Of note is that despite variability in aP2 induction, all cells demonstrated comparable PPAR $\gamma$  expression levels (Figure 6.15b). These results suggest that the dominant negative inhibition by mutant receptors observed on the human aP2 gene promoter *in vitro* (Figure 6.13), appears to correlate with reduced aP2 induction in response to PPAR $\gamma$  activation in novel mutation-containing cells *ex vivo*.

To exclude the possibility that the attenuated aP2 induction observed with R357X mutation-containing cells *ex vivo* might be the result of haploinsufficiency as a consequence of nonsense-mediated decay of the R357X mRNA transcript (Culbertson, 1999), we investigated expression of the mutant transcript in immature dendritic cells generated from the proband. Because the presence of the R357X mutation destroys a Cac8I restriction enzyme site, which is present in the wild type sequence, it was possible to test for the presence of both the mutant and wild type mRNA transcripts in R357X cells using this restriction fragment length polymorphism. In addition to the two fragments of 161bp and 74bp corresponding to the pattern of Cac8I digestion of cDNA from wild type allele, an extra specific band of 235bp corresponding to an undigested cDNA fragment was detected only in the cells harboring the R357X allele (Figure 6.17). Moreover, Western blotting revealed expression of both wild type and truncated R357X mutant PPAR $\gamma$  proteins in immature dendritic cells (Figure 6.18). These observations indicate that the mutant R357X transcript is not subject to nonsense-mediated decay.



To determine whether the differences in PPAR $\gamma$  responsiveness between novel mutation (C114R, R357X) versus FS mutation-containing cells were observed in other target gene contexts, we compared expression profiles of other PPAR $\gamma$ -responsive genes identified from extensive microarray profiling of normal IDCs (Szatmari & Nagy, manuscript in preparation); target gene responses to PPAR $\gamma$  agonist in DBD (C114R) and (R357X) LBD truncation mutation-containing cells were markedly attenuated whereas FS mutation-containing cells exhibited intermediate responses that were either similar to or only slightly attenuated compared to WT cells (Figure 6.16).

Finally, we determined whether dominant negative inhibition by a novel, non DNA-binding PPAR $\gamma$  mutant (C114R) could interfere with a receptor-mediated biological process. Compared to control non-transduced, WT PPAR $\gamma$  or GFP adenovirus treated cells, both adipocyte differentiation (Figure 6.19a) and aP2 target gene expression (Figure 6.19b) in human preadipocytes transduced with C114R mutant PPAR $\gamma$  adenovirus were significantly attenuated.

Primer number	Forward Primer sequence 5'-3'	Reverse Primer Sequence 5'-3'
200	TGATATCAGAGAGCCCAATGGA	CGGTAATCCCAGCAATCAA
220	GGTTTCTCCCCTCAACCAAG	TCAAACAGTGGGCTAAAACA
23	CGGACATTTTCCACACAGAAG	GAAGTGGTCAGTTTCACCATCA
260	TGACTGGCAGACACATTATGACA	GCTCCGGCTCTTGTCTTTTC
280	TTTTGGTCAAATAATAATGGCACA	GTTAAAGCCTGGCACCATTG
300	AACCAAATTTGTCTCTTTTGTGAAA	TGCAGCATCTTTGAAGCAGA
22	TGATTGAATTTCCCCCTGTG	TGGCTTCCAAATCTTCCCTG
24	AGAAGATGCAGTCCCAGAAAAA	TTCGATTACTGGCTTCCAAATC
25	TCCCAACAATCATTTGTTCTCAT	GCAGCATCTTTGAAGCAGAAA
320	ATAGCCTGCAAGGATTTCCC	AACCCCTCTGCTTTATTTGGAA
340	CTGCTTCCAGAGATGAAAGGAA	ACGGAGCTTTCTGCTGATGA
360	GAAGAAGCAAATCCATGGTGA	AGGGGCAAGGTATTTGCATT
380	CTGGCAGCAAAGAAGTCCCTG	TCATCATCCTTACCATTGCCA
400	CCATTGAGATACGTCGGCAT	GACACATCTGCTGTGATTGCC
420	CTGAGCGAACATAACCGCAAT	TTTTCCCTGACTTTCCAGAACA
440	TCAGGATAATAGCCCACAGCA	CAGCACACTGTTTCTTGGCA
460	GTGAAGACGTGTGGGGAAAA	TTCATGTGGATCAAACGCTG
480	GCCCATCGAGGTAAAGGAAA	GACCCATGAGGATTCTTCCAC
500	GGAGAAATGTGGCACTGGAA	ACAGCAATTGCCTGCTCATT
520	GCCATTGTGCATTCTGCTTT	GGTGCTTCTCAATACCCTGGA
540	TGAGCAGGCAATTGCTGTAG	TCATGCCTTGCTTCTTCCAT
560	TGCATAGGCCAGATTTTCCA	TGCCTTGAGCTTGACTTTCC
580	GCAAGGCATGAAAATGAAGG	CCCAGGATAGCCAGGACAAT
600	CAAGCTCAAGGCAACGAATC	CCCATTACCAATCCAAATG

**Table 6.1** Sequences of primers used to amplify and sequence the coding region of the *PPP1R3A* gene (exons 1-4).

h36B4 Probe	<i>FAM-AGGCTGTGGTGCTGATGGGCAAGAA</i>
h36B4 Reverse primer	ATATGAGGCAGCAGTTTCTCCAG
h36B4 Forward primer	AGATGCAGCAGATCCGCAT
hFABP4 Probe	<i>FAM-ATTCCACCACCAGTTTATCATCCTCTCGTT</i>
hFABP4 Reverse primer	GGAAGTGACGCCTTTCATGA
hFABP4 Forward primer	GGATGGAAAATCAACCACCA
hPPAR $\gamma$ Probe	<i>FAM-CAAACCTGGGCGGTCTCCACTGAG</i>
hPPAR $\gamma$ Reverse primer	CTTCAATGGGCTTCACATTCA
hPPAR $\gamma$ Forward primer	GATGACAGCGACTTGGCAA
PPAR-FOR	CTCCTTGATGAATAAAGATGGGG
PPAR-REV	ATGTCTTCAATGGGCTTCACAT

**Table 6.2** Sequences of primers and probes used to amplify and quantitate gene expression in immature dendritic cells by qPCR. FAM = 6-carboxy-fluorescein; PPAR-FOR and PPAR-REV are primers used to detect wild type and R357X mutant cDNAs in IDCs

Subject	S1	S2	S3	Reference
Mutation	C114R	C131Y	R357X	
Gender	F	F	F	
Age (and at presentation)(yr)	41 (34)	42 (35)	35 (26)	
BMI (kg/m <sup>2</sup> )	30.8	24.2	29.3	Non obese <30
WC	97	80	96	Female <80 cm
Blood Pressure	155/95*	220/120	125/80*	<130/85 (mmHg)
Diabetes (age at diagnosis)(yr)	T2DM (41)	T2DM (42)	T2DM(26)	
Lipodystrophy	Y	Y	Y	
PCOS	Y	Y	Y	
Hepatic steatosis	Y	Y	Y	
Fasting insulin	310	174	170*	<60 pmol/L
Triglycerides	8.9*	4.5	34.8*	<1.7 mmol/L
HDL Cholesterol	0.47*	0.89	0.56*	>1.29 mmol/L
Predicted total body fat (%)	37.4	28.8	36.4	
Measured total body fat (%)	26 <sup>-0.8</sup>	23 <sup>-1.2</sup>	21 <sup>-1.1</sup>	
Measured lower limb fat (%)	20	17	11	
Measured truncal fat (%)	30	27	28	

**Table 6.3** Clinical, biochemical and body composition data from index cases harbouring the 3 novel PPAR $\gamma$  mutations. All biochemical analyses were performed on fasting samples. BMI, body mass index; WC, waist circumference; T2DM, type 2 diabetes mellitus; PCOS, polycystic ovarian syndrome; HDL, high density lipoprotein; Predicted total body fat was calculated as follows (Black *et al.*, 1983): males % fat = (1.281xBMI) – 10.13; females % fat: (1.48xBMI) – 7.00; Measured total and depot-specific body fat were determined using dual-energy X-ray absorptiometry – with corresponding z-scores for total body fat shown in superscript; Hepatic steatosis was diagnosed according to standard radiological criteria; F, female, \* on therapy

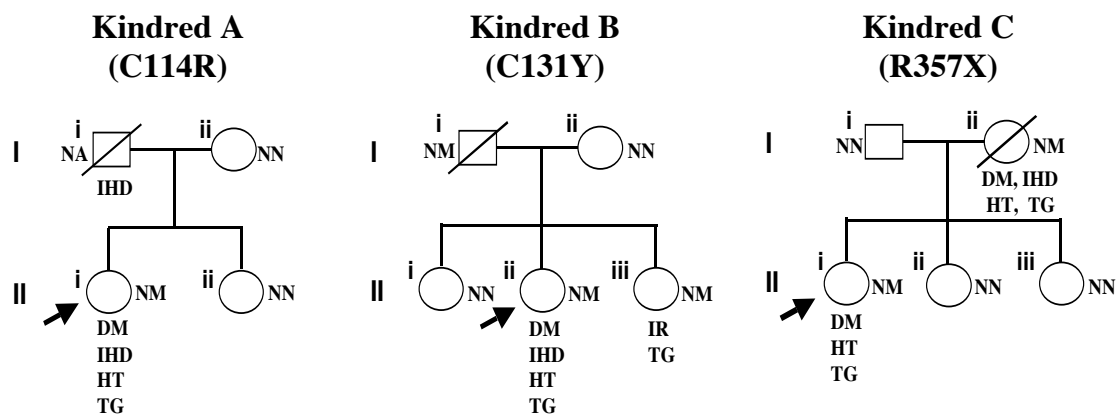


**Figure 6.1** Identification of novel mutations in PPAR $\gamma$  gene in subjects with partial lipodystrophy and insulin resistance. N denotes wild type, M mutant, and NA not available for testing. Squares represent male family members, circles female family member, symbols with a slash deceased family members. Arrows denote probands (S1-S3). DM, type 2 diabetes mellitus; IGT, impaired glucose tolerance; IHD, ischaemic heart disease; HT, hypertension; TG, hypertriglyceridaemia.



**Figure 6.2** Subject 1 (S1), a 43-year-old female was heterozygous for a cysteine-114-arginine (C114R) PPAR $\gamma$  mutation. She presented with subfertility and oligoamenorrhoea aged 34yrs at which time hyperlipidaemia was incidentally noted. Two subsequent pregnancies were uneventful. At the time of investigation aged 41yrs medication included fenofibrate and atorvastatin and clinical examination revealed partial lipodystrophy. Diabetes mellitus was diagnosed aged 41yrs on oral glucose tolerance testing and subsequently managed with dietary treatment. Investigation for secondary amenorrhoea and hyperprolactinaemia revealed an incidental pituitary mesoadenoma treated with cabergoline with restoration of menses. She developed ischaemic heart disease aged 42yrs with severe triple vessel disease confirmed at coronary angiography. Despite percutaneous revascularisation, triple anti-anginal medical therapy and smoking cessation, she continued to suffer from ischaemic cardiac pain. Her mother and sister were unaffected at the PPAR $\gamma$  locus; her father (genotype unknown) died aged 60yrs from a myocardial infarction.

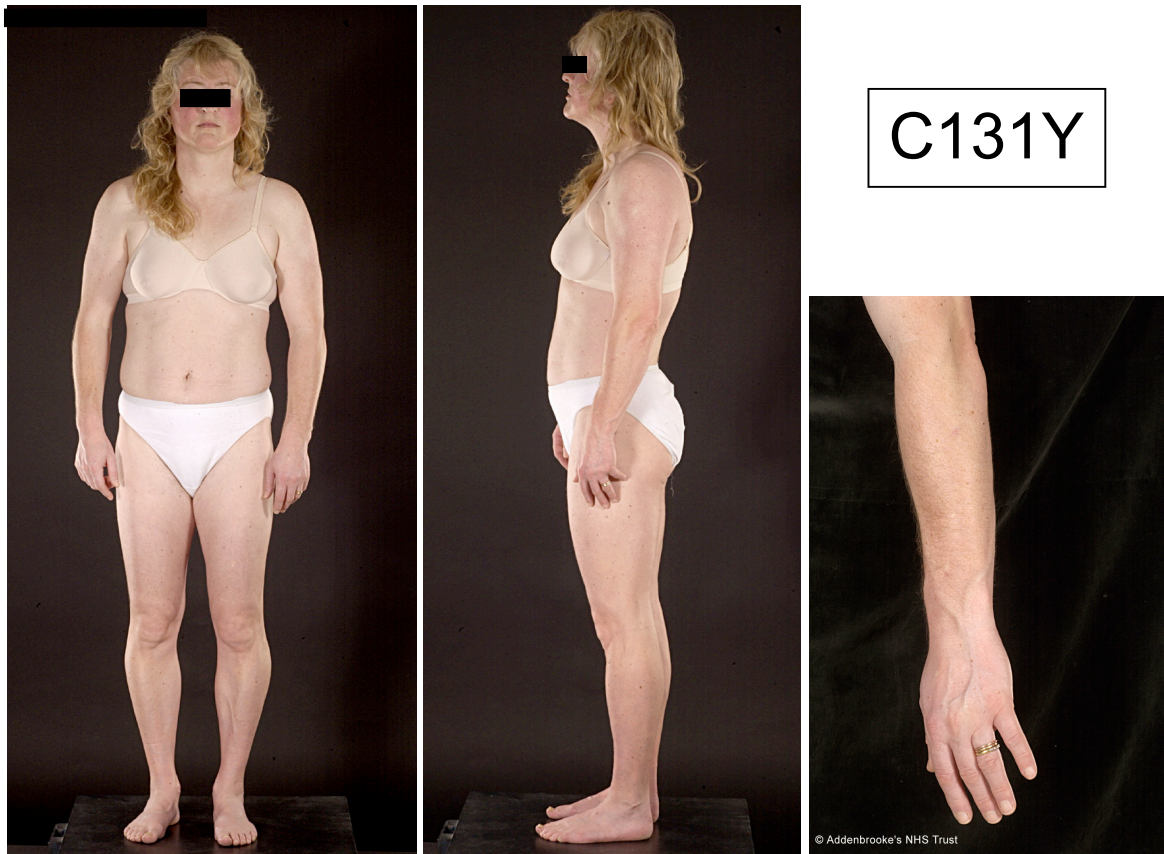


**Figure 6.3** Subject 2 (S2), a 45-year-old female was heterozygous for a cysteine-131-tyrosine (C131Y) PPAR $\gamma$  mutation. She presented aged 35yrs with hypertension and syncopal episodes presumed secondary to rebound hypoglycaemia associated with severe hyperinsulinaemia. Initial clinical examination and investigation highlighted partial lipodystrophy and dyslipidaemia. PCOS was diagnosed on the basis of oligomenorrhoea and confirmatory pelvic ultrasound. Diabetes mellitus diagnosed aged 42yrs was managed with dietary treatment. At the time of investigation aged 35yrs medication consisted of lacidipine and lisinopril. As a lifelong non-smoker she developed ischaemic heart disease aged 44yrs. Angiography confirmed single vessel disease which is managed medically. Her mother and older sister were unaffected at the PPAR $\gamma$  locus but family screening confirmed the C131Y mutation in her younger sister and father. At the time of investigation the sister (a 34-year-old triathlon athlete) was asymptomatic but hyperinsulinaemic and hypertriglyceridaemic. The father, a 74-year old male, showed no evidence of metabolic disturbance in the context of a lifelong “slim” body habitus (BMI at investigation 22.5). As a long-term smoker he developed inoperable lung carcinoma aged 73yrs which was treated palliatively and he died aged 74yrs.



R357X



**Figure 6.4** Subject 3 (S3), a 38-year-old female, heterozygous for an arginine-357-stop (R357X) mutation, presented with oligomenorrhoea and hirsutism following menarche aged 11yrs. Gestational diabetes and hypertension were diagnosed aged 26yrs and her pregnancy was complicated by pre-eclampsia. Persistent hyperglycaemia and hypertension post-partum required metformin and atenolol therapy respectively and glycaemic control remained poor despite subsequent introduction of insulin. Dyslipidaemia was diagnosed aged 29yrs and she commenced fibrate treatment following two episodes of acute pancreatitis. Clinical examination revealed partial lipodystrophy and axillary acanthosis. At the time of investigation her treatment included insulin, metformin, atenolol and fenofibrate. Genetic screening found her mother, now deceased, to also be heterozygous for the R357X mutation. The mother had suffered from longstanding menstrual irregularity and hirsutism, was diagnosed with hypertension in her thirties, type 2 diabetes and dyslipidaemia in her forties and suffered a sudden cardiac death aged 57yrs.



WT



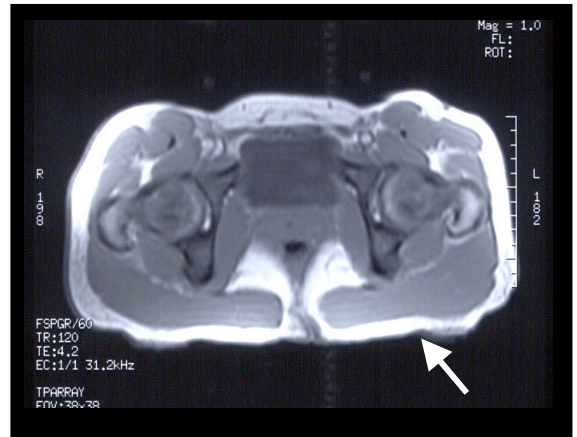
R357X



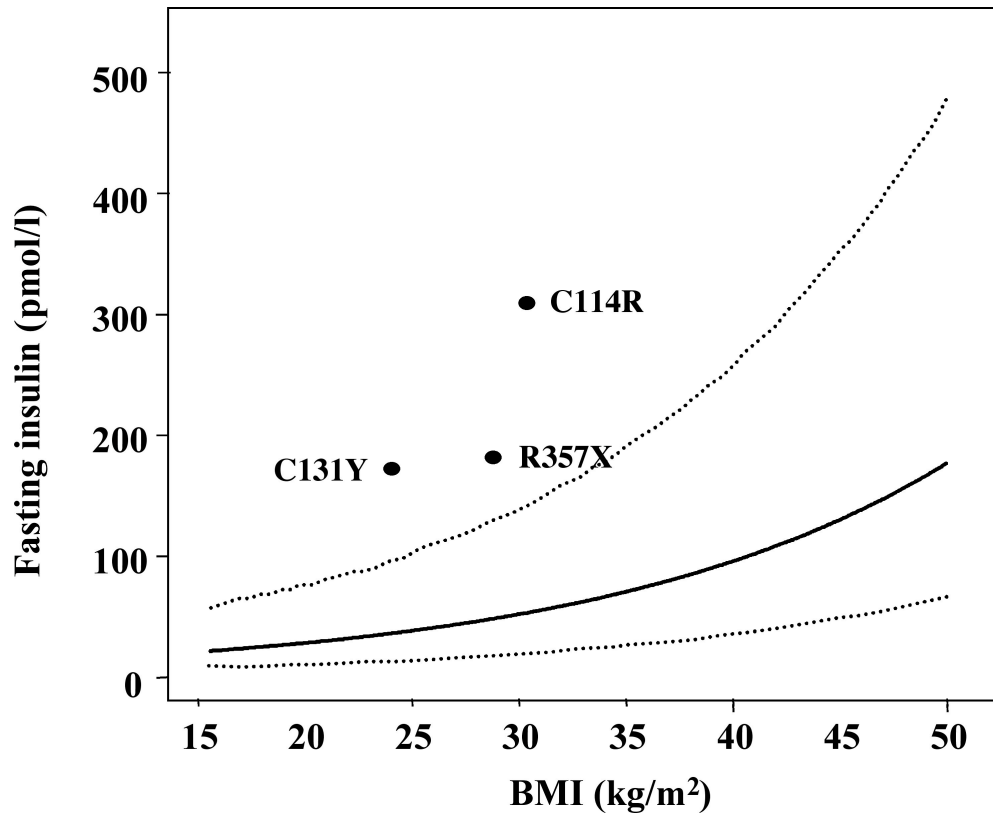
C114R



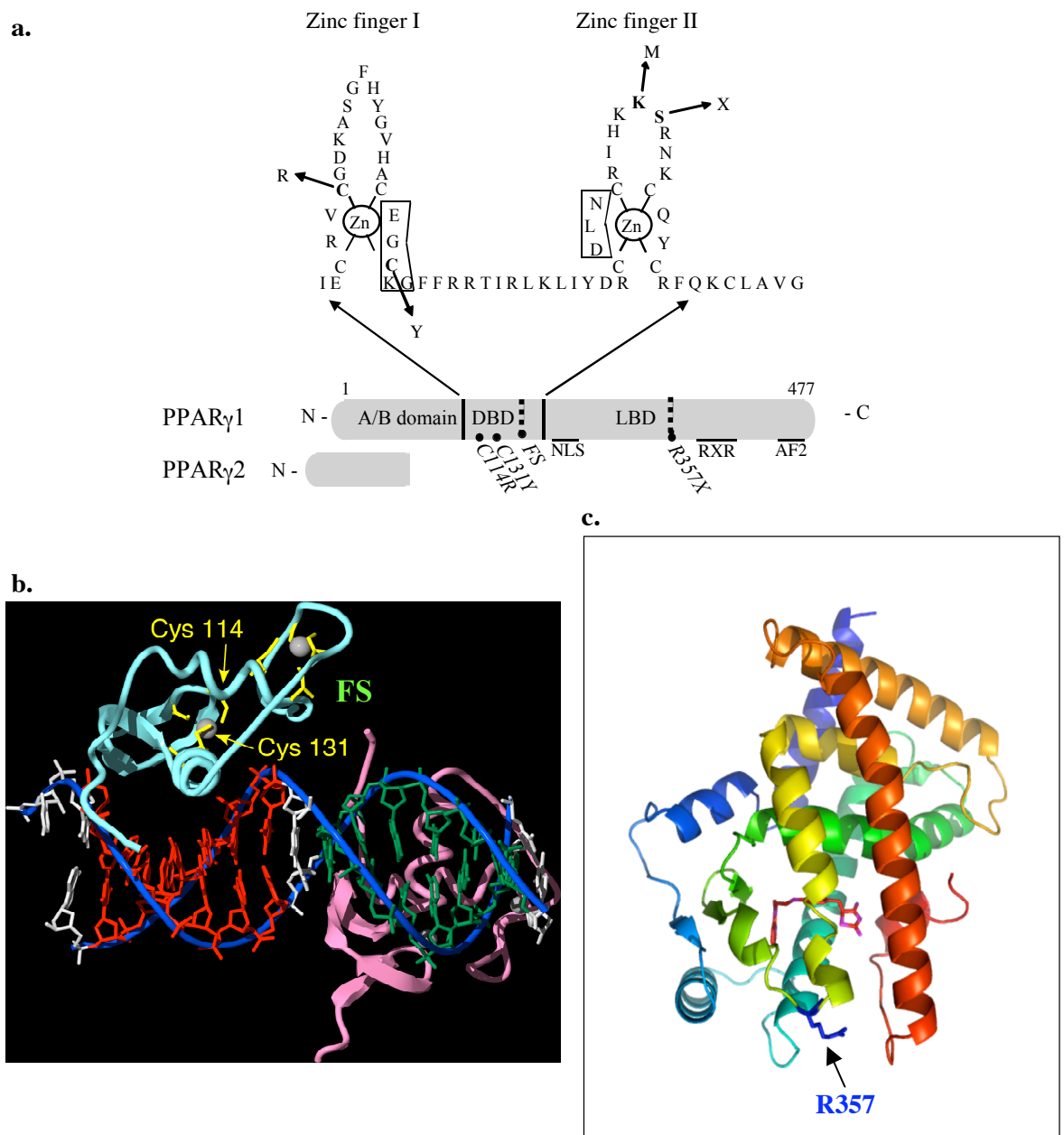
C131Y



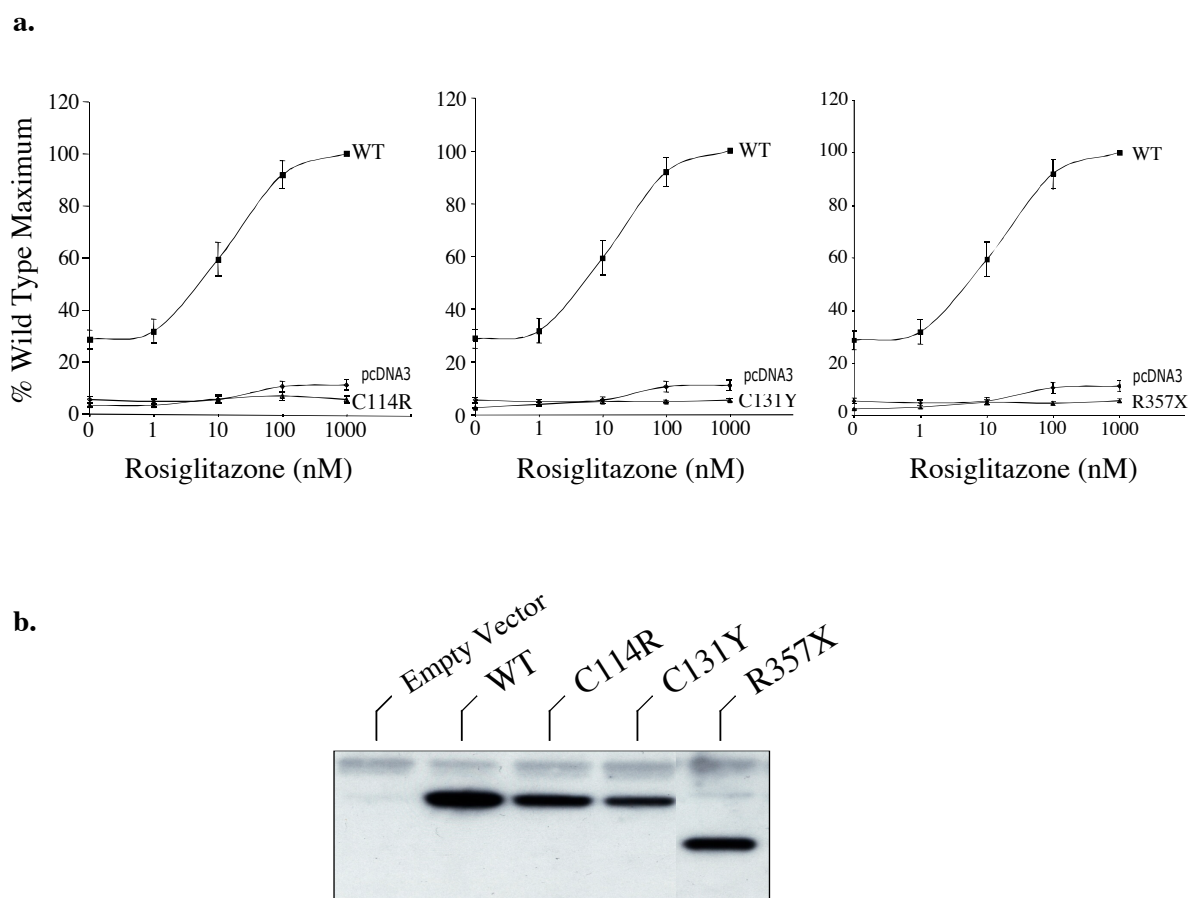
**Figure 6.5** T1-weighted MRI images at the level of the gluteal fat pad in a lean healthy female (WT, top panel on the left) and in the R357X, C114R and C131Y probands. Note the decreased amount of gluteal subcutaneous fat (arrowed) in the affected individuals as compared with the control.



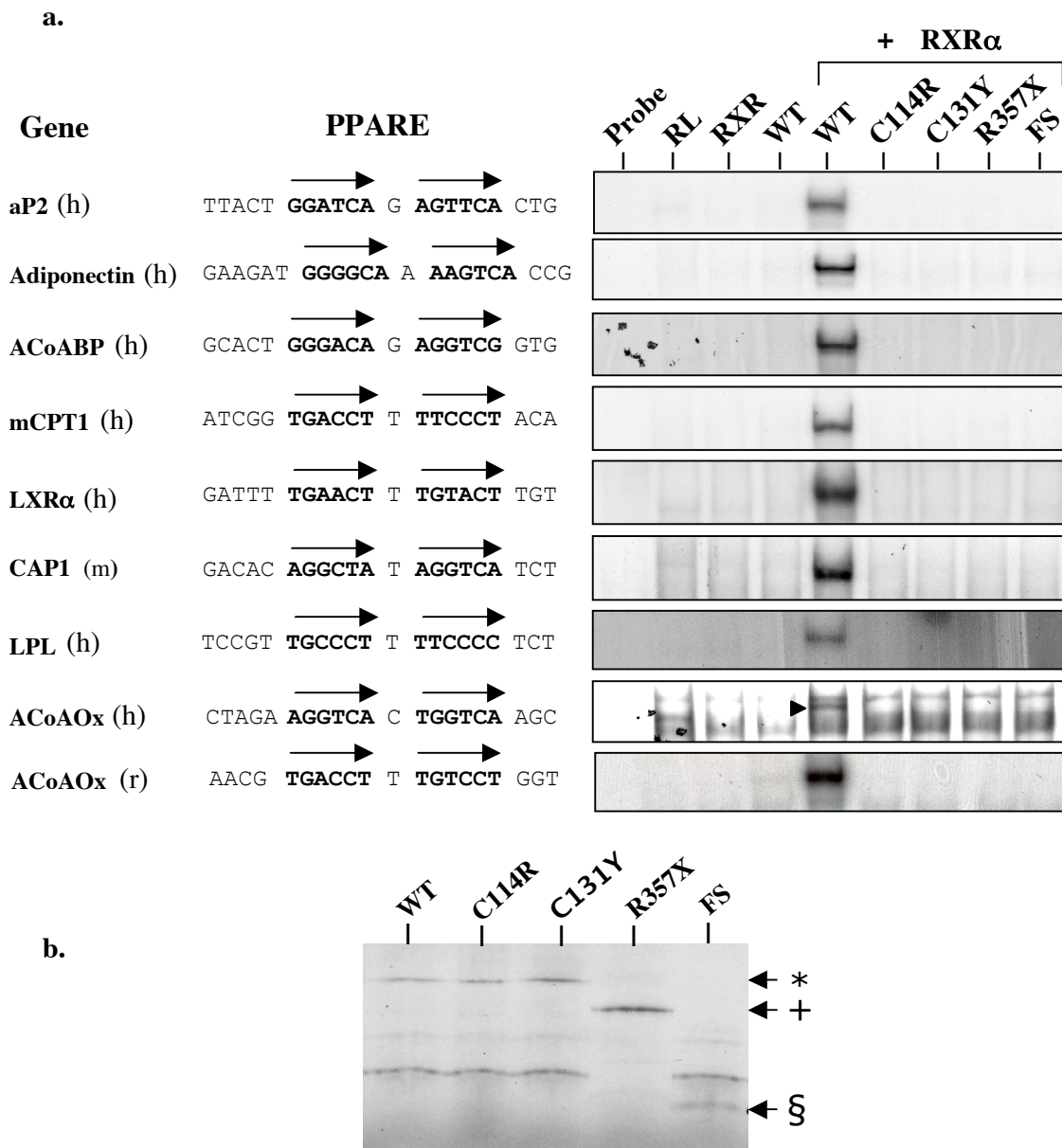
**Figure 6.6** Fasting plasma insulin concentrations versus body mass index (BMI, kg/m<sup>2</sup>) showing that probands (S1-S3) exhibit marked hyperinsulinaemia when compared with normal subjects. The solid black line represents the log-linear regression between fasting insulin levels and BMI in 1121 normal subjects recruited to on MRC (UK) Ely population-based cohort study. The 95% confidence intervals are shown as dotted lines.



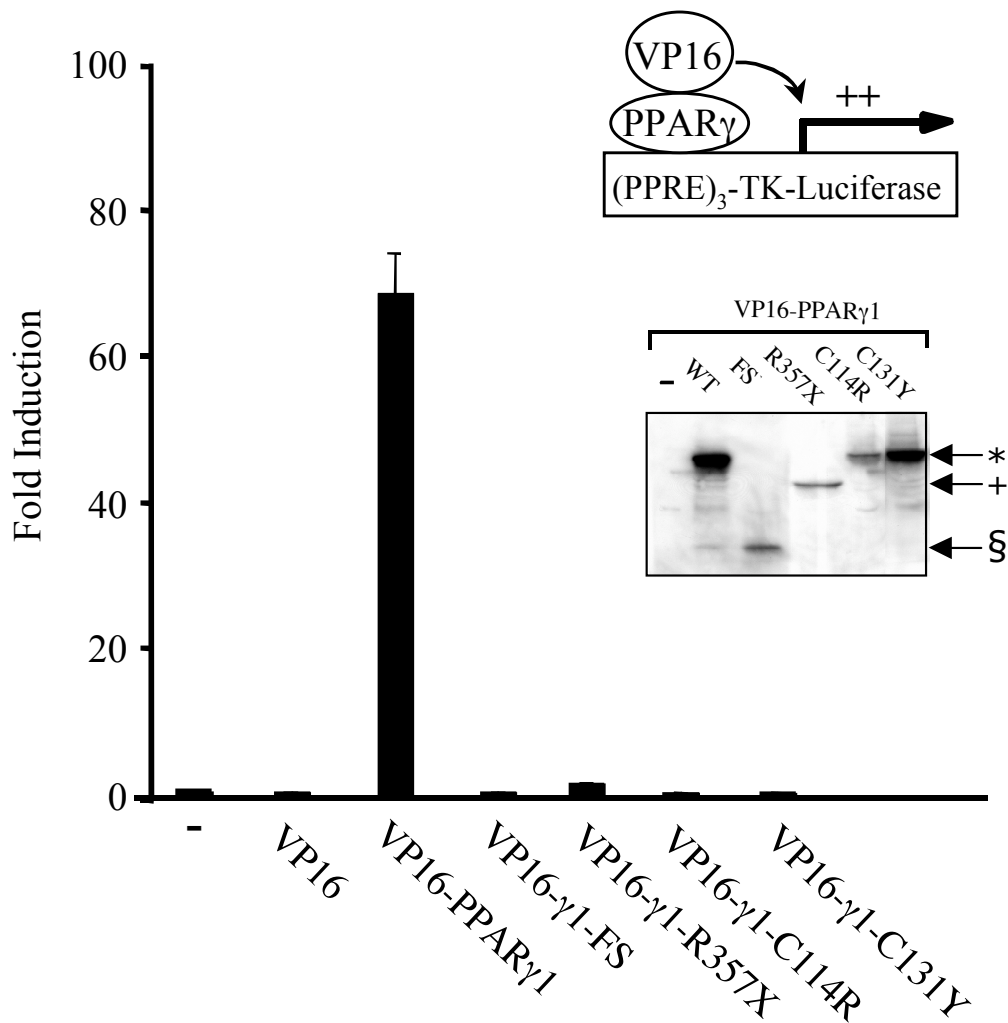
**Figure 6.7 a.** Schematic representation of the structural and functional organization of PPAR $\gamma$  showing the amino-terminal (A/B), DNA binding (DBD) and ligand-binding (LBD) domains. The position of the three novel mutations and the previously described FS mutation (Chapter 5) is indicated. Two mutations involve cysteine residues (shown in bold) in the first zinc-finger of the DBD (C114R and C131Y respectively), the third mutation introduces a stop codon in the LBD (R357X). **b.** and **c.** Crystallographic modelling of the DNA binding domain and the ligand-binding domain of PPAR $\gamma$  showing the location of the novel mutations and previously described mutation (FS). In pale blue are represented the two zinc-fingers with the cysteine residues in yellow co-ordinating binding of a zinc atom (**b.**). Ribbon representation of the LBD of PPAR $\gamma$  bound to rosiglitazone (in red). Arginine at codon 357 is shown in blue (**c.**). The arrows indicate the position of the novel mutations.



**Figure 6.8** The PPAR $\gamma$  mutant receptors are transcriptionally inactive. **a.** Transcriptional activity of wild type (WT) and mutant (C114R, C131Y and R357X) receptors in response to increasing concentrations of Rosiglitazone. 24-wells plates of 293EBNA cells were transfected with 100ng of wild type, mutant or empty (pcDNA3) expression vector together with a reporter gene (PPARE)<sub>3</sub>TKLUC (500ng) and the internal control plasmid Bos- $\beta$ -gal (100ng). Data shown are expressed as a percentage of the maximum activation obtained with WT $\gamma$ 1 and as the mean  $\pm$  s.e.m. of at least three independent experiments, each performed in triplicate, with a correction for transfection efficiency using the  $\beta$ -galactosidase activity. **b.** Comparable expression levels of wild type and mutant PPAR $\gamma$  in transfected 293EBNA cells. Whole cell lysates were immunoprecipitated with anti-PPAR $\gamma$  antibody and Western-blotted.

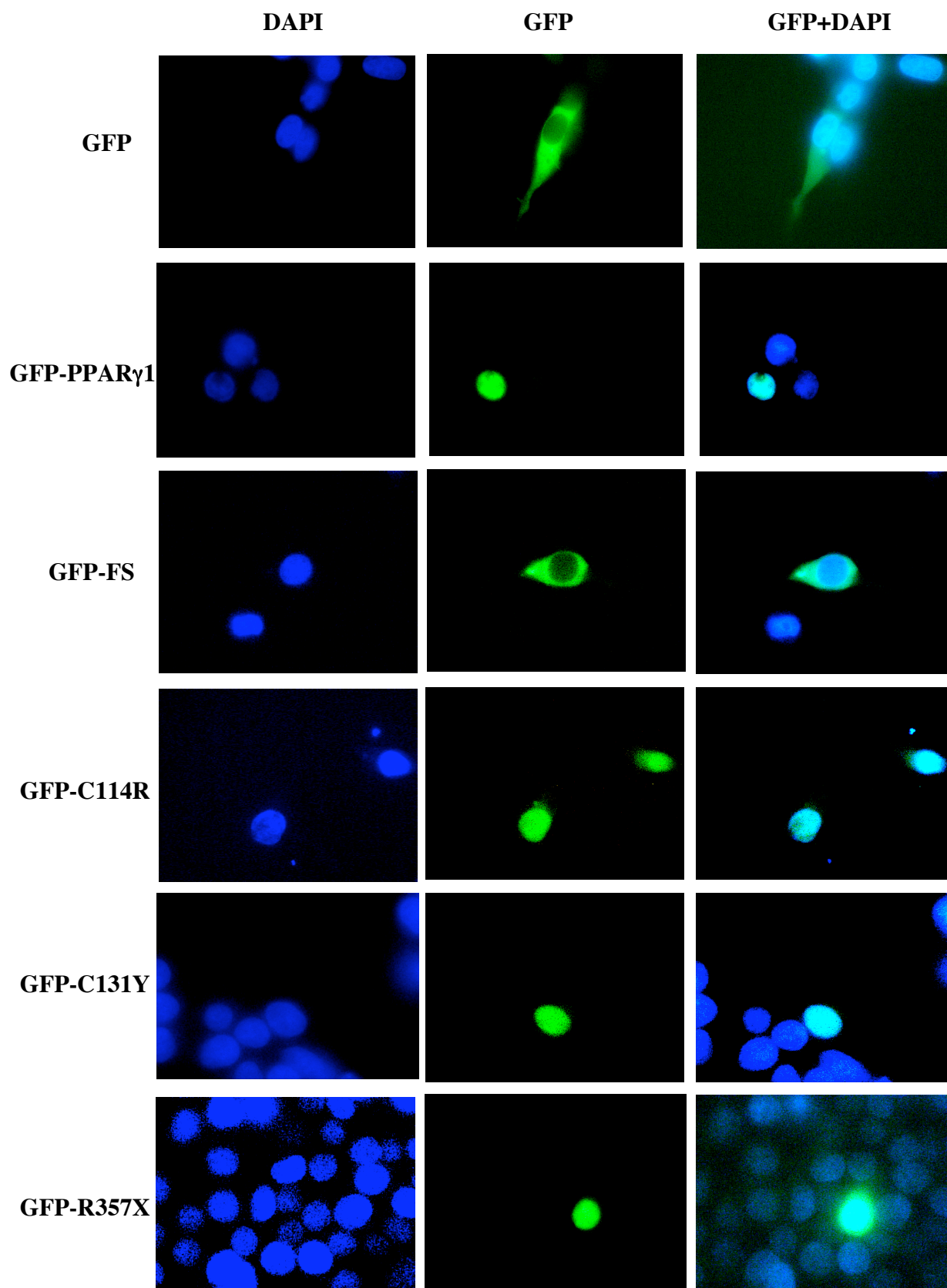


**Figure 6.9** Novel PPAR $\gamma$  mutants are unable to bind to DNA. **a.** Electrophoretic mobility shift assays (EMSA) in which *in vitro* translated wild type (WT) or mutant (C114R, C131Y, R357X and FS) PPAR $\gamma$ 1 were co-incubated with RXR $\alpha$  and oligonucleotide duplexes encoding various native PPREs. Note the complete absence of DNA binding by all mutants compared to the WT-RXR $\alpha$  heterodimer. **b.** Coomassie-stained gel of  $^{35}$ S-labeled *in vitro* translated proteins used in the EMSAs confirms comparable expression of WT and mutant receptors. The various arrows indicate the size of full length WT and C114R, C131Y (\*), R357X (+) and FS (§) receptor proteins. aP2, adipocyte protein 2 (FABP4); ACoABP, acyl coenzyme A binding protein; mCPT1, muscle carnitine palmitoyl transferase 1; LXR $\alpha$ , liver X receptor; CAP1, cbl associated protein; LPL, lipoprotein lipase, ACoAOx, acyl coenzyme A oxidase; h, human; m, mouse; r, rat.

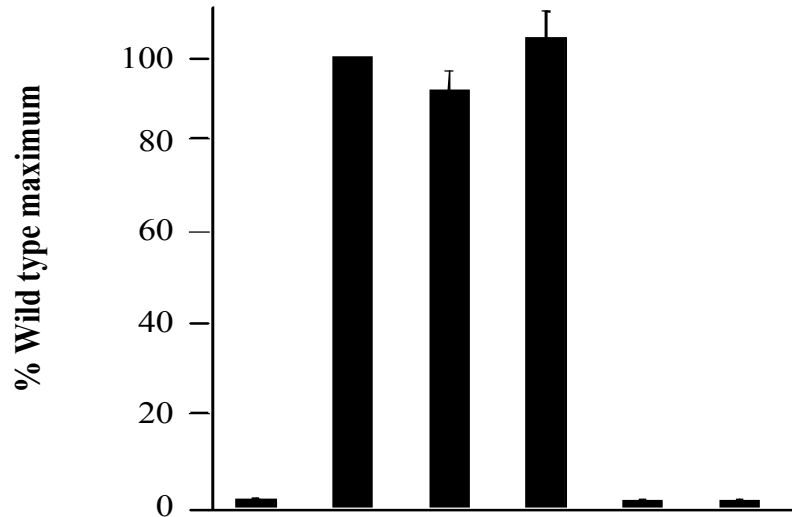
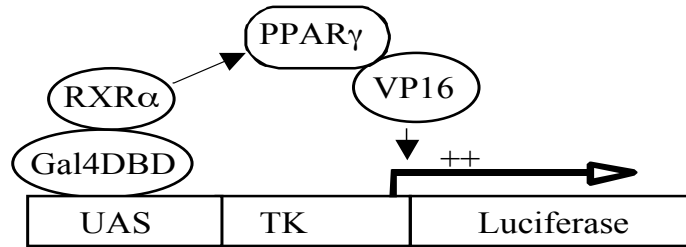


**Figure 6.10** Chimaeric fusion proteins consisting of the VP16 activation domain linked to the amino-terminus of full-length PPAR $\gamma$ 1 (WT or mutants) were co-expressed in 293EBNA cells with a PPARE-containing reporter gene [(PPARE) $_3$ TKLUC]. Interaction of WT VP16-PPAR $\gamma$  with (PPARE) $_3$ TKLUC markedly increased transactivation, whereas reporter gene activity in cells expressing mutant chimaeras was similar to mock-transfected cells. 96-well plates of 293EBNA cells were transfected with 9ng of (PPARE) $_3$ TKLUC, 1.6ng of Bos- $\beta$ -gal, and 1.6ng of the respective VP16-PPAR $\gamma$ 1 chimaeras as shown. Results are expressed as fold induction relative to cells transfected with VP16 alone and represent the mean  $\pm$  s.e.m. of at least three independent experiments, each performed in triplicate. *Inset*,  $^{35}$ S-labeled *in vitro* translated wild type and mutant VP16-PPAR $\gamma$  fusion proteins. Arrows indicate the position of WT, C114R, C131Y (\*), R357X (+) and FS (§) fusion protein products.

**Figure 6.11** C114R, C131Y and R357X PPAR $\gamma$  mutants translocate to the nucleus whereas the FS PPAR $\gamma$  mutant remains cytoplasmic. DAPI-staining (blue) of 293EBNA nuclei (left panels) and cellular location of GFP fluorescence (middle panels) are shown. Merged images (right panels) confirm nuclear translocation of wild type (WT) PPAR $\gamma$ 1 and the C114R, C131Y and R357X mutants (with co-localisation of the green fluorescent and DAPI signals), but not the FS mutant. 293EBNA cells were transfected with expression vectors (1 $\mu$ g) encoding EGFP alone (GFP), or GFP-PPAR $\gamma$ 1 [wild type (WT) or mutant] fusion proteins as shown. This figure has been kindly provided by Dr Erik Schoenmakers.







<b>Gal4-RXRα</b>	<b>+</b>	<b>+</b>	<b>+</b>	<b>+</b>	<b>+</b>	<b>+</b>
<b>VP16</b>	<b>+</b>	<b>-</b>	<b>-</b>	<b>-</b>	<b>-</b>	<b>-</b>
<b>VP16-WT</b>	<b>-</b>	<b>+</b>	<b>-</b>	<b>-</b>	<b>-</b>	<b>-</b>
<b>VP16-C114R</b>	<b>-</b>	<b>-</b>	<b>+</b>	<b>-</b>	<b>-</b>	<b>-</b>
<b>VP16-C131Y</b>	<b>-</b>	<b>-</b>	<b>-</b>	<b>+</b>	<b>-</b>	<b>-</b>
<b>VP16-R357X</b>	<b>-</b>	<b>-</b>	<b>-</b>	<b>-</b>	<b>+</b>	<b>-</b>
<b>VP16-FS</b>	<b>-</b>	<b>-</b>	<b>-</b>	<b>-</b>	<b>-</b>	<b>+</b>

**Figure 6.12** Interaction between VP16-WT or mutant PPAR $\gamma$  fusions and Gal4-RXR $\alpha$  chimeras. 293EBNA cells were transfected with 50ng of VP16-PPAR $\gamma$  and Gal-4 RXR $\alpha$  expression vectors together with 500ng of UASTKLUC reporter and 100ng of Bos- $\beta$ -Gal internal control to correct for transfection efficiency. The results are expressed as a percentage of the WT maximum response and are the mean  $\pm$  s.e.m. of three independent experiments each done in triplicate.

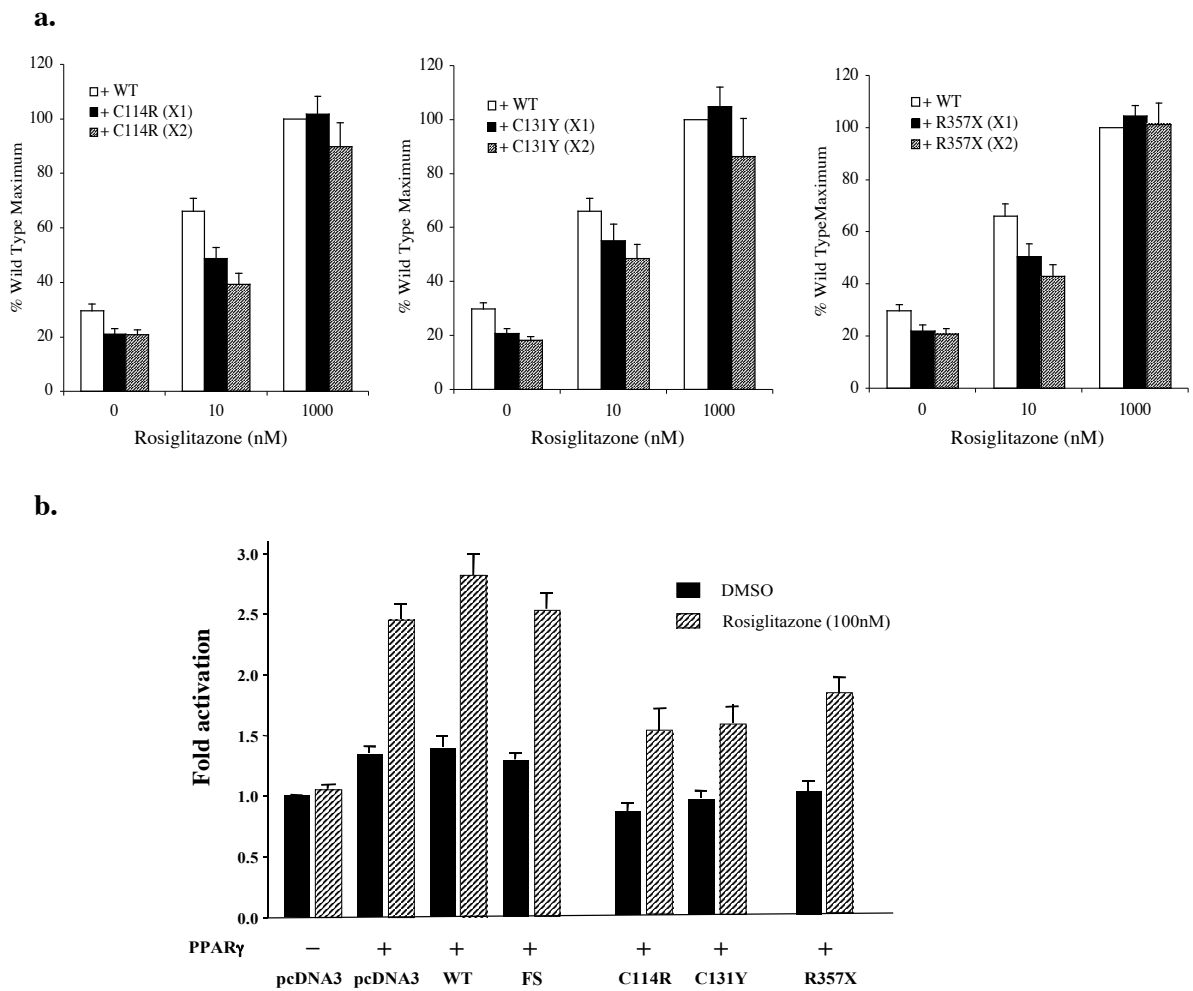


**Figure 6.13** Dominant negative inhibition of wild type receptor activity by mutant receptors. **a.** 293EBNA cells were cotransfected with 25ng of wild type plus an equal amount of either wild type (white bar) or each mutant expression vector (black bar), together with the (PPARE)<sub>3</sub>TKLUC reporter gene (500ng) in the presence of increasing concentrations of ligand (Rosiglitazone). The striped bars denote cotransfection of 25ng of wild type plus a two fold excess (X2) of mutant receptors. The transcriptional responses mediated by either 25ng, 50ng or 75ng of WT receptor were virtually identical (data not shown). Results are expressed as a percentage of WT maximum response, corrected for Bos- $\beta$ -gal activity (100ng). **b.** 3T3-L1 cells were cotransfected with 33ng of wild type plus an equal amount of either empty (pcDNA3), wild type (WT) or each mutant expression vector, together with a human aP2-LUC reporter gene in the presence of DMSO (black bar) or 100nM Rosiglitazone (striped bar). Unlike the FS mutation, which did not exhibit any dominant negative activity, the C114R, C131Y and R357X mutant receptors were able to inhibit WT function. The results shown are the mean  $\pm$  s.e.m. of at least five independent experiments, each done in triplicate, with correction for transfection efficiency using the  $\beta$ -galactosidase activity.

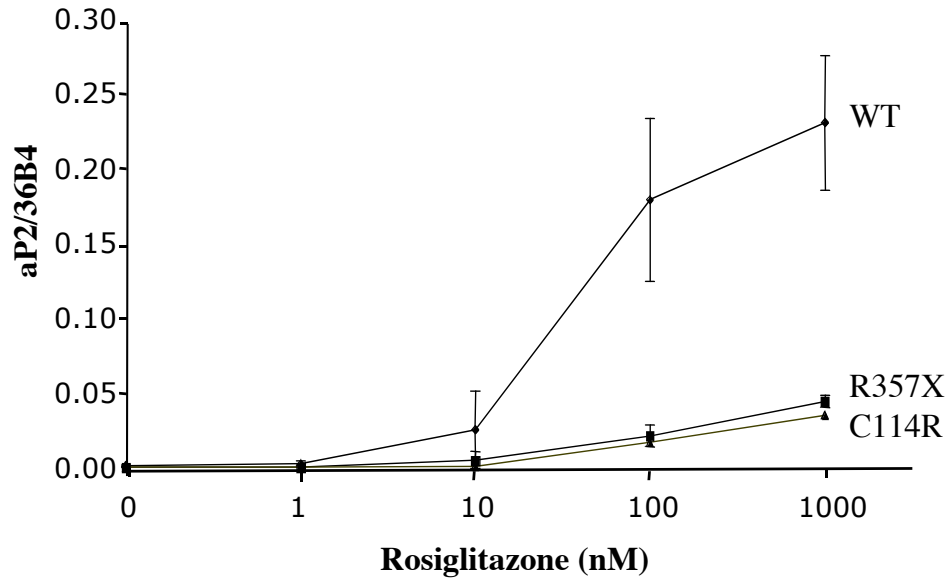


**Figure 6.14** Comparison of aP2 (FABP4) expression in cells from a normal control subject (WT) and patients carrying the R357X or C114R PPAR $\gamma$  mutations. Monocytes were cultured for 24 hours in the presence of 500U/ml IL-4 and 800U/ml GM-CSF to generate immature dendritic cells (IDCs) together with increasing concentrations of rosiglitazone. The mRNA levels for aP2 were determined by real-time quantitative qPCR as described in the section 6.2.8. Data are expressed as a ratio of the aP2 transcripts relative to 36B4 expression and represent the mean expression  $\pm$  s.e.m. of three independent experiments. Although all cells showed comparable PPAR $\gamma$  expression (data not shown), ligand-dependent induction of aP2 expression in R357X and C114R mutation-containing IDCs was markedly impaired in comparison to the response in WT cells.

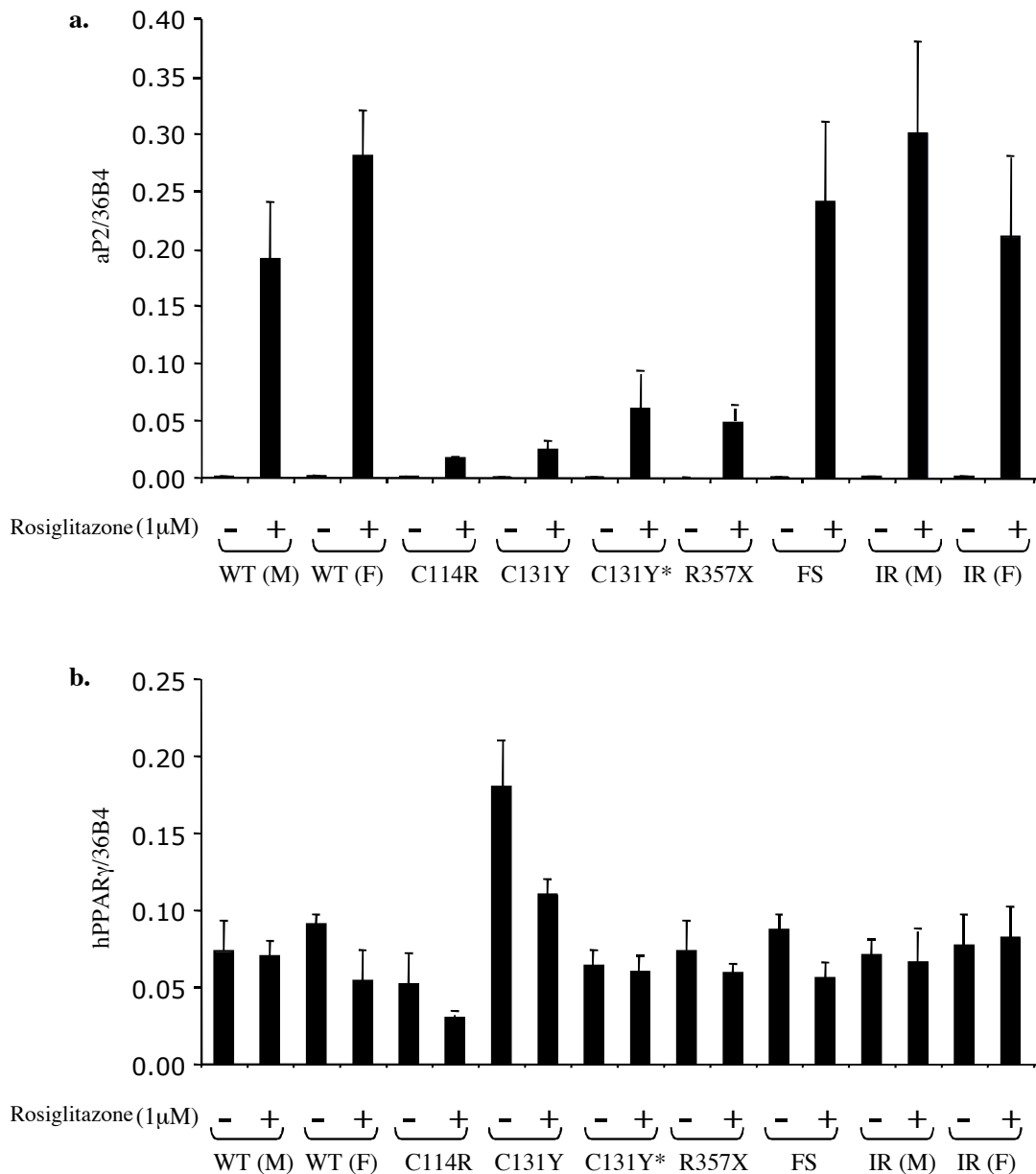


**Figure 6.15** Levels of aP2 (FABP4) (**a.**) and PPAR $\gamma$  (**b.**) gene expression in cells from normal controls and individuals carrying mutations in PPAR $\gamma$ . Peripheral blood monocytes obtained from two healthy individuals (WT), two insulin resistant subjects without mutations in PPAR $\gamma$  and patients with C114R, C131Y, R357X or FS mutations were cultured for 24 hours as described in section 6.2.7 to generate immature dendritic cells (IDCs) in absence (-) or presence of 1 $\mu$ M rosiglitazone (+). The levels of aP2 and PPAR $\gamma$  gene expression were determined by real-time quantitative qPCR (Taqman assays) as described in section 6.2.8. Data are expressed as a ratio of aP2 (**a.**) or PPAR $\gamma$  (**b.**) transcripts relative to 36B4 expression and represent the mean  $\pm$  s.e.m. of at least three independent experiments. M, male; F, female; \* denotes the father of the C131Y index case.

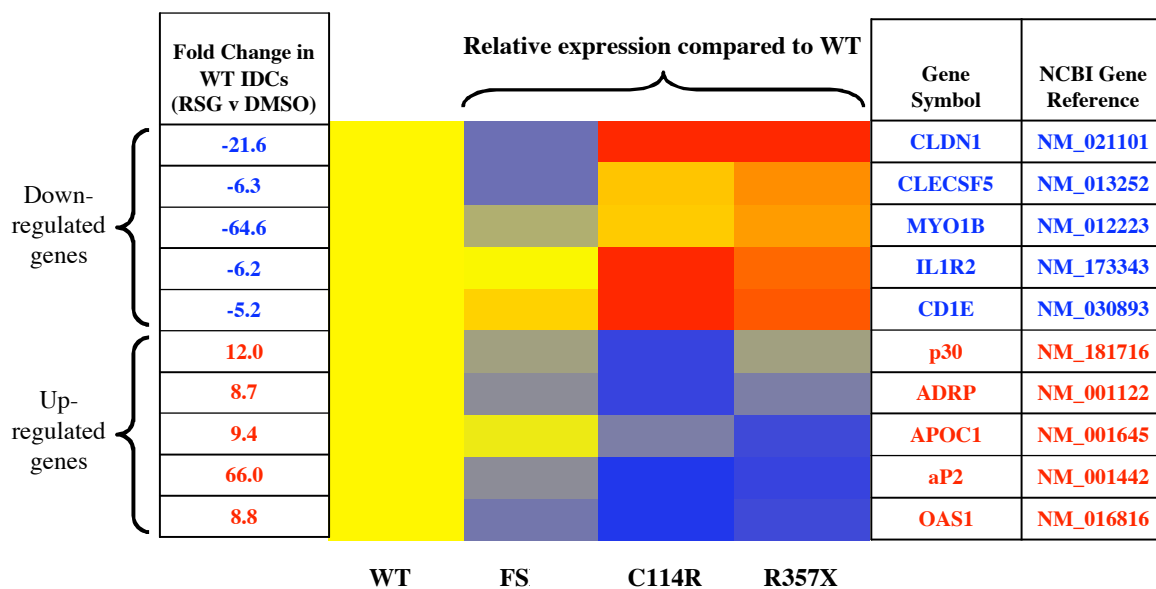


**Figure 6.16** Relative expression of several PPAR $\gamma$  target genes (5 down-regulated and 5 up-regulated right panel) in WT and receptor mutation-containing (FS, C114R, R357X) IDCs, quantified by real-time quantitative qPCR using Taqman Low Density Arrays (TLDA). Gene expression in ligand-treated (1 $\mu$ M rosiglitazone) WT versus mutant cells IDCs was compared and the results are shown as heat maps. Thus, red indicates higher, and blue lower, levels of gene expression relative to rosiglitazone-treated WT cells, whose levels have been uniformly designated yellow. The fold changes in expression of each gene in rosiglitazone (RSG) versus vehicle (DMSO) treated WT cells is also listed (left panel).

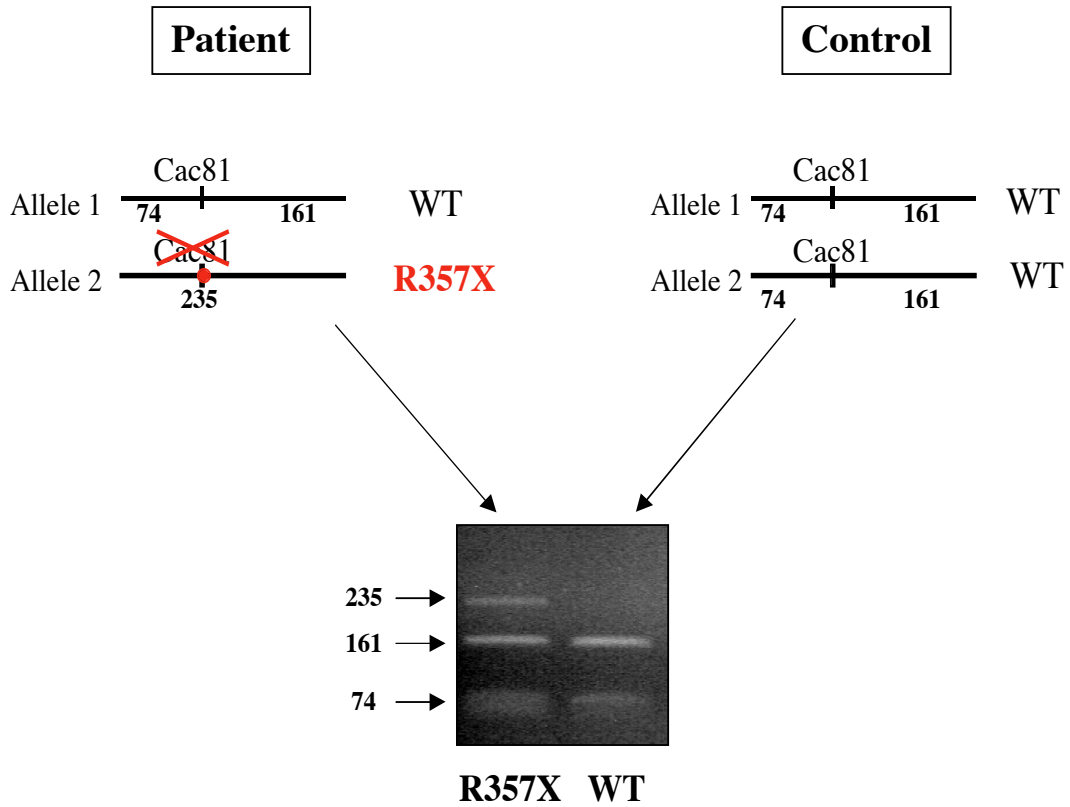


**Figure 6.17** RT-PCR with cDNA amplification confirms the presence of both the mutant and wild type mRNA transcripts in the R357X patient. Following reverse transcription of RNA from wild type (WT) or R357X mutation-containing immature dendritic cells, the cDNAs were amplified by PCR and digested with Cac8I enzyme. The size of the DNA following digestion was determined by electrophoresis on a 2% (w/v) agarose gel. The presence of the R357X mutation destroys a Cac8I restriction site in one allele and as consequence an undigested fragment of 235bp was detected only in cells from the patient.

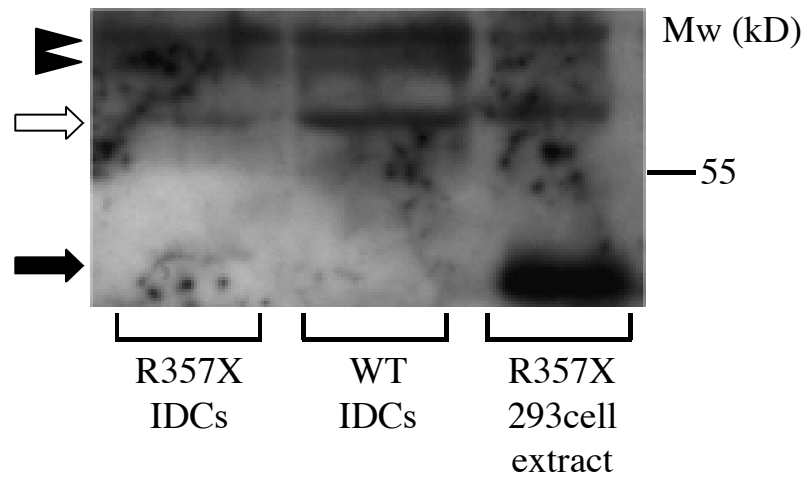
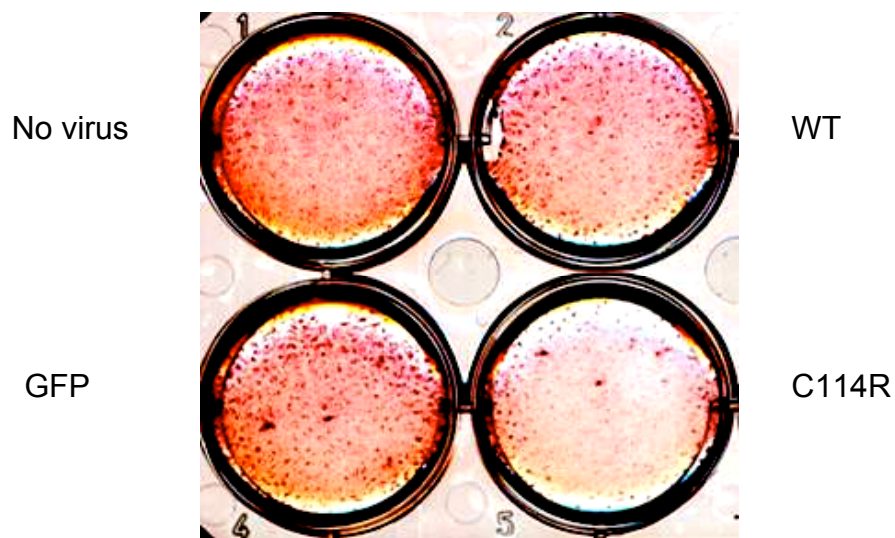


**Figure 6.18** R357X mutant PPAR $\gamma$  is expressed in peripheral blood monocyte derived immature dendritic cells (IDCs). IDCs were generated from S3 and an age- and sex-matched control subject as described in paragraph 6.2.7. Whole cell lysates of WT and R357X mutation-containing IDCs were immunoprecipitated with anti-PPAR $\gamma$  antibody and Western-blotted together with a control extract of 293EBNA cells transfected with R357X mutant PPAR $\gamma$ . An open arrow denotes the position of WT PPAR $\gamma$ , a solid arrow shows R357X protein and non-specific bands are denoted by solid arrow heads.

a.



b.

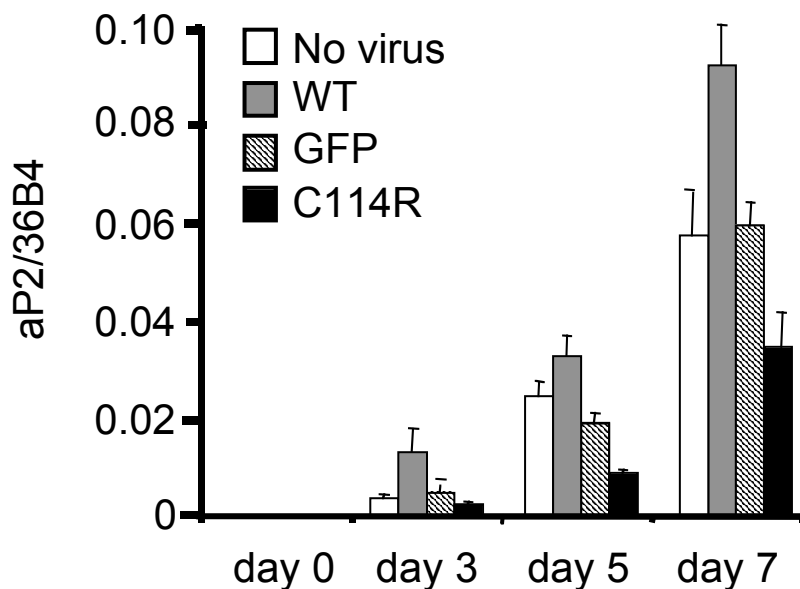


**Figure 6.19** Adenoviral expression of C114R mutant PPAR $\gamma$  inhibits rosiglitazone-induced preadipocyte differentiation. **a.** Human preadipocyte (Chub-S7) cells were cultured in 6-wells plates and differentiated in the presence of rosiglitazone (100nM). 24 hours prior to differentiation, cells were mock infected or transduced with  $2 \times 10^7$  pfu/well of recombinant adenoviruses expressing either GFP alone, GFP and WT PPAR $\gamma$ , or GFP and C114R PPAR $\gamma$ . Comparable degrees of viral infection efficiency were verified by fluorescence microscopy. Following differentiation Chub-S7 cells were fixed and stained with Oil-red-O to show accumulation of intracellular lipid. **b.** aP2 (FABP4) gene expression was determined by real-time quantitative RT-PCR at days 0, 3, 5 and 7 of differentiation. This figure has been kindly provided by Dr Erik Schoenmakers.



## 6.4 Discussion

In this chapter I have reported the functional characterization of three novel mutations in the human *PPARG* gene, identified in a cohort of patients with clinical features of partial lipodystrophy together with insulin resistance, dyslipidemia and hypertension, which extend the range of heterozygous PPAR $\gamma$  mutations identified to date. The first two mutations to be reported (P467L and V290M) were able to bind DNA but showed significant impairment of transcriptional activation and coactivator recruitment in response to synthetic (Barroso *et al.*, 1999) or putative natural ligands (Chapter 4; Agostini *et al.*, 2004) as a consequence of the mutations destabilizing the C-terminal alpha helix (AF2) of PPAR $\gamma$  (Kallenberger *et al.*, 2003), which is crucial for ligand and coactivator interaction. Moreover, they have been shown to exert dominant negative activity over their wild type counterpart (Barroso *et al.*, 1999; Agostini *et al.*, 2004). Subsequently, we described another heterozygous frameshift/premature stop mutation (FS) in the DNA binding domain of PPAR $\gamma$  in an unrelated kindred. The functional characterization of this mutation revealed properties which were in marked contrast to those of the previously described mutations. Consistent with the mutation truncating its DBD, the FS PPAR $\gamma$  mutant lacked DNA binding and transcriptional activity and did not exert dominant negative activity over its WT counterpart. Significantly, in this kindred only individuals who were doubly heterozygous for the FS mutant and an additional defects in an unrelated gene, *PPP1R3A*, exhibited severe insulin resistance (Chapter 5; Savage *et al.*, 2002). Interestingly however, a heterozygous loss-of-function mutation in the promoter region of PPAR $\gamma$ 4 has been reported in a proband with partial lipodystrophy (Al-Shali *et al.*, 2004), whilst a further heterozygous nonsense mutation Y355X (Y327X in PPAR $\gamma$ 1) within the LBD, whose protein product *in vitro* was transcriptionally inactive, with no apparent dominant negative activity (Francis *et al.*, 2006) have been recently reported. Very recently, another frameshift mutation designated as E138fs $\Delta$ AATG has been identified in a subject with partial lipodystrophy, with the mutant allele predicted to encode a truncated protein lacking the DNA and ligand-binding domain (Hegele *et al.*, 2006). In these cases, it has been proposed that the clinical phenotype is a consequence of PPAR $\gamma$  haploinsufficiency, which contrasts with the absence of insulin resistance in FS mutation containing

subjects reported by us (Savage *et al.*, 2002).

Two of the three novel mutations (C114R and C131Y) reported in this chapter are situated in the DBD and the third (R357X) within the LBD of the receptor. Specifically, the two DBD mutations (C114R and C131Y) involve two of the four highly conserved zinc-coordinating cysteines in the first zinc-finger, whose intact structure is required to permit DNA binding (Figure 6.7). Accordingly, their ability to bind DNA as heterodimer with RXR was assessed using electrophoretic mobility shift assays. The results showed that C114R and C131Y were unable to bind to a variety of PPAREs from well known PPAR $\gamma$  target genes in the presence of RXR $\alpha$  (Figure 6.9a). Similar results were recently reported by Temple and colleagues, who created three different mutations in the P-box region of zinc-finger one of PPAR $\gamma$  in order to elucidate the role of DNA binding in PPAR $\gamma$  function; two of their mutants maintained the structure of the zinc-finger and a third mutation at cysteine 131, analogous to a mutation shown previously to prevent DNA binding of thyroid receptor (Chatterjee *et al.*, 1989), disrupted the entire zinc-finger I structure. Interestingly, only this third mutation was incapable of binding DNA under any conditions, highlighting the importance of the cysteine residue to maintain tetrahedral coordination of a zinc ion and subsequently the stability of the entire zinc-finger structure. Without the tertiary structure of the DBD being intact, the protein cannot make contact with the DNA (Temple *et al.*, 2005).

Despite the presence of an intact DBD, the R357X mutant also failed to bind to the panel of PPAREs (Figure 6.9a). However, this finding was not unexpected as the R357X premature stop mutation results in a protein which is truncated between helices 6 and 7 of the LBD of the receptor and lacks the carboxy-terminal region which contains a key dimerization interface with RXR. Subsequently, R357X was shown to be unable to form a heterodimeric complex with RXR and therefore failed to bind DNA (Figure 6.9). A mammalian two-hybrid assay with Gal4-RXR $\alpha$  and the different VP16-full length PPAR $\gamma$  mutants confirmed defective dimerisation of R357X with RXR, whereas all the DBD mutants recruited RXR similarly to the WT receptor, in keeping with preservation of this dimerisation interface within their intact LBD (Figure 6.12). Consistent with their inability to bind DNA, C114R, C131Y and R357X showed markedly impaired transactivation profiles (Figure 6.8). However, in contrast to the previously described FS mutant, which lacks the putative

nuclear localization signal (NLS) and remained cytoplasmic, all the novel mutant PPAR $\gamma$  (C114R, C131Y, R357X) proteins, which have a preserved hinge region containing the NLS, retain the ability to translocate appropriately to the nucleus (Figure 6.11).

Such retention of nuclear translocation function prompted us to examine whether the novel receptor mutants might be able to interfere with the transcriptional function of WT PPAR $\gamma$ . The novel mutants inhibited PPAR $\gamma$ -mediated transactivation of both a reporter gene [(PPARE)<sub>3</sub>TKLUC] containing a synthetic, multimerised PPARE as well as a reporter gene (haP2-LUC) containing a natural target gene promoter, whereas the FS mutant lacked dominant negative activity in either context (Figure 6.13). Significantly, these observations with cotransfected receptors and reporter genes *in vitro*, were mirrored by profiles of PPAR $\gamma$ -mediated aP2 induction in mutation-containing primary blood mononuclear-derived cells from subjects studied *ex vivo* (Figures 6.14 and 6.15). More extended gene expression profiling supported these differences, with induction of other PPAR $\gamma$  target genes being markedly attenuated in novel mutation-containing versus WT cells with FS mutation-containing cells exhibiting an intermediate profile (Figure 6.16). Taken together, these data suggest that the FS null mutation limits PPAR $\gamma$  responsiveness via haploinsufficiency of functional receptor, whereas the greater restriction of PPAR $\gamma$  action in the novel DBD and LBD mutation-containing cells is attributable to their dominant negative activity. Recently, Francis and colleagues have reported a novel nonsense mutation, causing premature termination at tyrosine 355 in PPAR $\gamma$ 2 (or Y327X in PPAR $\gamma$ 1), in a Canadian patient with insulin resistance and partial lipodystrophy (Francis *et al.*, 2006). This mutation, similar to our R357X codon change, results in a protein which is truncated in the LBD of the receptor. However, the *in vitro* characterization of this truncation mutant showed, in contrast to our findings, that the Y327X protein was transcriptionally inactive and markedly unstable, with no dominant negative interference with wild type receptor function, leading the authors to conclude that the clinical phenotype in their kindred was due to haploinsufficiency (Francis *et al.*, 2006). However, the manner in which the mutant receptor expression vector was generated for *in vitro* studies was somewhat unusual. In contrast to their wild type PPAR $\gamma$  construct, all DNA sequences downstream of the stop codon at R327 were deleted. Clearly this could result in altered

transcription or stability of RNA and thus protein translation from this vector, in comparison with the wild type construct. Moreover, their *in vitro* observations were not tested with any *ex vivo* studies using mutation-containing cells from patients.

We have shown previously that dominant negative inhibition by P467L and V290M PPAR $\gamma$  is abolished by disrupting their ability to interact with corepressors (Chapter 4; Agostini *et al.*, 2004), suggesting transcriptional interference via repression of target genes by DNA-bound mutant receptors, analogous to mechanisms of dominant negative inhibition by mutant nuclear receptors (e.g. the v-erbA oncogene, thyroid hormone receptor  $\beta$  mutants in Resistance to Thyroid Hormone, PZLF-RAR $\alpha$  fusion proteins in promyelocytic leukaemia) in other contexts (Love *et al.*, 2000). In contrast, the missense DBD and LBD R357X truncation mutants are unable to bind DNA, yet can inhibit WT PPAR $\gamma$  action, suggesting a different mechanism of transcriptional interference. Meyer and colleagues postulated competition for shared cofactors by receptors to explain antagonism of progesterone and estrogen receptor signalling (Meyer *et al.*, 1989) and the subsequent observation that SRC-1, a shared coactivator, could relieve such “squenching”, validated this hypothesis (Onate *et al.*, 1995). Following this, it has been shown that ligand-dependent activation of nuclear receptors can inhibit either their own function (Baretino *et al.*, 1994) or that of heterologous receptors (Zhang *et al.*, 1996), by limiting the availability of coactivators that are recruited to their C-terminal activation function 2 (AF-2) domains. In keeping with this observation, we have tested the ability of the novel mutant receptors to recruit a variety of coactivators. Protein-protein interaction assays showed ligand-dependent binding of SRC-1 or TRAP220 to the DBD mutants with an intact AF-2 domain while the R357X with a preserved DBD domain showed interaction with PGC-1 $\alpha$  or PDIP (data generated by E. Schoenmakers and not shown but published in Agostini *et al.*, 2006).

Overall our observations therefore provide a plausible mechanism whereby non DNA-binding PPAR $\gamma$  mutants can titrate functionally limiting coactivator(s) to restrict WT receptor function (Figure 6.20). It is quite conceivable that multiple different coactivators or cofactor complexes could be limiting in different tissue and target gene contexts *in vivo*. Evidence from other biological contexts provides support for similar mechanisms operating to inhibit PPAR signalling *in vivo*: analogous to our natural, PPAR $\gamma$  DBD mutant inhibiting human adipocyte

differentiation (Figure 6.19), others have generated artificial, dominant negative, PPAR $\gamma$  DBD mutants which block either adipogenesis (Park *et al.*, 2003) or neural stem cell differentiation (Wada *et al.*, 2006) in the murine context;  $\gamma$ ORF4, a human PPAR $\gamma$  splice variant in which the LBD is truncated at residues 273 which has dominant negative activity, is selectively overexpressed in colorectal carcinoma cells and cancer tissues (Sabatino *et al.*, 2005); a dominant negative, PPAR $\alpha$  splice variant with a truncated LBD ( $\alpha\alpha174$ ) is expressed in human tissues including liver (Gervois *et al.*, 1999).

In summary, in this chapter I have described three novel non-DNA binding PPAR $\gamma$  mutations (two missense DBD and one truncated LBD receptor mutants), occurring in unrelated kindreds, which extend the range of heterozygous mutations reported to date. Each index case exhibited clinical features of insulin resistance with fasting hyperinsulinaemia (Figure 6.6), partial lipodystrophy (Figure 6.5), dyslipidaemia and early-onset hypertension (Table 6.3) described in the first subjects in whom dominant negative PPAR $\gamma$  mutations were identified (Barroso *et al.*, 1999; Savage *et al.*, 2003). The functional characterization of these receptor mutants has provided evidence that they act through a novel dominant negative mechanism involving transcriptional limitation by sequestration of coactivators or cofactors complexes, which has not been yet described in any other inherited human disorder caused by nuclear receptor defects.

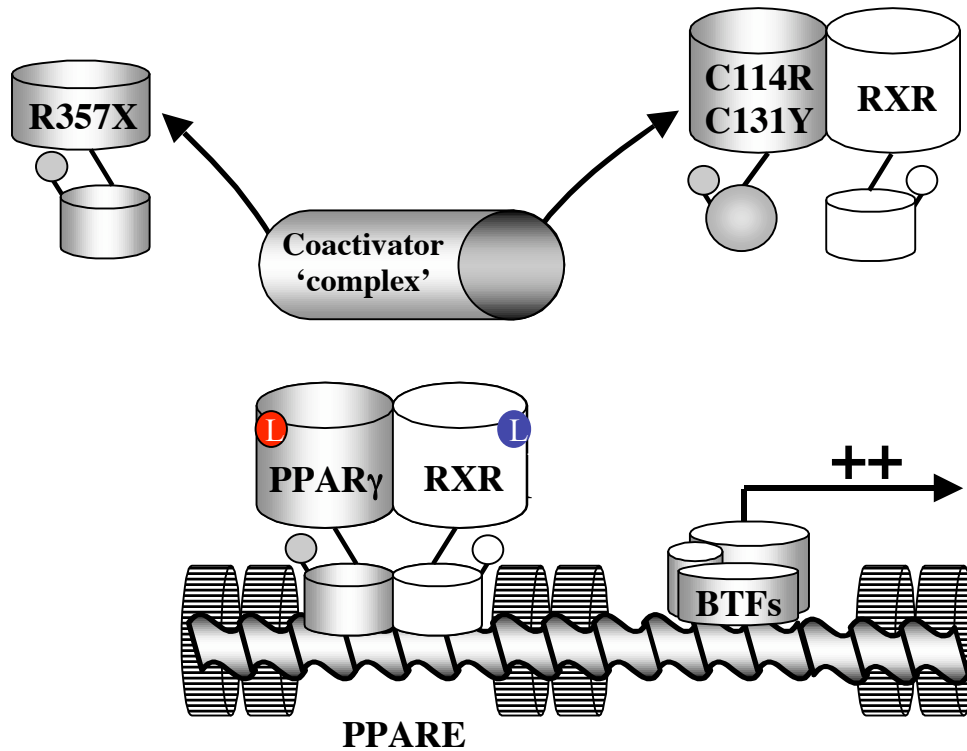


**Figure 6.20** Proposed model of transcriptional interference by naturally occurring PPAR $\gamma$  R357X, C114R and C131Y mutants. Although unable to bind DNA, the natural mutants which translocate to the nucleus, can interfere with the transcriptional activity of the WT receptor by sequestering component(s) of the coactivator complex that are limiting in certain target gene or cellular context.

## Chapter 7

### CONCLUDING DISCUSSION

The work reported in this thesis describes abnormal nuclear receptor signaling and human disease, principally focusing upon the study of the molecular properties of the thyroid hormone receptor (TR) and the peroxisome proliferator-activated receptor gamma (PPAR $\gamma$ ) in genetic disorders of thyroid hormone and insulin action respectively.

**Chapter 3** reports the functional characterization of three novel RTH mutations (S314C, S314F, S314Y), due to different nucleotide substitutions in the same codon, occurring in six separate families. These mutant receptors showed marked differences in their functional impairment. Molecular modelling of the different mutations using the crystal structure of TR $\beta$  explains how ligand binding is perturbed and why phenylalanine or tyrosine substitutions at this codon are more deleterious than cysteine. Our data suggest that there may be a correlation between mutant receptor function *in vitro* and resistance within the pituitary-thyroid axis *in vivo*.

Until now attempts to correlate individual mutations with clinical phenotype has not proved successful, because of the extreme variability of RTH, with kindreds with the same TR $\beta$  mutation showing different degree of resistance in the same tissues and even different spectra of resistance in different tissues in the same individual. In collaboration with the Clinical Biochemistry Department, Addenbrooke's Hospital, we will continue to screen for TR $\beta$  mutations in subjects with thyroid function tests that are consistent with a diagnosis of RTH. Although with much lower frequency, we are still identifying novel mutations, which offer an opportunity to enhance our understanding of structure-function relationships in the receptor. For example, we have recently found a novel *de novo* mutation in a sporadic case of RTH with the typical biochemistry, which results in mutation of a highly conserved glutamic acid to glutamine (E457Q) in helix 12. A homologous mutation (E457A) in a murine model, which has been recently described by Ortiga-Carvalho and colleagues, completely abolished coactivator recruitment by mutant receptor *in vitro*, but

preserved normal T3 binding and corepressor interactions (Ortiga-Carvalho *et al.*, 2005). These animals showed abnormal regulation of the hypothalamic-pituitary-thyroid axis suggesting that the AF2 domain of TR $\beta$  is required for both positive and negative transcriptional regulation by TH *in vivo* (Ortiga-Carvalho *et al.*, 2005). In keeping with these results, preliminary functional characterization of the human E457Q TR $\beta$  mutant has revealed normal ligand binding and dissociation from corepressors, but complete transcriptional inactivity due an inability to recruit coactivator (Mitchell and Agostini, unpublished data). This observation that negative transcriptional regulation in the pituitary-thyroid axis in both human and murine contexts is mediated by cofactors that are recruited to TR in a ligand-dependent manner may be of significance in identifying candidate genes that can be screened in cases of RTH where no TR $\beta$  mutations have been identified.

Recently, using cDNA microarray analysis, Moeller and colleagues have identified several genes regulated by TH in human skin fibroblasts, whose expression is attenuated in skin fibroblasts from patients with RTH. These findings suggest that profiling of gene expression patterns may have a key role to play in the study of individuals with defects of TH action (Moeller *et al.*, 2005). Thus, in addition to continued screening for TR $\beta$  mutations, we are also planning to study gene expression profiles of peripheral blood-derived cells (T cells, B cells and macrophages) from RTH patients, which are more widely and readily accessible. This will provide an opportunity to further understand the molecular actions of TR $\beta$  mutants and to elucidate the affected cellular pathways *in vivo*. Through comparison of microarray profiles from RTH patients versus normal subjects we may be able to determine specific cell types with altered patterns of T3-dependent gene expression that indicate hormone signaling mediated predominantly via either  $\alpha$  or  $\beta$  receptors. We may therefore be able to identify peripheral target genes whose expression correlates with the dominant negative potency of TR $\beta$  mutants as suggested in Chapter 3, or alternatively to identify genes regulated mainly via TR $\alpha$ , whose altered expression correlates with the degree of thyrotoxic symptoms in patients.

Whereas most cases of RTH are associated with TR $\beta$  gene mutations, 15% of cases are of unknown etiology without TR $\beta$  gene defects. Potential mechanisms of non-TR $\beta$ -mediated RTH include abnormalities in cofactors or other proteins, which mediate thyroid hormone action. It will be of particular interest to compare gene



expression profiles of blood cells derived from these “non-TR $\beta$ ” RTH cases with those obtained from TR $\beta$  mutation-containing cells. A distinctly different expression profile may identify a novel candidate gene or pathogenetic mechanisms mediating this disorder.

**Chapters 4, 5 and 6** outline the results of functional studies of several naturally occurring human mutations in the PPAR $\gamma$  gene and their role in the human metabolic syndrome.

P467L and V290M (both involving residues in the ligand binding domain of the receptor) were the first missense, loss-of-function mutations to be identified in three patients with severe insulin resistance. Initial functional studies showed that the mutant receptors were transcriptionally impaired with reduced ligand binding and coactivator recruitment and, analogous to TR $\beta$  mutations in RTH, the mutants inhibited wild type PPAR $\gamma$  action in a dominant negative manner. In **chapter 4** I have extended the functional characterization of these mutations showing clearly that P467L and V290M destabilize helix 12 favouring receptor interaction with corepressor and resulting in dominant negative activity via repression of target genes by DNA-bound mutant receptors. Using fluorescence anisotropy these deleterious mutations have been shown to enhance the mobility of helix 12 in PPAR $\gamma$ , supporting my experimental findings (Kallenberger *et al.*, 2003). Consistent with this model, dominant negative inhibition by the P467L mutant is abolished by introduction of an additional artificial mutation (L318A) that disrupts corepressor interaction (Agostini *et al.*, 2004). Furthermore, I have shown that a higher-affinity, tyrosine-based agonist, such as farglitazar, has the potential to overcome this proposed disease mechanism in both mutant receptors *in vitro*, and thus represents a more rational therapeutic approach to restoring mutant receptor function and ameliorating insulin resistance in our patients.

Subsequently, two other groups have independently identified mutations in the ligand-binding domain of the PPAR $\gamma$  (F388L and R425C in PPAR $\gamma$ 2; F360L and R397C in PPAR $\gamma$ 1) in patients with partial lipodystrophy and insulin resistance. Although the authors reported F388L as a mutant lacking dominant negative activity, subsequent studies in our own laboratory with both the F360L and R397C receptor mutants have shown that these two mutants can interfere with wild type receptor

signalling (Figure 7.1), in a dominant negative manner similar to that seen with the P467L and V290M mutants.

More recently, we have identified five, novel heterozygous mutations in unrelated cases of lipodystrophic insulin resistance: three missense mutations (C114R, C131Y, C161W) involve highly conserved cysteine residues in the DBD and two premature stop mutations (FS315X, R357X) in the LBD of PPAR $\gamma$  (Agostini *et al.*, 2006). In **chapter 6** I have described the functional properties of C114R, C131Y and R357X. Unlike P467L and V290M, these mutant receptors lack the ability to bind to DNA. However despite this, they retain the ability to translocate to the nucleus, bind PPAR $\gamma$  coactivators and inhibit wild type PPAR $\gamma$  action in a dominant negative manner, possibly via a novel mechanism of transcriptional interference which involves sequestration of functionally-limiting cofactor(s) to restrict WT receptor function (Figure 6.20). *In vitro* observations of dominant negative activity were mirrored by profiles of PPAR $\gamma$ -mediated target gene (aP2/FABP4) expression in mutation-containing primary blood mononuclear-derived cells from subjects studied *ex vivo* (Figure 6.15).

In contrast, **chapter five** describes a different, digenic mechanism of insulin resistance in a large UK family, with a combination of loss-of-mutations in PPAR $\gamma$  and PPP1R3 (muscle-specific protein-phosphatase 1 regulatory subunit 3) genes. In this kindred only individuals who were doubly heterozygous for frameshift stop mutations in both PPAR $\gamma$  and PPP1R3 were severely insulin resistant, whereas two individuals who were heterozygous only for the PPAR $\gamma$  mutation and two other subjects who were heterozygous only for the PPP1R3 mutation had normal fasting insulin levels. This family illustrates that mutations in different proteins regulating separate metabolic pathway in adipose tissue or skeletal muscle can combine to result in extreme insulin resistance, while alone they have only modest metabolic effects. This represents the first clear-cut demonstration of gene/gene interaction mediating insulin resistance in humans.

The complete loss-of-function together with absence of dominant negative activity of the FS null mutation suggests that it limits PPAR $\gamma$  signaling via haploinsufficiency of functional receptor. Consistent with this, an individual who was heterozygous for the FS PPAR $\gamma$  mutation did not exhibit insulin resistance or

other metabolic abnormalities associated with other patients harboring dominant negative mutations in PPAR $\gamma$ .

Overall, our observations together with those of other groups have documented 14 different human genetic mutations in *PPARG* associated with clinical phenotypes. Except for a PPAR $\gamma$ 2 P115Q mutation which was identified in four morbidly obese subjects (Ristow *et al.*, 1998), all of the other mutations have been associated with a stereotyped syndrome of severe insulin resistance with or without partial lipodystrophy (Barroso *et al.*, 1999; Agarwal and Garg, 2002; Hegele *et al.*, 2002; Savage *et al.*, 2002; Savage *et al.*, 2003; Al-Shali *et al.*, 2004; Agostini *et al.*, 2006; Francis *et al.*, 2006; Hegele *et al.*, 2006).

Unlike RTH where the majority of natural mutations in TR $\beta$  are located in the carboxy-terminal part of the receptor, clustering in three “hot” areas around the ligand-binding pocket (Collingwood *et al.*, 1998), PPAR $\gamma$  mutations are distributed across several domains of the receptor (Figure 7.2a). Moreover these mutations have been shown to have different functional properties leading to disease through mechanisms of either: i) gain-of-function; ii) dominant negative activity; or iii) haploinsufficiency.

A P115Q substitution in PPAR $\gamma$  is the only “gain of function” mutation described to date. This amino acid change, with constitutive transcriptional function and enhanced adipogenic activity due to defective phosphorylation of the adjacent serine 114, was originally described in four morbidly obese German patients. However, recently another German individual carrying the same P115Q mutation was reported to be only moderately overweight, contrasting with the finding of the original study (Bluher and Pashke, 2003). Further studies are required to clarify the role of this particular genetic variant in the development of obesity in the general population.

To date, we have described seven different dominant negative PPAR $\gamma$  mutations, which can either compete directly with the wild type receptor for binding to a PPARE in the promoter region of target genes or indirectly interfere with the wild type receptor function by reducing the availability of other components of the transcriptional machinery, such as coactivators, through sequestration. Two further receptor mutations (PPAR $\gamma$ 2 F388L, R425C or PPAR $\gamma$ 1 F360L, R397C) do exhibit dominant negative activity when tested in some assays (Figure 7.1) but not by others

(Hegele *et al.*, 2002). All the cases described (including another female patient with the P467L mutation in an unrelated kindred [Gurnell and Chatterjee, unpublished data]) show very similar clinical phenotype whose main features are summarized in Figure 7.2b.

However, several loss-of-function mutations in PPAR $\gamma$  are likely to operate via a haploinsufficiency mechanism, yet have been associated with a similar clinical phenotype which includes severe insulin resistance. A heterozygous, single nucleotide substitution in the PPAR $\gamma$ 4 promoter (-14A>G, Al-Shali *et al.*, 2004), leading to reduced receptor expression from one allele of the PPAR $\gamma$  gene, can only lead to receptor haploinsufficiency; two other mutations, described either by another group (E138fs $\Delta$ AATG, Hegele *et al.*, 2006) or us (FS, Savage *et al.*, 2002), generate prematurely-truncated receptor variants and we have shown that the latter is clearly devoid of dominant negative activity. However, the FS PPAR $\gamma$  mutation was only associated with insulin resistance when combined with a second gene defect and this possibility was not excluded in the other published cases with haploinsufficient receptor mutations (Al-Shali *et al.*, 2004; Hegele *et al.*, 2006). Recently, on going surveillance of our subject with a haploinsufficient PPAR $\gamma$  mutation (FS), has provided evidence for a mechanism other than a second genetic defect, which could generate the clinical phenotype. When first studied in 2002, our subject with the FS mutation showed normal circulating insulin and lipid levels. However, in response to an altered lifestyle (over-nutrition and reduced physical activity) he gained weight substantially and his phenotype has changed markedly (Table 7.1), with the development of numerous features (insulin resistance, dyslipidaemia) of metabolic syndrome. In this context, it is noteworthy that the patients harbouring the -14A>G and E138fs $\Delta$ AATG mutations presented with hyperinsulinaemia and dyslipidaemia also on a background of significantly increased body weight (BMI 34.4 kg/m<sup>2</sup> and 33 kg/m<sup>2</sup> respectively) (Al-Shali *et al.*, 2004; Hegele *et al.*, 2006). Expression profiling of PPAR $\gamma$  target genes in peripheral blood mononuclear cells has shown that gene expression in dominant negative mutation-containing versus WT cells is markedly attenuated, whereas haploinsufficient FS mutation-containing cells exhibit an intermediate phenotype (Chapter 6, Figure 6.16). It would be very interesting to expression profile blood cell from all the published cases described to date as this may help to distinguish true dominant negative versus haploinsufficient states.

On the basis of our genetic and phenotypic observations, we propose a model in which limitation of PPAR $\gamma$  function, either alone, or together with environmental or other genetic factors, can cause a metabolic phenotype in the human context (Figure 7.3). PPAR $\gamma$  plays a pivotal role in the regulation of target genes mediating both adipocyte formation (differentiation) and function (lipogenesis) (Lehrke and Lazar, 2005). Therefore, it is plausible that any reduction in cellular PPAR $\gamma$  activity occurring either through haploinsufficiency (50% loss-of-function) or dominant negative mechanisms (>50% loss-of-function), is deleterious in the human context.

The identification of further novel receptor mutations and the characterization of murine models of natural human mutations will enable us to better understand the biological role of PPAR $\gamma$  and its involvement in human metabolic disease. Therefore, we will continue screening for further PPAR $\gamma$  mutations in different cohorts of patients presenting with: (i) partial lipodystrophy; (ii) severe insulin resistance; (iii) preeclampsia plus severe insulin resistance; (iv) PCOS plus severe insulin resistance but with a lean phenotype. However, regarding the use of mouse models, there may be significant physiological differences between humans and mice. For example, the adverse metabolic consequences of human PPAR $\gamma$  haploinsufficiency (Al-Shali *et al.*, 2004; Hegele *et al.*, 2006; Table 7.1) are in contrast to the preservation of insulin sensitivity seen in heterozygous PPAR $\gamma$  null mice even following high-fat diet (Kubota *et al.*, 1999; Miles *et al.*, 2000) or in heterozygous P465L animals (equivalent to the human P467L mutation) which do not have a metabolic phenotype unless they are crossed with severely obese, leptin deficient (ob/ob) mice and challenged with extreme positive energy balance (Gray *et al.*, 2006). These observations suggest that mouse metabolic physiology is different and does not become deranged unless the dietary load is severe, whereas human physiology is more sensitive; therefore caution needs to be exercised when translating insights from rodent models to humans. On the other hand, it is interesting to note that the P465L PPAR $\gamma$  mutation mouse model does exhibit hypertension as in the human cases, indicating that this feature is probably truly associated with PPAR $\gamma$  dysfunction.

PPAR $\gamma$  is highly expressed in macrophages within human atherosclerotic lesions as well as in normal human blood monocyte-derived macrophages (HMDMs). It is activated by oxidised LDL and its derivatives and the receptor regulates genes

mediating both cholesterol uptake (e.g. CD36) and efflux (e.g. ABCA1, ABCG1) pathways. PPAR $\gamma$  regulates macrophage expression of LXR, and this receptor independently regulates macrophage cholesterol homeostasis and inflammation. Interestingly, in our human PPAR $\gamma$  mutation cohort three females (C131Y, C114R, R357X) with no other obvious risk factors, have developed significant coronary atherosclerosis prematurely (age 35-52yrs). We therefore wish to study PPAR $\gamma$  function in mutation-containing HMDMs *ex vivo*. Using microarray and qPCR analyses we will investigate expression profile of these cells and compare this with profiles from normal controls in the absence and presence of both PPAR $\gamma$  and LXR selective ligands to explore the potential link between abnormal PPAR $\gamma$  and/or LXR signalling and the atherosclerotic phenotype. Preliminary microarray data indicates that PPAR $\gamma$  agonist-dependent induction of many known target genes (e.g. FABP4, CD36, ApoE, LPL) is attenuated in C131Y mutation-containing HMDM cells. Finally, another observation worthy of note is that heterozygous females with PPAR $\gamma$  mutations appear to be more severely affected than male carriers. However, ascertainment of additional subjects and families and detailed physiological studies are required to define a link between gender and phenotypic severity in syndromes of human PPAR $\gamma$  insufficiency and to elucidate the mechanisms that mediate this divergence.

Subject	vi		
Mutation	FS		
Gender	M		
Age (and at presentation) (yr)	32 (32)	34	36
BMI (kg/m <sup>2</sup> ) [non obese <30]	25.8 2002	27.5 2004	29.6 2006
WC (cm) [M <94; F <80]	nd	nd	103
BP (mmHg) [< 130/85]	125/90	nd	140/80
T2DM/IGT (age at diagnosis - yr)	N/A	N/A	N/A
TG (mmol/L) [< 1.7]	1.5	3.4	5.7
HDL-C (mmol/L) [M>1.03; F>1.29]	1.02	0.84	0.56
FI (pmol/L) [<60]	46	51	146
Predicted total body fat (%)	22.9	25.1	27.8
Measured total body fat (%)	nd	20 <sup>+0.1</sup>	23 <sup>+0.5</sup>
Measured lower limb fat (%)	nd	14	16
Measured truncal fat (%)	nd	27	30

**Table 7.1** Changes in clinical, biochemical and body composition parameters in the subject carrying the FS mutation (Subject vi in Figure 5.1) between 2002 when he was first studied and later in 2006. Key: BMI, body mass index; WC, waist circumference; BP, blood pressure; T2DM, type 2 diabetes mellitus; IGT, impaired glucose tolerance; TG, triglycerides; HDL-C, high density lipoprotein cholesterol; FI, fasting insulin; Predicted total body fat was calculated as follows (Black et al, 1983): males % fat = (1.281×BMI) – 10.13; Measured total and depot-specific body fat were determined using dual-energy X-ray absorptiometry – with corresponding z-scores for total body fat shown as superscript; M, male; healthy adult values where available are shown in parentheses [ ]; N/A, not applicable; nd, not determined.

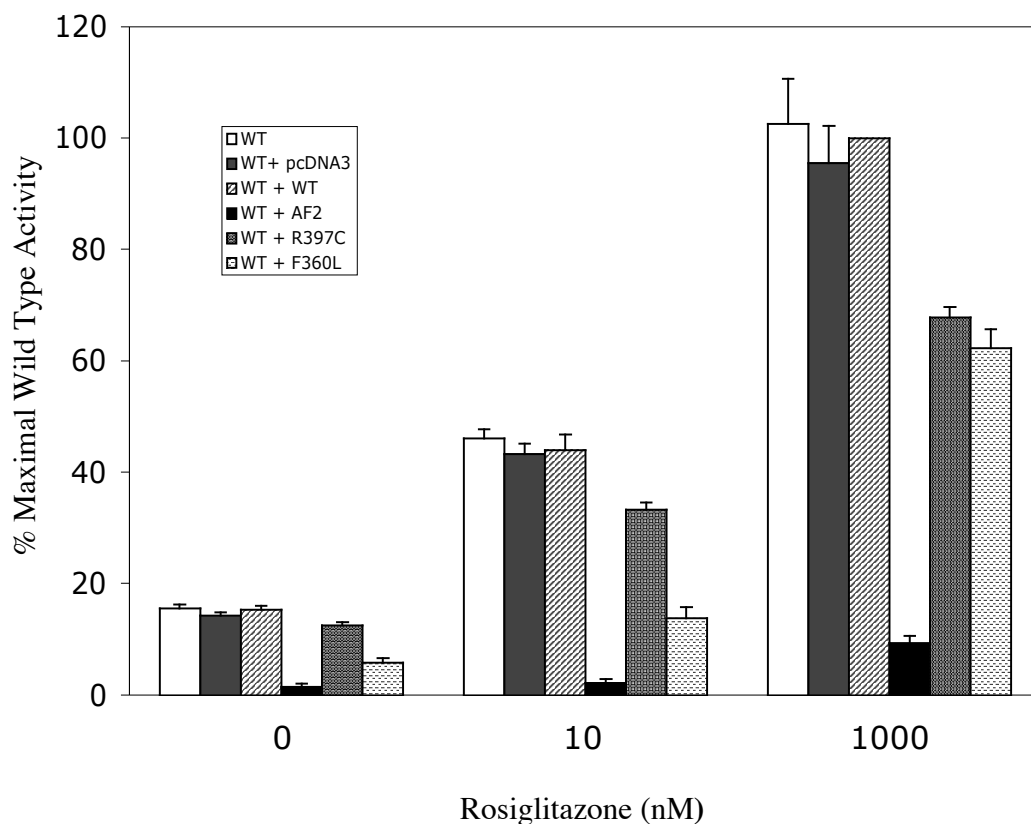


**Figure 7.1** R397C and F360L human PPAR $\gamma$ 1 mutants exhibit dominant negative activity when coexpressed with their wild type receptor (WT) counterpart. 293EBNA cells were transfected with WT alone or with an equal amount of either empty vector (pcDNA3), or additional WT, or mutant receptors (R397C or F360L) together with (PPARE) $_3$ TKLUC reporter gene (500ng) in the presence of increasing concentrations of ligand. As a control an artificial mutant (AF2), which we have previously shown to exhibit strong dominant negative inhibition (Gurnell *et al.*, 2000), was also tested in this experiment. Both R397C and F360L receptor mutants exhibit significant dominant negative activity even at the maximal levels of ligand. Dominant negative inhibition by those mutant receptors was also evident when tested using a human  $\alpha$ P2 reporter gene in 3T3-L1 adipocyte cells (Schoenmakers, unpublished data). The results shown are the mean  $\pm$  s.e.m. of at least five independent experiments, each done in triplicate, with a correction for transfection efficiency using  $\beta$ -galactosidase activity.



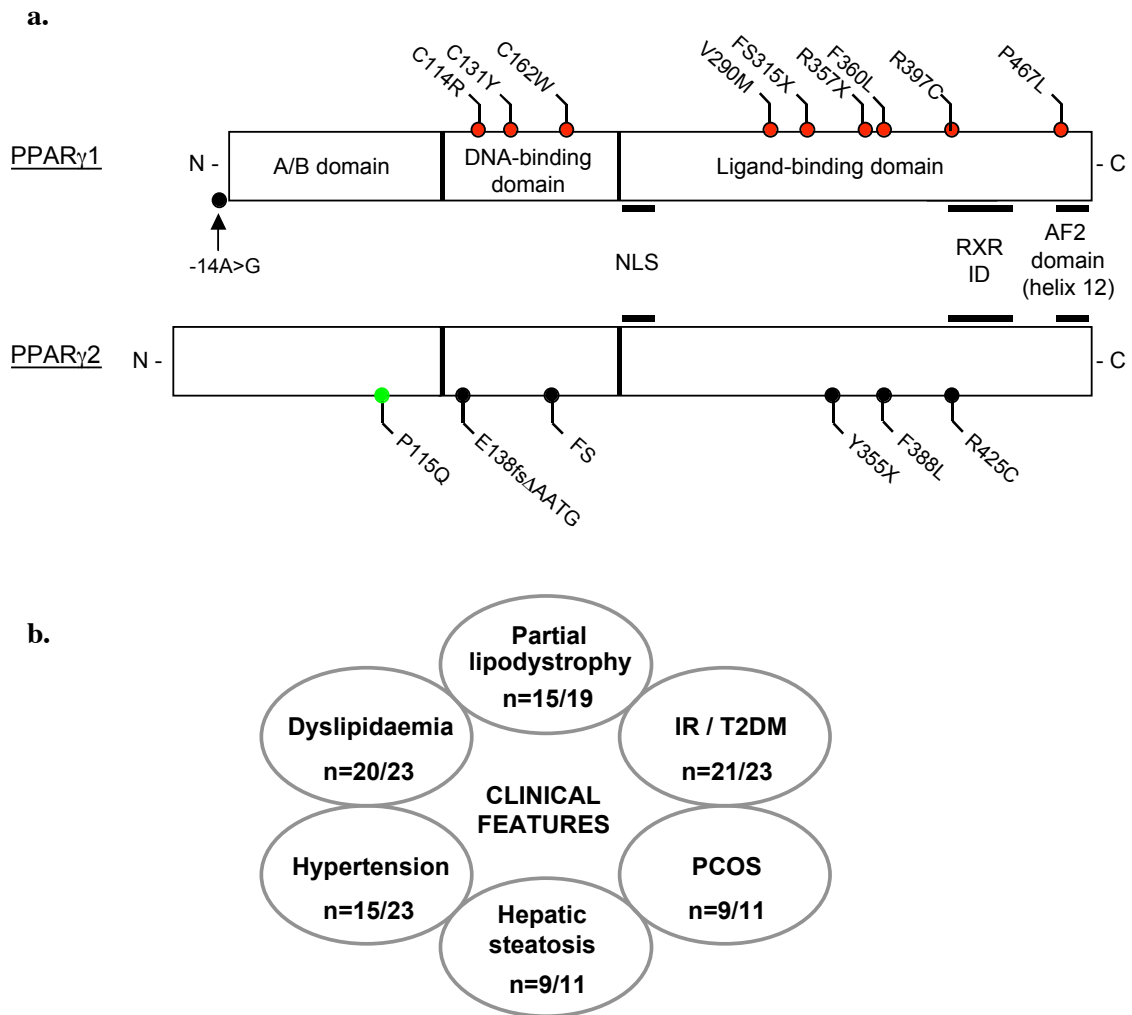


**Figure 7.2** Mutations in human PPAR $\gamma$  causing either receptor insufficiency or gain-of-function. **a.** Schematic representation of PPAR $\gamma$  1 and 2 isoforms showing the position of known natural genetic mutations identified to date. Except for the -14A>G nucleotide substitution, which is in the PPAR $\gamma$  4 promoter controlling expression of PPAR $\gamma$ 1, all other mutations affect both receptor isoforms. Note that mutations are shown on either the  $\gamma$ 1 or  $\gamma$ 2 background depending on the nomenclature used by authors in their publications. Mutants documented to have dominant negative activity (red) or leading to receptor haploinsufficiency (black) are shown. The P115Q (green) mutation results in a constitutively active receptor. **b.** Overview of phenotypic characteristics of subjects with loss-of-function PPAR $\gamma$  mutations. The denominator n refers to the number of subjects for whom information is available.

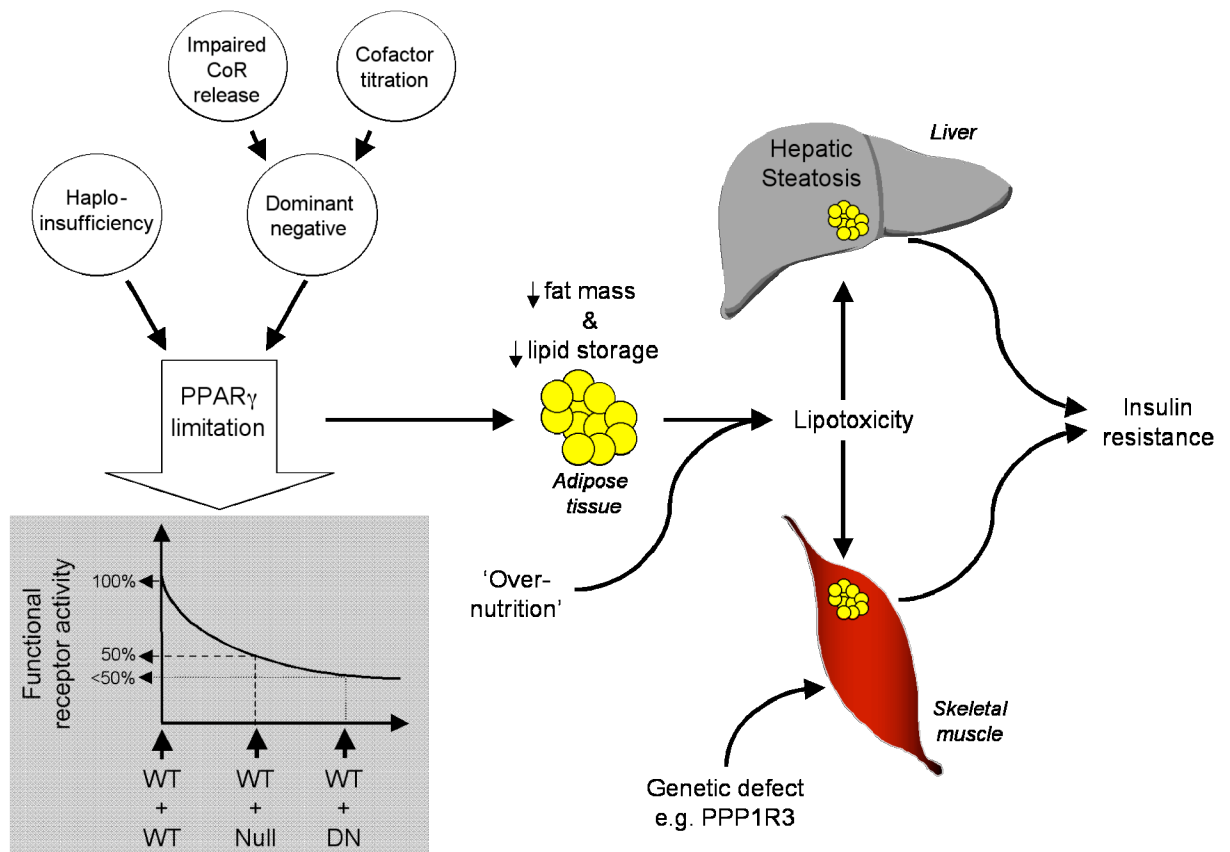


**Figure 7.3** Schematic representation of the pathogenesis of insulin resistance in subjects with PPAR $\gamma$  mutations. Mutations in the *PPARG* gene variably limit receptor activity, leading to a reduction in both adipocyte mass and function. Consequently, the ability to metabolize and store a dietary lipid load is compromised, with subsequent deposition and toxicity of lipid intermediates mediating insulin resistance in target tissues (e.g. liver, skeletal muscle). Dominant negative PPAR $\gamma$  mutations, associated with greater restriction of WT receptor function (>50%), can mediate a clinical phenotype, whereas PPAR $\gamma$  haploinsufficiency (50% loss-of-function) may require a second “hit” (e.g. overnutrition/dietary excess or combination with an unrelated genetic defect) to cause metabolic dysfunction.

## REFERENCES

- Abel, E. D., Boers, M.-E., Pazos-Moura, C., Moura, E., Kaulbach, H., Zakaria, M., Lowell, B., Radovick, S., Liberman, M. C., and Wondisford, F. (1999). Divergent roles for thyroid hormone receptor  $\beta$  isoforms in the endocrine axis and auditory system. *Journal of Clinical Investigation* *104*, 291-300.
- Abel, E. D., Peroni, O., Kim, J. K., Kim, Y. B., Boss, O., Hadro, E., Minnemann, T., Shulman, G. I., and Kahn, B. B. (2001). Adipose-selective targeting of the GLUT4 gene impairs insulin action in muscle and liver. *Nature* *409*, 729-733.
- Adams, M., Matthews, C. H., Collingwood, T. N., Tone, Y., Beck Peccoz, P., and K., C. V. K. (1994). Genetic analysis of twenty-nine kindreds with generalised and pituitary resistance to thyroid hormone. *Journal of Clinical Investigation* *94*, 506-515.
- Adams, M., Reginato, M. J., Shao, D., Lazar, M. A., and Chatterjee, V. K. K. (1997). Transcriptional activation by peroxisome proliferator-activated receptor  $\gamma$  is inhibited by phosphorylation at a consensus mitogen-activated protein kinase site. *Journal of Biological Chemistry* *272*, 5128-5132.
- Adams, M. D., Celniker, S. E., Holt, R. A., Evans, C. A., Gocayne, J. D., Amanatides, P. G., Scherer, S. E., Li, P. W., Hoskins, R. A., Galle, R. F., *et al.* (2000). The genome sequence of *Drosophila melanogaster*. *Science* *287*, 2185-2195.
- Agarwal, A. K., and Garg, A. (2002). A novel heterozygous mutation in peroxisome proliferator-activated receptor-gamma gene in a patient with familial partial lipodystrophy. *J Clin Endocrinol Metab* *87*, 408-411.
- Agostini, M., Gurnell, M., Savage, D. B., Wood, E. M., Smith, A. G., Rajanayagam, O., Garnes, K. T., Levinson, S. H., Xu, H. E., Schwabe, J. W., *et al.* (2004). Tyrosine agonists reverse the molecular defects associated with dominant-negative mutations in human peroxisome proliferator-activated receptor gamma. *Endocrinology* *145*, 1527-1538.
- Agostini, M., Schoenmakers, E., Mitchell, C. S., Szatmari, I., Savage, D. B., Smith, A. G., Rajanayagam, O., Semple, R. K., Luan, J., Bath, L., *et al.* (2006). Non-DNA binding, dominant-negative, human PPAR $\gamma$  mutations associated with lipodystrophic insulin resistance. *Cell Metabolism* *4*, 1-9.
- Ahima, R. S., and Flier, J. S. (2000). Adipose tissue as an endocrine organ. *Trends Endocrinol Metab* *11*, 327-332.
- Alland, L., Muhle, R., Hou, H., Jr., Potes, J., Chin, L., Schreiber-Agus, N., and DePinho, R. A. (1997). Role for N-CoR and histone deacetylase in Sin3-mediated transcriptional repression [see comments]. *Nature* *387*, 49-55.

Al-Shali, K., Cao, H., Knoers, N., Hermus, A. R., Tack, C. J., and Hegele, R. A. (2004). A single-base mutation in the peroxisome proliferator-activated receptor gamma4 promoter associated with altered in vitro expression and partial lipodystrophy. *J Clin Endocrinol Metab* 89, 5655-5660.

Altincicek, B., Tenbaum, S. P., Dressel, U., Thormeyer, D., Renkawitz, R., and Baniahmad, A. (2000). Interaction of the corepressor Alien with DAX-1 is abrogated by mutations of DAX-1 involved in adrenal hypoplasia congenita. *J Biol Chem* 275, 7662-7667.

Altiok, S., Xu, M., and Spiegelman, B. M. (1997). PPARgamma induces cell cycle withdrawal: inhibition of E2F/DP DNA-binding activity via down-regulation of PP2A. *Genes Dev* 11, 1987-1998.

Altshuler, D., Hirschhorn, J. N., Klannemark, M., Lindgren, C. M., Vohl, M. C., Nemesh, J., Lane, C. R., Schaffner, S. F., Bolk, S., Brewer, C., *et al.* (2000). The common PPARgamma Pro12Ala polymorphism is associated with decreased risk of type 2 diabetes. *Nat Genet* 26, 76-80.

Aranda, A., and Pascual, A. (2001). Nuclear hormone receptors and gene expression. *Physiol Rev* 81, 1269-1304.

Auboeuf, D., Rieusset, J., Fajas, L., Vallier, P., Frering, V., Riou, J. P., Staels, B., Auwerx, J., Laville, M., and Vidal, H. (1997). Tissue distribution and quantification of the expression of mRNAs of peroxisome proliferator-activated receptors and liver X receptor-alpha in humans: no alteration in adipose tissue of obese and NIDDM patients. *Diabetes* 46, 1319-1327.

Au-Fliegner, M., Helmer, E., Casanova, J., Raaka, B. M., and Samuels, H. H. (1993). The conserved ninth C-terminal heptad in thyroid hormone and retinoic acid receptors mediates diverse responses by affecting heterodimer but not homodimer formation. *Mol Cell Biol* 13, 5725-5737.

Ayer, D. E., Lawrence, Q. A., and Eisenman, R. N. (1995). Mad-Max transcriptional repression is mediated by ternary complex formation with mammalian homologs of yeast repressor Sin3. *Cell* 80, 767-776.

Baker, K. D., Shewchuk, L. M., Kozlova, T., Makishima, M., Hassell, A., Wisely, B., Caravella, J. A., Lambert, M. H., Reinking, J. L., Krause, H., *et al.* (2003). The *Drosophila* orphan nuclear receptor DHR38 mediates an atypical ecdysteroid signaling pathway. *Cell* 113, 731-742.

Baniahmad, A., Ha, I., Reinberg, D., Tsai, S., Tsai, M. J., and O'Malley, B. W. (1993). Interaction of human thyroid hormone receptor beta with transcription factor TFIIB may mediate target gene derepression and activation by thyroid hormone. *Proc Natl Acad Sci U S A* 90, 8832-8836.

Baniahmad, A., Kohne, A. C., and Renkawitz, R. (1992). A transferable silencing domain is present in the thyroid hormone receptor, in the v-erbA oncogene product and in the retinoic acid receptor. *Embo J* 11, 1015-1023.

- Baretino, D., Vivanco Ruiz, M. D. M., and Stunnenberg, H. G. (1994). Characterization of the ligand-dependent transactivation domain of thyroid hormone receptor. *EMBO Journal* *13*, 3039-3049.
- Barroso, I., Gurnell, M., Crowley, V. E. F., Agostini, M., Schwabe, J. W., Soos, M. A., Maslen, G. L. I., Williams, T. D. M., Lewis, H., Schafer, A. J., *et al.* (1999). Dominant negative mutations in human PPAR $\gamma$  are associated with severe insulin resistance, diabetes mellitus and hypertension. *Nature* *402*, 880-883.
- Baumann, C. A., Chokshi, N., Saltiel, A. R., and Ribon, V. (2000). Cloning and characterization of a functional peroxisome proliferator activator receptor-gamma-responsive element in the promoter of the CAP gene. *J Biol Chem* *275*, 9131-9135.
- Beamer, B. A., Yen, C.-J., Andersen, R. E., Muller, D., Elahi, D., Cheskin, L. J., and *al, e.* (1998). Association of the Pro12Ala variant in the peroxisome proliferator-activated receptor- $\gamma$ 2 gene with obesity in two Caucasian populations. *Diabetes* *47*, 1806-1808.
- Beck-Peccoz, P., and Chatterjee, V. K. (1994). The variable clinical phenotype in thyroid hormone resistance syndrome. *Thyroid* *4*, 225-232.
- Bell-Parikh, L. C., Ide, T., Lawson, J. A., McNamara, P., Reilly, M., and FitzGerald, G. A. (2003). Biosynthesis of 15-deoxy-delta12,14-PGJ2 and the ligation of PPARgamma. *J Clin Invest* *112*, 945-955.
- Benbrook, D., and Pfahl, M. (1987). A novel thyroid hormone receptor encoded by a cDNA clone from a human testis library. *Science* *238*, 788-791.
- Berger, J., Tanen, M., Elbrecht, A., Hermanowski-Vosatka, A., Moller, D. E., Wright, S. D., and Thieringer, R. (2001). Peroxisome proliferator-activated receptor-gamma ligands inhibit adipocyte 11beta -hydroxysteroid dehydrogenase type 1 expression and activity. *J Biol Chem* *276*, 12629-12635.
- Berger, J. P., Petro, A. E., Macnaul, K. L., Kelly, L. J., Zhang, B. B., Richards, K., Elbrecht, A., Johnson, B. A., Zhou, G., Doebber, T. W., *et al.* (2003). Distinct properties and advantages of a novel peroxisome proliferator-activated protein [gamma] selective modulator. *Mol Endocrinol* *17*, 662-676.
- Berkenstam, A., and Gustafsson, J. A. (2005). Nuclear receptors and their relevance to diseases related to lipid metabolism. *Curr Opin Pharmacol* *5*, 171-176.
- Bianco, A. C., Salvatore, D., Gereben, B., Berry, M. J., and Larsen, P. R. (2002). Biochemistry, cellular and molecular biology, and physiological roles of the iodothyronine selenodeiodinases. *Endocr Rev* *23*, 38-89.
- Birnbaum, M. J. (2001). Diabetes. Dialogue between muscle and fat. *Nature* *409*, 672-673.

Bjorntorp, P., and Sjostrom, L. (1978). Carbohydrate storage in man: speculations and some quantitative considerations. *Metabolism* 27, 1853-1865.

Black, D., James, W. P. T., Besser, G. M., Brock, C. G. D., Craddock, D., Garrow, J. S., Hockaday, T. D. R., Lewis, B., Pilkington, T. R. E., Silverstone, J. T., *et al.* (1983). Obesity: a report of the College of Physicians. *Journal of the Royal College of Physicians of London* 17, 5-65.

Bluher, M., and Paschke, R. (2003). Analysis of the relationship between PPAR-gamma 2 gene variants and severe insulin resistance in obese patients with impaired glucose tolerance. *Exp Clin Endocrinol Diabetes* 111, 85-90.

Bookout, A. L., Jeong, Y., Downes, M., Yu, R. T., Evans, R. M., and Mangelsdorf, D. J. (2006). Anatomical profiling of nuclear receptor expression reveals a hierarchical transcriptional network. *Cell* 126, 789-799.

Bourguet, W., Ruff, M., Chambon, P., Gronemeyer, H., and Moras, D. (1995). Crystal structure of the ligand binding domain of the human nuclear receptor RXR- $\alpha$ . *Nature* 375, 377-382.

Bourguet, W., Vivat, V., Wurtz, J. M., Chambon, P., Gronemeyer, H., and Moras, D. (2000). Crystal structure of a heterodimeric complex of RAR and RXR ligand-binding domains. *Mol Cell* 5, 289-298.

Braissant, O., Foufelle, F., Scotto, C., Dauca, M., and Wahli, W. (1996). Differential expression of peroxisome proliferator-activated receptors (PPARs): tissue distribution of PPAR-alpha, -beta, and -gamma in the adult rat. *Endocrinology* 137, 354-366.

Brown, K. K., Henke, B. R., Blanchard, S. G., Cobb, J. E., Mook, R., Kaldor, I., Kliewer, S. A., Lehmann, J. M., Lenhard, J. M., Harrington, W. W., *et al.* (1999). A novel N-aryl tyrosine activator of peroxisome proliferator-activated receptor-gamma reverses the diabetic phenotype of the Zucker diabetic fatty rat. *Diabetes* 48, 1415-1424.

Bruning, J. C., Winnay, J., Bonner-Weir, S., Taylor, S. I., Accili, D., and Kahn, C. R. (1997). Development of a novel polygenic model of NIDDM in mice heterozygous for IR and IRS-1 null alleles. *Cell* 88, 561-572.

Brzozowski, A. M., Pike, A. C., Dauter, Z., Hubbard, R. E., Bonn, T., Engstrom, O., Ohman, L., Greene, G. L., Gustafsson, J. A., and Carlquist, M. (1997). Molecular basis of agonism and antagonism in the oestrogen receptor. *Nature* 389, 753-758.

Burant, C. F., Sreenan, S., Hirano, K.-i., Tai, T.-A. C., Lohmiller, J., Lukens, J., Davidson, N. O., Ross, S., and Graves, R. A. (1997). Troglitazone action is independent of adipose tissue. *Journal of Clinical Investigation* 100, 2900-2908.

Cao, H., and Hegele, R. A. (2000). Nuclear lamin A/C R482Q mutation in canadian kindreds with Dunnigan-type familial partial lipodystrophy. *Hum Mol Genet* 9, 109-112.

- Casas, F., Busson, M., Grandemange, S., Seyer, P., Carazo, A., Pessemesse, L., Wrutniak-Cabello, C., and Cabello, G. (2006). Characterization of a novel thyroid hormone receptor alpha variant involved in the regulation of myoblast differentiation. *Mol Endocrinol* *20*, 749-763.
- Cavaillès, V., Dauvois, S., L'Horset, F., Lopez, G., Hoare, S., Kushner, P. J., and Parker, M. G. (1995). Nuclear factor RIP140 modulates transcriptional activation by the estrogen receptor. *EMBO Journal* *14*, 3741-3751.
- Chakravarti, D., LaMorte, V. J., Nelson, M. C., Nakajima, T., Schulman, I. G., Juguilon, H., Montminy, M., and Evans, R. M. (1996). Role of CBP/P300 in nuclear receptor signalling. *Nature* *383*, 99-103.
- Chao, L., Marcus-Samuels, B., Mason, M. M., Moitra, J., Vinson, C., Arioglu, E., Gavrilova, O., and Reitman, M. L. (2000). Adipose tissue is required for the antidiabetic, but not for the hypolipidemic, effect of thiazolidinediones. *J Clin Invest* *106*, 1221-1228.
- Chatterjee, V. K. K. (1997). Molecular genetics and pathophysiology of thyroid hormone resistance. In *Current Opinion in Endocrinology and Diabetes*, pp. 371-376.
- Chatterjee, V. K. K. (2001). Resistance to thyroid hormone, and peroxisome-proliferator-activated receptor  $\gamma$  resistance. *Biochemical Society Transactions* *29*, 227-231.
- Chatterjee, V. K. K., Lee, J.-K., Rentoumis, A., and Jameson, J. L. (1989). Negative regulation of the TSH $\alpha$ -subunit gene by thyroid hormone: a response element localizes to the TATA box. *Proceedings of the National Academy of Science, USA* *86*, 9114-9118.
- Chatterjee, V. K. K., Nagaya, T., Madison, L. D., Datta, S., Rentoumis, A., and Jameson, J. L. (1991). Thyroid hormone resistance syndrome: inhibition of normal receptor function by mutant thyroid receptors. *Journal of Clinical Investigation* *87*, 1977-1984.
- Chawla, A., Barak, Y., Nagy, L., Liao, D., Tontonoz, P., and Evans, R. M. (2001). PPAR-gamma dependent and independent effects on macrophage-gene expression in lipid metabolism and inflammation. *Nat Med* *7*, 48-52.
- Chen, H., Lin, R. J., Schiltz, R. L., Chakravarti, D., Nash, A., Nagy, L., Privalsky, M. L., Nakatani, Y., and Evans, R. M. (1997). Nuclear receptor coactivator ACTR is a novel histone acetyltransferase and forms a multimeric activation complex with P/CAF and CBP/p300. *Cell* *90*, 569-580.
- Chen, J. D., and Evans, R. M. (1995). A transcriptional corepressor that interacts with nuclear hormone receptors. *Nature* *377*, 454-457.

Chen, S., Johnson, B., Li, Y., McKeever, B., Moller, D. E., and Zhou, G. (1999). Mapping of the PPAR $\gamma$  coactivator interaction by 3D NMR spectroscopy and site-directed mutagenesis. Paper presented at: The PPARs: transcriptional links to obesity, diabetes and cardiovascular disease (Keystone, Colorado).

Cheng, S. Y. (2005). Isoform-dependent actions of thyroid hormone nuclear receptors: lessons from knockin mutant mice. *Steroids* 70, 450-454.

Chinetti, G., Lestavel, S., Bocher, V., Remaley, A. T., Neve, B., Torra, I. P., Teissier, E., Minnich, A., Jaye, M., Duverger, N., *et al.* (2001). PPAR-alpha and PPAR-gamma activators induce cholesterol removal from human macrophage foam cells through stimulation of the ABCA1 pathway. *Nature Medicine* 7, 53-58.

Clifton-Bligh, R. J., de Zegher, F., Wagner, R. L., Collingwood, T. N., Francois, I., van Helvoirt, M., and Chatterjee, V. K. K. (1998). A novel TR $\beta$  mutation (R383H) in resistance to thyroid hormone predominantly impairs corepressor release and negative transcriptional regulation. *Molecular Endocrinology* 12, 609-621.

Codina, A., Love, J. D., Li, Y., Lazar, M. A., Neuhaus, D., and Schwabe, J. W. (2005). Structural insights into the interaction and activation of histone deacetylase 3 by nuclear receptor corepressors. *Proc Natl Acad Sci U S A* 102, 6009-6014.

Collingwood, T. N., Adams, M., Tone, Y., and Chatterjee, V. K. K. (1994). Spectrum of transcriptional dimerization and dominant negative properties of twenty different mutant thyroid hormone  $\beta$  receptors in thyroid hormone resistance syndrome. *Molecular Endocrinology* 8, 1262-1277.

Collingwood, T. N., Rajanayagam, O., Adams, M., Wagner, R., Cavailles, V., Kalkhoven, E., Matthews, C., Nystrom, E., Stenlof, K., Lindstedt, G., *et al.* (1997). A natural transactivation mutation in the thyroid hormone  $\beta$  receptor: impaired interaction with putative transcriptional mediators. *Proceedings of the National Academy of Science, USA* 94, 248-253.

Collingwood, T. N., Wagner, R., Matthews, C. H., Clifton-Bligh, R. J., Gurnell, M., Rajanayagam, O., Agostini, M., Fletterick, R. J., Beck Peccoz, P., Reinhardt, W., *et al.* (1998). A role of helix 3 of the TR $\beta$  ligand binding domain in coactivator recruitment identified by characterization of a third cluster of mutations in resistance to thyroid hormone. *EMBO Journal* 17, 4760-4770.

Colombo, C., Cutson, J. J., Yamauchi, T., Vinson, C., Kadowaki, T., Gavrilova, O., and Reitman, M. L. (2002). Transplantation of adipose tissue lacking leptin is unable to reverse the metabolic abnormalities associated with lipodystrophy. *Diabetes* 51, 2727-2733.

Combs, T. P., Wagner, J. A., Berger, J., Doebber, T., Wang, W. J., Zhang, B. B., Tanen, M., Berg, A. H., O'Rahilly, S., Savage, D. B., *et al.* (2002). Induction of adipocyte complement-related protein of 30 kilodaltons by PPARgamma agonists: a potential mechanism of insulin sensitization. *Endocrinology* 143, 998-1007.



Conneely, O. M., Sullivan, W. P., Toft, D. O., Birnbaumer, M., Cook, R. G., Maxwell, B. L., Zarucki-Schulz, T., Greene, G. L., Schrader, W. T., and O'Malley, B. W. (1986). Molecular cloning of the chicken progesterone receptor. *Science* 233, 767-770.

Cox, P. J., Ryan, D. A., Hollis, F. J., Harris, A. M., Miller, A. K., Vousden, M., and Cowley, H. (2000). Absorption, disposition, and metabolism of rosiglitazone, a potent thiazolidinedione insulin sensitizer, in humans. *Drug Metabolism and Disposition* 28, 772-780.

Culbertson, M. R. (1999). RNA surveillance. Unforeseen consequences for gene expression, inherited genetic disorders and cancer. *Trends Genet* 15, 74-80.

Damm, K., Thompson, C. C., and Evans, R. M. (1989). Protein encoded by v-erbA functions as a thyroid-hormone receptor antagonist. *Nature* 339, 593-597.

Darimont, C., Zbinden, I., Avanti, O., Leone-Vautravers, P., Giusti, V., Burckhardt, P., Pfeifer, A. M., and Mace, K. (2003). Reconstitution of telomerase activity combined with HPV-E7 expression allow human preadipocytes to preserve their differentiation capacity after immortalization. *Cell Death Differ* 10, 1025-1031.

Dayton, A. I., Selden, J. R., Laws, G., Dorney, D. J., Finan, J., Tripputi, P., Emanuel, B. S., Rovera, G., Nowell, P. C., and Croce, C. M. (1984). A human c-erbA oncogene homologue is closely proximal to the chromosome 17 breakpoint in acute promyelocytic leukemia. *Proc Natl Acad Sci U S A* 81, 4495-4499.

Deeb, S. S., Fajas, L., Nemoto, M., Pihlajamaki, J., Mykkanen, L., Kuusisto, J., Laakso, M., Fujimoto, W., and Auwerx, J. (1998). A Pro12Ala substitution in PPAR $\gamma$ 2 associated with decreased receptor activity, lower body mass index and improved insulin sensitivity. *Nature Genetics* 20, 284-287.

Demetri, G. D., Fletcher, C. D., Mueller, E., Sarraf, P., Naujoks, R., Campbell, N., Spiegelman, B. M., and Singer, S. (1999). Induction of solid tumor differentiation by the peroxisome proliferator-activated receptor-gamma ligand troglitazone in patients with liposarcoma. *Proc Natl Acad Sci U S A* 96, 3951-3956.

Desvergne, B., and Wahli, W. (1999). Peroxisome proliferator-activated receptors: nuclear control of metabolism. *Endocrine Reviews* 20, 649-688.

Di Renzo, J., Soderstrom, M., Kurokawa, R., Ogliastro, M.-H., Ricote, M., Ingrey, S., Horlein, A., Rosenfeld, M. G., and Glass, C. K. (1997). Peroxisome proliferator-activated receptors and retinoic acid receptors differentially control the interactions of retinoid X receptor heterodimers with ligands, coactivators and corepressors. *Molecular and Cellular Biology* 17, 2166-2176.

Doi, K., Itoh, H., Fukunaga, Y., Tanaka, T., Yamashita, J., Chun, T. H., Inoue, M., Masatsugu, K., Sawada, N., and Nakao, K. (1998). PPAR $\gamma$  modulates endothelial function: effects of thiazolidinediones on endothelial cell growth and secretion of endothelin (ET) and C-type natriuretic peptide (CNP). *Circulation* 98, 192.

Dumitrescu, A. M., Liao, X. H., Abdullah, M. S., Lado-Abeal, J., Majed, F. A., Moeller, L. C., Boran, G., Schomburg, L., Weiss, R. E., and Refetoff, S. (2005). Mutations in SECISBP2 result in abnormal thyroid hormone metabolism. *Nat Genet* 37, 1247-1252.

Dumitrescu, A. M., Liao, X. H., Best, T. B., Brockmann, K., and Refetoff, S. (2004). A novel syndrome combining thyroid and neurological abnormalities is associated with mutations in a monocarboxylate transporter gene. *Am J Hum Genet* 74, 168-175.

Elstner, E., Muller, C., Koshizuka, K., Williamson, E. A., Park, D., Asou, H., Shintaku, P., Said, J. W., Heber, D., and Koeffler, H. P. (1998). Ligands for peroxisome proliferator-activated receptor-gamma and retinoic acid receptor inhibit growth and induce apoptosis of human breast cancer cells in vitro and in BNX mice. *Proc Natl Acad Sci U S A* 95, 8806-8811.

Escriva, H., Safi, R., Hanni, C., Langlois, M. C., Saumitou-Laprade, P., Stehelin, D., Capron, A., Pierce, R., and Laudet, V. (1997). Ligand binding was acquired during evolution of nuclear receptors. *Proc Natl Acad Sci U S A* 94, 6803-6808.

Evans, R. M., Barish, G. D., and Wang, Y. X. (2004). PPARs and the complex journey to obesity. *Nat Med* 10, 355-361.

Fajas, L., Auboeuf, D., Raspe, E., Schoonjans, K., Lefebvre, A. M., Saladin, R., Najib, J., Laville, M., Fruchart, J. C., Deeb, S., *et al.* (1997). The organization, promoter analysis, and expression of the human PPARgamma gene. *J Biol Chem* 272, 18779-18789.

Fajas, L., Debril, M. B., and Auwerx, J. (2001). Peroxisome proliferator-activated receptor-gamma: from adipogenesis to carcinogenesis. *J Mol Endocrinol* 27, 1-9.

Farooqi, I. S., Jebb, S. A., Langmack, G., Lawrence, E., Cheetham, C. H., Prentice, A. M., Hughes, I. A., McCamish, M. A., and O'Rahilly, S. (1999). Effects of recombinant leptin therapy in a child with congenital leptin deficiency. *N Engl J Med* 341, 879-884.

Fernandes, I., Bastien, Y., Wai, T., Nygard, K., Lin, R., Cormier, O., Lee, H. S., Eng, F., Bertos, N. R., Pelletier, N., *et al.* (2003). Ligand-dependent nuclear receptor corepressor LCoR functions by histone deacetylase-dependent and -independent mechanisms. *Mol Cell* 11, 139-150.

Fiedorek, F. T., Wilson, G. G., Frith, L., Patel, J., and Abou-Donia, M. (2000). Monotherapy with G1262570, a tyrosine-based non-thiazolidinedione PPAR $\gamma$  agonist, improves metabolic control in type 2 diabetes mellitus patients. *Diabetes* 49(Suppl 1), Abst 157-OR.

Flamant, F., and Samarut, J. (2003). Thyroid hormone receptors: lessons from knockout and knock-in mutant mice. *Trends Endocrinol Metab* 14, 85-90.

- Floeth, M., and Bruckner-Tuderman, L. (1999). Digenic junctional epidermolysis bullosa: mutations in COL17A1 and LAMB3 genes. *Am J Hum Genet* 65, 1530-1537.
- Fondell, J. D., Ge, H., and Roeder, R. G. (1996). Ligand induction of a transcriptionally active thyroid hormone receptor coactivator complex. *Proc Natl Acad Sci U S A* 93, 8329-8333.
- Fondell, J. D., Roy, A. L., and Roeder, R. G. (1993). Unliganded thyroid hormone receptor inhibits formation of a functional preinitiation complex: implications for active repression. *Genes Dev* 7, 1400-1410.
- Forman, B. M., and Samuels, H. H. (1990). Interactions among a family of nuclear receptors: the regulatory zipper model. *Molecular Endocrinology* 4, 1293-1301.
- Forman, B. M., Tontonoz, P., Chen, J., Brun, R. P., Spiegelman, B. M., and Evans, R. M. (1995). 15-Deoxy-delta 12, 14-prostaglandin J2 is a ligand for the adipocyte determination factor PPAR $\gamma$ . *Cell* 83, 803-812.
- Forrest, D., Hanebuth, E., Smeyne, R. J., Everds, N., Stewart, C. L., Wehner, J. M., and Curran, T. (1996). Recessive resistance to thyroid hormone in mice lacking thyroid hormone receptor  $\beta$ : evidence for tissue-specific modulation of receptor function. *The EMBO Journal* 15, 3006-3015.
- Francis, G. A., Li, G., Casey, R., Wang, J., Cao, H., Leff, T., and Hegele, R. A. (2006). Peroxisomal proliferator activated receptor-gamma deficiency in a Canadian kindred with familial partial lipodystrophy type 3 (FPLD3). *BMC Med Genet* 7, 3.
- Frank-Raue, K., Lorenz, A., Haag, C., Hoppner, W., Boll, H. U., Knorr, D., Hentze, S., and Raue, F. (2004). Severe form of thyroid hormone resistance in a patient with homozygous/hemizygous mutation of T3 receptor gene. *Eur J Endocrinol* 150, 819-823.
- Friesema, E. C., Grueters, A., Biebermann, H., Krude, H., von Moers, A., Reeser, M., Barrett, T. G., Mancilla, E. E., Svensson, J., Kester, M. H., *et al.* (2004). Association between mutations in a thyroid hormone transporter and severe X-linked psychomotor retardation. *Lancet* 364, 1435-1437.
- Gampe, J., R. T., Montana, V. G., Lambert, M. H., Miller, A. B., Bledsoe, R. K., Milburn, M. V., Kliewer, S. A., Willson, T. M., and Xu, H. E. (2000). Asymmetry in the PPAR $\gamma$ /RXR $\alpha$  crystal structure reveals the molecular basis of heterodimerization among nuclear receptors. *Molecular Cell* 5, 545-555.
- Germain, P., Staels, B., Dacquet, C., Spedding, M., and Laudet, V. (2006). Overview of nomenclature of nuclear receptors. *Pharmacological Review* 58, 685-704.
- Gershengorn, M. C., and Weintraub, B. D. (1975). Thyrotropin-induced hyperthyroidism caused by selective pituitary resistance to thyroid hormone. A new syndrome of inappropriate secretion of TSH. *Journal of Clinical Investigation* 56, 633-642.

Gervois, P., Torra, I. P., Chinetti, G., Grotzinger, T., Dubois, G., Fruchart, J. C., Fruchart-Najib, J., Leitersdorf, E., and Staels, B. (1999). A truncated human peroxisome proliferator-activated receptor alpha splice variant with dominant negative activity. *Mol Endocrinol* 13, 1535-1549.

Gobinet, J., Carascossa, S., Cavailles, V., Vignon, F., Nicolas, J. C., and Jalaguier, S. (2005). SHP represses transcriptional activity via recruitment of histone deacetylases. *Biochemistry* 44, 6312-6320.

Goldberg, A. F., and Molday, R. S. (1996). Defective subunit assembly underlies a digenic form of retinitis pigmentosa linked to mutations in peripherin/rds and rom-1. *Proc Natl Acad Sci U S A* 93, 13726-13730.

Goodson, M., Jonas, B. A., and Privalsky, M. A. (2005). Corepressors: custom tailoring and alterations while you wait. *Nucl Recept Signal* 3, e003.

Graves, R. A., Tontonoz, P., Platt, K. A., Ross, S. R., and Spiegelman, B. M. (1992). Identification of a fat cell enhancer: analysis of requirements for adipose tissue-specific gene expression. *J Cell Biochem* 49, 219-224.

Gray, S. L., Nora, E. D., Grosse, J., Manieri, M., Stoeger, T., Medina-Gomez, G., Burling, K., Wattler, S., Russ, A., Yeo, G. S., *et al.* (2006). Leptin deficiency unmasks the deleterious effects of impaired peroxisome proliferator-activated receptor gamma function (P465L PPARgamma) in mice. *Diabetes* 55, 2669-2677.

Green, S., Walter, P., Kumar, V., Krust, A., Bornert, J. M., Argos, P., and Chambon, P. (1986). Human oestrogen receptor cDNA: sequence, expression and homology to v-erb-A. *Nature* 320, 134-139.

Greene, M. E., Blumberg, B., McBride, O. W., Yi, H. F., Kronquist, K., Kwan, K., Hsieh, L., Greene, G., and Nimer, S. D. (1995). Isolation of the human peroxisome proliferator activated receptor gamma cDNA: expression in hematopoietic cells and chromosomal mapping. *Gene Expr* 4, 281-299.

Griffith, A. J., Szymko, Y. M., Kaneshige, M., Quinonez, R. E., Kaneshige, K., Heintz, K. A., Mastroianni, M. A., Kelley, M. W., and Cheng, S. Y. (2002). Knock-in mouse model for resistance to thyroid hormone (RTH): an RTH mutation in the thyroid hormone receptor beta gene disrupts cochlear morphogenesis. *J Assoc Res Otolaryngol* 3, 279-288.

Grignani, F., De Matteis, S., Nervi, C., Tomassoni, L., Gelmetti, V., Cioce, M., Fanelli, M., Ruthardt, M., Ferrara, F. F., Zamir, I., *et al.* (1998). Fusion proteins of the retinoic acid receptor-alpha recruit histone deacetylase in promyelocytic leukaemia. *Nature* 391, 815-818.

Gronemeyer, H., Gustafsson, J. A., and Laudet, V. (2004). Principles for modulation of the nuclear receptor superfamily. *Nat Rev Drug Discov* 3, 950-964.

Gronemeyer, H., and Laudet, V. (1995). Transcription factors 3: nuclear receptors. *Protein Profile* 2, 1173-1308.

- Guan, H. P., Ishizuka, T., Chui, P. C., Lehrke, M., and Lazar, M. A. (2005). Corepressors selectively control the transcriptional activity of PPAR $\gamma$  in adipocytes. *Genes Dev* 19, 453-461.
- Guan, H.-P., Li, Y., Jensen, M. V., Newgard, C. B., Steppan, C. M., and Lazar, M. A. (2002). A futile metabolic cycle activated in adipocytes by antidiabetic agents. *Nature Medicine* 8, 1122-1128.
- Guenther, M. G., Barak, O., and Lazar, M. A. (2001). The SMRT and N-CoR corepressors are activating cofactors for histone deacetylase 3. *Mol Cell Biol* 21, 6091-6101.
- Gurnell, M., Savage, D. B., Chatterjee, V. K., and O'Rahilly, S. (2003). The metabolic syndrome: peroxisome proliferator-activated receptor gamma and its therapeutic modulation. *J Clin Endocrinol Metab* 88, 2412-2421.
- Gurnell, M., Wentworth, J. M., Agostini, M., Adams, M., Collingwood, T. N., Provenzano, C., Browne, P. O., Rajanayagam, O., Burris, T. P., Schwabe, J. W., *et al.* (2000). A dominant negative Peroxisome Proliferator-activated Receptor  $\gamma$  (PPAR $\gamma$ ) mutant is a constitutive repressor and inhibits PPAR $\gamma$ -mediated adipogenesis. *Journal of Biological Chemistry* 275, 5754-5759.
- Halachmi, S., Marden, E., Martin, G., MacKay, H., Abbondanza, C., and Brown, M. (1994). Estrogen receptor-associated proteins: possible mediators of hormone-induced transcription. *Science* 264, 1455-1458.
- Harris, M. I., Flegal, K. M., Cowie, C. C., Eberhardt, M. S., Goldstein, D. E., Little, R. R., Wiedmeyer, H. M., and Byrd-Holt, D. D. (1998). Prevalence of diabetes, impaired fasting glucose, and impaired glucose tolerance in U.S. adults. The Third National Health and Nutrition Examination Survey, 1988-1994. *Diabetes Care* 21, 518-524.
- Hashimoto, K., Curty, F. H., Borges, P. P., Lee, C. E., Abel, E. D., Elmquist, J. K., Cohen, R. N., and Wondisford, F. E. (2001). An unliganded thyroid hormone receptor causes severe neurological dysfunction. *Proc Natl Acad Sci U S A* 98, 3998-4003.
- Hayashi, Y., Weiss, R. E., Sarne, D. H., Yen, P. M., Sunthornthepvarakul, T., Marcocci, C., Chin, W. W., and Refetoff, S. (1995). Do clinical manifestations of resistance to thyroid hormone correlate with the functional alteration of the corresponding mutant thyroid hormone  $\beta$  receptors? *Journal of Clinical Endocrinology and Metabolism* 80, 3246-3256.
- Hayashi, Y., Xie, J., Weiss, R. E., Pohlenz, J., and Refetoff, S. (1998). Selective pituitary resistance to thyroid hormone produced by expression of a mutant thyroid hormone receptor  $\beta$  gene in the pituitary gland of transgenic mice. *Biochemical and Biophysical Research Communications* 245, 204-210.

He, L.-Z., Guidez, F., Tribioli, C., Peruzzi, D., Ruthardt, M., Zelent, A., and Pandolfi, P. P. (1998). Distinct interactions of PML-RAR $\alpha$  and PLZF-RAR $\alpha$  with co-repressors determine differential responses to RA in APL. *Nature Genetics* 18, 126-135.

Heery, D. M., Kalkhoven, E., Hoare, S., and Parker, M. G. (1997). A signature motif in transcriptional coactivators mediates binding to nuclear receptors. *Nature* 387, 733-736.

Hegele, R. A., Cao, H., Frankowski, C., Mathews, S. T., and Leff, T. (2002). PPARG F388L, a transactivation-deficient mutant, in familial partial lipodystrophy. *Diabetes* 51, 3586-3590.

Hegele, R. A., Ur, E., Ransom, T. P., and Cao, H. (2006). A frameshift mutation in peroxisome-proliferator-activated receptor-gamma in familial partial lipodystrophy subtype 3 (FPLD3; MIM 604367). *Clin Genet* 70, 360-362.

Heinzel, T., Lavinsky, R. M., Mullen, T.-M., Soderstrom, M., Laherty, C. D., Torchia, J., Yang, W.-M., Brard, G., Ngo, S. D., Davie, J. R., *et al.* (1997). A complex containing N-CoR, mSin3 and histone deacetylase mediates transcriptional repression. *Nature* 387, 43-48.

Helledie, T., Grontved, L., Jensen, S. S., Kiilerich, P., Rietveld, L., Albrektsen, T., Boysen, M. S., Nohr, J., Larsen, L. K., Fleckner, J., *et al.* (2002). The gene encoding the Acyl-CoA-binding protein is activated by peroxisome proliferator-activated receptor gamma through an intronic response element functionally conserved between humans and rodents. *J Biol Chem* 277, 26821-26830.

Henke, B. R., Blanchard, S. G., Brackeen, M. F., Brown, K. K., Cobb, J. E., Collins, J. L., Harrington, W. W. J., Hashim, M. A., Hull-Ryde, E. A., Kaldor, I., *et al.* (1998). *N*-(2-Benzoylphenyl)-L-tyrosine PPAR $\gamma$  agonists. 1. Discovery of a novel series of potent antihyperglycemic and antihyperlipidemic agents. *The Journal of Medicinal Chemistry* 41, 5020-5036.

Hevener, A. L., He, W., Barak, Y., Le, J., Bandyopadhyay, G., Olson, P., Wilkes, J., Evans, R. M., and Olefsky, J. (2003). Muscle-specific Pparg deletion causes insulin resistance. *Nat Med* 9, 1491-1497.

Hodin, R. A., Lazar, M. A., Wintman, B. I., Darling, D. S., Koenig, R. J., Larsen, P. R., Moore, D. D., and Chin, W. W. (1989). Identification of a thyroid hormone receptor that is pituitary-specific. *Science* 244, 76-79.

Hollenberg, A. N., Monden, T., and Wondisford, F. E. (1995). Ligand-independent and dependent function of thyroid hormone receptor isoforms depend upon their distinct amino termini. *Journal of Biological Chemistry* 270, 14274-14280.

Hollenberg, S. M., Weinberger, C., Ong, E. S., Cerelli, G., Oro, A., Lebo, R., Thompson, E. B., Rosenfeld, M. G., and Evans, R. M. (1985). Primary structure and expression of a functional human glucocorticoid receptor cDNA. *Nature* 318, 635-641.

Horlein, A. J., Naar, A. M., Heinzl, T., Torchia, J., Gloss, B., Kurokawa, R., Ryan, A., Kamei, Y., Soderstrom, M., Glass, C. J., and Rosenfeld, M. G. (1995). Ligand-independent repression by the thyroid hormone receptor mediated by a nuclear receptor corepressor. *Nature* 377, 397-404.

Hu, E., Tontonoz, P., and Spiegelman, B. M. (1995). Transdifferentiation of myoblasts by the adipogenic transcription factors PPAR gamma and C/EBP alpha. *Proc Natl Acad Sci U S A* 92, 9856-9860.

Hu, X., and Lazar, M. A. (1999). The CoRNR motif controls the recruitment of corepressors by nuclear hormone receptors. *Nature* 402, 93-96.

Huang, J. T., Welch, J. S., Ricote, M., Binder, C. J., Willson, T. M., Kelly, C., Witztum, J. L., Funk, C. D., Conrad, D., and Glass, C. K. (1999). Interleukin-4-dependent production of PPAR- $\gamma$  ligands in macrophages by 12/15-lipoxygenase. *Nature* 400, 378-382.

Huang, T. H., Peng, G., Kota, B. P., Li, G. Q., Yamahara, J., Roufogalis, B. D., and Li, Y. (2005). Anti-diabetic action of Punica granatum flower extract: activation of PPAR-gamma and identification of an active component. *Toxicol Appl Pharmacol* 207, 160-169.

Hummasti, S., and Tontonoz, P. (2006). The peroxisome proliferator-activated receptor N-terminal domain controls isotype-selective gene expression and adipogenesis. *Mol Endocrinol* 20, 1261-1275.

Iijima, K., Yoshizumi, M., Ako, J., Eto, M., Kim, S., Hashimoto, M., Sugimoto, N., Liang, Y. Q., Sudoh, N., Toba, K., and Ouchi, Y. (1998). Expression of peroxisome proliferator-activated receptor  $\gamma$  (PPAR $\gamma$ ) in rat aortic smooth muscle cells. *Biochemical and Biophysical Research Communications* 247, 353-356.

Ijpenberg, A., Jeannin, E., Wahli, W., and Desvergne, B. (1997). Polarity and specific sequence requirements of peroxisome proliferator-activated receptor (PPAR)/retinoid X receptor heterodimer binding to DNA. A functional analysis of the malic enzyme gene PPAR response element. *J Biol Chem* 272, 20108-20117.

Inzucchi, S. E., Maggs, D. G., Spollett, G. R., Page, S. L., Rife, F. S., Walton, V., and Shulman, G. I. (1998). Efficacy and metabolic effects of metformin and troglitazone in type II diabetes mellitus. *New England Journal of Medicine* 338, 867-872.

Issemann, I., and Green, S. (1990). Activation of a member of the steroid hormone receptor superfamily by peroxisome proliferators [see comments]. *Nature* 347, 645-650.

Iwaki, M., Matsuda, M., Maeda, N., Funahashi, T., Matsuzawa, Y., Makishima, M., and Shimomura, I. (2003). Induction of adiponectin, a fat-derived antidiabetic and antiatherogenic factor, by nuclear receptors. *Diabetes* 52, 1655-1663.

Jepsen, K., and Rosenfeld, M. G. (2002). Biological roles and mechanistic actions of co-repressor complexes. *J Cell Sci* 115, 689-698.

Juge-Aubry, C., Pernin, A., Favez, T., Burger, A. G., Wahli, W., Meier, C. A., and Desvergne, B. (1997). DNA binding properties of peroxisome proliferator-activated receptor subtypes on various natural peroxisome proliferator response elements. Importance of the 5'-flanking region. *J Biol Chem* 272, 25252-25259.

Kallenberger, B. C., Love, J. D., Chatterjee, V. K., and Schwabe, J. W. (2003). A dynamic mechanism of nuclear receptor activation and its perturbation in a human disease. *Nat Struct Biol* 10, 136-140.

Kamiya, Y., Zhang, X. Y., Ying, H., Kato, Y., Willingham, M. C., Xu, J., O'Malley, B. W., and Cheng, S. Y. (2003). Modulation by steroid receptor coactivator-1 of target-tissue responsiveness in resistance to thyroid hormone. *Endocrinology* 144, 4144-4153.

Kaneshige, M., Kaneshige, K., Zhu, X., Dace, A., Garrett, L., Carter, T. A., Kazlauskaitė, R., Pankratz, D. G., Wynshaw-Boris, A., Refetoff, S., *et al.* (2000). Mice with a targeted mutation in the thyroid hormone beta receptor gene exhibit impaired growth and resistance to thyroid hormone. *Proc Natl Acad Sci U S A* 97, 13209-13214.

Katsanis, N., Ansley, S. J., Badano, J. L., Eichers, E. R., Lewis, R. A., Hoskins, B. E., Scambler, P. J., Davidson, W. S., Beales, P. L., and Lupski, J. R. (2001). Triallelic inheritance in Bardet-Biedl syndrome, a Mendelian recessive disorder. *Science* 293, 2256-2259.

Kelley, D. E., and Goodpaster, B. H. (2001). Effects of exercise on glucose homeostasis in Type 2 diabetes mellitus. *Med Sci Sports Exerc* 33, S495-501; discussion S528-499.

Kim, K. R., Lee, J. H., Kim, S. J., Rhee, S. D., Jung, W. H., Yang, S. D., Kim, S. S., Ahn, J. H., and Cheon, H. G. (2006). KR-62980: a novel peroxisome proliferator-activated receptor gamma agonist with weak adipogenic effects. *Biochem Pharmacol* 72, 446-454.

Kitajima, K., Nagaya, T., and Jameson, J. L. (1995). Dominant negative and DNA-binding properties of mutant thyroid hormone receptors that are defective in homodimerization but not heterodimerization. *Thyroid* 5, 343-353.

Kliwer, S. A., Lenhard, J. M., Willson, T. M., Patel, I., Morris, D. C., and Lehmann, J. M. (1995). A prostaglandin J2 metabolite binds peroxisome proliferator-activated receptor gamma and promotes adipocyte differentiation. *Cell* 83, 813-819.

Kliwer, S. A., Sundseth, S. S., Jones, S. A., Brown, P. J., Wisely, G. B., Koble, C. S., Devchand, P., Wahli, W., Willson, T. M., Lenhard, J. M., and Lehmann, J. M. (1997). Fatty acids and eicosanoids regulate gene expression through direct interactions with peroxisome proliferator-activated receptors alpha and gamma. *Proc Natl Acad Sci U S A* 94, 4318-4323.



- Korzus, E., Torchia, J., Rose, D. W., Xu, L., Kurokawa, R., McInerney, E. M., Mullen, T. M., Glass, C. K., and Rosenfeld, M. G. (1998). Transcription factor-specific requirements for coactivators and their acetyltransferase functions. *Science* 279, 703-707.
- Kraus, W. L., McInerney, E. M., and Katzenellenbogen, B. S. (1995). Ligand-dependent, transcriptionally productive association of the amino- and carboxyl-terminal regions of a steroid hormone nuclear receptor. *Proc Natl Acad Sci U S A* 92, 12314-12318.
- Krentz, A. J., Bailey, C. J., and Melander, A. (2000). Thiazolidinediones for type 2 diabetes. New agents reduce insulin resistance but need long term clinical trials. *British Medical Journal* 321, 252-253.
- Kroll, T. G., Sarraf, P., Pecciarini, L., Chen, C. J., Mueller, E., Spiegelman, B. M., and Fletcher, J. A. (2000). PAX8-PPAR $\gamma$ 1 fusion oncogene in human thyroid carcinoma. *Science* 289, 1357-1360.
- Kubota, N. T., Miki, H., Tamemoto, H., Yamauchi, T., Komeda, K., Satoh, S., Nakano, R., Ishii, C., Sugiyama, T., Eto, K., Tsubamoto, Y., *et al.* (1999). PPAR $\gamma$  mediates high-fat diet-induced adipocyte hypertrophy and insulin resistance. *Molecular Cell* 4, 597-609.
- Kumar, R., and Thompson, E. B. (1999). The structure of the nuclear hormone receptors. *Steroids* 64, 310-319.
- Laffitte, B. A., Joseph, S. B., Walczak, R., Pei, L., Wilpitz, D. C., Collins, J. L., and Tontonoz, P. (2001). Autoregulation of the human liver X receptor alpha promoter. *Mol Cell Biol* 21, 7558-7568.
- Lanz, R. B., McKenna, N. J., Onate, S. A., Albrecht, U., Wong, J., Tsai, S. Y., Tsai, M. J., and O'Malley, B. W. (1999). A steroid receptor coactivator, SRA, functions as an RNA and is present in an SRC-1 complex. *Cell* 97, 17-27.
- Laudet, V. (1997). Evolution of the nuclear receptor superfamily: early diversification from an ancestral orphan receptor. *J Mol Endocrinol* 19, 207-226.
- Lazar, M. A. (1993). Thyroid hormone receptors: multiple forms, multiple possibilities. *Endocrine Reviews* 14, 184-193.
- Lazar, M. A., Berrodin, T. J., and Harding, H. P. (1991). Differential DNA binding by monomeric, homodimeric, and potentially heteromeric forms of the thyroid hormone receptor. *Mol Cell Biol* 11, 5005-5015.
- Lefebvre, A.-M., Chen, I., Desreumaux, P., Najib, J., Fruchart, J.-C., Geboes, K., Briggs, M., Heyman, R., and Auwerx, J. (1998). Activation of the peroxisome proliferator-activated receptor  $\gamma$  promotes the development of colon tumours in C57BL/6J-APC<sup>Min/+</sup> mice. *Nature Medicine* 4, 1053-1057.

Lehmann, J. M., Moore, L. B., Smith-Oliver, T. A., Wilkison, W. O., Willson, T. M., and Kliewer, S. A. (1995). An antidiabetic thiazolidinedione is a high affinity ligand for peroxisome proliferator-activated receptor  $\gamma$  (PPAR $\gamma$ ). *Journal of Biological Chemistry* *270*, 12953-12956.

Lehrke, M., and Lazar, M. A. (2005). The many faces of PPAR $\gamma$ . *Cell* *123*, 993-999.

Li, Y., Lambert, M. H., and Xu, H. E. (2003). Activation of nuclear receptors: a perspective from structural genomics. *Structure* *11*, 741-746.

Libby, P., and *al, e.* (1999). PPAR $\gamma$  activation in human endothelial cells increases plasminogen activator inhibitor type-1 expression: PPAR $\gamma$  as a potential mediator in vascular disease. *Arterioscler Thromb Vasc Biol* *19*, 546-551.

Lin, J. R., Nagy, L., Satoshi, I., Shao, W., Miller, W., and Evans, R. M. (1998). Role of the histone deacetylase complex in acute promyelocytic leukaemia. *Nature* *391*, 811-814.

Liu, K., Black, R. M., Acton, J. J., 3rd, Mosley, R., Debenham, S., Abola, R., Yang, M., Tschirret-Guth, R., Colwell, L., Liu, C., *et al.* (2005). Selective PPAR $\gamma$  modulators with improved pharmacological profiles. *Bioorg Med Chem Lett* *15*, 2437-2440.

Lonard, D. M., and O'Malley, B. W. (2005). Expanding functional diversity of the coactivators. *Trends Biochem Sci* *30*, 126-132.

Love, J. D., Gooch, J. T., Nagy, L., Chatterjee, V. K. K., and Schwabe, J. W. R. (2000). Transcriptional repression by nuclear receptors: mechanisms and role in disease. *Biochemical Society Transactions* *28*, 390-396.

Maeda, N., Takahashi, M., Funahashi, T., Kihara, S., Nishizawa, H., Kishida, K., Nagaretani, H., Matsuda, M., Komuro, R., Ouchi, N., *et al.* (2001). PPAR $\gamma$  ligands increase expression and plasma concentrations of adiponectin, an adipose-derived protein. *Diabetes* *50*, 2094-2099.

Makowski, A., Brzostek, S., Cohen, R. N., and Hollenberg, A. N. (2003). Determination of nuclear receptor corepressor interactions with the thyroid hormone receptor. *Mol Endocrinol* *17*, 273-286.

Mamasiri, S., Yesil, S., Dumitrescu, A. M., Liao, X. H., Demir, T., Weiss, R. E., and Refetoff, S. (2006). Mosaicism of a thyroid hormone receptor-beta gene mutation in resistance to thyroid hormone. *J Clin Endocrinol Metab* *91*, 3471-3477.

Mangelsdorf, D. J., and Evans, R. M. (1995). The RXR heterodimers and orphan receptors. *Cell* *83*, 841-850.

- Martin, G., Schoonjans, K., Lefebvre, A. M., Staels, B., and Auwerx, J. (1997). Coordinate regulation of the expression of the fatty acid transport protein and acyl-CoA synthetase genes by PPARalpha and PPARgamma activators. *J Biol Chem* 272, 28210-28217.
- Mascaro, C., Acosta, E., Ortiz, J. A., Marrero, P. F., Hegardt, F. G., and Haro, D. (1998). Control of human muscle-type carnitine palmitoyltransferase I gene transcription by peroxisome proliferator-activated receptor. *J Biol Chem* 273, 8560-8563.
- Masugi, J., Tamori, Y., Mori, H., Koike, T., and Kasuga, M. (2000). Inhibitory effect of a proline-to-alanine substitution at codon 12 of peroxisome proliferator-activated receptor-gamma 2 on thiazolidinedione-induced adipogenesis. *Biochem Biophys Res Commun* 268, 178-182.
- Matthews, D. R., Hosker, J. P., Rudenski, A. S., Naylor, B. A., Treacher, D. F., and Turner, R. C. (1985). Homeostasis model assessment: insulin resistance and  $\beta$ -cell function from fasting plasma glucose and insulin concentrations in man. *Diabetologia* 28, 412-419.
- McGarry, J. D. (1992). What if Minkowski had been ageusic? An alternative angle on diabetes. *Science* 258, 766-770.
- McKenna, N. J., Lanz, R. B., and O'Malley, B. W. (1999). Nuclear receptor coregulators: cellular and molecular biology. *Endocr Rev* 20, 321-344.
- McKenna, N. J., and O'Malley, B. W. (2002). Combinatorial control of gene expression by nuclear receptors and coregulators. *Cell* 108, 465-474.
- Meier, C. A., Dickstein, B. M., Ashizawa, K., McClaskey, J. H., Muchmore, P., Ransom, S. C., Menke, J. B., Hao, E.-N., Usala, S. J., Bercu, B. B., *et al.* (1992). Variable transcriptional activity and ligand binding of mutant  $\beta$ 1 3,5,3'-triiodothyronine receptors from four families with generalised resistance to thyroid hormone. *Molecular Endocrinology* 6, 248-258.
- Meier, C. A., Parkison, C., Chen, A., Ashizawa, K., Meier-Heusler, S. C., Muchmore, P., Cheng, S.-Y., and Weintraub, B. D. (1993). Interaction of human  $\beta$ 1 thyroid hormone receptor and its mutants with DNA and retinoid X receptor  $\beta$ . T3 response element-dependent dominant negative potency. *The Journal of Clinical Investigation* 92, 1986-1993.
- Meyer, M. E., Gronemeyer, H., Turcotte, B., Bocquel, M. T., Tasset, D., and Chambon, P. (1989). Steroid hormone receptors compete for factors that mediate their enhancer function. *Cell* 57, 433-442.
- Miesfeld, R., Rusconi, S., Godowski, P. J., Maler, B. A., Okret, S., Wikstrom, A. C., Gustafsson, J. A., and Yamamoto, K. R. (1986). Genetic complementation of a glucocorticoid receptor deficiency by expression of cloned receptor cDNA. *Cell* 46, 389-399.

- Miles, P. D., Barak, Y., He, W., Evans, R. M., and Olefsky, J. M. (2000). Improved insulin-sensitivity in mice heterozygous for PPAR-gamma deficiency. *J Clin Invest* 105, 287-292.
- Misra, P., Chakrabarti, R., Vikramadithyan, R. K., Bolusu, G., Juluri, S., Hiriyani, J., Gershon, C., Rajjak, A., Kashireddy, P., Yu, S., *et al.* (2003). PAT5A: a partial agonist of peroxisome proliferator-activated receptor gamma is a potent antidiabetic thiazolidinedione yet weakly adipogenic. *J Pharmacol Exp Ther* 306, 763-771.
- Moeller, L.C., Dumitresco, A.M., Walker, R.L., Meltzer, P. S., and Refetoff, S. (2005). Thyroid hormone responsive genes in cultured human fibroblasts. 3 *J Clin Endocrinol Metab*, 90(2), 936-943 937.
- Mueller, E., Drori, S., Aiyer, A., Yie, J., Sarraf, P., Chen, H., Hauser, S., Rosen, E. D., Ge, K., Roeder, R. G., and Spiegelman, B. M. (2002). Genetic analysis of adipogenesis through peroxisome proliferator-activated receptor gamma isoforms. *J Biol Chem* 277, 41925-41930.
- Mueller, E., Smith, M., Sarraf, P., Kroll, T., Aiyer, A., Kaufman, D. S., Oh, W., Demetri, G., Figg, W. D., Zhou, X. P., *et al.* (2000). Effects of ligand activation of peroxisome proliferator-activated receptor gamma in human prostate cancer. *Proceedings of the National Academy of Sciences, USA* 97, 10990-10995.
- Mukherjee, R., Davies, P. J. A., Crombie, D. L., Dischoff, E. D., Cesario, R. M., Jow, L., Hamann, L. G., F., B. M., Mondon, C. E., Nadzan, A. M., *et al.* (1997). Sensitization of diabetic and obese mice to insulin by retinoid X receptor agonists. *Nature* 386, 407-410.
- Nagaya, T., and Jameson, J. L. (1993). Thyroid hormone receptor dimerization is required for dominant negative inhibition by mutations that cause thyroid hormone resistance. *Journal of Biological Chemistry* 268, 15766-15771.
- Nagaya, T., Madison, L. D., and Jameson, J. L. (1992). Thyroid hormone receptor mutants that cause resistance to thyroid hormone: evidence for receptor competition for DNA sequences in target genes. *Journal of Biological Chemistry* 267, 13014-13019.
- Nagy, L., Kao, H.-Y., Chakravarti, D., Lin, R. J., Hassig, C. A., Ayer, D. E., Schreiber, S. L., and Evans, R. M. (1997). Nuclear receptor repression mediated by a complex containing SMRT, mSin3A and histone deacetylase. *Cell* 89, 373-380.
- Nagy, L., Kao, H.-Y., Love, J. D., Li, C., Banayo, E., Gooch, J. T., Chatterjee, V. K. K., Evans, R. M., and Schwabe, J. W. R. (1999). Mechanism of co-repressor binding and release from nuclear hormone receptors. *Genes and Development* 13, 3209-3216.
- Nagy, L., Tontonoz, P., A., A. J. G., Chen, H., and Evans, R. M. (1998). Oxidized LDL regulates macrophage gene expression through ligand activation of PPAR $\gamma$ . *Cell* 93, 229-240.

- Nakamura, Y., Ohya, Y., Onaka, U., Fujii, K., Abe, I., and Fujishima, M. (1998). Inhibitory action of insulin-sensitizing agents on calcium channels in smooth muscle cells from resistance arteries of guinea-pig. *British Journal of Pharmacology* *123*, 675-682.
- Newgard, C. B., Brady, M. J., O'Doherty, R. M., and Saltiel, A. R. (2000). Organizing glucose disposal: emerging roles of the glycogen targeting subunits of protein phosphatase-1. *Diabetes* *49*, 1967-1977.
- Nielsen, J. N., Derave, W., Kristiansen, S., Ralston, E., Ploug, T., and Richter, E. A. (2001). Glycogen synthase localization and activity in rat skeletal muscle is strongly dependent on glycogen content. *J Physiol* *531*, 757-769.
- Nolte, R. T., B., W. G., Westin, S., Cobb, J. E., Lambert, M. H., Kurokawa, R., Rosenfeld, M. G., Willson, T. M., Glass, C. K., and Milburn, M. V. (1998). Ligand binding and coactivator assembly of the peroxisome proliferator-activated receptor- $\gamma$ . *Nature* *395*, 137-143.
- Norris, A. W., Chen, L., Fisher, S. J., Szanto, I., Ristow, M., Jozsi, A. C., Hirshman, M. F., Rosen, E. D., Goodyear, L. J., Gonzalez, F. J., *et al.* (2003). Muscle-specific PPAR $\gamma$ -deficient mice develop increased adiposity and insulin resistance but respond to thiazolidinediones. *J Clin Invest* *112*, 608-618.
- Ogihara, T., Rakugi, H., Ikegama, H., and *al, e.* (1995). Enhancement of insulin sensitivity by troglitazone lowers blood pressure in diabetic hypertensives. *American Journal of Hypertension* *8*, 316-320.
- Okuno, A., Tamemoto, H., Tobe, K., Ueki, K., Mori, Y., Iwamoto, K., Umesono, K., Akanuma, Y., Fujiwara, T., Horikoshi, H., *et al.* (1998). Troglitazone increases the number of small adipocytes without the change of white adipose tissue mass in obese Zucker rats. *J Clin Invest* *101*, 1354-1361.
- Olefsky, J. M. (2000). Treatment of insulin resistance with peroxisome proliferator-activated receptor gamma agonists. *J Clin Invest* *106*, 467-472.
- Onate, S. A., Tsai, S. Y., Tsai, M.-J., and O'Malley, B. W. (1995). Sequence and characterization of a coactivator for the steroid hormone receptor superfamily. *Science* *270*.
- Ono, S., Schwartz, I. D., Mueller, O. T., Root, A. W., Usala, S. J., and Bercu, B. B. (1991). Homozygosity for a dominant negative thyroid hormone receptor gene responsible for generalized resistance to thyroid hormone. *Journal of Clinical Endocrinology and Metabolism* *73*, 990-994.
- Oppenheimer, J. H., Schwartz, H. L., Koerner, D., and Surks, M. I. (1974). Limited binding capacity sites for L-triiodothyronine in rat liver nuclei. Nuclear-cytoplasmic interrelation, binding constants, and cross-reactivity with L-thyroxine. *J Clin Invest* *53*, 768-777.

O'Rahilly, S. (2002). Insights into obesity and insulin resistance from the study of extreme human phenotypes. *Eur J Endocrinol* *147*, 435-441.

Oral, E. A., Simha, V., Ruiz, E., Andewelt, A., Premkumar, A., Snell, P., Wagner, A. J., DePaoli, A. M., Reitman, M. L., Taylor, S. I., *et al.* (2002). Leptin-replacement therapy for lipodystrophy. *N Engl J Med* *346*, 570-578.

Ortiga-Carvalho, T. M., Shibusawa, N., Nikrodhanond, A., Oliveira, K. J., Machado, D. S., Liao, X. H., Cohen, R. N., Refetoff, S., and Wondisford, F. E. (2005). Negative regulation by thyroid hormone receptor requires an intact coactivator-binding surface. *J Clin Invest* *115*, 2517-2523.

O'Shea, P. J., Harvey, C. B., Suzuki, H., Kaneshige, M., Kaneshige, K., Cheng, S. Y., and Williams, G. R. (2003). A thyrotoxic skeletal phenotype of advanced bone formation in mice with resistance to thyroid hormone. *Mol Endocrinol* *17*, 1410-1424.

Park, K. S., Ciaraldi, T. P., Lindgren, K., Abrams-Carter, L., Mudaliar, S., Nikoulina, S. E., Tufari, S. R., Veerkamp, J. H., Vidal-Puig, A., and Henry, R. R. (1998). Troglitazone effects on gene expression in human skeletal muscle of type II diabetes involve up-regulation of peroxisome proliferator-activated receptor- $\gamma$ . *Journal of Clinical Endocrinology and Metabolism* *83*, 2830-2835.

Park, M. Y., Lee, K. S., and Sung, M. K. (2005). Effects of dietary mulberry, Korean red ginseng, and banaba on glucose homeostasis in relation to PPAR-alpha, PPAR-gamma, and LPL mRNA expressions. *Life Sci* *77*, 3344-3354.

Park, Y., Freedman, B. D., Lee, E. J., Park, S., and Jameson, J. L. (2003). A dominant negative PPARgamma mutant shows altered cofactor recruitment and inhibits adipogenesis in 3T3-L1 cells. *Diabetologia* *46*, 365-377.

Parker, M. G., Christian, M., and White, R. (2006). The nuclear receptor co-repressor RIP140 controls the expression of metabolic gene networks. *Biochem Soc Trans* *34*, 1103-1106.

Pascual, G., Fong, A. L., Ogawa, S., Gamliel, A., Li, A. C., Perissi, V., Rose, D. W., Willson, T. M., Rosenfeld, M. G., and Glass, C. K. (2005). A SUMOylation-dependent pathway mediates transrepression of inflammatory response genes by PPAR-gamma. *Nature* *437*, 759-763.

Pascual, G., and Glass, C. K. (2006). Nuclear receptors versus inflammation: mechanisms of transrepression. *Trends Endocrinol Metab* *17*, 321-327.

Pazin, M. J., and Kadonaga, J. T. (1997). SWI2/SNF2 and related proteins: ATP-driven motors that disrupt protein-DNA interactions? *Cell* *88*, 737-740.

Pelton, P. D., Zhou, L., Demarest, K. T., and Burris, T. P. (1999). PPAR $\gamma$  activation induces the expression of the adipocyte fatty acid binding protein gene in human monocytes. *Biochemical and Biophysical Research Communications* *261*, 456-458.

- Perissi, V., Staszewski, L. M., McInerney, E. M., Kurokawa, R., Krones, A., Rose, D. W., Lambert, M. H., Milburn, M. V., Glass, C. K., and Rosenfeld, M. G. (1999). Molecular determinants of nuclear receptor-corepressor interaction. *Genes & Development* *13*, 3198-3208.
- Pershadsingh, H. A., Szollosi, J., Benson, S., Hyun, W. C., Feuerstein, B. G., and Kurtz, T. W. (1993). Effects of ciglitazone on blood pressure and intracellular calcium metabolism. *Hypertension* *21*, 1020-1023.
- Petkovich, M., Brand, N. J., Krust, A., and Chambon, P. (1987). A human retinoic acid receptor which belongs to the family of nuclear receptors. *Nature* *330*, 444-450.
- Picard, F., and Auwerx, J. (2002). PPAR( $\gamma$ ) and glucose homeostasis. *Annu Rev Nutr* *22*, 167-197.
- Piedrafita, F. J., Bendik, I., Ortiz, M. A., and Pfahl, M. (1995). Thyroid hormone receptor homodimers can function as ligand-sensitive repressors. *Molecular Endocrinology* *9*, 563-578.
- Pohlenz, J., Weiss, R. E., Macchia, P. E., Pannain, S., Lau, I. T., Ho, H., and Refetoff, S. (1999). Five new families with resistance to thyroid hormone not caused by mutations in the thyroid hormone receptor  $\beta$  gene. *The Journal of Clinical Endocrinology and Metabolism* *84*, 3919-3928.
- Potter, G. B., Beaudoin, G. M., 3rd, DeRenzo, C. L., Zarach, J. M., Chen, S. H., and Thompson, C. C. (2001). The hairless gene mutated in congenital hair loss disorders encodes a novel nuclear receptor corepressor. *Genes Dev* *15*, 2687-2701.
- Privalsky, M. L. (2004). The role of corepressors in transcriptional regulation by nuclear hormone receptors. *Annu Rev Physiol* *66*, 315-360.
- Puigserver, P., and Spiegelman, B. M. (2003). Peroxisome proliferator-activated receptor- $\gamma$  coactivator 1  $\alpha$  (PGC-1  $\alpha$ ): transcriptional coactivator and metabolic regulator. *Endocr Rev* *24*, 78-90.
- Puigserver, P., Wu, Z., Park, C. W., Graves, R., Wright, M., and Spiegelman, B. M. (1998). A cold-inducible coactivator of nuclear receptors linked to adaptive thermogenesis. *Cell* *92*, 829-839.
- Quigley, C. A., De Bellis, A., Marschke, K. B., el-Awady, M. K., Wilson, E. M., and French, F. S. (1995). Androgen receptor defects: historical, clinical, and molecular perspectives [published erratum appears in *Endocr Rev* 1995 Aug;16(4):546]. *Endocr Rev* *16*, 271-321.
- Rachez, C., Lemon, B. D., Suldan, Z., Bromleigh, V., Gamble, M., Naar, A. M., Erdjument-Bromage, H., Tempst, P., and Freedman, L. P. (1999). Ligand-dependent transcription activation by nuclear receptors requires the DRIP complex. *Nature* *398*, 824-828.

Rangwala, S. M., Rhoades, B., Shapiro, J. S., Rich, A. S., Kim, J. K., Shulman, G. I., Kaestner, K. H., and Lazar, M. A. (2003). Genetic modulation of PPAR $\gamma$  phosphorylation regulates insulin sensitivity. *Dev Cell* 5, 657-663.

Rasmussen, S. K., Hansen, L., Frevert, E. U., Cohen, P. T., Kahn, B. B., and Pedersen, O. (2000). Adenovirus-mediated expression of a naturally occurring Asp905Tyr variant of the glycogen-associated regulatory subunit of protein phosphatase-1 in L6 myotubes. *Diabetologia* 43, 718-722.

Rastinejad, F., Perlmann, T., Evans, R. M., and Sigler, P. (1995). Structural determinants of nuclear receptor assembly on DNA direct repeats. *Nature* 375, 203-211.

Refetoff, S., De Wind, L. T., and De Groot, L. J. (1967). Familial syndrome combining deaf-mutism, stippled epiphyses, goiter and abnormally high PBI: possible target organ refractoriness to thyroid hormone. *Journal of Clinical Endocrinology and Metabolism* 27, 279-294.

Refetoff, S., Sadow, P. M., Reutrakul, S., Dennis, K., Mannavola, D., Pohlenz, J., and Weiss, R. E. (2004). Resistance to thyroid hormone in the absence of mutations in the thyroid hormone receptor genes. In *Syndrome of hormone resistance on the hypothalamic-pituitary-thyroid axis*, P. Beck-Peccoz, ed. (Boston, Kluwer Academic Publishers).

Refetoff, S., Weiss, R. E., and Usala, S. J. (1993). The syndromes of resistance to thyroid hormone. *Endocrine Reviews* 14, 348-399.

Reginato, M. J., Bailey, S. T., Krakow, S. L., Minami, C., Ishii, S., Tanaka, H., and Lazar, M. A. (1998). A potent antidiabetic thiazolidinedione with unique peroxisome proliferator-activated receptor  $\gamma$ -activating properties. *Journal of Biological Chemistry* 273, 32679-32684.

Ren, D., Collingwood, T. N., Rebar, E. J., Wolffe, A. P., and Camp, H. S. (2002). PPAR $\gamma$  knockdown by engineered transcription factors: exogenous PPAR $\gamma$ 2 but not PPAR $\gamma$ 1 reactivates adipogenesis. *Genes Dev* 16, 27-32.

Renaud, J.-P., Rochel, N., Ruff, M., Vivat, V., Chambon, P., Gronemeyer, H., and Moras, D. (1995). Crystal structure of the RAR-ligand-binding domain bound to all-*trans* retinoic acid. *Nature* 378, 681-689.

Rewers, M., and Hamman, R. F. (1995). Risk factors for non-insulin-dependent diabetes. In *Diabetes in America*, 2nd Edition, N. D. D. Group, ed. (Bethesda, National Institutes of Health), pp. 179-220.

Rico-Sanz, J., Thomas, E. L., Jenkinson, G., Mierisova, S., Iles, R., and Bell, J. D. (1999). Diversity in levels of intracellular total creatine and triglycerides in human skeletal muscles observed by (1)H-MRS. *J Appl Physiol* 87, 2068-2072.



Ricote, M., Huang, J., Fajas, L., Li, A., Welch, J., Najib, J., Witztum, J. L., Auwerx, J., Palinski, W., and Glass, C. K. (1998). Expression of the peroxisome proliferator-activated receptor  $\gamma$  (PPAR $\gamma$ ) in human atherosclerosis and regulation in macrophages by colony stimulating factors and oxidized low density lipoprotein. *Proceedings of the National Academy of Science, USA* 95, 7614-7619.

Ridker, P. M., Cook, N. R., Cheng, S., Erlich, H. A., Lindpaintner, K., Plutzky, J., and Zee, R. Y. (2003). Alanine for proline substitution in the peroxisome proliferator-activated receptor gamma-2 (PPARG2) gene and the risk of incident myocardial infarction. *Arterioscler Thromb Vasc Biol* 23, 859-863.

Ristow, M., Muller-Wieland, D., Pfeiffer, A., Krone, W., and Kahn, C. R. (1998). Obesity associated with a mutation in a genetic regulator of adipocyte differentiation. *New England Journal of Medicine* 339, 953-959.

Rival, Y., Stennevin, A., Puech, L., Rouquette, A., Cathala, C., Lestienne, F., Dupont-Passelaigue, E., Patoiseau, J. F., Wurch, T., and Junquero, D. (2004). Human adipocyte fatty acid-binding protein (aP2) gene promoter-driven reporter assay discriminates nonlipogenic peroxisome proliferator-activated receptor gamma ligands. *J Pharmacol Exp Ther* 311, 467-475.

Robinson-Rechavi, M., Carpentier, A. S., Duffraisse, M., and Laudet, V. (2001). How many nuclear hormone receptors are there in the human genome? *Trends Genet* 17, 554-556.

Rocchi, S., Picard, F., Vamecq, J., Gelman, L., Potier, N., Zeyer, D., Dubuquoy, L., Bac, P., Champy, M. F., Plunket, K. D., *et al.* (2001). A unique PPARgamma ligand with potent insulin-sensitizing yet weak adipogenic activity. *Mol Cell* 8, 737-747.

Rochette-Egly, C., Oulad-Abdelghani, M., Staub, A., Pfister, V., Scheuer, I., Chambon, P., and Gaub, M. P. (1995). Phosphorylation of the retinoic acid receptor-alpha by protein kinase A. *Mol Endocrinol* 9, 860-871.

Rosen, E. D., Hsu, C. H., Wang, X., Sakai, S., Freeman, M. W., Gonzalez, F. J., and Spiegelman, B. M. (2002). C/EBPalpha induces adipogenesis through PPARgamma: a unified pathway. *Genes Dev* 16, 22-26.

Sabatino, L., Casamassimi, A., Peluso, G., Barone, M. V., Capaccio, D., Migliore, C., Bonelli, P., Pedicini, A., Febbraro, A., Ciccodicola, A., and Colantuoni, V. (2005). A novel peroxisome proliferator-activated receptor gamma isoform with dominant negative activity generated by alternative splicing. *J Biol Chem* 280, 26517-26525.

Saez, E., Rosenfeld, J., Livolsi, A., Olson, P., Lombardo, E., Nelson, M., Banayo, E., Cardiff, R. D., Izpisua-Belmonte, J. C., and Evans, R. M. (2004). PPAR gamma signaling exacerbates mammary gland tumor development. *Genes Dev* 18, 528-540.

Saez, E., Tontonoz, P., Nelson, M. C., Alvarez, J. G., Ming, U. T., Baird, S. M., Thomazy, V. A., and Evans, R. M. (1998). Activators of the nuclear receptor PPARgamma enhance colon polyp formation. *Nat Med* 4, 1058-1061.

- Safer, J. D., Cohen, R. N., Hollenberg, A. N., and Wondisford, F. E. (1998). Defective release of corepressor by hinge mutants of the thyroid hormone receptor found in patients with resistance to thyroid hormone. *Journal of Biological Chemistry* 273, 30175-30182.
- Sakurai, A., Nakai, A., and DeGroot, L. J. (1990). Structural analysis of human thyroid hormone receptor beta gene. *Molecular and Cellular Endocrinology* 71, 83-91.
- Sallusto, F., and Lanzavecchia, A. (1994). Efficient presentation of soluble antigen by cultured human dendritic cells is maintained by granulocyte/macrophage colony-stimulating factor plus interleukin 4 and downregulated by tumor necrosis factor alpha. *J Exp Med* 179, 1109-1118.
- Sambrook, J., Fritsch, E. F., and Maniatis, T. (1989). In *Molecular cloning: a laboratory manual* (New York, Cold Spring Harbor Laboratory Press).
- Samuels, H. H., and Shapiro, L. E. (1976). Thyroid hormone stimulates de novo growth hormone synthesis in cultured GH1 cells: evidence for the accumulation of a rate limiting RNA species in the induction process. *Proc Natl Acad Sci U S A* 73, 3369-3373.
- Sap, J., Munoz, A., Damm, K., Goldberg, Y., Ghysdael, J., Leutz, A., Beug, H., and Vennstrom, B. (1986). The c-erb-A protein is a high-affinity receptor for thyroid hormone. *Nature* 324, 635-640.
- Sarraf, P., Mueller, E., Jones, D., King, F. J., DeAngelo, D. J., Partridge, J. B., Holden, S. A., Chen, L. B., Singer, S., Fletcher, C., and Spiegelman, B. M. (1998). Differentiation and reversal of malignant changes in colon cancer through PPARgamma. *Nature Medicine* 4, 1046-1052.
- Sarraf, P., Mueller, E., Smith, W. M., Wright, H. M., Kum, J. B., Aaltonen, L. A., de la Chappelle, A., Spiegelman, B. M., and Eng, C. (1999). Loss-of-function mutations in PPAR $\gamma$  associated with human colon cancer. *Molecular Cell* 3, 799-804.
- Sasaki, S., Lesoon-Wood, L. A., Dey, A., Kuwata, T., Weintraub, B. D., Humphrey, G., Yang, W. M., Seto, E., Yen, P. M., Howard, B. H., and Ozato, K. (1999). Ligand-induced recruitment of a histone deacetylase in the negative-feedback regulation of the thyrotropin beta gene. *Embo J* 18, 5389-5398.
- Satoh, H., Tsukamoto, K., Hashimoto, Y., Hashimoto, N., Togo, M., Hara, M., Maekawa, H., Isoo, N., Kimura, S., and Watanabe, T. (1999). Thiazolidinediones suppress endothelin-1 secretion from bovine vascular endothelial cells: A new possible role of PPAR $\gamma$  on vascular endothelial function. *Biochemical and Biophysical Research Communications* 254, 757-763.
- Savage, D. B. (2005). PPARgamma as a metabolic regulator: insights from genomics and pharmacology. *Expert Rev Mol Med* 2005, 1-16.

Savage, D. B., Agostini, M., Barroso, I., Gurnell, M., Luan, J., Meirhaeghe, A., Harding, A. H., Ihrke, G., Rajanayagam, O., Soos, M. A., *et al.* (2002). Digenic inheritance of severe insulin resistance in a human pedigree. *Nat Genet* 31, 379-384.

Savage, D. B., Sewter, C. P., Klenk, E. S., Segal, D. G., Vidal-Puig, A., Considine, R. V., and O'Rahilly, S. (2001). Resistin / Fizz3 expression in relation to obesity and peroxisome proliferator-activated receptor-gamma action in humans. *Diabetes* 50, 2199-2202.

Savage, D. B., Tan, G. D., Acerini, C. L., Jebb, S. A., Agostini, M., Gurnell, M., Williams, R. L., Umpleby, A. M., Thomas, E. L., Bell, J. D., *et al.* (2003). Human metabolic syndrome resulting from dominant-negative mutations in the nuclear receptor peroxisome proliferator-activated receptor-gamma. *Diabetes* 52, 910-917.

Schoonjans, K., Staels, B., and Auwerx, J. (1996). Role of the peroxisome proliferator-activated receptor (PPAR) in mediating the effects of fibrates and fatty acids on gene expression. *J Lipid Res* 37, 907-925.

Schoonjans, K., Watanabe, M., Suzuki, H., Mahfoudi, A., Krey, G., Wahli, W., Grimaldi, P., Staels, B., Yamamoto, T., and Auwerx, J. (1995). Induction of the acyl-coenzyme A synthetase gene by fibrates and fatty acids is mediated by a peroxisome proliferator response element in the C promoter. *J Biol Chem* 270, 19269-19276.

Schreiber-Agus, N., Chin, L., Chen, K., Torres, R., Rao, G., Guida, P., Skoultchi, A. I., and DePinho, R. A. (1995). An amino-terminal domain of Mx11 mediates anti-Myc oncogenic activity and interacts with a homolog of the yeast transcriptional repressor SIN3. *Cell* 80, 777-786.

Semple, R. K., Chatterjee, V. K., and O'Rahilly, S. (2006). PPARgamma and human metabolic disease. *J Clin Invest* 116, 581-589.

Shackleton, S., Lloyd, D. J., Jackson, S. N., Evans, R., Niermeijer, M. F., Singh, B. M., Schmidt, H., Brabant, G., Kumar, S., Durrington, P. N., *et al.* (2000). LMNA, encoding lamin A/C, is mutated in partial lipodystrophy. *Nat Genet* 24, 153-156.

Shibusawa, N., Hashimoto, K., Nikrodhanond, A. A., Liberman, M. C., Applebury, M. L., Liao, X. H., Robbins, J. T., Refetoff, S., Cohen, R. N., and Wondisford, F. E. (2003). Thyroid hormone action in the absence of thyroid hormone receptor DNA-binding in vivo. *J Clin Invest* 112, 588-597.

Shikama, N., Lyon, L., and La Thangue, N. B. (1997). The p300/CBP family: integrating signals with transcription factors and chromatin. *Trends Cell Biol* 7, 230-236.

Sibley, C. H., and Tomkins, G. M. (1974). Mechanisms of steroid resistance. *Cell* 2, 221-227.

Sluder, A. E., Mathews, S. W., Hough, D., Yin, V. P., and Maina, C. V. (1999). The nuclear receptor superfamily has undergone extensive proliferation and diversification in nematodes. *Genome Res* 9, 103-120.

- Sorbera, L. A., Leeson, P. A., Martin, L., and Castaner, J. (2001). Farglitazar. Antidiabetic PPAR $\gamma$  agonist. *Drugs of the Future* 26, 354-363.
- Speckman, R. A., Garg, A., Du, F., Bennett, L., Veile, R., Arioglu, E., Taylor, S. I., Lovett, M., and Bowcock, A. M. (2000). Mutational and haplotype analyses of families with familial partial lipodystrophy (Dunnigan variety) reveal recurrent missense mutations in the globular C-terminal domain of lamin A/C. *Am J Hum Genet* 66, 1192-1198.
- Spencer, T. E., Jenster, G., Burcin, M. M., Allis, C. D., Zhou, J., Mizzen, C. A., McKenna, N. J., Onate, S. A., Tsai, S. Y., Tsai, M. J., and O'Malley, B. W. (1997). Steroid receptor coactivator-1 is a histone acetyltransferase. *Nature* 389, 194-198.
- Steppan, C. M., Bailey, S. T., Bhat, S., Brown, E. J., Banerjee, R. R., Wright, C. M., Patel, H. R., Ahima, R. S., and Lazar, M. A. (2001). The hormone resistin links obesity to diabetes. *Nature* 409, 307-312.
- Steppan, C. M., and Lazar, M. A. (2002). Resistin and obesity-associated insulin resistance. *Trends Endocrinol Metab* 13, 18-23.
- Sundvold, H., and Lien, S. (2001). Identification of a novel peroxisome proliferator-activated receptor (PPAR) gamma promoter in man and transactivation by the nuclear receptor RORalpha1. *Biochem Biophys Res Commun* 287, 383-390.
- Suzuki, H., Willingham, M. C., and Cheng, S. Y. (2002). Mice with a mutation in the thyroid hormone receptor beta gene spontaneously develop thyroid carcinoma: a mouse model of thyroid carcinogenesis. *Thyroid* 12, 963-969.
- Suzuki, Y., Lanner, C., Kim, J. H., Vilardo, P. G., Zhang, H., Yang, J., Cooper, L. D., Steele, M., Kennedy, A., Bock, C. B., *et al.* (2001). Insulin control of glycogen metabolism in knockout mice lacking the muscle-specific protein phosphatase PP1G/RGL. *Mol Cell Biol* 21, 2683-2694.
- Szatmari, I., Gogolak, P., Im, J. S., Dezso, B., Rajnavolgyi, E., and Nagy, L. (2004). Activation of PPARgamma specifies a dendritic cell subtype capable of enhanced induction of iNKT cell expansion. *Immunity* 21, 95-106.
- Tagami, T., Madison, L. D., Nagaya, T., and Jameson, J. L. (1997). Nuclear receptor corepressors activate rather than suppress basal transcription of genes that are negatively regulated by thyroid hormone. *Molecular and Cellular Biology* 17, 2642-2648.
- Tagami, T., Park, Y., and Jameson, J. L. (1999). Mechanisms that mediate negative regulation of the thyroid-stimulating hormone alpha gene by the thyroid hormone receptor. *J Biol Chem* 274, 22345-22353.
- Tang, P. M., Bondor, J. A., Swiderek, K. M., and DePaoli-Roach, A. A. (1991). Molecular cloning and expression of the regulatory (RG1) subunit of the glycogen-associated protein phosphatase. *J Biol Chem* 266, 15782-15789.

- Tata, J. R. (1963). Inhibition of the biological action of thyroid hormones by actinomycin D and puromycin. *Nature* 197, 1167-1168.
- Tata, J. R., and Widnell, C. C. (1966). Ribonucleic acid synthesis during the early action of thyroid hormones. *Biochem J* 98, 604-620.
- Temple, K. A., Cohen, R. N., Wondisford, S. R., Yu, C., Deplewski, D., and Wondisford, F. E. (2005). An intact DNA-binding domain is not required for peroxisome proliferator-activated receptor gamma (PPARgamma) binding and activation on some PPAR response elements. *J Biol Chem* 280, 3529-3540.
- Terauchi, Y., Iwamoto, K., Tamemoto, H., Komeda, K., Ishii, C., Kanazawa, Y., Asanuma, N., Aizawa, T., Akanuma, Y., Yasuda, K., *et al.* (1997). Development of non-insulin-dependent diabetes mellitus in the double knockout mice with disruption of insulin receptor substrate-1 and beta cell glucokinase genes. Genetic reconstitution of diabetes as a polygenic disease. *J Clin Invest* 99, 861-866.
- Thomas, E. L., Saeed, N., Hajnal, J. V., Brynes, A., Goldstone, A. P., Frost, G., and Bell, J. D. (1998). Magnetic resonance imaging of total body fat. *J Appl Physiol* 85, 1778-1785.
- Thompson, C. C., Weinberger, C., Lebo, R., and Evans, R. M. (1987). Identification of a novel thyroid hormone receptor expressed in the mammalian central nervous system. *Science* 237, 1610-1614.
- Thorpe, K. L., Schafer, A. J., Genin, E., Trowsdale, J., and Beck, S. (1999). Detection of polymorphism in the RING3 gene by high-throughput fluorescent SSCP analysis. *Immunogenetics* 49, 256-265.
- Tone, Y., Collingwood, T. N., Adams, M., and Chatterjee, V. K. K. (1994). Functional analysis of a transactivation domain in the thyroid hormone  $\beta$  receptor. *Journal of Biological Chemistry* 269, 31157-31161.
- Tontonoz, P., Hu, E., Devine, J., Beale, E. G., and Spiegelman, B. M. (1995). PPAR gamma 2 regulates adipose expression of the phosphoenolpyruvate carboxykinase gene. *Mol Cell Biol* 15, 351-357.
- Tontonoz, P., Hu, E., Graves, R. A., Budavari, A. I., and Spiegelman, B. M. (1994a). mPPAR $\gamma$ 2: tissue-specific regulator of an adipocyte enhancer. *Genes and Development* 8, 1224-1234.
- Tontonoz, P., Hu, E., and Spiegelman, B. M. (1994b). Stimulation of adipogenesis in fibroblasts by PPAR $\gamma$ 2, a lipid-activated transcription factor. *Cell* 79, 1147-1156.
- Tontonoz, P., Singer, S., Forman, B. M., Sarraf, P., Fletcher, J. A., Fletcher, C. D., Brun, R. P., Mueller, E., Altiock, S., Oppenheim, H., *et al.* (1997). Terminal differentiation of human liposarcoma cells induced by ligands for peroxisome proliferator-activated receptor gamma and the retinoid X receptor. *Proceedings of the National Academy of Sciences, USA* 94, 237-241.

- Torchia, J., Rose, D. W., Inostroza, J., Kamei, Y., Westin, S., Glass, C. K., and Rosenfeld, M. G. (1997). The transcriptional co-activator p/CIP binds CBP and mediates nuclear-receptor function [see comments]. *Nature* 387, 677-684.
- Torres-Arzayus, M. I., Font de Mora, J., Yuan, J., Vazquez, F., Bronson, R., Rue, M., Sellers, W. R., and Brown, M. (2004). High tumor incidence and activation of the PI3K/AKT pathway in transgenic mice define AIB1 as an oncogene. *Cancer Cell* 6, 263-274.
- Tsai, Y. S., Kim, H. J., Takahashi, N., Kim, H. S., Hagaman, J. R., Kim, J. K., and Maeda, N. (2004). Hypertension and abnormal fat distribution but not insulin resistance in mice with P465L PPARgamma. *J Clin Invest* 114, 240-249.
- Tzamelis, I., Fang, H., Ollero, M., Shi, H., Hamm, J. K., Kievit, P., Hollenberg, A. N., and Flier, J. S. (2004). Regulated production of a peroxisome proliferator-activated receptor-gamma ligand during an early phase of adipocyte differentiation in 3T3-L1 adipocytes. *J Biol Chem* 279, 36093-36102.
- Uppenberg, J., Svensson, C., Jaki, M., Bertilsson, G., Jendeberg, L., and Berkenstam, A. (1998). Crystal structure of the ligand binding domain of the human nuclear receptor PPARgamma. *J Biol Chem* 273, 31108-31112.
- Usala, S. J., Bale, A. E., Gesundheit, N., Weinberger, C., Lash, R. W., Wondisford, F. E., McBride, O. W., and Weintraub, B. D. (1988). Tight linkage between the syndrome of generalized thyroid hormone resistance and the human c-erbA  $\beta$  gene. *Molecular Endocrinology* 2, 1217-1220.
- Varanasi, U., Chu, R., Huang, Q., Castellon, R., Yeldandi, A. V., and Reddy, J. K. (1996). Identification of a peroxisome proliferator-responsive element upstream of the human peroxisomal fatty acyl coenzyme A oxidase gene. *J Biol Chem* 271, 2147-2155.
- Wada, K., Nakajima, A., Katayama, K., Kudo, C., Shibuya, A., Kubota, N., Terauchi, Y., Tachibana, M., Miyoshi, H., Kamisaki, Y., *et al.* (2006). Peroxisome proliferator-activated receptor gamma-mediated regulation of neural stem cell proliferation and differentiation. *J Biol Chem* 281, 12673-12681.
- Wade, P. A., and Wolffe, A. P. (1999). Transcriptional regulation: SWItching circuitry. *Curr Biol* 9, R221-224.
- Wagner, R. L., Apriletti, J. W., McGrath, M. E., West, B. L., Baxter, J. D., and Fletterick, R. J. (1995). A structural role for hormone in the thyroid hormone receptor. *Nature* 378, 690-697.
- Walker, A. B., Chattington, P. D., Buckingham, R. E., and Williams, G. (1999). The thiazolidinedione rosiglitazone (BRL-49653) lowers blood pressure and protects against impairment of endothelial function in Zucker fatty rats. *Diabetes* 48, 1448-1453.

- Wang, Z., Benoit, G., Liu, J., Prasad, S., Aarnisalo, P., Liu, X., Xu, H., Walker, N. P., and Perlmann, T. (2003). Structure and function of Nurr1 identifies a class of ligand-independent nuclear receptors. *Nature* 423, 555-560.
- Watkins, R. E., Wisely, G. B., Moore, L. B., Collins, J. L., Lambert, M. H., Williams, S. P., Willson, T. M., Klierer, S. A., and Redinbo, M. R. (2001). The human nuclear xenobiotic receptor PXR: structural determinants of directed promiscuity. *Science* 292, 2329-2333.
- Webb, P., Anderson, C. M., Valentine, C., Nguyen, P., Marimuthu, A., West, B. L., Baxter, J. D., and Kushner, P. J. (2000). The nuclear receptor corepressor (N-CoR) contains three isoleucine motifs (I/LXXII) that serve as receptor interaction domains (IDs). *Mol Endocrinol* 14, 1976-1985.
- Weinberger, C., Thompson, C. C., Ong, E. S., Lebo, R., Gruol, D. J., and Evans, R. M. (1986). The c-erb-A gene encodes a thyroid hormone receptor. *Nature* 324, 641-646.
- Weiss, R. E., Hayashi, Y., Nagaya, T., Petty, K. J., Murata, Y., Tunca, H., Seo, H., and Refetoff, S. (1996). Dominant inheritance of resistance to thyroid hormone not linked to defects in the thyroid hormone receptor  $\alpha$  or  $\beta$  genes may be due to a defective cofactor. *Journal of Clinical Endocrinology and Metabolism* 81, 4196-4203.
- Weiss, R. E., Weinberg, M., and Refetoff, S. (1993). Identical mutations in unrelated families with generalized resistance to thyroid hormone occur in cytosine-guanine-rich areas of the thyroid hormone receptor  $\beta$  gene. *Journal of Clinical Investigation* 91, 2408-2415.
- Weiss, R. E., Xu, J., Ning, G., Pohlenz, J., O'Malley, B. W., and Refetoff, S. (1999). Mice deficient in the steroid receptor coactivator 1 (SRC-1) are resistant to thyroid hormone. *EMBO Journal* 18, 1900-1904.
- Wikstrom, L., Johansson, C., Salto, C., Barlow, C., Campos-Barros, A., Baas, F., Forrest, D., Thoren, P., and Vennstrom, B. (1998). Abnormal heart rate and body temperature in mice lacking thyroid hormone receptor  $\alpha$ 1. *EMBO Journal* 17, 455-461.
- Williams, G. R. (2000). Cloning and characterization of two novel thyroid hormone receptor beta isoforms. *Mol Cell Biol* 20, 8329-8342.
- Willson, T. M., Brown, P. J., Sternbach, D. D., and Henke, B. R. (2000). The PPARs: from orphan receptors to drug discovery. *J Med Chem* 43, 527-550.
- Wondisford, F. E., Steinfelder, H. J., Nations, M., and Radovick, S. (1993). AP-1 antagonizes thyroid hormone receptor action on the thyrotropin beta-subunit gene. *J Biol Chem* 268, 2749-2754.

Wong, R., Vasilyev, V. V., Ting, Y.-T., Kutler, D. I., Willingham, M. C., Weintraub, B. D., and Cheng, S.-Y. (1997). Transgenic mice bearing a human mutant thyroid hormone  $\beta$ 1 receptor manifest thyroid function anomalies, weight reduction and hyperactivity. *Molecular Medicine* 3, 303-314.

Wu, C. (1997). Chromatin remodeling and the control of gene expression. *J Biol Chem* 272, 28171-28174.

Wu, Y., Chin, W. W., Wang, Y., and Burris, T. P. (2003). Ligand and coactivator identity determines the requirement of the charge clamp for coactivation of the peroxisome proliferator-activated receptor gamma. *J Biol Chem* 278, 8637-8644.

Wu, Z., Xie, Y., Morrison, R. F., Bucher, N. L., and Farmer, S. R. (1998). PPARgamma induces the insulin-dependent glucose transporter GLUT4 in the absence of C/EBPalpha during the conversion of 3T3 fibroblasts into adipocytes. *J Clin Invest* 101, 22-32.

Xu, H. E., Stanley, T. B., Montana, V. G., Lambert, M. H., Shearer, B. G., Cobb, J. E., McKee, D. D., Galardi, C. M., Plunket, K. D., Nolte, R. T., *et al.* (2002). Structural basis for antagonist-mediated recruitment of nuclear co-repressors by PPAR $\alpha$ . *Nature* 415, 813-817.

Xu, P. L., Shan, S. F., Kong, Y. Y., Xie, Y. H., and Wang, Y. (2003). Characterization of a strong repression domain in the hinge region of orphan nuclear receptor hB1F/hLRH-1. *Sheng Wu Hua Xue Yu Sheng Wu Wu Li Xue Bao (Shanghai)* 35, 909-916.

Yamashita, D., Yamaguchi, T., Shimizu, M., Nakata, N., Hirose, F., and Osumi, T. (2004). The transactivating function of peroxisome proliferator-activated receptor gamma is negatively regulated by SUMO conjugation in the amino-terminal domain. *Genes Cells* 9, 1017-1029.

Yamauchi, T., Waki, H., Kamon, J., Murakami, K., Motojima, K., Komeda, K., Miki, H., Kubota, N., Terauchi, Y., Tsuchida, A., *et al.* (2001). Inhibition of RXR and PPARgamma ameliorates diet-induced obesity and type 2 diabetes. *J Clin Invest* 108, 1001-1013.

Ye, J. M., Dzamko, N., Cleasby, M. E., Hegarty, B. D., Furler, S. M., Cooney, G. J., and Kraegen, E. W. (2004). Direct demonstration of lipid sequestration as a mechanism by which rosiglitazone prevents fatty-acid-induced insulin resistance in the rat: comparison with metformin. *Diabetologia* 47, 1306-1313.

Yeh, S., and Chang, C. (1996). Cloning and characterization of a specific coactivator, ARA70, for the androgen receptor in human prostate cells. *Proc Natl Acad Sci U S A* 93, 5517-5521.

Yen, P. M. (2003). Molecular basis of resistance to thyroid hormone. *Trends Endocrinol Metab* 14, 327-333.



Yen, P. M., Darling, D. S., Carter, R. L., Forgoine, M., Umeda, P. M., and Chin, W. W. (1992). Triiodothyronine (T3) decreases binding to DNA by T3-receptor homodimers but not receptor auxiliary protein heterodimers. *Journal of Biological Chemistry* 267, 3565-3568.

Yen, P. M., Wilcox, E. C., Hayashi, Y., Refetoff, S., and Chin, W. W. (1995). Studies on the repression of basal transcription (silencing) by artificial and natural human thyroid hormone receptor- $\beta$  mutants. *Endocrinology* 136, 2845-2851.

Ying, H., Furuya, F., Willingham, M. C., Xu, J., O'Malley, B. W., and Cheng, S. Y. (2005). Dual functions of the steroid hormone receptor coactivator 3 in modulating resistance to thyroid hormone. *Mol Cell Biol* 25, 7687-7695.

Yoh, S. M., Chatterjee, V. K. K., and Privalsky, M. L. (1997). Thyroid hormone resistance syndrome manifests as an aberrant interaction between mutant T3 receptors and transcriptional corepressors. *Molecular Endocrinology* 11, 470-480.

Young, P. W., Cawthorne, M. A., Coyle, P. J., Holder, J. C., Holman, G. D., Kozka, I. J., Kirkham, D. M., Lister, C. A., and Smith, S. A. (1995). Repeat treatment of obese mice with BRL49653, a new and potent insulin sensitizer, enhances insulin action in white adipocytes: Association with increased insulin binding and cell-surface GLUT4 as measured by photoaffinity labelling. *Diabetes* 44, 1087-1092.

Yuan, C. X., Ito, M., Fondell, J. D., Fu, Z. Y., and Roeder, R. G. (1998). The TRAP220 component of a thyroid hormone receptor-associated protein (TRAP) coactivator complex interacts directly with nuclear receptors in a ligand-dependent fashion [published erratum appears in *Proc Natl Acad Sci U S A* 1998 Nov 24;95(24):14584]. *Proc Natl Acad Sci U S A* 95, 7939-7944.

Zamir, I., Zhang, J., and Lazar, M. A. (1997). Stoichiometric and steric principles governing repression by nuclear hormone receptors. *Genes and Development* 11, 835-846.

Zhang, J., Fu, M., Cui, T., Xiong, C., Xu, K., Zhong, W., Xiao, Y., Floyd, D., Liang, J., Li, E., *et al.* (2004). Selective disruption of PPAR $\gamma$  2 impairs the development of adipose tissue and insulin sensitivity. *Proc Natl Acad Sci U S A* 101, 10703-10708.

Zhang, J., Zamir, I., and Lazar, M. A. (1997). Differential recognition of liganded and unliganded thyroid hormone receptor by retinoid X receptor regulates transcriptional repression. *Molecular and Cellular Biology* 17, 6887-6897.

Zhang, X., Jeyakumar, M., and Bagchi, M. K. (1996). Ligand-dependent cross-talk between steroid and thyroid hormone receptors. Evidence for common transcriptional coactivator(s). *J Biol Chem* 271, 14825-14833.

Zhang, X. K., Hoffmann, B., Tran, P. B., Graupner, G., and Pfahl, M. (1992). Retinoid X receptor is an auxiliary protein for thyroid hormone and retinoic acid receptors. *Nature* 355, 441-446.

## APPENDIX

### PUBLICATIONS

**Agostini M.**, Schoenmakers E., Mitchell C., Szatmari I., Savage D., Smith A., Rajanayagam O., Semple R., Luan J., Bath L., Zalin A., Labib M., Kumar S., Simpson H., Blom D., Marais D., Schwabe J, Barroso I., Trembath R., Wareham N., Nagy L., Gurnell M., O'Rahilly S., Chatterjee K. (2006). Non-DNA binding, dominant-negative, human PPAR $\gamma$  mutations cause lipodystrophic insulin resistance. **Cell Metabolism** (4), 1–9.

Baris I., Arisoy A.E, Smith A., **Agostini M.**, Mitchell C.S., Park S.M., Halefoglu A., Zengin E., Chatterjee V.K., Battaloglu E. (2006). A novel missense mutation in human TTF-2 (FKHL15) gene associated with congenital hypothyroidism but not athyreosis **J Clin Endocrin Metab** 91 (10), 4183-7.

**Agostini M.**, Gurnell M., Savage D.B., Wood E., Smith A., Rajanayagam O., Garnes K.T., Levinson S.H., Xu H.E., Schwabe J.W., Willson T.M., O'Rahilly S., Chatterjee V.K. (2004). Tyrosine agonists reverse the molecular defects associated with dominant-negative mutations in human peroxisome proliferator-activated receptor  $\gamma$ . **Endocrinology** 145 (4), 1527-1538.

Savage D.B., Tan G.D., Acerini C.L., Jebb S.A., **Agostini M.**, Gurnell M., Williams R.L., Umpleby A.M., Thomas E.L., Bell J.D., Dixon A.K., Dunne F., Boiani R., Cinti S., Vidal-Puig A., Karpe F., Chatterjee V.K., O'Rahilly S. (2003). Human metabolic syndrome resulting from dominant negative mutations in the nuclear receptor peroxisome proliferator-activated receptor gamma. **Diabetes** 52 (4), 910-917.

**Agostini M.**, Savage D.B., Barroso I., Gurnell M., Luan J., Meirhaeghe A., Harding A.H., Ihrke G., Rajanayagam O., Soos M.A., George S., Berger D., Thomas E.L., Bell J.D., Meeran K., Ross R.J., Vidal-Puig A., Wareham N.J., O'Rahilly S., Chatterjee V.K., Schafer A.J. (2002). Digenic inheritance of severe insulin resistance in a human pedigree. **Nature Genetics** 31, 379-384.

Canale D., **Agostini M.**, Giorgilli G., Caglieresi C., Scartabelli G., Nardini V., Jannini E.A., Martino E., Pinchera A., Macchia E. (2001). Thyroid hormone receptors in neonatal, prepubertal, and adult rat testis. **Journal of Andrology** 22, 284-288.

Wentworth J.M., **Agostini M.**, Love J., Schwabe J.W., Chatterjee V.K.K.(2000). St John's wort, a herbal antidepressant, activates the steroid X receptor. **Journal of Endocrinology** 166, R11-R16.

Gurnell M., Wentworth J.M., **Agostini M.**, Adams M., Collingwood T.N., Provenzano C., Browne P.O., Rajanayagam O., Burriss T.P., Schwabe J.W., Lazar M.A., Chatterjee V.K.K. (2000). A dominant-negative peroxisome proliferator-activated receptor  $\gamma$  (PPAR $\gamma$ ) mutant is a constitutive repressor and inhibits PPAR $\gamma$ -mediated adipogenesis. **Journal of Biological Chemistry** 275, (8) 5754-5759.

Barroso I., Gurnell M., Crowley V.E.F., **Agostini M.**, Schwabe J.W., Soos M.A., Maslen G.L.I., Williams T.D.M., Lewis H., Schafer A.J., Chatterjee V.K.K., O’Rahilly S. (1999). Dominant negative mutations in human PPAR $\gamma$  are associated with severe insulin resistance, diabetes mellitus and hypertension. **Nature** 402, 880-883.

**Agostini M.**, Gurnell M., Rajanayagam O., Clifton-Bligh R.J.D., Wang T., Zelissen P.M.J., Van Der Horst F., Van De Wiel A., Macchia E., Pinchera A., Schwabe J.W.R., Chatterjee V.K.K. (1999). Three novel mutations at serine 314 in the thyroid hormone  $\beta$  receptor differentially impair ligand binding in the syndrome of resistance to thyroid hormone. **Endocrinology** 140 (12), 5901-5906.

Colligwood T.N., Wagner R., Mattheus C.H., Clifton-Bligh R.J., Gurnell M., Rajanayagam O., **Agostini M.**, Fletterick J., Beck-Peccoz P., Reinhardt W., Binder G., Ranke M.B., Hermus A., Hesh R.D., Lazarus J., Newrick P., Parfitt V., Raggatt P., Zegher F., Chatterjee V.K.K. (1998). A role for helix 3 of the TR $\beta$  ligand-binding domain in coactivator recruitment identified by characterisation of a third cluster of mutations in resistance to thyroid hormone. **EMBO Journal** 17 (16), 4760-4770.

**I attended and presented my work at the following conferences:**

- 1999 26<sup>th</sup> Annual Meeting of the European Thyroid Association (Milan, Italy) - **oral presentation**
- 2000 Nuclear Receptors 2000 (Steamboat Spring, Colorado) - **poster**
- 2000 11<sup>th</sup> International Congress of Endocrinology (Sydney, Australia) - **poster**
- 2000 Departmental Research Day, (Hinxton Hall, UK) - **oral presentation**
- 2000 1<sup>st</sup> European Nuclear Receptor Net-Work (Debrecen, Hungary)
- 2001 The PPARs: A transcription odyssey (Keystone, Colorado) -**poster**
- 2001 First International Symposium "PPARs: from basic science to clinical application". (Florence, Italy)
- 2001 5<sup>th</sup> Workshop on Resistance to Thyroid Hormone (Verbania, Italy)
- 2001 5<sup>th</sup> European Congress of Endocrinology (Turin, Italy) - **poster**
- 2001 Nuclear Receptor in Health and Disease (Mont Ste Odile, Alsace)
- 2001 2<sup>nd</sup> European Nuclear Receptor Net-Work (Strasbourg, France)
- 2001 Departmental Research Day, (Hinxton Hall, UK)
- 2002 Autumn Meeting of the Medical Research Society (London, UK) - **oral presentation**
- 2002 Nuclear Receptor Superfamily (Snowbird, Utah) - **poster**
- 2002 3<sup>rd</sup> European Nuclear Receptor Net-Work (Cambridge, UK) - **oral presentation**
- 2003 PPARs: Transcriptional Regulators of Metabolism and Metabolic Disease (Keystone, Colorado) - **poster**
- 2003 Second International Symposium "PPARs: from basic science to clinical application". (Florence, Italy) - **oral presentation**
- 2003 CIMR Research Retreat (Hinxton Hall, UK)
- 2003 British Endocrine Societies (Glasgow, UK) - **oral presentation**
- 2003 4<sup>th</sup> European Nuclear Receptor Net-Work (Stockholm, Sweden) – **oral presentation**

- 2004 Nuclear Receptor: Orphan Brothers (Keystone, Colorado) - **poster**
- 2004 Departmental Research Day, (Hinxton Hall, UK)
- 2004 23rd Joint Meeting of the British Endocrine Societies (Brighton, UK) - **poster**
- 2004 Biosciences Post-Grad Club Seminars (University of Hertfordshire, UK) – **oral presentation**
- 2004 5<sup>th</sup> European Nuclear Receptor Net-Work (Debrecen, Hungary)
- 2005 PPAR/LXR (Whistler, Canada) - **poster**
- 2005 CIMR Research Retreat (Hinxton Hall, UK) - **poster**
- 2005 Nuclear Receptors from Chromatin to Disease (EMBO Conference, Lake of Garda, Italy) - **poster**
- 2005 Departmental Research Day, (Hinxton Hall, UK)
- 2006 CIMR Research Retreat (Hinxton Hall, UK)
- 2006 Departmental Research Day, (Hinxton Hall, UK)
- 2007 Department of Internal Medicine Seminars (University of Cape Town, SA) - **oral presentation**
- 2007 Nuclear Receptors Pathways to Metabolic Regulation (Steamboat Springs, Colorado) - **poster**

I have also attended and presented at the Research Seminars of the Cambridge Institute for Diabetes, Endocrinology and Metabolism.

I regularly attend the journal club once every two weeks and seminars related to my work at the Cambridge Institute for Medical Research.

*Publications arising from this thesis*

# Three Novel Mutations at Serine 314 in the Thyroid Hormone $\beta$ Receptor Differentially Impair Ligand Binding in the Syndrome of Resistance to Thyroid Hormone\*

M. GURNELL†‡, O. RAJANAYAGAM†, M. AGOSTINI†§, R. J. D. CLIFTON-BLIGH||, T. WANG, P. M. J. ZELISSEN, F. VAN DER HORST, A. VAN DE WIEL, E. MACCHIA, A. PINCHERA, J. W. R. SCHWABE, AND V. K. K. CHATTERJEE

*Department of Medicine, University of Cambridge, Addenbrooke's Hospital (M.G., O.R., M.A., R.J.D.C.-B., V.K.K.C.), Cambridge, United Kingdom CB2 2QQ; the Dipartimento di Endocrinologia e Metabolismo, Università di Pisa (M.A., E.M., A.P.), 56124 Pisa, Italy; the Department of Clinical Biochemistry, Leicester Royal Infirmary (T.W.), Leicester, United Kingdom LE1 5WW; the Department of Endocrinology, University Hospital (P.M.J.Z.), Utrecht, The Netherlands; the Department of Clinical Chemistry, Eemland Hospital (F.v.d.H.), 3800 BM Amersfoort, The Netherlands; and the Medical Research Council Laboratory of Molecular Biology (J.W.R.S.), Cambridge, United Kingdom CB2 2QH; Department of Endocrinology (Ar.d.W), Eemland Hospital, 3800 BM Amersfoort, The Netherlands*

## ABSTRACT

The syndrome of resistance to thyroid hormone is associated with diverse mutations in the ligand-binding domain of the thyroid hormone  $\beta$  receptor, localizing to three clusters around the hormone binding cavity. Here, we report three novel resistance to thyroid hormone mutations (S314C, S314F, and S314Y), due to different nucleotide substitutions in the same codon, occurring in six separate families. Functional characterization of these mutant receptors showed marked differences in their properties. S314F and S314Y receptor mutants exhibited significant transcriptional impairment in keeping with negligible ligand binding and were potent dominant

negative inhibitors of wild-type receptor action. In contrast, the S314C mutant bound ligand with reduced affinity, such that its functional impairment and dominant negative activity manifest at low concentrations of thyroid hormone, but are more reversible at higher  $T_3$  concentrations. The degree of functional impairment of mutant receptors *in vitro* may correlate with the magnitude of thyroid dysfunction *in vivo*. Modelling these mutations using the crystal structure of thyroid hormone receptor  $\beta$  shows why ligand binding is perturbed and why the phenylalanine/tyrosine mutations are more deleterious than cysteine. (*Endocrinology* 140: 5901–5906, 1999)

RECOGNITION that the syndrome of resistance to thyroid hormone (RTH) is linked to the thyroid hormone  $\beta$  receptor (TR $\beta$ ) gene locus (1) has led to the identification of an increasing number of natural mutations whose functional characterization has provided important insights into structure-function relationships in this receptor. RTH is characterized by elevated serum free thyroid hormones (FT<sub>4</sub> and FT<sub>3</sub>) in the presence of unsuppressed TSH levels, reflecting resistance to the normal negative feedback mechanisms within the hypothalamus and pituitary (2). The degree of resistance within peripheral tissues determines whether thyrotoxic clinical features are associated with the condition (3). An autosomal dominant mode of inheritance, in conjunction with the recognition that receptor mutants are functionally impaired, has led to the proposal that these abnormal pro-

teins are able to inhibit the function of their wild-type (WT) counterparts in a dominant negative manner (4, 5). Such dominant negative inhibition requires the preservation of DNA-binding and heterodimerization functions in mutant receptors (6–8), consonant with the observation that no RTH mutants have hitherto been reported in the DNA-binding or dimerization domains of TR $\beta$ . In fact the majority of natural mutations cluster around the ligand binding pocket (9) and impair hormone binding.

Here we describe three novel single nucleotide substitutions in TR $\beta$  associated with RTH that result in different missense mutations at residue 314 (S314C, S314F, and S314Y). Examination of the crystal structure of TR $\beta$  suggests that Ser<sup>314</sup> plays a structural role in ligand binding. Functional characterization of the natural mutants allowed us to study how the different amino acid substitutions at this position affected receptor function. Although all the mutations affected ligand binding, there were significant differences in the extent of the alteration with corresponding variation in their transcriptional and dominant negative properties.

## Materials and Methods

### Clinical and genetic analyses

Serum FT<sub>4</sub> and FT<sub>3</sub> levels were measured with a Delfia fluoroimmunoassay (Wallac, Inc., Milton Keynes, UK). TSH levels were

Received May 13, 1999.

Address all correspondence and requests for reprints to: Dr. V. K. K. Chatterjee, Department of Medicine, University of Cambridge, Level 5, Addenbrooke's Hospital, Hills Road, Cambridge, United Kingdom CB2 2QQ. E-mail:kkc1@mole.bio.cam.ac.uk.

\* This work was supported by the Wellcome Trust.

† M.G., O.R., and M.A. contributed equally to this work.

‡ Wellcome Training Fellow.

§ Supported by a British Council-Centro Nazionale Recherche grant.

|| Commonwealth Foundation Research Scholar.

determined with a sensitive second generation assay (Delfia, Wallac, Inc.). The coefficient of variation was less than 10% in all instances.

Genomic DNA was extracted from peripheral blood leukocytes using standard techniques. Exons 7–10 of TR $\beta$ 1 from each index case were amplified by PCR using intronic primers and sequenced as previously described (10). Each mutation was verified in three independent reactions, and other family members were screened for the presence of the identified mutation.

### Plasmid constructs

Receptor mutations were generated by site-directed mutagenesis of WT human TR $\beta$ 1 complementary DNA and confirmed by direct sequencing as reported previously (6). Both wild-type and mutant receptors were subcloned into pGEM7z and the eukaryotic expression vector RSV (containing the Rous sarcoma virus enhancer and promoter) for *in vitro* and *in vivo* studies, respectively. For functional assays, a reporter gene containing a direct repeat thyroid response element (TRE) spaced by four nucleotides (DR+4) from the malic enzyme gene upstream of the thymidine kinase promoter and luciferase (MAL-TKLUC) was cotransfected with receptor expression vectors and a  $\beta$ -galactosidase reference plasmid (Bos- $\beta$ gal) as described previously (6).

### Hormone and DNA binding assays

Receptor proteins were synthesized by coupled transcription and translation (Promega Corp., Southampton, UK). T<sub>3</sub> binding affinities were determined using a modification of a filter assay, and binding affinity constants (K<sub>a</sub>) were calculated using Scatchard analyses from three separate experiments on independently generated protein samples (11).

Receptor binding to DNA was assessed by electrophoretic mobility shift assays using *in vitro* translated receptors quantitated by SDS-PAGE analysis and a <sup>32</sup>P-labeled oligonucleotide duplex corresponding to an everted repeat (F2) TRE from the chick lysozyme gene. TR exhibits both homodimeric and heterodimeric [with the retinoid X receptor (RXR)] binding to this TRE, with dissociation of the homodimer on addition of ligand. Details of the oligonucleotide duplex sequences and reaction conditions have been described previously (6).

### Cell culture and transient transfection assays

JEG-3 (human choriocarcinoma) cells were grown in Optimem containing 2% (vol/vol) FCS and 1% (vol/vol) penicillin, streptomycin, and

fungizone (Life Technologies, Inc., Paisley, Scotland). Eighteen hours before transfection the medium was changed to Optimem with 2% charcoal-stripped FCS. Twenty-four-well plates of cells were transfected by a 5-h exposure to calcium phosphate containing the reporter plasmid MAL-TKLUC (500 ng), TR $\beta$ 1 expression vectors (50 ng), and the internal control plasmid Bos- $\beta$ gal (200 ng). After an additional 36 h, cells were lysed, and extracts were assayed for luciferase and  $\beta$ -galactosidase activity using standard methods (11).

## Results

### Clinical and genetic analyses

The clinical features and biochemistry in six families with RTH are shown in Table 1. All patients exhibited thyroid function tests characteristic of RTH: namely, elevated serum free T<sub>4</sub> and free T<sub>3</sub> with an inappropriately normal TSH. Although index cases presented with goiter or thyrotoxic symptoms, most affected family members were asymptomatic and were detected by screening. One patient (no. IV) first presented with Graves' disease, but subsequent thyroid function tests in remission were consistent with RTH. Direct sequencing of exons 7–10 of TR $\beta$ 1 of index cases showed that each individual was heterozygous for a single nucleotide substitution at codon 314 in exon 9. A single nucleotide change in the WT sequence TCC (serine), corresponding to a missense mutation, was noted in each family: cases I, II, and III, TTC (phenylalanine)-S314F; cases IV and V, TAC (tyrosine)-S314Y; and case VI, TGC (cysteine)-S314C. There was complete concordance between the presence of a receptor defect and the abnormal biochemistry associated with RTH, suggesting that these receptor abnormalities were highly likely to be causative.

### Hormone and DNA binding

All natural mutations in TR $\beta$  cluster in the ligand binding domain, and consequently, the majority exhibit reduced hormone binding. Accordingly, each mutation was introduced

**TABLE 1.** Biochemical and genetic data from six RTH families

Case <sup>a</sup>	Age (yr)/sex	Clinical features <sup>b</sup>	FT <sub>4</sub> (9.0–20 pmol/liter)	FT <sub>3</sub> (3.0–7.5 pmol/liter)	TSH (0.4–4.0 mU/liter)	Nucleotide change	Codon change <sup>c</sup>
I	35/F	Goiter, thyrotoxic	24	6.4 <sup>d</sup>	2.3	1226 TCC to TTC	S314F
I.I f	69/M	Asymptomatic	21	4.7 <sup>e</sup>	2.6	1226 TCC to TTC	S314F
I.II b	31/M	Asymptomatic	28	9.5	5.1	1226 TCC to TTC	S314F
I.III s	28/F	Asymptomatic	24	8.5	2.1	1226 TCC to TTC	S314F
I.IV b	33/M	Asymptomatic	36	12	0.9	1226 TCC to TTC	S314F
II	37/M	Goiter	37	11	0.6	1226 TCC to TTC	S314F
II.I so	5/M	Goiter, otitis media	38	15	3.0	1226 TCC to TTC	S314F
III	51/M	Asymptomatic	41	13	1.0	1226 TCC to TTC	S314F
IV <sup>f</sup>	47/F	AITD	28	13	1.5	1226 TCC to TAC	S314Y
IV.I so	29/M	Asymptomatic	34	17	1.9	1226 TCC to TAC	S314Y
IV.II b	48/M	Asymptomatic	23	9.4	1.2	1226 TCC to TAC	S314Y
IV.III n	10/F	Failure to thrive, ADHD	55	16	2.3	1226 TCC to TAC	S314Y
V <sup>g</sup>	51/F	Goiter	30	11	6.1	1226 TCC to TAC	S314Y
V.I so	13/M	Asymptomatic	48	17	1.1	1226 TCC to TAC	S314Y
VI	26/F	Goiter, anxiety, palpitations	24	9	1.5	1226 TCC to TGC	S314C
VI.I b	40/M	Goiter, anxiety, palpitations	25	11	1.3	1226 TCC to TGC	S314C
VI.II m	63/F	Goiter, anxiety, palpitations	25	9	0.9	1226 TCC to TGC	S314C

<sup>a</sup> Index case and affected relatives: f, father; m, mother; so, son; s, sister; b, brother; n, niece.

<sup>b</sup> ADHD, Attention deficit hyperactivity disorder; AITD, autoimmune thyroid disease.

<sup>c</sup> Codon nomenclature based on a predicted protein sequence of 1–461 residues (22).

<sup>d</sup> Free T<sub>3</sub> on other occasions, 10.7, 8.0, and 8.3.

<sup>e</sup> Free T<sub>3</sub> on another occasion, 9.5.

<sup>f</sup> Thyroid function tests when AITD in remission.

<sup>g</sup> Subtotal thyroidectomy, no thyroid hormone replacement therapy.



into the WT TR $\beta$ 1 complementary DNA, and *in vitro* synthesized proteins were assayed for binding of [ $^{125}$ I]T $_3$ . As expected from their location within the ligand binding domain, mutant receptors demonstrated impaired binding compared with wild-type receptor. Scatchard analyses indicated that their ligand affinities were reduced with a marked difference in the magnitude of the abnormality between mutations. Thus, in comparison with a wild-type  $K_a$  ( $\pm$ SEM) of  $0.68 \times 10^{10} \text{ M}^{-1}$  (0.11), the S314C mutant bound ligand with a slightly reduced affinity [ $K_a$ ,  $0.48 \times 10^{10}$  (0.07)  $\text{M}^{-1}$ ]. In contrast, with the S314F and S314Y mutant receptor proteins no specific radiolabeled T $_3$  binding was detected, suggesting a marked ligand binding defect.

Previous studies have shown that TR is able to bind DNA as both a homodimer and a heterodimer with RXR and that homodimeric complexes dissociate after binding of ligand (12). We tested homo- and heterodimeric binding of WT and mutant receptors using an everted repeat TRE configuration and hypothesized that mutant receptor homodimer dissociation would be variably altered depending on the degree of impairment in hormone binding. In the absence of ligand, WT receptor formed homo- and heterodimer complexes and after the addition of 100 nM T $_3$ , the homodimer complex dissociated readily (Fig. 1). In comparison, the addition of 100 nM T $_3$  resulted in a differential displacement of ho-

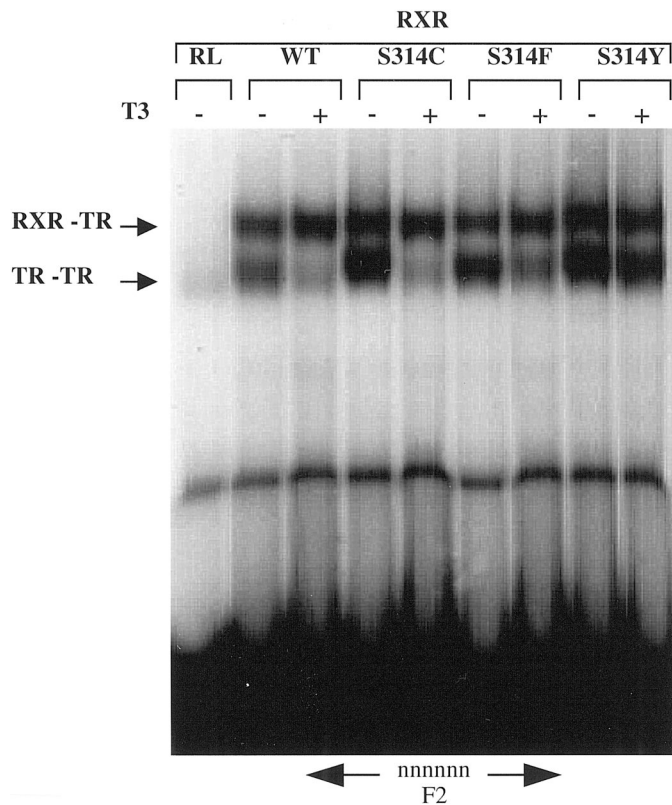


FIG. 1. Differential dissociation of TR $\beta$  homodimers in response to T $_3$  on the F2 everted repeat TRE. Using an electrophoretic mobility supershift assay, *in vitro* translated TR $\beta$  (WT or mutants: S314C, S314F, and S314Y) and RXR were coincubated with the chick lysozyme F2 TRE in the absence or presence of T $_3$  (100 nM). Complexes were resolved by PAGE. The locations of homodimer (TR-TR) and heterodimer (RXR-TR) complexes are indicated.

modimer between mutants, with a rank order of WT > S314C > S314F > S314Y.

#### Functional activity and dominant negative inhibition

To evaluate their transcriptional properties, expression vectors encoding WT or mutant receptors were cotransfected with a reporter gene (MAL-TKLUC) containing a direct repeat TRE configuration. In comparison with WT receptor, S314Y was transcriptionally inactive even at the highest concentration of T $_3$  (1000 nM), whereas S314F produced detectable activity (10–15% of the maximal WT response) only at 100 and 1000 nM T $_3$ . In marked contrast, although impaired relative to WT at the lower concentrations of ligand (0.1 and 1.0 nM), the S314C mutant exhibited a right-shifted activation profile, attaining a maximal transcriptional response comparable to that of WT at 100 nM T $_3$  (Fig. 2).

Consonant with its dominant mode of inheritance, it has been suggested that the mutant receptors in RTH inhibit the action of their WT counterparts in a dominant negative manner (4, 5). We therefore examined the dominant negative potency of each RTH mutant in transient transfection analyses using the same TRE. Either WT receptor alone or equal amounts of WT and mutant receptor were cotransfected with MAL-TKLUC, and transcriptional activity was assayed at either low (1 nM) or high (1000 nM) T $_3$  concentrations. At 1 nM T $_3$ , coexpressed S314F or S314Y mutants reduced *trans*-activation by WT receptor comparably (WT alone 100%; WT plus S314F or WT plus S314Y, 45%), whereas cotransfected S314C mutant was less inhibitory (WT, 100%; WT plus S314C, 68%). Similarly, at the higher T $_3$  concentration, dominant negative inhibition by the S314C mutant was less marked with 80% *trans*-activation of WT alone, whereas S314F and S314Y continued to exert significant inhibitory effects (*trans*-activation, 60% of WT alone; Fig. 3).

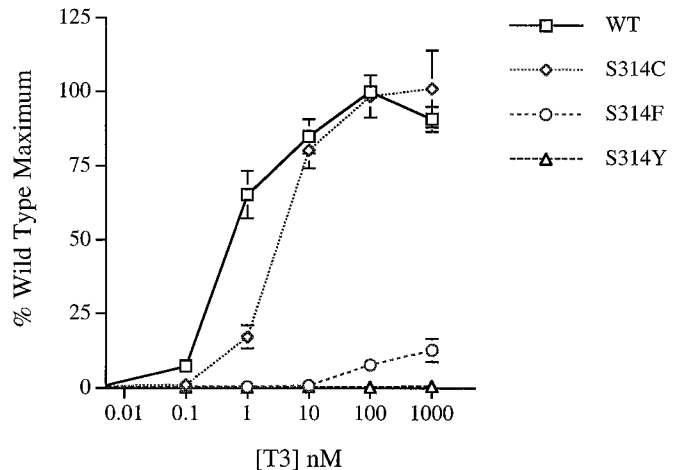


FIG. 2. T $_3$ -dependent transcriptional activation of the malic enzyme (MAL-TKLUC) reporter gene by WT and mutant (S314C, S314F, S314Y) TRs. JEG-3 cells were cotransfected with WT or mutant TR $\beta$  expression plasmids together with the reporter construct MAL-TKLUC and an internal control plasmid (Bos- $\beta$ gal). Hormone-dependent activation in response to increasing amounts of T $_3$  was normalized against the internal control and expressed as a percentage of the maximum WT receptor response. The data shown represent the mean  $\pm$  SEM of at least three experiments, each performed in triplicate.

In view of the marked differences in ligand binding affinity, *trans*-activation, and dominant negative activity of the S314 mutants *in vitro*, we sought to determine whether this might be reflected in the degree of resistance to thyroid hormone action *in vivo*. A previous study has suggested that the magnitude of elevation of circulating free T<sub>4</sub> (reflecting the degree of resistance within the pituitary-thyroid axis) may correlate with the degree of impairment in hormone binding affinities of mutant receptor proteins *in vitro* (13). We therefore compared circulating free T<sub>4</sub> levels in individuals harboring the three different codon 314 mutations (Fig. 4). Interestingly, those with the S314Y or F mutation, on the average, exhibited higher FT<sub>4</sub> levels than patients with the S314C mutation, with a trend that, although not significant,

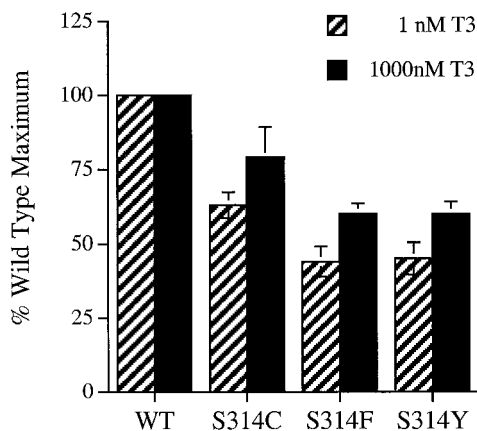


FIG. 3. Dominant negative inhibition of wild-type (WT) receptor activity by mutant receptors. JEG-3 cells were cotransfected with 500 ng of the reporter plasmid MAL-TKLUC, 200 ng of the internal control Bos- $\beta$ gal and either 100 ng WT expression vector alone or 50 ng each of wild-type and mutant receptor vectors. Corrected luciferase activity was measured after incubation with low (1 nM) or high (1000 nM) T<sub>3</sub> concentrations, and values are expressed as a percentage of the maximal WT receptor response. The data shown represent the mean  $\pm$  SEM of at least three experiments, each performed in triplicate.

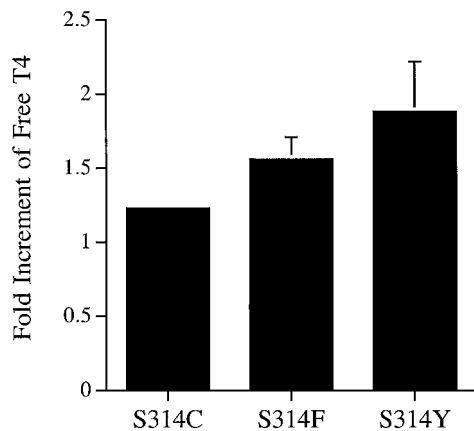


FIG. 4. Circulating FT<sub>4</sub> levels in individuals harboring each of the three codon 314 mutations. FT<sub>4</sub> levels, expressed as the fold increment relative to the upper limit of the normal reference range (denoted 1.0), were calculated for all individuals shown in Table 1, except the index case in pedigree V, in whom the pituitary-thyroid axis had been altered by previous thyroid surgery. For each mutation, values shown represent the mean  $\pm$  SEM.

suggests a correlation between the degree of resistance and the extent of mutant receptor dysfunction.

## Discussion

We have identified six kindreds with RTH harboring three different amino acid substitutions (S314C, S314F, and S314Y) at the same codon in the TR $\beta$  gene. All affected individuals exhibited pathognomonic biochemical features with elevated circulating free thyroid hormones and nonsuppressed TSH, in keeping with the idea that this disorder is characterized by resistance within the hypothalamic-pituitary-thyroid axis. Two of the mutations (S314F and S314Y) were identified in separate families with no apparent shared ancestry, suggesting that they had arisen independently in a mutation-prone GC-rich region as has been documented previously in RTH (14). Most affected individuals were asymptomatic or noted to have a goiter, but in four cases thyrotoxic features were present. There was no clear correlation between clinical features and the underlying genetic defect, underscoring the variable clinical phenotype in this disorder (3).

RTH also exhibits molecular heterogeneity, being associated with diverse mutations that all localize to the ligand binding domain of the TR $\beta$  gene. On the basis of their transcriptional and hormone binding properties, it has been suggested that RTH mutants can be subdivided into three categories (15): type I mutants exhibit reduced *trans*-activation consistent with the degree of impairment in their ability to bind ligand, type II mutants show a disproportionate loss of *trans*-activation relative to their altered ligand binding affinity, and type III mutants exhibit negligible ligand binding and comparably impaired *trans*-activation. In this study, the mutations we have identified in codon 314 of TR $\beta$  exhibited divergent functional properties. The S314C substitution resulted in a moderate impairment in hormone binding. Consonant with this, it exhibited a type I *trans*-activation profile, with functional impairment at lower T<sub>3</sub> levels but full *trans*-activation at higher T<sub>3</sub> concentrations. In contrast, the S314F and S314Y substitutions resulted in severely attenuated ligand binding. These mutants showed type III transcriptional responses, with S314Y being unable to activate transcription, and S314F achieving only 15% of the maximal WT response at 1000 nM T<sub>3</sub>.

We have shown that all three codon 314 mutants are able to inhibit the transcriptional activity of WT TR when they are coexpressed. This dominant negative effect has been observed previously with a large number of other RTH mutants and is in keeping with the dominant mode of inheritance of this disorder (6, 11, 16). Gel mobility shift assays indicate that all three codon 314 mutants retain the ability to bind to DNA and heterodimerize with RXR. This observation supports previous hypotheses that DNA binding and heterodimerization are functional properties that are critical for RTH mutants to exert dominant negative activity (6–8). In addition to differences in transcriptional function, our studies suggest that the three S314 mutants differ in dominant negative potency, as at both low (1 nM) and high (1000 nM) concentrations of T<sub>3</sub>, the S314F and S314Y mutants inhibited WT receptor function more strongly than S314C. It has been suggested that the ability of some RTH mutants to form TR

homodimers that constitutively repress basal transcription may contribute to their dominant negative inhibitory potency (17–19). In keeping with this hypothesis, we note that the weaker dominant negative mutant S314C formed TR homodimers that dissociated more readily with T<sub>3</sub>, whereas the more potent S314F and S314Y mutants formed homodimer complexes that were less T<sub>3</sub> reversible. Interestingly, the extent of thyroid dysfunction *in vivo* appeared consistent with the magnitude of receptor dysfunction *in vitro*.

To investigate the potential reasons for the marked divergence in their functional properties, we modelled the effect of the different amino acid changes in Ser<sup>314</sup> in human TR $\beta$  (20). Figure 5a shows that the side-chain of Ser<sup>314</sup> plays a structural role in the periphery of the hydrophobic ligand binding cavity, consistent with our functional data indicating its importance in hormone binding. When viewed in greater

detail (Fig. 5b), it is evident that this serine is tightly packed in van der Waal's contact with the side-chains of Ile<sup>353</sup>, Ile<sup>431</sup>, and Leu<sup>428</sup>, with the hydroxyl group of Ser<sup>314</sup> within hydrogen bonding distance of the carbonyls of Met<sup>310</sup> and Glu<sup>311</sup>. Mutation of Ser<sup>314</sup> to a cysteine would probably weaken these hydrogen bonds. However, as the side-chain volumes of serine and cysteine are so similar, few structural perturbations might be anticipated, explaining the relatively modest effect on ligand binding. In contrast, when Ser<sup>314</sup> is replaced by a phenylalanine, the bulky aromatic side-chain of the latter clashes sterically with Ile<sup>431</sup>, Met<sup>310</sup>, and ligand (Fig. 5c). Rotation of the side-chain of Met<sup>310</sup> to accommodate this results in a clash with His<sup>435</sup> and Phe<sup>459</sup>. We suggest that such steric effects may be more deleterious, and indeed, it is known that different substitutions of His<sup>435</sup> in TR $\beta$  markedly impair ligand binding (21).

In conclusion, we have described three novel mutations in

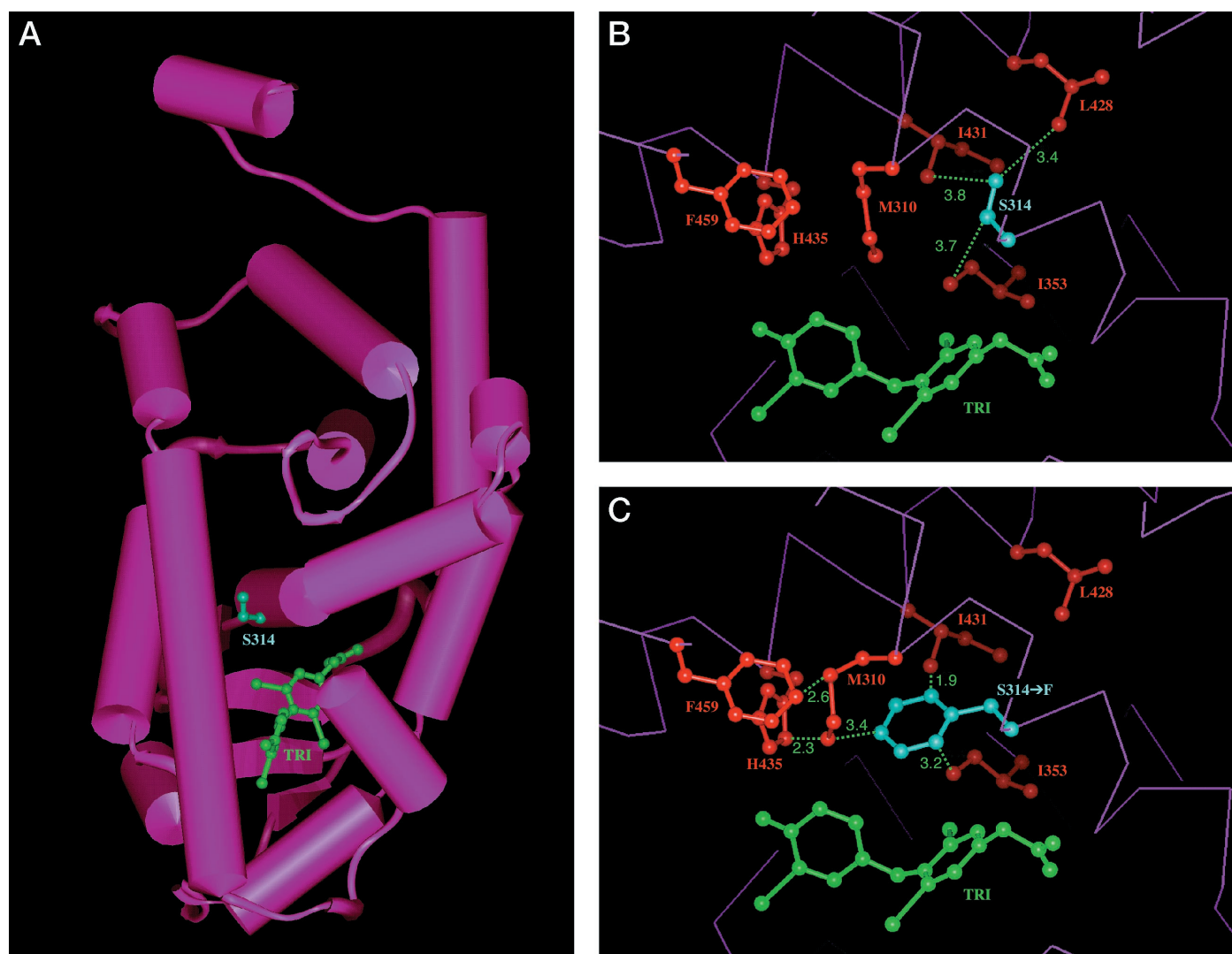


FIG. 5. a, The crystal structure of human TR $\beta$  is shown, with Ser<sup>314</sup> located in the periphery of the ligand binding cavity. b, Enlarged view showing the residues in contact with Ser<sup>314</sup>. c, The mutation of Ser<sup>314</sup> to Phe was modelled by replacing the side-chain and then selecting the most favorable rotamer conformation. The orientation for the phenylalanine shown here is the only one that did not clash badly with the peptide backbone. However, this orientation clashed with the side-chains of Met<sup>310</sup> and Ile<sup>431</sup>. The orientation of Met<sup>310</sup> could be adjusted to avoid the clash with the phenylalanine, but this caused it to clash with both Phe<sup>459</sup> and His<sup>435</sup>. In conclusion, the bulky aromatic side-chain cannot readily be accommodated without significant structural perturbations.

TR $\beta$  in RTH due to distinct nucleotide substitutions at a single codon (314) that differentially impair receptor function. Our data suggest that the degree of functional impairment *in vitro* correlates with the extent to which interaction of Ser<sup>314</sup> with T<sub>3</sub> is disrupted and might also be related to the magnitude of thyroid dysfunction *in vivo*.

### Acknowledgments

We thank R. Wagner and R. Fletterick for providing the coordinates for the human TR $\beta$  crystal structure.

### References

- Usala SJ, Bale AE, Gesundheit N, Weinberger C, Lash RW, Wondisford FE, McBride OW, Weintraub BD 1988 Tight linkage between the syndrome of generalized thyroid hormone resistance and the human *c-erbA*  $\beta$  gene. *Mol Endocrinol* 2:1217-1220
- Refetoff S, Weiss RE, Usala SJ 1993 The syndromes of resistance to thyroid hormone. *Endocr Rev* 14:348-399
- Beck-Peccoz P, Chatterjee VKK 1994 The variable clinical phenotype in thyroid hormone resistance syndrome. *Thyroid* 4:225-232
- Sakurai A, Miyamoto T, Refetoff S, DeGroot LJ 1990 Dominant negative transcriptional regulation by a mutant thyroid hormone receptor  $\beta$  in a family with generalised resistance to thyroid hormone. *Mol Endocrinol* 4:1988-1994
- Chatterjee VKK, Nagaya T, Madison LD, Datta S, Rentoumis A, Jameson JL 1991 Thyroid hormone resistance syndrome: inhibition of normal receptor function by mutant thyroid hormone receptors. *J Clin Invest* 87:1977-1984
- Collingwood TN, Adams M, Tone Y, Chatterjee VKK 1994 Spectrum of transcriptional, dimerization and dominant negative properties of twenty different mutant thyroid hormone  $\beta$ -receptors in thyroid hormone resistance syndrome. *Mol Endocrinol* 8:1262-1277
- Nagaya T, Madison LD, Jameson JL 1992 Thyroid hormone receptor mutants that cause resistance to thyroid hormone: evidence for receptor competition for DNA sequences in target genes. *J Biol Chem* 267:13014-13019
- Nagaya T, Jameson JL 1993 Thyroid hormone receptor dimerization is required for dominant negative inhibition by mutations that cause thyroid hormone resistance. *J Biol Chem* 268:15766-15771
- Clifton-Bligh RJ, de Zegher F, Wagner RL, Collingwood TN, Francois I, van Helvoirt M, Chatterjee VKK 1998 A novel TR $\beta$  mutation (R383H) in resistance to thyroid hormone predominantly impairs corepressor release and negative transcriptional regulation. *Mol Endocrinol* 8:1262-1277
- Adams M, Matthews C, Collingwood TN, Tone Y, Beck-Peccoz P, Chatterjee VKK 1994 Genetic analysis of 29 kindreds with generalized and pituitary resistance to thyroid hormone. *J Clin Invest* 94:506-515
- Collingwood TN, Wagner R, Matthews CH, Clifton-Bligh RJ, Gurnell M, Rajanayagam O, Agostini M, Fletterick RJ, Beck-Peccoz P, Reinhardt W, Binder G, Ranke MB, Hermus A, Hesch RD, Lazarus J, Newrick P, Parfitt V, Raggatt P, de Zegher F, Chatterjee VKK 1998 A role for helix 3 of the TR $\beta$  ligand binding domain in coactivator recruitment identified by characterization of a third cluster of mutations in resistance to thyroid hormone. *EMBO J* 17:4760-4770
- Yen PM, Darling DS, Carter RL, Forgione M, Umeda PM, Chin WW 1992 Triiodothyronine (T<sub>3</sub>) decreases binding to DNA by T<sub>3</sub>-receptor homodimers but not receptor auxiliary protein heterodimers. *J Biol Chem* 267:3565-3568
- Hayashi Y, Weiss RE, Sarne DH, Yen PM, Sunthornthepvarakul T, Marcocci C, Chin WW, Refetoff S 1995 Do clinical manifestations of resistance to thyroid hormone correlate with the functional alteration of the corresponding mutant thyroid hormone  $\beta$  receptors? *J Clin Endocrinol Metab* 80:3246-3256
- Weiss RE, Weinberg M, Refetoff S 1993 Identical mutations in unrelated families with generalised resistance to thyroid hormone occur in cytosine-guanine-rich areas of the thyroid hormone receptor beta gene. *J Clin Invest* 91:2408-2415
- Meier CA, Parkison C, Chen A, Ashizawa K, Meier-Hausler SC, Muchmore P, Cheng S-Y, Weintraub BD 1993 Interaction of human  $\beta$ 1 thyroid hormone receptor and its mutants with DNA and retinoid X receptor  $\beta$ . T<sub>3</sub> response element-dependent dominant negative potency. *J Clin Invest* 92:1986-93
- Meier CA, Dickstein BM, Ashizawa K, McClaskey JH, Muchmore P, Ransom SC, Menke JB, Hao E-N, Usala SJ, Bercu BB, Cheng S-Y, Weintraub BD 1992 Variable transcriptional activity and ligand binding of mutant  $\beta$ 1 3,5,3'-triiodothyronine receptors from four families with generalised resistance to thyroid hormone. *Mol Endocrinol* 6:248-258
- Piedrafita FJ, Bendik I, Ortiz MA, Pfahl M 1995 Thyroid hormone receptor homodimers can function as ligand-sensitive repressors. *Mol Endocrinol* 9:563-578
- Yen PM, Wilcox EC, Hayashi Y, Refetoff S, Chin WW 1995 Studies on the repression of basal transcription (silencing) by artificial and natural human thyroid hormone receptor- $\beta$  mutants. *Endocrinology* 136:2845-2851
- Kitajima K, Nagaya T, Jameson JL 1995 Dominant negative and DNA-binding properties of mutant thyroid hormone receptors that are defective in homodimerization but not heterodimerization. *Thyroid* 5:343-353
- Feng W, Ribeiro RCJ, Wagner RL, Nguyen H, Apriletti JW, Fletterick RJ, Baxter JD, Kushner PJ, West BL 1998 Hormone-dependent coactivator binding to a hydrophobic cleft on nuclear receptors. *Science* 280:1747-1749
- Tsukaguchi H, Yoshimasa Y, Fujimoto K, Ishii H, Yamamoto T, Yoshimasa T, Yagura T, Takamatsu J 1995 Three novel mutations of thyroid hormone receptor  $\beta$  gene in unrelated patients with resistance to thyroid hormone: two mutations of the same codon (H435L and H435Q) produce separate subtypes of resistance. *J Clin Endocrinol Metab* 80:3613-3616
- Sakurai A, Nakai A, DeGroot LJ 1990 Structural analysis of human thyroid hormone receptor  $\beta$  gene. *Mol Cell Endocrinol* 71:83-91

# Tyrosine Agonists Reverse the Molecular Defects Associated with Dominant-Negative Mutations in Human Peroxisome Proliferator-Activated Receptor $\gamma$

MAURA AGOSTINI, MARK GURNELL, DAVID B. SAVAGE, EMILY M. WOOD, AARON G. SMITH, ODELIA RAJANAYAGAM, KEITH T. GARNES, SIDNEY H. LEVINSON, H. ERIC XU, JOHN W. R. SCHWABE, TIMOTHY M. WILLSON, STEPHEN O'RAHILLY, AND V. KRISHNA CHATTERJEE

Departments of Medicine (M.A., M.G., D.B.S., E.M.W., A.G.S., O.R., S.O., K.C.) and Clinical Biochemistry (D.B.S., S.O.), University of Cambridge, Addenbrooke's Hospital, Cambridge CB2 2QQ, United Kingdom; GlaxoSmithKline (K.T.G., S.H.L.), Isotope Chemistry, Upper Merion, Pennsylvania 19406; GlaxoSmithKline (H.E.X., T.M.W.), Nuclear Receptor Discovery Research, Research Triangle Park, North Carolina 27709; and Medical Research Council Laboratory of Molecular Biology (J.W.R.S.), Addenbrooke's Hospital, Cambridge CB2 2QH, United Kingdom

Loss-of-function mutations in the ligand-binding domain of human peroxisome proliferator-activated receptor  $\gamma$  (PPAR $\gamma$ ) are associated with a novel syndrome characterized by partial lipodystrophy and severe insulin resistance. Here we have further characterized the properties of natural dominant-negative PPAR $\gamma$  mutants (P467L, V290M) and evaluated the efficacy of putative natural ligands and synthetic thiazolidinedione (TZD) or tyrosine-based (TA) receptor agonists in rescuing mutant receptor function. A range of natural ligands failed to activate the PPAR $\gamma$  mutants and their transcriptional responses to TZDs (e.g. pioglitazone, rosiglitazone) were markedly attenuated, whereas TAs (e.g. farglitazar) corrected defects in ligand binding and coactivator recruitment by the PPAR $\gamma$  mutants, restoring transcriptional function comparable with wild-type receptor. Transcriptional silencing via recruitment of corepressor contributes to dominant-negative inhibition of wild type by the P467L and V290M mu-

tants and the introduction of an artificial mutation (L318A) disrupting corepressor interaction abrogated their dominant-negative activity. More complete ligand-dependent corepressor release and reversal of dominant-negative inhibition was achieved with TA than TZD agonists. Modeling suggests a structural basis for these observations: both mutations destabilize helix 12 to favor receptor-corepressor interaction; conversely, farglitazar makes more extensive contacts than rosiglitazone within the ligand-binding pocket, to stabilize helix 12, facilitating corepressor release and transcriptional activation. Farglitazar was a more potent inducer of PPAR $\gamma$  target gene (aP2) expression in peripheral blood mononuclear cells with the P467L mutation. Having shown that rosiglitazone is of variable and limited efficacy in these subjects, we suggest that TAs may represent a more rational therapeutic approach. (*Endocrinology* 145: 1527–1538, 2004)

**P**EROXISOME PROLIFERATOR-ACTIVATED RECEPTOR  $\gamma$  (PPAR $\gamma$ ), a member of the nuclear receptor superfamily, was first characterized as a transcriptional regulator of adipocyte-specific gene expression (1) and preadipocyte differentiation (2). A number of unsaturated fatty acids (arachidonic, linoleic,  $\gamma$ -linolenic, eicosapentaenoic) activate PPAR $\gamma$  and may represent endogenous ligands for the receptor in this context (3, 4). Eicosanoid derivatives of fatty acids can act as endogenous PPAR $\gamma$  activators in other biological processes: in the macrophage, hydroxyoctadecadi-

enoic acid (HODE) and hydroxyeicosatetraenoic acid (HETE), the 15-lipoxygenase products of arachidonic and linoleic acids, inhibit the production of inflammatory cytokines (5) and promote the uptake and catabolism of oxidized low-density lipoprotein (6); 15-deoxy  $\Delta^{12,14}$  prostaglandin J<sub>2</sub> (15d-PGJ<sub>2</sub>), a terminal metabolite of prostaglandin D<sub>2</sub>, which binds PPAR $\gamma$  and promotes adipocyte differentiation, has been most widely studied as a putative naturally occurring ligand (7, 8).

The thiazolidinediones (TZDs) were synthesized as potentially hypolipidemic derivatives of clofibrate but then developed as antidiabetic agents because of their unexpected insulin sensitizing action *in vivo*. TZDs are high-affinity PPAR $\gamma$  ligands (9), with the rank order of their binding affinities mirroring antihyperglycemic activity, suggesting a role for this receptor in mediating their antidiabetic action. In keeping with this, we have previously described two different mutations (P467L, V290M) in the ligand-binding domain (LBD) of human PPAR $\gamma$  (10) in two families, with affected subjects exhibiting severe insulin resistance and early-onset type 2 diabetes mellitus (T2DM), together with other features of the human metabolic syndrome (e.g. dyslipidemia [low

Abbreviations: aP2, Adipocyte P2; CBP, CREB (cAMP response element binding protein) binding protein; 15d-PGJ<sub>2</sub>, 15-deoxy  $\Delta^{12,14}$  prostaglandin J<sub>2</sub>; GST, glutathione-S-transferase; HETE, hydroxyeicosatetraenoic acid; HODE, hydroxyoctadecadienoic acid; LBD, ligand-binding domain; NCoR, nuclear receptor corepressor; PBMC, peripheral blood mononuclear cell; PPAR $\gamma$ , peroxisome proliferator-activated receptor  $\gamma$ ; RAR, retinoic acid receptor; RTH, resistance to thyroid hormone; SMRT, silencing mediator of retinoid and thyroid receptors; TA, tyrosine-based receptor agonist; T2DM, type 2 diabetes mellitus; TR $\beta$ , thyroid hormone  $\beta$ -receptor; TZD, thiazolidinedione; WT, wild-type.

*Endocrinology* is published monthly by The Endocrine Society (<http://www.endo-society.org>), the foremost professional society serving the endocrine community.

high-density lipoprotein cholesterol, high triglycerides], hypertension). Consonant with a central role for PPAR $\gamma$  in adipogenesis, these individuals also exhibit a stereotyped pattern of partial lipodystrophy (11), a feature that has also been observed in other reported cases with receptor mutations (12, 13).

In addition to being functionally impaired, the P467L and V290M mutant receptors inhibit wild-type (WT) PPAR $\gamma$  action in a dominant-negative manner, consistent with heterozygosity for mutant PPAR $\gamma$  in affected subjects and dominant inheritance of the disorder in one family (10). The syndrome of resistance to thyroid hormone (RTH), a disorder characterized by elevated circulating thyroid hormones with tissue refractoriness to thyroid hormone action, is associated with similar dominant-negative mutations in the human thyroid hormone  $\beta$ -receptor (TR $\beta$ ) (14). Here functional studies have shown that higher concentrations of ligand can overcome dominant-negative inhibition by many TR $\beta$  mutants *in vitro* (15) and that the administration of supraphysiological doses of thyroid hormone can restore target tissue responsiveness *in vivo* (16). By analogy, we reasoned that the administration of a PPAR $\gamma$  agonist to enhance mutant receptor function and reverse dominant-negative activity might represent a rational approach to the treatment of the severe metabolic disturbance observed in our affected subjects. Three TZD PPAR $\gamma$  agonists have been developed for clinical use: troglitazone, the first insulin-sensitizing antidiabetic agent to be licensed, was later withdrawn due to unpredictable and potentially fatal hepatotoxicity; however, the newer agents, pioglitazone and rosiglitazone, offer comparable efficacy and appear to be devoid of this side effect (17). Clinical studies with rosiglitazone in two subjects harboring the P467L and V290M PPAR $\gamma$  mutations have demonstrated variable efficacy in ameliorating the insulin resistance and metabolic phenotype (11), suggesting a role for more potent receptor agonists. Recently high-affinity tyrosine-based PPAR $\gamma$  agonists, with potent glucose-lowering activity *in vivo* (18) and proven antidiabetic efficacy in patients with T2DM (19), have been developed. The lead compound, farglitazar (GI262570), is currently being evaluated in human clinical trials.

Here we report more detailed functional characterization of the previously reported dominant-negative natural PPAR $\gamma$  mutants. Consonant with the severe clinical phenotype, an array of putative endogenous natural ligands were unable to activate mutant PPAR $\gamma$ . The mutant receptors exhibited markedly impaired transcriptional responses with TZDs, but in contrast, tyrosine-based receptor agonists (TAs) corrected defects in ligand-binding, corepressor release, and coactivator recruitment, permitting transcriptional activation comparable with WT receptor. In comparison with the TZD rosiglitazone, the TA farglitazar completely reversed dominant-negative inhibition by both mutant receptors *in vitro* and activated PPAR $\gamma$  target gene (adipocyte P2) expression in P467L mutant peripheral blood mononuclear cells (PBMCs) more effectively. Crystallographic modeling suggests a structural basis for these observations: both mutations in PPAR $\gamma$  destabilize helix 12 (20), and, as in the recently elucidated PPAR $\alpha$ /silencing mediator of retinoid and thyroid receptors (SMRT) structure (21), this may facil-

itate corepressor interaction; conversely, unlike rosiglitazone, the synthetic ligand farglitazar is able to make additional contacts within the receptor ligand-binding pocket, thereby providing additional stability to helix 12, which mediates transactivation. Tyrosine-based PPAR $\gamma$  agonists, rather than TZDs, may therefore represent a more rational approach to restoring mutant receptor function *in vivo*, thereby ameliorating insulin resistance in our patients.

## Materials and Methods

### Plasmid constructs

Full-length human PPAR $\gamma$ 1 cDNA was cloned by RT-PCR from total human preadipocyte RNA and introduced into the pcDNA3 expression vector (Invitrogen, Groningen, The Netherlands). The P467L and V290M natural mutants and L318A artificial mutant were generated by site-directed mutagenesis of the WT receptor template as previously described (10). DNA sequences encoding residues 173–477 of the WT and mutant PPAR $\gamma$ 1 LBDs were cloned into pGEX4T (Amersham Pharmacia Biotech, Buckinghamshire, UK) and AASV (22) to yield glutathione-S-transferase (GST)-PPAR $\gamma$  and VP16-PPAR $\gamma$  LBD fusions, respectively. Gal4-SMRT consists of the 468 C-terminal amino acids of SMRT fused in-frame to the Gal4 DNA-binding domain in pCMX (23). Gal4-ID1 (amino acids 2302–2352), Gal4-ID2 (amino acids 2131–2201), and Gal4-ID1 + 2 (amino acids 2131–2352) contain one or more of the nuclear receptor interaction domains of SMRT as reported previously (24). PPAR $\gamma$ -RETCLUC (7) and UASTKLUC (22) have been described previously.

### Protein-protein interaction assays

Bacterially expressed GST fusion proteins were prepared according to standard protocols (10). After purification, proteins bound to glutathione-Sepharose beads (Amersham Pharmacia Biotech) in binding buffer [40 mM HEPES (pH 7.8), 100 mM KCl, 5 mM MgCl<sub>2</sub>, 0.2 mM EDTA, 1% Nonidet P-40, 10% glycerol, 2 mM dithiothreitol, 4 mg/ml BSA] were mixed with 5  $\mu$ l of <sup>35</sup>S-labeled *in vitro*-translated cAMP response element-binding protein (CBP) together with ligand or vehicle and incubated at 4 C for 2 h. After washing with NETN buffer [20 mM Tris (pH 8.0), 100 mM NaCl, 1 mM EDTA, 0.5% Nonidet P-40], bound CBP was determined by SDS-PAGE. Comparable loading of the GST-PPAR $\gamma$  LBD fusion proteins was confirmed with Coomassie staining before autoradiography. The assay shown is representative of three separate experiments with similar results.

### Ligand-binding assays

[<sup>3</sup>H]-farglitazar was synthesized as follows: Crabtree's catalyst (25) (3 mg, 200 mol %) was added to a solution of farglitazar (1.0 mg) in methylene chloride (1.0 ml). The mixture was subjected to three freeze-pump-thaw cycles on a steel manifold before introduction of 1.96 Ci tritium gas. The reaction mixture was allowed to warm to room temperature and vigorously stirred for 18 h. After workup and exchange of labile tritium, 129 mCi crude [<sup>3</sup>H]-farglitazar was obtained at 50% radiochemical purity by HPLC. A 25.8-mCi portion of the crude product was purified by HPLC (Zorbax SB C18, 5  $\mu$ m, 4.6  $\times$  250 mm, 70:30:0.1 acetonitrile/water/trifluoroacetic acid at 1.0 ml/min, UV detection at 240 nm). The desired product fraction was collected, concentrated *in vacuo*, frozen, and lyophilized under vacuum to give a pale yellow solid. The solid was dissolved in 5 ml of absolute ethanol to provide 6.05 mCi [<sup>3</sup>H]-farglitazar (1.21 mCi/ml; 41 Ci/mmol) at 97.6% radiochemical purity by HPLC: <sup>1</sup>H-NMR (CDCl<sub>3</sub>, 400 MHz), 8.84 (m, 1H), 7.94 (m, 2H), 7.58 (m, 2H), 7.51 (m, 1H), 7.46 (m, 1H), 7.43 (m, 2H), 7.38 (m, 2H), 7.34 (m, 1H), 7.21 (m, 2H), 6.80 (m, 2H), 6.69 (d, J = 8.3 Hz, 1H), 6.61 (ddd, J = 7.6, 7.6, 0.9 Hz, 1H), 4.38 (m, 1H), 4.134 (t, J = 6.6 Hz, 2H), 3.25 (dd, J = 13.9, 5.7 Hz, 1H), 3.14 (dd, J = 13.9, 7.1 Hz, 1H), 2.94 (t, J = 6.6 Hz, 2H), 2.33 (s, <sup>3</sup>H). <sup>3</sup>H-NMR (CDCl<sub>3</sub>, 426 MHz) 8.03 (dm, J = 1.2 Hz). Hormone-binding assays were performed using bacterially expressed GST-PPAR $\gamma$  LBD fusion proteins and the PPAR $\gamma$  ligands [<sup>3</sup>H]-rosiglitazone (9) and [<sup>3</sup>H]-farglitazar in a modification of a previously described filter binding assay (26). Filters were preincubated with BSA (1%) and Tween (1%) to reduce nonspecific binding with the [<sup>3</sup>H]-

farglitazar compound. Again, addition of comparable amounts of PPAR $\gamma$  LBD fusion proteins was confirmed through Coomassie staining of aliquots subjected to SDS-PAGE. Results denote the mean  $\pm$  SEM of experiments performed on three separate occasions.

### Transfection assays

Calcium phosphate-mediated transfection was performed in 24-well plates of 293EBNA cells. Each well was cotransfected with 50–100 ng of receptor expression vector, 500 ng of reporter construct, 100 ng of the internal control plasmid Bos- $\beta$ -gal, and, where indicated, 50–100 ng of additional construct. Cells were harvested and assayed as described previously (15). Results represent the mean  $\pm$  SEM of at least three independent experiments, each performed in triplicate.

### *aP2* assays in PBMCs

Blood was obtained from the index case harboring the P467L PPAR $\gamma$  mutation (10) and PBMCs were isolated by ficoll gradient centrifugation, washed in PBS, and cultured in RPMI 1640 (Sigma-Aldrich, Dorset, UK) with 1% charcoal-stripped fetal bovine serum in 6-well plates with  $3 \times 10^6$  cells/well. After exposure to either rosiglitazone or farglitazar for 24 h, RNA was isolated from cells using a commercial kit (Qiagen, West Sussex, UK) and reverse transcribed to generate first-strand cDNA. This was serially diluted and analyzed by quantitative PCR as described previously (27). Results shown are the mean of two independent experiments in the individual carrying the P467L mutation (a deterioration in her clinical condition precluded venesection for a third determination).

### Statistical analyses

All results are expressed as mean  $\pm$  SEM; where appropriate, comparisons between values were made using the Student's *t* test.

## Results

The transcriptional activities of WT receptor and PPAR $\gamma$  mutants were assayed by cotransfection of receptor expression vectors together with a reporter gene (PPARETKLUC) containing three copies of the PPARE from the acyltransferase-coenzyme A oxidase gene linked to the thymidine kinase promoter and luciferase, in the absence or presence of an array of putative natural ligands (Fig. 1). Western blotting of cell extracts after transfection of WT PPAR $\gamma$  or P467L and V290M mutants confirmed that their expression levels were equivalent in these assays (data not shown). As has been previously described, WT PPAR $\gamma$  exhibited some constitutive basal transcriptional activity (28) but showed a transcriptional response to unsaturated fatty acids (linoleic acid,

arachidonic acid,  $\gamma$ -linolenic acid), 15d-PGJ<sub>2</sub>, and eicosanoids (13-HODE, 15-HETE), which ranged from 50% to 80% of that obtained with a synthetic PPAR $\gamma$  agonist rosiglitazone (1  $\mu$ M). In contrast, the P467L and V290M mutants were completely unresponsive to all the natural ligands tested, despite their partial response to the synthetic receptor agonist.

To evaluate the potential therapeutic role of synthetic PPAR $\gamma$  agonists, we next examined the function of PPAR $\gamma$  mutants with each of the TZDs, including rosiglitazone, which is the most potent receptor agonist in this class that is licensed for clinical use. In comparison with WT PPAR $\gamma$ , the P467L and V290M mutant receptors were virtually unresponsive to both troglitazone (Fig. 2C) and pioglitazone (Fig. 2D), achieving only 40–50% of WT receptor activity at the highest concentration (10  $\mu$ M) of ligand. Similarly, only 1–10  $\mu$ M rosiglitazone elicited partial transcriptional responses (50–75% of WT) from the mutant receptors (Fig. 2E). Replacement of the 2,4-thiazolidinedione head group (Fig. 2A) with tyrosine-based substituents has led to the development of a series of high-affinity PPAR $\gamma$  agonists (Fig. 2B). In marked contrast to the TZDs, these compounds showed greater activity with PPAR $\gamma$  mutants. GW1929 (Fig. 2F) and GW7845 (Fig. 2G) induced significant transcriptional activation by both P467L and V290M mutant receptors even at low concentrations (10–100 nM) of ligand, enabling both mutants to achieve maximal responses comparable with WT receptor. Farglitazar, which is being developed for clinical use, showed the greatest activity, with the PPAR $\gamma$  mutants achieving greater than 75% of WT receptor activity at 10 nM concentration of ligand (Fig. 2H). Importantly, such greater potency of tyrosine agonists, compared with thiazolidinediones, was more evident with PPAR $\gamma$  mutants than WT receptor. Thus, whereas farglitazar was 100 times more potent than rosiglitazone with WT PPAR $\gamma$  [WT activation with 100 nM rosiglitazone (Fig. 2E) *vs.* 1 nM farglitazar (Fig. 2H)], the tyrosine agonist was up to 1000 times more potent than rosiglitazone with the PPAR $\gamma$  mutants [P467L and V290M activation with 10,000 nM rosiglitazone (Fig. 2E) *vs.* 10 nM farglitazar (Fig. 2H)].

We have shown previously that the impaired transcriptional function of the P467L PPAR $\gamma$  mutant reflects a com-

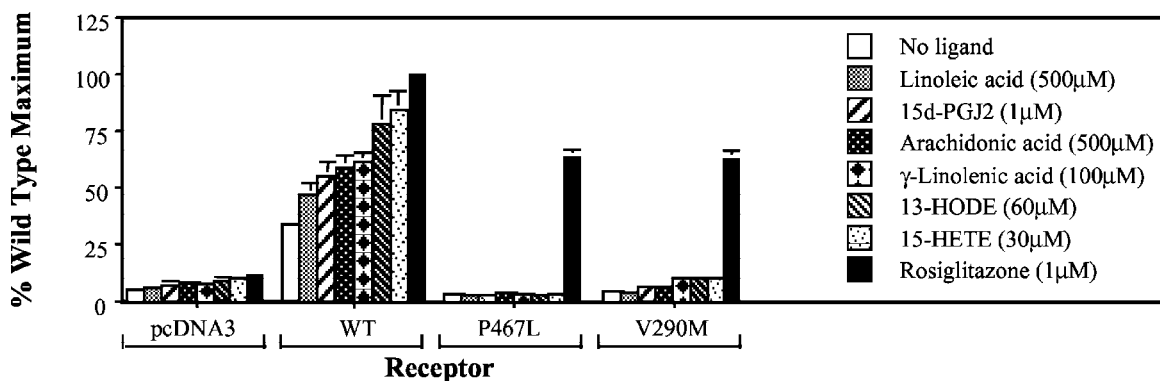


FIG. 1. A panel of putative endogenous ligands fail to transactivate mutant PPAR $\gamma$ . Twenty-four-well plates of 293EBNA cells were transfected with 500 ng of PPARETKLUC reporter gene, 100 ng of Bos- $\beta$ -gal control plasmid, and 100 ng of receptor expression vector as shown. Transcriptional activity in response to a variety of endogenous ligands is shown. Results are expressed as a percentage of the maximal WT observed response.

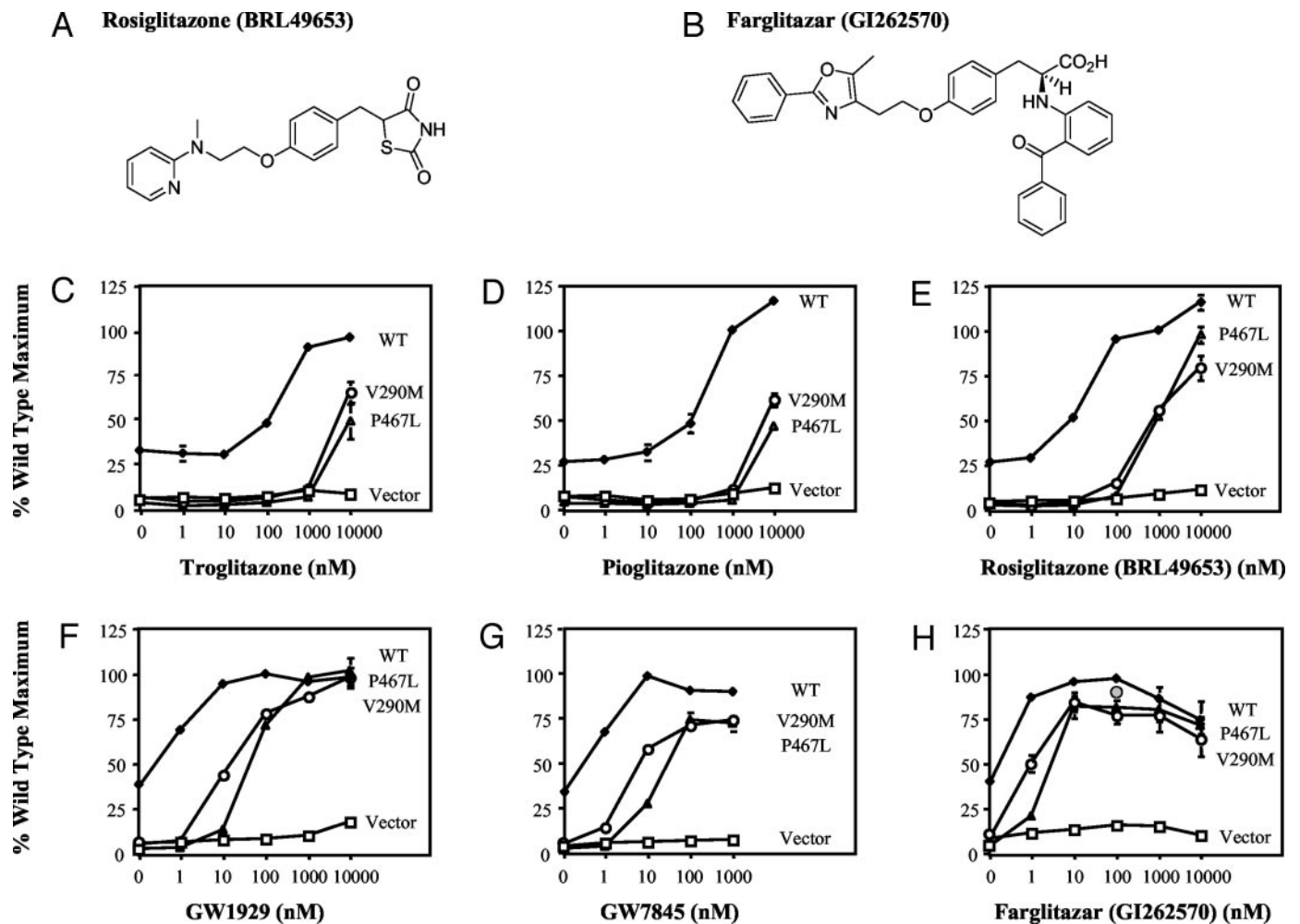


FIG. 2. A and B, Synthetic PPAR $\gamma$  agonists. Comparison of the chemical structures of rosiglitazone (thiazolidinedione, A) and farglitazar (tyrosine agonist, B). C–H, Tyrosine-based but not thiazolidinedione receptor agonists restore the transcriptional activity of P467L and V290M PPAR $\gamma$  mutants. Twenty-four-well plates of 293EBNA cells were transfected as outlined in Fig. 1. Transcriptional activity in response to ligand is shown for troglitazone (C) pioglitazone (D) rosiglitazone (E) GW1929 (F) GW7845 (G) and farglitazar (H). Results are expressed as a percentage of the WT maximum. The gray circle in H denotes the transcriptional response of WT PPAR $\gamma$  to 100 nM rosiglitazone, indicating that it is of the same magnitude as the receptor response to farglitazar.

combination of defects in binding to ligand and recruitment of coactivator (10). We therefore compared these properties of the P467L and V290M receptor mutants with TZD *vs.* tyrosine-based PPAR $\gamma$  agonists. In ligand-binding assays with bacterially expressed WT or mutant GST-PPAR $\gamma$  LBD fusion proteins and [ $^3$ H]-rosiglitazone or [ $^3$ H]-farglitazar, neither mutant receptor exhibited detectable specific binding to the radiolabeled TZD, whereas both mutant proteins showed significant specific binding to the TA (Fig. 3A). In a protein-protein interaction assay, both rosiglitazone and farglitazar mediated strong recruitment of the  $^{35}$ S-labeled coactivator CBP to WT receptor. However, the P467L and V290M mutants showed negligible coactivator binding even at high concentrations (10  $\mu$ M) of TZD, whereas a lower concentration (1  $\mu$ M) of TA promoted recruitment of CBP (Fig. 3B). Some members of the nuclear receptor family [*e.g.* TR and retinoic acid receptor (RAR)] are able to silence basal gene transcription through ligand-independent interaction with specific corepressor proteins such as nuclear receptor corepressor (NCoR) (29) and SMRT (23), with ligand-binding

promoting corepressor dissociation. We therefore examined the effects of the P467L and V290M mutant receptors on basal gene transcription and their interaction with corepressor. In comparison with cells transfected with empty expression vector, WT PPAR $\gamma$  activated basal reporter gene activity (~5-fold); in striking contrast, both PPAR $\gamma$  mutants not only lacked such activation but also significantly repressed basal gene transcription (pcDNA3 = 1.0; P467L = 0.44; V290M = 0.53) (Fig. 4A), suggesting that they might interact aberrantly with corepressors *in vivo*. Several studies have identified domains (ID1 and ID2) within NCoR and SMRT that mediate interaction with nuclear receptors (24, 30, 31).

To study the interaction between PPAR $\gamma$  mutants and corepressor, mammalian two-hybrid assays were performed, with cotransfection of fusions consisting of the ID1 + 2, ID1, or ID2 domains of SMRT linked to the DNA-binding domain of Gal4, together with VP16 linked to WT, P467L, or V290M PPAR $\gamma$  LBDs. In the absence of ligand, WT receptor and both PPAR $\gamma$  mutants were recruited comparably with Gal4-ID1 + 2, and additional experiments with



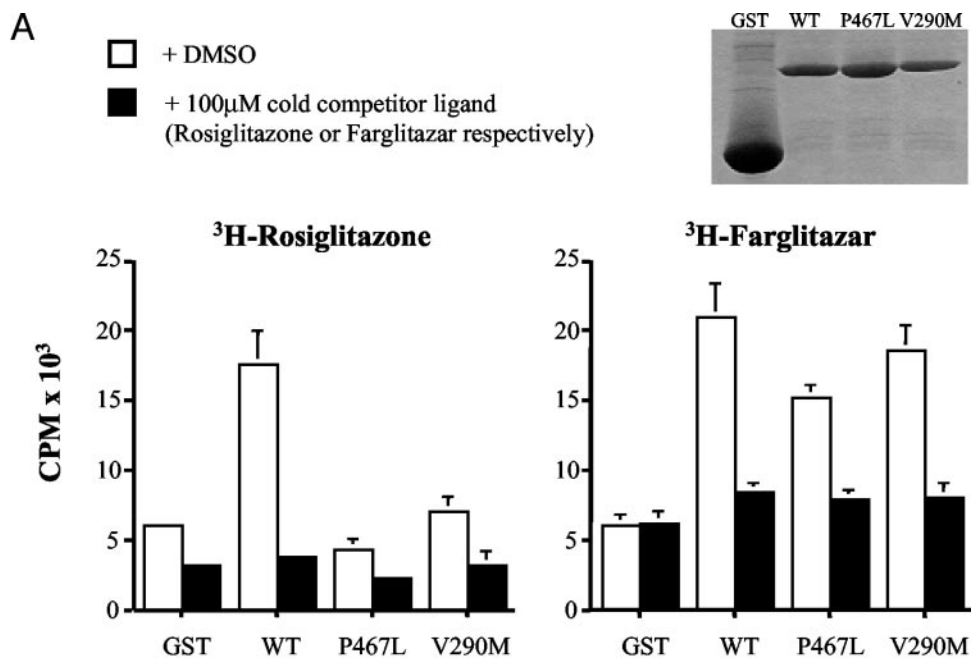
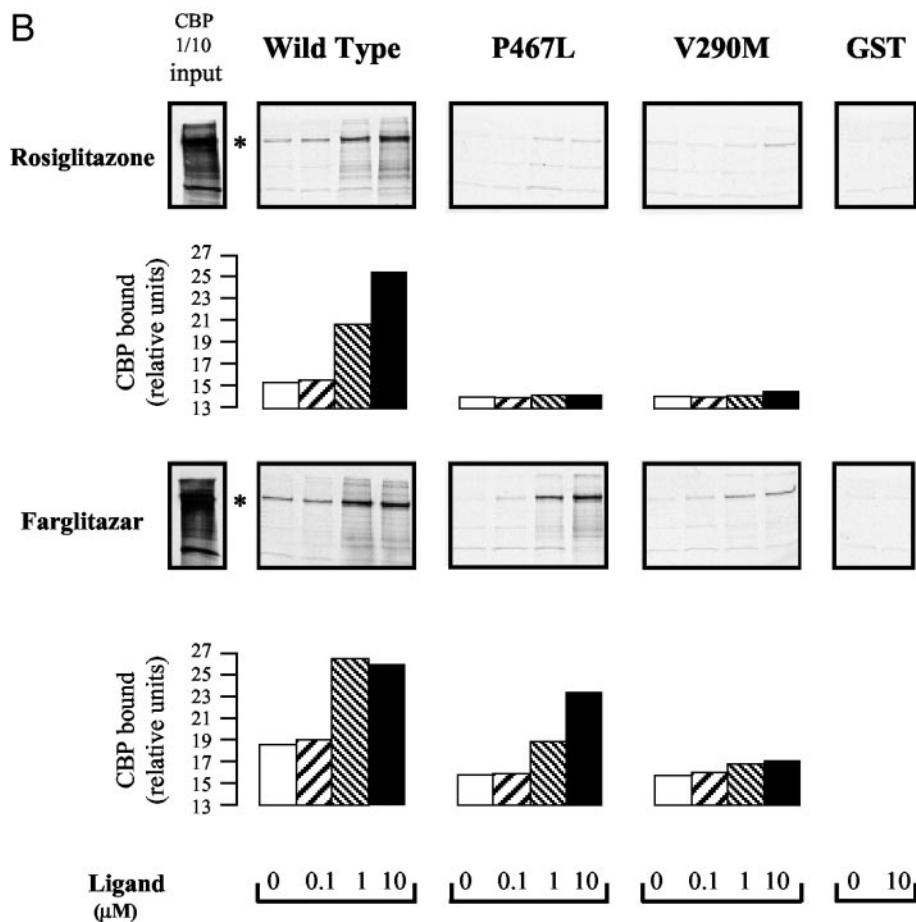


FIG. 3. A, Binding of thiazolidinedione (<sup>3</sup>H-rosiglitazone) and tyrosine agonist (<sup>3</sup>H-farglitazar) radioligands to GST-PPAR $\gamma$  LBD chimaeras. Bacterially expressed GST-PPAR $\gamma$  LBD fusion proteins were incubated with radioligand as indicated in the absence or presence of 10  $\mu$ M cold competing ligand (rosiglitazone or farglitazar, respectively). *Inset*, Coomassie-stained gel of proteins used in ligand-binding assays confirming comparable expression of WT and mutant receptors, with GST present in slight excess. B, Coactivator recruitment to mutant PPAR $\gamma$  is greater with TA (farglitazar) than thiazolidinedione (rosiglitazone). WT and mutant GST-PPAR $\gamma$  LBD fusion proteins (quantitated as in A) were tested for interaction with <sup>35</sup>S-labeled *in vitro*-translated CBP in the presence of increasing concentrations of ligand (rosiglitazone or farglitazar). Control assays were performed with GST alone. Histograms below each panel quantify the amount of CBP bound. An asterisk (\*) denotes the band corresponding to full-length CBP.



individual ID domain fusions indicated that this interaction was mediated through the ID1 region (Fig. 4B). Next, we examined the effect of thiazolidinedione *vs.* tyrosine-based

PPAR $\gamma$  agonists on receptor-corepressor interaction. With the addition of increasing concentrations (100–1000 nM) of TZD ligand (rosiglitazone), both mutant receptors exhibited

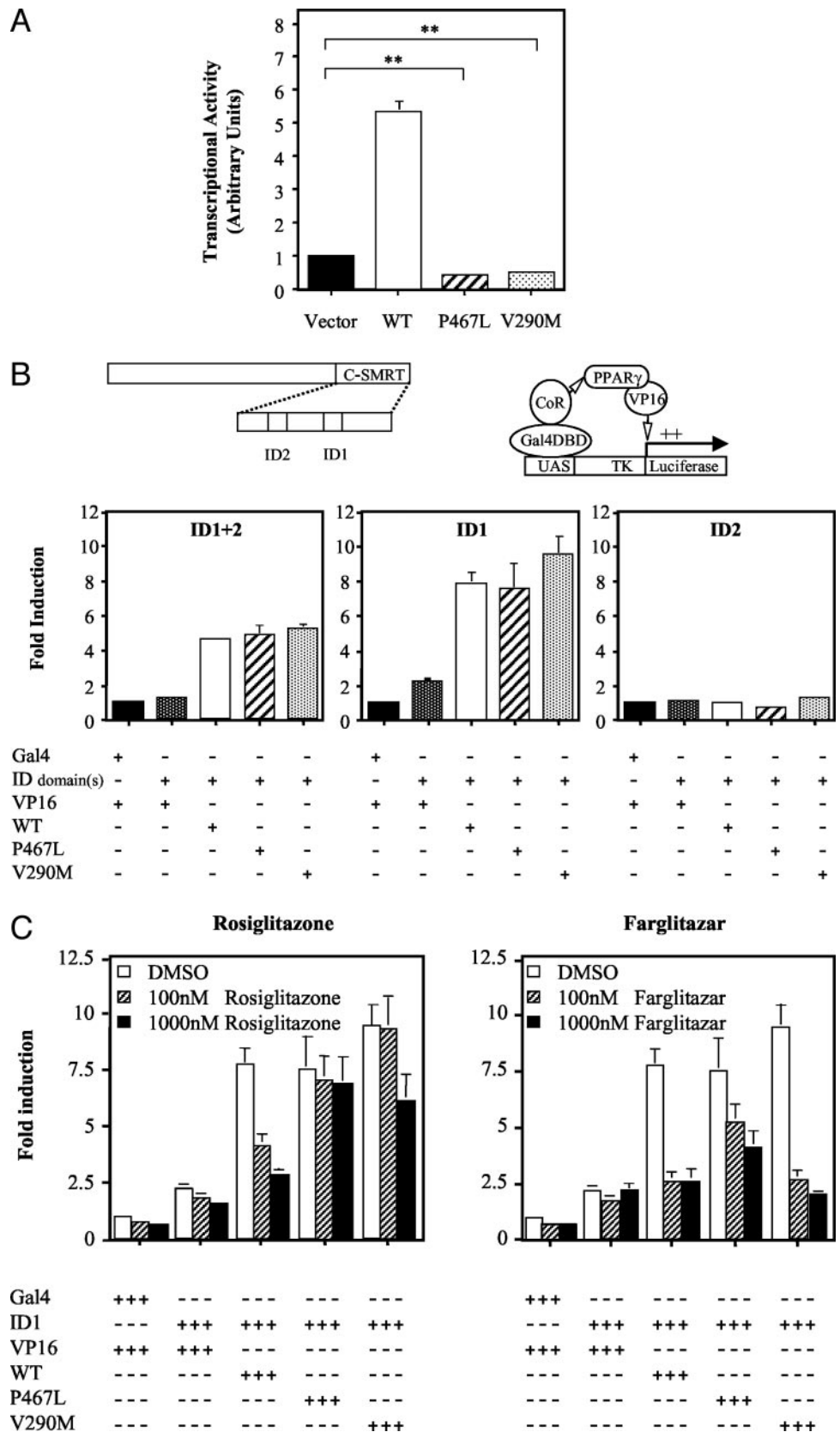


FIG. 4. PPAR $\gamma$  mutants repress basal transcription and are recruited to the ID1 domain of the corepressor SMRT. A, Unlike their WT counterpart, both the P467L and V290M mutants silence basal gene transcription. 293EBNA cells were transfected with 500 ng reporter gene (PPARETKLUC), 100 ng Bos- $\beta$ -gal (internal control), and 100 ng of receptor construct (empty vector, WT, P467L, or V290M). B, WT and mutant PPAR $\gamma$  interact with the ID1 domain of SMRT. 293EBNA cells were transfected with 500 ng of the reporter construct UASTKLUC, 100 ng of the internal control Bos- $\beta$ -gal, 50 ng of expression vectors encoding the Gal4 DNA-binding domain (Gal4) alone or fused to the ID1, ID2, or ID1 + 2 domains of SMRT, and 50 ng of expression vector encoding VP16 alone or VP16 fused to the LBD of WT PPAR $\gamma$  (WT), P467L PPAR $\gamma$  (P467L), or V290M PPAR $\gamma$  (V290M). C, Farglitazar is more effective than rosiglitazone in promoting corepressor dissociation from mutant PPAR $\gamma$ . 293EBNA cells were transfected as in B and treated with vehicle (dimethylsulfoxide, DMSO), rosiglitazone, or farglitazar. \*\*,  $P < 0.001$ .

significantly attenuated and incomplete dissociation from a Gal4-ID1 corepressor fusion when compared with the WT receptor (Fig. 4C). However, the addition of TA (farglitazar) induced progressive and nearly complete dissociation of both mutant receptors from Gal4-ID1 in a manner comparable with WT PPAR $\gamma$  (Fig. 4C).

Our previous studies indicated that inhibition of WT receptor function by the P467L and V290M PPAR $\gamma$  mutants is a likely mechanism for impaired receptor action *in vivo* (10). We therefore compared the relative efficacy of both natural and synthetic agonists in ameliorating such dominant-negative inhibition by PPAR $\gamma$  mutants. Cells transfected with WT receptor plus an equal amount of either P467L or V290M PPAR $\gamma$  mutants were studied with increasing concentrations of natural (15d-PGJ<sub>2</sub>) or synthetic ligands (rosiglitazone or farglitazar). In keeping with their transcriptional activities with each ligand when tested alone, the P467L and V290M mutants exhibited significant dominant-negative inhibition (30–35%) of WT receptor function even at maximal concentrations of 15d-PGJ<sub>2</sub> (Fig. 5). Moreover, both mutants exerted strong dominant-negative activity at low (10 nM) concentrations of TZD, and such inhibition was retained at higher (1  $\mu$ M) levels of ligand with the V290M mutant (Fig. 5). In contrast, low (10 nM) or high (1  $\mu$ M) concentrations of farglitazar completely reversed dominant-negative inhibition by the PPAR $\gamma$  mutants (Fig. 5).

Failure of ligand-dependent corepressor release has been shown to mediate dominant-negative inhibition by natural TR $\beta$  mutants in RTH (32). We therefore sought to determine whether corepressor interaction is important for dominant-negative activity of the natural PPAR $\gamma$  mutants. The crystal

structure of a PPAR $\alpha$ -SMRT complex has recently been elucidated (21), and residues in PPAR $\alpha$  that mediate binding to a polypeptide from SMRT are highly conserved in PPAR $\gamma$  (see Fig. 8B). One of these conserved residues in PPAR $\gamma$  (Leu 318) was mutated to alanine on either WT or P467L mutant PPAR $\gamma$  backgrounds, with comparison of their transcriptional properties in the absence of ligand. The L318A receptor mutant showed comparable constitutive activity to WT PPAR $\gamma$ ; however, the P467L/L318A double mutation exhibited attenuated repression of basal transcription when compared with the P467L mutant (Fig. 6A: pcDNA3 = 1.0; P467L = 0.48; P467L/L318A = 0.85). Consistent with this, in a mammalian two-hybrid assay, the L318A mutation abolished interaction of the P467L mutant with the ID1 domain of SMRT corepressor (Fig. 6A, *inset*). Moreover, in comparison with the P467L mutation alone, the P467L/L318A double mutant exhibited almost negligible dominant-negative inhibition of WT PPAR $\gamma$  activity (Fig. 6B).

The adipocyte P2 (aP2) gene, a well-validated PPAR $\gamma$  target gene, has previously been shown to be expressed and regulated by PPAR $\gamma$  ligands in PBMCs (33). To determine whether the differences in mutant PPAR $\gamma$  responses to synthetic agonists observed *in vitro* might correlate with ligand-dependent responses in cells from our affected subjects, we examined the ability of both rosiglitazone and farglitazar to induce aP2 expression in cultured PBMCs taken from the index case harboring the P467L mutation (10). Rosiglitazone induced aP2 expression in patient PBMCs in a dose-dependent manner, but with farglitazar the dose-response curve of the target gene activation was significantly left shifted (Fig. 7). The magnitude of maximal aP2 target gene induction in

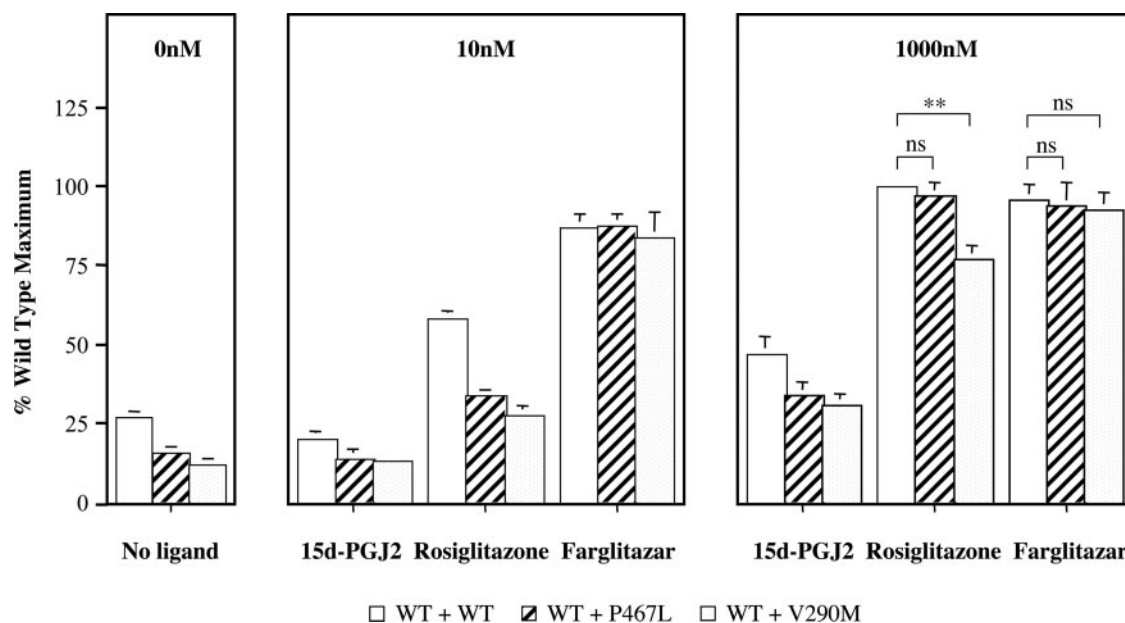


FIG. 5. TA (farglitazar) reverses dominant-negative inhibition by PPAR $\gamma$  mutants more fully than natural ligand (15d-PGJ<sub>2</sub>) or thiazolidinedione (rosiglitazone). 293EBNA cells were transfected with 100 ng of WT receptor plus an equal amount of either WT or mutant (P467L; V290M) expression vector (with the same reporter gene and internal control constructs as described in Fig. 1) in the presence of increasing concentrations of ligand. The transcriptional responses mediated by either 100 or 200 ng of WT receptor were virtually identical (data not shown). Results are expressed as a percentage of the WT maximum response. \*\*,  $P < 0.001$ ; ns, not significant.

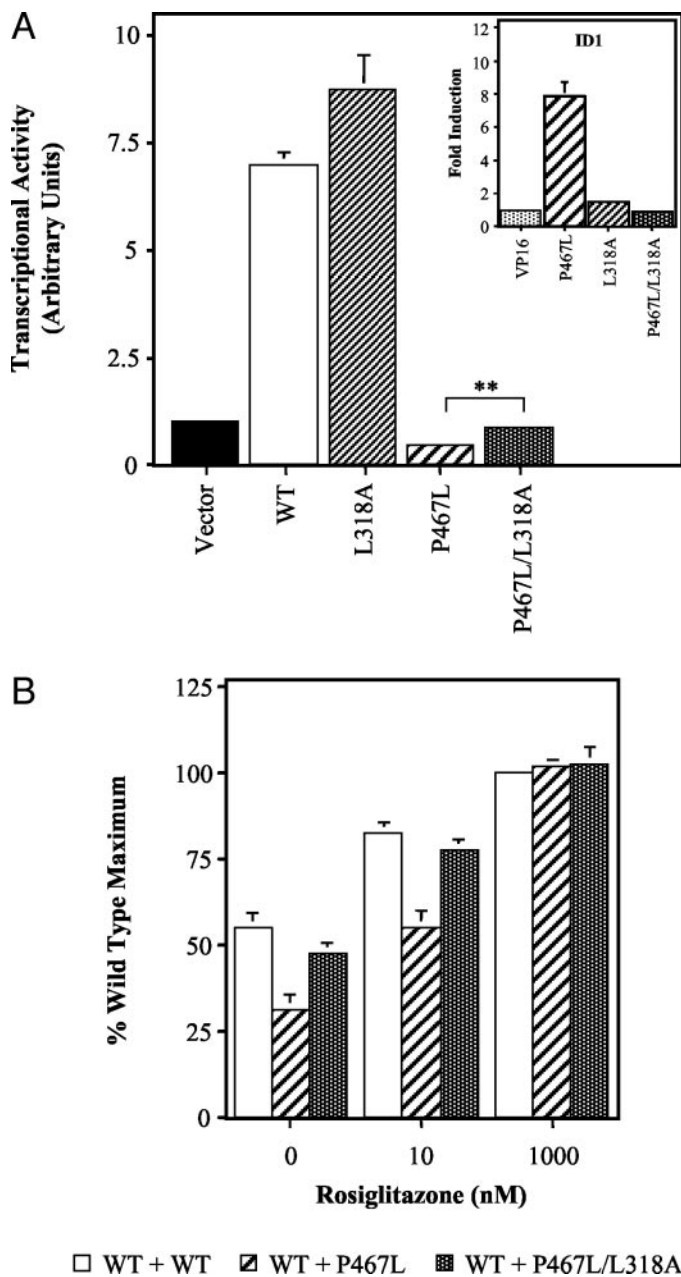


FIG. 6. Introduction of the L318A mutation attenuates both transcriptional repression and dominant-negative activity of P467L through abolition of its interaction with corepressor. A, Basal transcriptional repression by the P467L natural mutant is reversed, but constitutive activity of WT PPAR $\gamma$  is not affected by the addition of an L318A mutation. *Inset*, Interaction of P467L with the ID1 domain of SMRT is abolished after introduction of the L318A mutation. 293EBNA cells were transfected and results analyzed as in Fig. 4, A and B. B, Introduction of the L318A mutation significantly attenuates the dominant-negative activity of P467L. 293EBNA cells were transfected as in Fig. 5 and treated with vehicle (dimethylsulfoxide, DMSO) or rosiglitazone. \*\*,  $P < 0.001$ .

response to either ligand was similar. The results suggest that the tyrosine agonist is a more potent activator of PPAR $\gamma$ -mediated transcription than its thiazolidinedione counterpart in primary cells from an affected subject.

## Discussion

We have previously described two different heterozygous, loss-of-function mutations (P467L, V290M) in the LBD of human PPAR $\gamma$ . Affected individuals exhibited marked hyperinsulinemia and the skin lesion acanthosis nigricans, signifying severe insulin resistance; importantly, subjects had developed complications secondary to insulin resistance, including characteristic dyslipidemia (elevated triglycerides, low high-density lipoprotein cholesterol), ovarian dysfunction, and T2DM; they also showed early-onset hypertension unrelated to diabetic comorbidity (10). Whereas both receptor mutants were markedly functionally impaired and dominant-negative inhibitors of wild-type receptor action, they retained some transcriptional activity at the highest concentrations of ligand (10). We therefore reasoned that if either higher levels of endogenous natural ligands or synthetic receptor agonists could overcome the functional defect and dominant-negative inhibition by PPAR $\gamma$  mutants *in vitro*, they might be useful to treat the severe clinical phenotype when administered *in vivo*.

Despite being able to activate transcription via WT PPAR $\gamma$ , even micromolar concentrations of putative endogenous ligands, including omega-3 ( $\gamma$ -linolenic) and omega-6 (linoleic, arachidonic) polyunsaturated fatty acids, eicosanoids (13-HODE, 15-HETE) and 15d-PGJ<sub>2</sub>, were unable to induce transcriptional activity from the mutant receptors (Fig. 1). Furthermore, high levels of 15d-PGJ<sub>2</sub> were unable to reverse significant dominant-negative inhibition of WT receptor function by the P467L and V290M PPAR $\gamma$  mutants (Fig. 5). Such unresponsiveness of mutant receptors to endogenous ligands correlates with recent clinical findings of partial lipodystrophy in adults and significant insulin resistance, even in two young children aged 4 and 7 yr with the P467L mutation (11), which underscore the severity of the clinical

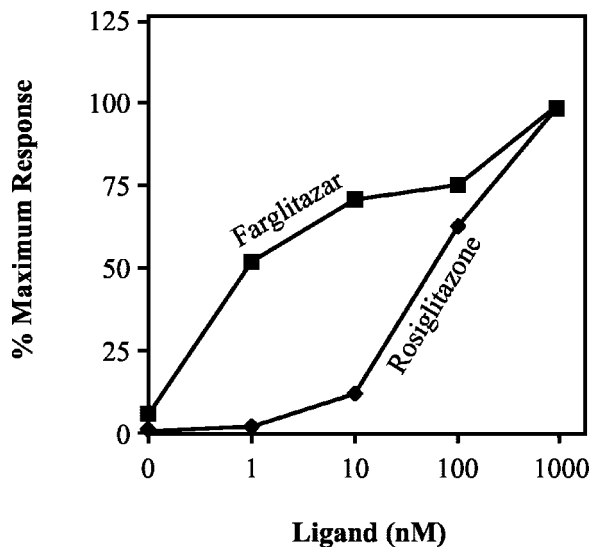


FIG. 7. The TA (farglitazar) enhances target gene (aP2) expression in P467L mutant receptor containing PBMCs more effectively than thiazolidinedione (rosiglitazone). After 24 h exposure to increasing concentrations of rosiglitazone or farglitazar, aP2 gene expression in PBMCs was quantitated by RT-PCR. The results are expressed as a percentage of the maximum observed response. The SEM was less than 10% and has been omitted for clarity.

phenotype. In addition, such unresponsiveness *in vitro* suggests that raising levels of endogenous PPAR $\gamma$  ligands in affected subjects is unlikely to be a successful therapeutic approach.

With thiazolidinedione PPAR $\gamma$  agonists, both the lower-affinity (WT PPAR $\gamma$  EC<sub>50</sub> = 500 nM) agents, troglitazone and pioglitazone, and the more potent (WT PPAR $\gamma$  EC<sub>50</sub> = 43 nM) rosiglitazone, induced significant transcriptional activity with the P467L and V290M mutants only at 10- or 1- $\mu$ M concentrations of ligand, respectively (Fig. 2, C–E). A novel class of synthetic PPAR $\gamma$  ligands (GW1929, GW7845, and farglitazar), where *N*-tyrosine moieties have been substituted for the 2,4-thiazolidinedione head group, have been developed (34) and are known to be higher-affinity (EC<sub>50</sub> = 0.3–6 nM) agonists for WT PPAR $\gamma$ . In marked contrast to TZDs, the TAs proved capable of rescuing mutant PPAR $\gamma$  function, even at low concentrations of ligand (1–10 nM), eliciting a maximal transcriptional response comparable with WT receptor (Fig. 2, F–H). Furthermore, the greater potency of tyrosine *vs.* thiazolidinedione agonist is more marked with the PPAR $\gamma$  mutants than WT receptor, indicating that this class of ligand acts specifically to restore mutant receptor function.

Further comparisons of rosiglitazone *vs.* farglitazar indicated that the ability of the TA to correct deficits in ligand binding, coactivator recruitment and corepressor displacement mediated its enhancement of mutant receptor function (Figs. 3 and 4). To elucidate the molecular basis for the observed differences between the two classes of PPAR $\gamma$  ligand, we examined the crystal structures of the PPAR $\gamma$ /retinoid X receptor- $\alpha$  heterodimer (35) complexed with either rosiglitazone or farglitazar. In keeping with other nuclear receptors, an amphipathic  $\alpha$ -helix (H12) at the receptor carboxyterminus mediates important interactions with both ligand and coactivator (steroid receptor coactivator-1) (36): in both crystal structures, Tyr473 makes contact with ligand, forming hydrogen bonds with either the 2,4-thiazolidinedione head group of rosiglitazone or the carboxylate head group of farglitazar; the side chain of Leu468 from the opposite side of H12 contributes to a hydrophobic cleft on the receptor surface, which accommodates the coactivator peptide, whereas Glu471 acts in concert with Lys301 to form a charge clamp that stabilizes interaction with coactivator. Pro467 forms the amino-terminal boundary of helix 12 and Val290 (within helix 3) packs against H12. We have previously demonstrated, using fluorescence anisotropy, that mutation of either residue disrupts the position and orientation of helix 12, thereby compromising interactions with both ligand and coactivator (20). Inspection of the TZD *vs.* TA-bound PPAR $\gamma$  structures reveals that farglitazar occupies more (~40% *vs.* 25%) of the ligand-binding pocket with a 5-methyl-2-phenyloxazole tail and benzophenone head group, making additional hydrophobic interactions in the cavity, which probably account for its increased PPAR $\gamma$ -binding affinity, compared with rosiglitazone (35) (Fig. 8A).

Unlike a subset of nuclear receptors (including TR and RAR), which are capable of repressing basal transcription in the absence of ligand through recruitment of corepressor proteins such as NCoR (29) and SMRT (23), WT PPAR $\gamma$  exhibits constitutive transcriptional activity (Fig. 4A) (28).

Whether such activity represents receptor activation by endogenous PPAR $\gamma$  ligands or is an intrinsic property of unliganded PPAR $\gamma$ , with H12 being in an active conformation in the apo-receptor crystal structure (36), remains unclear. In contrast, both the P467L and V290M PPAR $\gamma$  mutants not only lacked such constitutive activity but also acted as potent transcriptional repressors in the absence of exogenous ligand (Fig. 4A). These properties are similar to those of artificial dominant-negative human [L468A/E471A (37)] and murine [L466A (38)] PPAR $\gamma$  mutants described previously. However, in a two-hybrid assay, both WT and natural PPAR $\gamma$  mutants interacted with corepressor (Fig. 4B). To reconcile these apparently discordant observations, we suggest that corepressor is greatly overexpressed relative to endogenous coactivators in the two-hybrid assay, probably promoting its interaction with WT PPAR $\gamma$  in a manner that is not relevant to its normal action in cells containing more physiological levels of each cofactor type. Evidence in favor of this notion is provided by our observation that the introduction of a mutation (L318A), which disrupts corepressor interaction with both WT PPAR $\gamma$  and the P467L mutant, has no discernible effect on the constitutive transcriptional activity of WT receptor, whereas it reverses transcriptional silencing and dominant-negative inhibition by the P467L mutant (Fig. 6, A and B).

The ability to silence basal gene transcription is also a characteristic of dominant-negative inhibition by mutant nuclear receptors in other disorders, *e.g.* TR $\beta$  mutants in RTH (32), the promyelocytic leukemia-RAR fusion protein in acute promyelocytic leukemia (39), and the oncogene *v-erbA* (40). Furthermore, some TR $\beta$  mutants in RTH have been shown to interact aberrantly with corepressor, exhibiting failure to dissociate fully with ligand (41, 42) and corepressor interaction with PLZF-RAR fusions in acute promyelocytic leukemia is refractory to retinoic acid treatment (39, 43, 44). In this context, both PPAR $\gamma$  mutants exhibited delayed and incomplete corepressor release in the presence of saturating levels (1  $\mu$ M) of rosiglitazone (Fig. 4C), whereas a moderate concentration (100 nM) of farglitazar promoted near normal dissociation of corepressor (Fig. 4C). Furthermore, such failure of natural PPAR $\gamma$  mutants to release corepressor fully with TZD is analogous to the properties of the artificial helix 12 PPAR $\gamma$  mutants (L468A/E471A; L466A) described previously (37, 38).

Recently the crystal structure of a ternary complex consisting of the PPAR $\alpha$  LBD bound to an antagonist and a polypeptide motif from the corepressor SMRT has been solved (21). Notable features of this structure include displacement of helix 12 such that it adopts a different position, compared with its active conformation in the agonist-bound structure, and docking of a SMRT motif in a hydrophobic groove formed by helices 3, 4, and 5 of the receptor. The LBDs of PPAR $\gamma$  and PPAR $\alpha$  are similar (~71% homology) and an alignment of residues in helix 3 from the receptors (Fig. 8B) indicates striking homology, with 13 of 14 amino acids mediating PPAR $\alpha$ -SMRT interaction being identical in PPAR $\gamma$ . These observations permit crystallographic modeling to provide insights into how the natural PPAR $\gamma$  mutations (P467L, V290M) facilitate interaction with corepressor. Both mutations destabilize helix 12, preventing it from adopting the

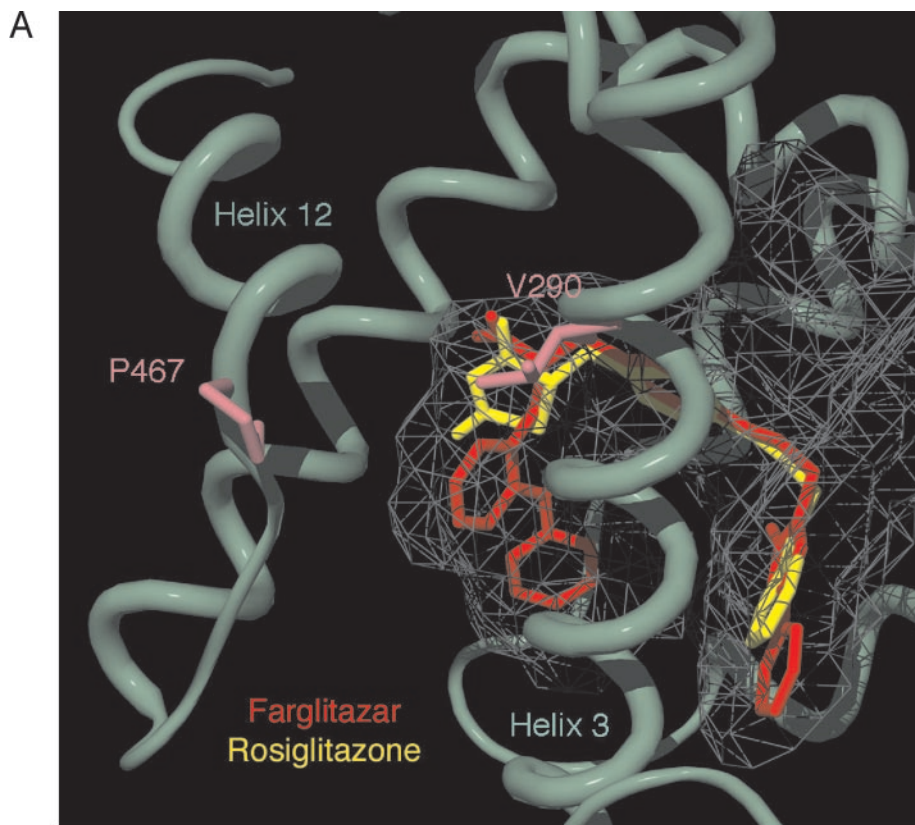
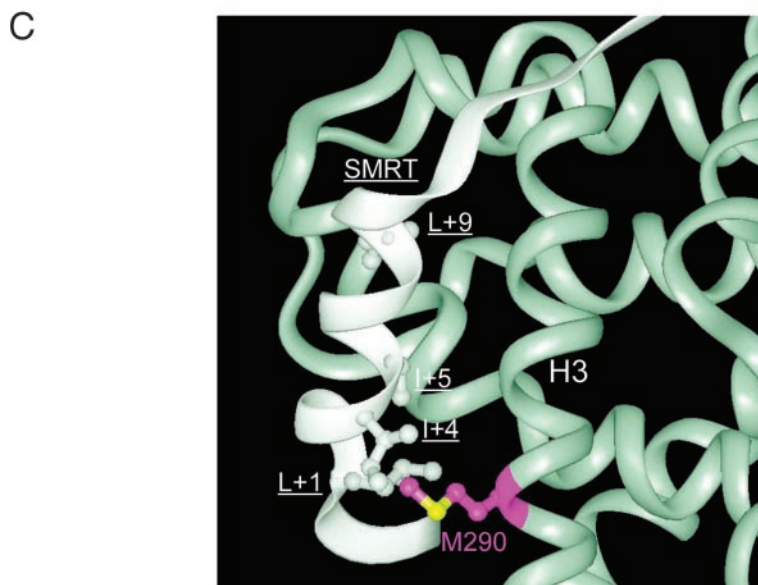


**FIG. 8. A,** Crystallographic modeling demonstrating how the TA (farglitazar) may preferentially stabilize helix 12 in mutant PPAR $\gamma$ . Superimposition of PPAR $\gamma$  structures bound to either tyrosine (farglitazar) or thiazolidinedione (rosiglitazone) agonists showing part of the cavities (*gray mesh*) containing either ligand. On the helical backbone (*green*), the side chains (*pink*) of residues (P467, V290), mutated in our patients with severe insulin resistance, are depicted. Both mutations are predicted to disrupt the orientation of helix 12 as described previously (10), thereby perturbing known important interactions of this helix with ligand [rosiglitazone (*yellow*) or farglitazar (*red*)] and coactivator. **B,** An alignment of amino acid sequences corresponding to the corepressor interaction interface in PPAR $\alpha$  in the three receptor subtypes. Residues in PPAR $\alpha$  mediating contact with the SMRT motif are highlighted (\*), and boxes denote complete conservation of 13 of 14 of these amino acids between the receptors. L318 in PPAR $\gamma$  is denoted in *bold*. **C,** A molecular model showing interface between SMRT (*white*) and PPAR $\gamma$  (*green*) with the V290M mutation (*purple*). The key SMRT residues that form the interface (I+4, I+5, L+1, L+9) are numbered as reported in the PPAR $\alpha$ /SMRT crystal structure (21).

**B**

PPAR $\alpha$	281	V	E	T	V	T	E	L	T	E	F	A	K	A	I	P	G	F	A	N	L	D	L	N	D	Q	V	T	L	L	K	Y	G	V	Y	314
PPAR $\gamma$	290	V	E	A	V	Q	E	I	T	E	Y	A	K	S	I	P	G	F	V	L	N	D	L	N	D	Q	V	T	L	L	K	Y	G	V	H	323
PPAR $\delta$	254	V	E	T	V	R	E	L	T	E	F	A	K	S	I	P	S	F	S	S	L	F	L	N	D	Q	V	T	L	L	K	Y	G	V	H	287



agonist-bound conformation (20). By analogy with the altered conformation of helix 12 in the antagonist-bound PPAR $\alpha$ /SMRT structure, we suggest that such displacement of H12 in the natural PPAR $\gamma$  mutants favors corepressor

recruitment. In addition, with the V290M mutation, an additional factor may stabilize corepressor binding. A crystallographic model of PPAR $\gamma$  complexed with SMRT (Fig. 8C) shows that the side chain of V290 is in contact with an

isoleucine residue (I + 4) of the SMRT motif. However, the interaction is relatively weak due to the distance ( $\sim 4$  Å) between the isoleucine and valine residues and the fact that these hydrophobic side chains are partially solvent exposed. In contrast, when residue 290 is substituted by methionine, its extended side chain has improved van der Waals contacts, predicting stabilization of corepressor interaction.

Whereas both PPAR $\gamma$  mutants inhibited WT receptor function significantly at lower (10 nM) concentrations of rosiglitazone (Fig. 5), the same concentration of farglitazar fully relieved dominant-negative inhibition by both mutant receptors (Fig. 5). To determine whether differential responses of the mutant receptors to the two ligands *in vitro* might translate into differences in clinical efficacy *in vivo*, we compared the ability of both rosiglitazone and farglitazar to induce PPAR $\gamma$  target gene (aP2) expression in PBMCs from one patient with the P467L receptor mutation. As anticipated, even at low concentrations (1–10 nM), farglitazar evoked a greater target gene response from mutant PBMCs than was observed with rosiglitazone, indicating greater efficacy of the tyrosine agonist *vs.* its TZD counterpart (Fig. 7). Although peak plasma drug levels after oral administration of farglitazar (5 mg) are slightly lower (300 nM) (45) than after 8 mg (1  $\mu$ M) of rosiglitazone (46), our studies indicate that they still exceed concentrations required to restore the function and abrogate dominant-negative activity of mutant receptors *in vitro*. Accordingly, the tyrosine-based PPAR $\gamma$  agonist may have greater potential efficacy *in vivo*, and future clinical studies will determine whether it does represent a more rational therapeutic approach to treating the severe insulin resistance in our affected patients.

### Acknowledgments

We thank Dr. Xue-Ming Shen for HPLC radiochemical purity analysis, Ms. Tong Ni for radioactive concentration analysis, and Dr. Alan Freyer for NMR assignments. We also acknowledge the secretarial expertise of Mrs. T. D. Wallman.

Received September 23, 2003. Accepted November 24, 2003.

Address all correspondence and requests for reprints to: V. K. Chatterjee, Department of Medicine, University of Cambridge, Level 5, Box 157, Addenbrooke's Hospital, Hills Road, Cambridge CB2 2QQ, United Kingdom. E-mail:kkc1@mole.bio.cam.ac.uk.

This work was supported by the Wellcome Trust (to V.K.C., S.O., and M.G.), a European Union network grant (to J.S. and V.K.C.), and the Raymond and Beverly Sackler Foundation (to M.G.).

M.A. and M.G. contributed equally to this work.

### References

- Tontonoz P, Hu E, Graves RA, Budavari AI, Spiegelman BM 1994 mPPAR $\gamma$ 2: tissue-specific regulator of an adipocyte enhancer. *Genes Dev* 8:1224–1234
- Tontonoz P, Hu E, Spiegelman BM 1994 Stimulation of adipogenesis in fibroblasts by PPAR $\gamma$ 2, a lipid-activated transcription factor. *Cell* 79:1147–1156
- Kliwer SA, Sundseth SS, Jones SA, Brown PJ, Wisely GB, Koble CS, Devchand P, Wahli W, Willson TM, Lenhard JM, Lehmann JM 1997 Fatty acids and eicosanoids regulate gene expression through direct interactions with peroxisome proliferator-activated receptors  $\alpha$  and  $\gamma$ . *Proc Natl Acad Sci USA* 94:4318–4323
- Desvergne B, Wahli W 1999 Peroxisome proliferator-activated receptors: nuclear control of metabolism. *Endocr Rev* 20:649–688
- Huang JT, Welch JS, Ricote M, Binder CJ, Willson TM, Kelly C, Witztum JL, Funk CD, Conrad D, Glass CK 1999 Interleukin-4-dependent production of PPAR- $\gamma$  ligands in macrophages by 12/15-lipoxygenase. *Nature* 400:378–382
- Nagy L, Tontonoz P, Alvarez JG, Chen H, Evans RM 1998 Oxidized LDL regulates macrophage gene expression through ligand activation of PPAR $\gamma$ . *Cell* 93:229–240
- Forman BM, Tontonoz P, Chen J, Brun RP, Spiegelman BM, Evans RM 1995 15-Deoxy- $\Delta$ 12, 14-prostaglandin J2 is a ligand for the adipocyte determination factor PPAR $\gamma$ . *Cell* 83:803–812
- Kliwer SA, Lenhard JM, Willson TM, Patel I, Morris DC, Lehmann JM 1995 A prostaglandin J2 metabolite binds peroxisome proliferator-activated receptor  $\gamma$  and promotes adipocyte differentiation. *Cell* 83:813–819
- Lehmann JM, Moore LB, Smith-Oliver TA, Wilkison WO, Willson TM, Kliwer SA 1995 An antidiabetic thiazolidinedione is a high affinity ligand for peroxisome proliferator-activated receptor  $\gamma$  (PPAR $\gamma$ ). *J Biol Chem* 270:12953–12956
- Barroso I, Gurnell M, Crowley VEF, Agostini M, Schwabe JW, Soos MA, Maslen GLL, Williams TDM, Lewis H, Schafer AJ, Chatterjee VKK, O'Rahilly S 1999 Dominant-negative mutations in human PPAR $\gamma$  are associated with severe insulin resistance, diabetes mellitus and hypertension. *Nature* 402:880–883
- Savage DB, Tan GD, Acerini CL, Jebb SA, Agostini M, Gurnell M, Williams R, Umpleby AM, Thomas EL, Bell JD, Dixon AK, Cinti S, Vidal-Puig A, Karpe F, Chatterjee VKK, O'Rahilly S 2003 Clinical and pathophysiological features of a metabolic syndrome resulting from mutations in the nuclear receptor PPAR $\gamma$ . *Diabetes* 52:910–917
- Agarwal AK, Garg A 2002 A novel heterozygous mutation in peroxisome proliferator-activated receptor- $\gamma$  gene in a patient with familial partial lipodystrophy. *J Clin Endocrinol Metab* 87:408–411
- Hegele RA, Cao H, Frankowski C, Mathews ST, Leff T 2002 PPARG F388L, a transactivation-deficient mutant, in familial partial lipodystrophy. *Diabetes* 51:3586–3590
- Refetoff S, Weiss RE, Usala SJ 1993 The syndromes of resistance to thyroid hormone. *Endocr Rev* 14:348–399
- Collingwood TN, Adams M, Tone Y, Chatterjee VKK 1994 Spectrum of transcriptional dimerization and dominant negative properties of twenty different mutant thyroid hormone  $\beta$  receptors in thyroid hormone resistance syndrome. *Mol Endocrinol* 8:1262–1277
- Hayashi Y, Weiss RE, Sarne DH, Yen PM, Sunthornthepvarakul T, Marcocci C, Chin WW, Refetoff S 1995 Do clinical manifestations of resistance to thyroid hormone correlate with the functional alteration of the corresponding mutant thyroid hormone  $\beta$  receptors? *J Clin Endocrinol Metab* 80:3246–3256
- Krentz AJ, Bailey CJ, Melander A 2000 Thiazolidinediones for type 2 diabetes. New agents reduce insulin resistance but need long term clinical trials. *BMJ* 321:252–253
- Brown KK, Henke BR, Blanchard SG, Cobb JE, Mook R, Kaldor I, Kliwer SA, Lehmann JM, Lenhard JM, Harrington WW, Novak PJ, Faison W, Binz JG, Hashim MA, Oliver WO, Brown HR, Parks DJ, Plunket KD, Tong WQ, Menius JA, Adkison K, Noble SA, Willson TM 1999 A novel N-aryl tyrosine activator of peroxisome proliferator-activated receptor- $\gamma$  reverses the diabetic phenotype of the Zucker diabetic fatty rat. *Diabetes* 48:1415–1424
- Fiedorek FT, Wilson GG, Frith L, Patel J, Abou-Donia M 2000 Monotherapy with G1262570, a tyrosine-based non-thiazolidinedione PPAR $\gamma$  agonist, improves metabolic control in type 2 diabetes mellitus patients. *Diabetes* 49(Suppl 1):157-OR (Abstract)
- Kallenberger BC, Love JD, Chatterjee VK, Schwabe JW 2003 A dynamic mechanism of nuclear receptor activation and its perturbation in a human disease. *Nat Struct Biol* 10:136–140
- Xu HE, Stanley TB, Montana VG, Lambert MH, Shearer BG, Cobb JE, McKee DD, Galardi CM, Plunket KD, Nolte RT, Parks DJ, Moore JT, Kliwer SA, Willson TM, Stimmel JB 2002 Structural basis for antagonist-mediated recruitment of nuclear co-repressors by PPAR $\alpha$ . *Nature* 415:813–817
- Tone Y, Collingwood TN, Adams M, Chatterjee VKK 1994 Functional analysis of a transactivation domain in the thyroid hormone  $\beta$  receptor. *J Biol Chem* 269:31157–31161
- Chen JD, Evans RM 1995 A transcriptional corepressor that interacts with nuclear hormone receptors. *Nature* 377:454–457
- Nagy L, Kao H-Y, Love JD, Li C, Banayo E, Gooch JT, Chatterjee VKK, Evans RM, Schwabe JWR 1999 Mechanism of co-repressor binding and release from nuclear hormone receptors. *Genes Dev* 13:3209–3216
- Shu AYL, Saunders D, Levinson SH, Landvatter SW, Mahoney A, Senderoff SG, Mack JF, Heys JR 1999 Direct tritium labeling of multifunctional compounds using organoiridium catalysis. *J Labelled Comp Radiopharm* 42:797–807
- Adams M, Matthews CH, Collingwood TN, Tone Y, Beck Peccoz P, K CVK 1994 Genetic analysis of twenty-nine kindreds with generalised and pituitary resistance to thyroid hormone. *J Clin Invest* 94:506–515
- Savage DB, Sewter CP, Klenk ES, Segal DG, Vidal-Puig A, Considine RV, O'Rahilly S 2001 Resistin/Fizz3 expression in relation to obesity and peroxisome proliferator-activated receptor- $\gamma$  action in humans. *Diabetes* 50:2199–2202
- Zamir I, Zhang J, Lazar MA 1997 Stoichiometric and steric principles governing repression by nuclear hormone receptors. *Genes Dev* 11:835–846
- Horlein AJ, Naar AM, Heinzel T, Torchia J, Gloss B, Kurokawa R, Ryan A, Kamei Y, Soderstrom M, Glass CJ, Rosenfeld MG 1995 Ligand-independent repression by the thyroid hormone receptor mediated by a nuclear receptor corepressor. *Nature* 377:397–404

30. **Hu X, Lazar MA** 1999 The CoNRN motif controls the recruitment of corepressors by nuclear hormone receptors. *Nature* 402:93–96
31. **Perissi V, Staszewski LM, McInerney EM, Kurokawa R, Kronen A, Rose DW, Lambert MH, Milburn MV, Glass CK, Rosenfeld MG** 1999 Molecular determinants of nuclear receptor-corepressor interaction. *Genes Dev* 13:3198–3208
32. **Yoh SM, Chatterjee VKK, Privalsky ML** 1997 Thyroid hormone resistance syndrome manifests as an aberrant interaction between mutant T3 receptors and transcriptional corepressors. *Mol Endocrinol* 11:470–480
33. **Pelton PD, Zhou L, Demarest KT, Burris TP** 1999 PPAR $\gamma$  activation induces the expression of the adipocyte fatty acid binding protein gene in human monocytes. *Biochem Biophys Res Commun* 261:456–458
34. **Henke BR, Blanchard SG, Brackeen MF, Brown KK, Cobb JE, Collins JL, Harrington WWJ, Hashim MA, Hull-Ryde EA, Kaldor I, Kliewer SA, Lake DH, Leesnitzer LM, Lehmann JM, Lenhard JM, Orband-Miller LA, Miller JF, Mook RAJ, Noble SA, Oliver WJ, Parks DJ, Plunket KD, Szewczyk JR, Willson TM** 1998 *N*-(2-Benzoylphenyl)-*L*-tyrosine PPAR $\gamma$  agonists. 1. Discovery of a novel series of potent antihyperglycemic and antihyperlipidemic agents. *J Med Chem* 41:5020–5036
35. **Gampe J, RT, Montana VG, Lambert MH, Miller AB, Bledsoe RK, Milburn MV, Kliewer SA, Willson TM, Xu HE** 2000 Asymmetry in the PPAR $\gamma$ /RXR $\alpha$  crystal structure reveals the molecular basis of heterodimerization among nuclear receptors. *Mol Cell* 5:545–555
36. **Nolte RT, Wisely BG, Westin S, Cobb JE, Lambert MH, Kurokawa R, Rosenfeld MG, Willson TM, Glass CK, Milburn MV** 1998 Ligand binding and coactivator assembly of the peroxisome proliferator-activated receptor- $\gamma$ . *Nature* 395:137–143
37. **Gurnell M, Wentworth JM, Agostini M, Adams M, Collingwood TN, Provenzano C, Browne PO, Rajanayagam O, Burris TP, Schwabe JW, Lazar MA, Chatterjee VKK** 2000 A dominant negative peroxisome proliferator-activated receptor  $\gamma$  (PPAR $\gamma$ ) mutant is a constitutive repressor and inhibits PPAR $\gamma$ -mediated adipogenesis. *J Biol Chem* 275:5754–5759
38. **Park Y, Freedman BD, Lee EJ, Park S, Jameson JL** 2003 A dominant negative PPAR $\gamma$  mutant shows altered cofactor recruitment and inhibits adipogenesis in 3T3-L1 cells. *Diabetologia* 46:365–377
39. **Lin JR, Nagy L, Satoshi I, Shao W, Miller W, Evans RM** 1998 Role of the histone deacetylase complex in acute promyelocytic leukaemia. *Nature* 391:811–814
40. **Damm K, Thompson CC, Evans RM** 1989 Protein encoded by *v-erbA* functions as a thyroid-hormone receptor antagonist. *Nature* 339:593–597
41. **Clifton-Bligh RJ, de Zegher F, Wagner RL, Collingwood TN, Francois I, van Helvoirt M, Chatterjee VKK** 1998 A novel TR $\beta$  mutation (R383H) in resistance to thyroid hormone predominantly impairs corepressor release and negative transcriptional regulation. *Mol Endocrinol* 12:609–621
42. **Safer JD, Cohen RN, Hollenberg AN, Wondisford FE** 1998 Defective release of corepressor by hinge mutants of the thyroid hormone receptor found in patients with resistance to thyroid hormone. *J Biol Chem* 273:30175–30182
43. **Grignani F, De Matteis S, Nervi C, Tomassoni L, Gelmetti V, Cioco M, Fanelli M, Ruthardt M, Ferrara FF, Zamir I, Seiser C, Lazar MA, Minucci S, Pelicci PG** 1998 Fusion proteins of the retinoic acid receptor- $\alpha$  recruit histone deacetylase in promyelocytic leukaemia. *Nature* 391:815–818
44. **He L-Z, Guidez F, Tribioli C, Peruzzi D, Ruthardt M, Zelent A, Pandolfi PP** 1998 Distinct interactions of PML-RAR $\alpha$  and PLZF-RAR $\alpha$  with co-repressors determine differential responses to RA in APL. *Nat Genet* 18:126–135
45. **Sorbera LA, Leeson PA, Martin L, Castaner J** 2001 Farglitazar. Antidiabetic PPAR $\gamma$  agonist. *Drugs of the Future* 26:354–363
46. **Cox PJ, Ryan DA, Hollis FJ, Harris AM, Miller AK, Vousden M, Cowley H** 2000 Absorption, disposition, and metabolism of rosiglitazone, a potent thiazolidinedione insulin sensitizer, in humans. *Drug Metab Dispos* 28:772–780

*Endocrinology* is published monthly by The Endocrine Society (<http://www.endo-society.org>), the foremost professional society serving the endocrine community.



# Digenic inheritance of severe insulin resistance in a human pedigree

David B. Savage<sup>1,2\*</sup>, Maura Agostini<sup>2\*</sup>, Inês Barroso<sup>3\*</sup>, Mark Gurnell<sup>2\*</sup>, Jian'an Luan<sup>4\*</sup>, Aline Meirhaeghe<sup>1,2</sup>, Anne-Helen Harding<sup>4</sup>, Gudrun Ihrke<sup>1</sup>, Odelia Rajanayagam<sup>2</sup>, Maria A. Soos<sup>1,2</sup>, Stella George<sup>1,2</sup>, Dirk Berger<sup>1,2</sup>, E. Louise Thomas<sup>5</sup>, Jimmy D. Bell<sup>5</sup>, Karim Meeran<sup>6</sup>, Richard J. Ross<sup>7</sup>, Antonio Vidal-Puig<sup>1,2</sup>, Nicholas J. Wareham<sup>4</sup>, Stephen O'Rahilly<sup>1,2</sup>, V. Krishna K. Chatterjee<sup>2</sup> & Alan J. Schafer<sup>3</sup>

\*These authors contributed equally to this work.

Published online: 15 July 2002, doi:10.1038/ng926

**Impaired insulin action is a key feature of type 2 diabetes and is also found, to a more extreme degree, in familial syndromes of insulin resistance. Although inherited susceptibility to insulin resistance may involve the interplay of several genetic loci, no clear examples of interactions among genes have yet been reported. Here we describe a family in which five individuals with severe insulin resistance, but no unaffected family members, were compound heterozygous with respect to frameshift/premature stop mutations in two unlinked genes, *PPARG* and *PPP1R3A* these encode peroxisome proliferator activated receptor  $\gamma$ , which is highly expressed in adipocytes, and protein phosphatase 1, regulatory subunit 3, the muscle-specific regulatory subunit of protein phosphatase 1, which are centrally involved in the regulation of carbohydrate and lipid metabolism, respectively. That mutant molecules primarily involved in either carbohydrate or lipid metabolism can combine to produce a phenotype of extreme insulin resistance provides a model of interactions among genes that may underlie common human metabolic disorders such as type 2 diabetes.**

As part of an investigation into the etiology of inherited syndromes of severe insulin resistance<sup>1</sup>, we identified a European pedigree (family A) with several affected members (Fig. 1). The grandparents (individuals Ii and Iii) had typical late-onset type 2 diabetes with no clinical features of severe insulin resistance. Three of their six children and two of their grandchildren had acanthosis nigricans, a dermatological marker of extreme insulin resistance. All five individuals with acanthosis nigricans had markedly elevated fasting plasma insulin levels, indicative of severe insulin resistance (Fig. 1). Using mutational screening (Fig. 1a), we identified a heterozygous frameshift resulting in a premature stop mutation of *PPARG* (A<sup>553</sup>ΔAAAiT)fs.185(stop 186) that was present in the grandfather (Ii), all five relatives with severe insulin resistance and one other relative with normal insulin levels (IIvi). Further candidate-gene studies (Fig. 1b) revealed a heterozygous frameshift/premature stop mutation in *PPP1R3A* (C<sup>1984</sup>ΔAG)fs.662(stop 668) that was also present in this family. In this case, the mutation was present in the grandmother (Iii), in all five individuals with severe insulin resistance and in one other relative (IIIii). Thus, all five family members with severe insulin resistance, and no other family members,

were compound heterozygous with respect to two frameshift mutations of these two unlinked genes. Fasting insulin levels in the singly heterozygous and wildtype family members were within the normal range. By contrast, the compound heterozygotes showed extreme hyperinsulinemia (Fig. 1d) and, to a variable extent, diabetes, hyperlipidemia and hypertension (Fig. 1c and Table 1). As diabetes, hypertension or dyslipidemia were also present in some other members of the kindred, these phenotypes do not seem to require mutations in both *PPARG* and *PPP1R3A*.

We screened our cohort of probands with syndromes of severe insulin resistance ( $n = 129$ ) for the *PPARG* and *PPP1R3A* frameshift mutations. The *PPARG* frameshift mutation was not detected in any other individuals, whereas one European individual carried the same heterozygous frameshift mutation of *PPP1R3A* that was found in family A. This individual (IIi, family B) presented with acanthosis nigricans at age 20 years. He had a body mass index (BMI) of 36.5 kg m<sup>-2</sup> and a fasting insulin level of 437 pmol l<sup>-1</sup> (normal <80 pmol/l). He inherited the mutation from his moderately obese father (BMI 30 kg m<sup>-2</sup>), who also has marked hyperinsulinemia (fasting insulin 178 pmol l<sup>-1</sup>; Fig. 1e). The two other family members who did not carry these mutations were clinically and biochemically normal. Notably, subject IIIi (family B) subsequently lost 40 kg and reduced his BMI to 27 kg m<sup>-2</sup>. By that time, his fasting insulin level had fallen to 93 pmol l<sup>-1</sup>.

The PPAR $\gamma$  protein is a ligand-inducible transcription factor that regulates target gene transcription as a heterodimer with the retinoid X receptor (RXR)<sup>2</sup>. This heterodimeric complex can be activated synergistically by antidiabetic PPAR $\gamma$  agonists (thiazolidinediones) and RXR-specific ligands<sup>3</sup>. The modular structure of PPAR $\gamma$  consists of a central DNA-binding domain, an amino-terminal activation domain, and a carboxy-terminal ligand-binding domain (Fig. 1a). The frameshift/premature stop mutation reported here is predicted to lead to a mutant receptor that is truncated within the second zinc finger of the DNA-binding domain. This region is common to both the  $\gamma 1$  and  $\gamma 2$  isoforms of the receptor (Fig. 1a) and is crucial in mediating receptor interaction with PPAR-specific response elements (PPAREs) in target gene promoters. We therefore examined whether the PPAR $\gamma$  mutants could bind to DNA as heterodimers with RXR, using an electrophoretic mobility shift assay. Unlike

Departments of <sup>1</sup>Clinical Biochemistry and <sup>2</sup>Medicine, University of Cambridge, Addenbrooke's Hospital, Hills Road, Cambridge CB2 2QQ, UK. <sup>3</sup>Incyte Genomics, 3160 Porter Drive, Palo Alto, California, USA. <sup>4</sup>Department of Public Health, University of Cambridge, Addenbrooke's Hospital, Cambridge, UK. <sup>5</sup>The Robert Steiner MRI Unit, MRC Clinical Sciences Centre, Imperial College School of Medicine, Hammersmith Hospital, London, UK. <sup>6</sup>Department of Endocrinology, Imperial College Faculty of Medicine, Charing Cross and Hammersmith Hospitals, London, UK. <sup>7</sup>Division of Clinical Sciences, University of Sheffield, Sheffield, UK. Correspondence should be addressed to S.O'R. (e-mail: sorahill@hgmp.mrc.ac.uk).



their wildtype counterparts, neither mutant PPAR $\gamma$  isoform formed heterodimeric complexes when co-incubated with a radiolabeled probe encoding the acyl-CoA oxidase PPARE (Fig. 2a). Accordingly, and in contrast to wildtype receptors, neither mutant receptor mediated transactivation when cotransfected with a reporter gene containing the PPARE and increasing concentrations of the thiazolidinedione rosiglitazone (Fig. 2b). Moreover, unlike the previously reported, naturally occurring missense PPAR $\gamma$  mutants (Pro467Leu and Val290Met)<sup>1</sup>, the truncated mutant proteins did not show dominant-negative activity when co-expressed with the wildtype receptor (Fig. 2c).

Is a loss-of-function mutation in a single allele of *PPARG* a plausible contributor to insulin resistance? It has been shown that PPAR $\gamma$  agonists enhance insulin sensitivity<sup>4</sup>, and humans with dominant-negative mutations in *PPARG*<sup>1</sup> and mice with severe

PPAR- $\gamma$  deficiency<sup>5</sup> show marked insulin resistance. Heterozygous PPAR- $\gamma$ -deficient mice seem to be less insulin resistant than their wildtype littermates<sup>6,7</sup>, however. Although both individuals from family A who carry only the *PPARG* frameshift mutation have fasting insulin levels in the normal range, the co-occurrence of this mutation with the *PPP1R3A* frameshift mutation results in severe insulin resistance. This might seem to conflict with the findings in heterozygous *Pparg* mice. There are several possible explanations for this apparent discrepancy. First, the combination of a genetic defect in muscle glycogen synthesis with the haploid *PPARG* state has not yet been examined in mice. Second, although the particular *PPARG* mutation found in family A does not seem to exert a dominant-negative effect, it might have some properties distinct from a purely null allele. Finally, it is possible that species differences in adipose-tissue biochemistry<sup>8</sup> may mean

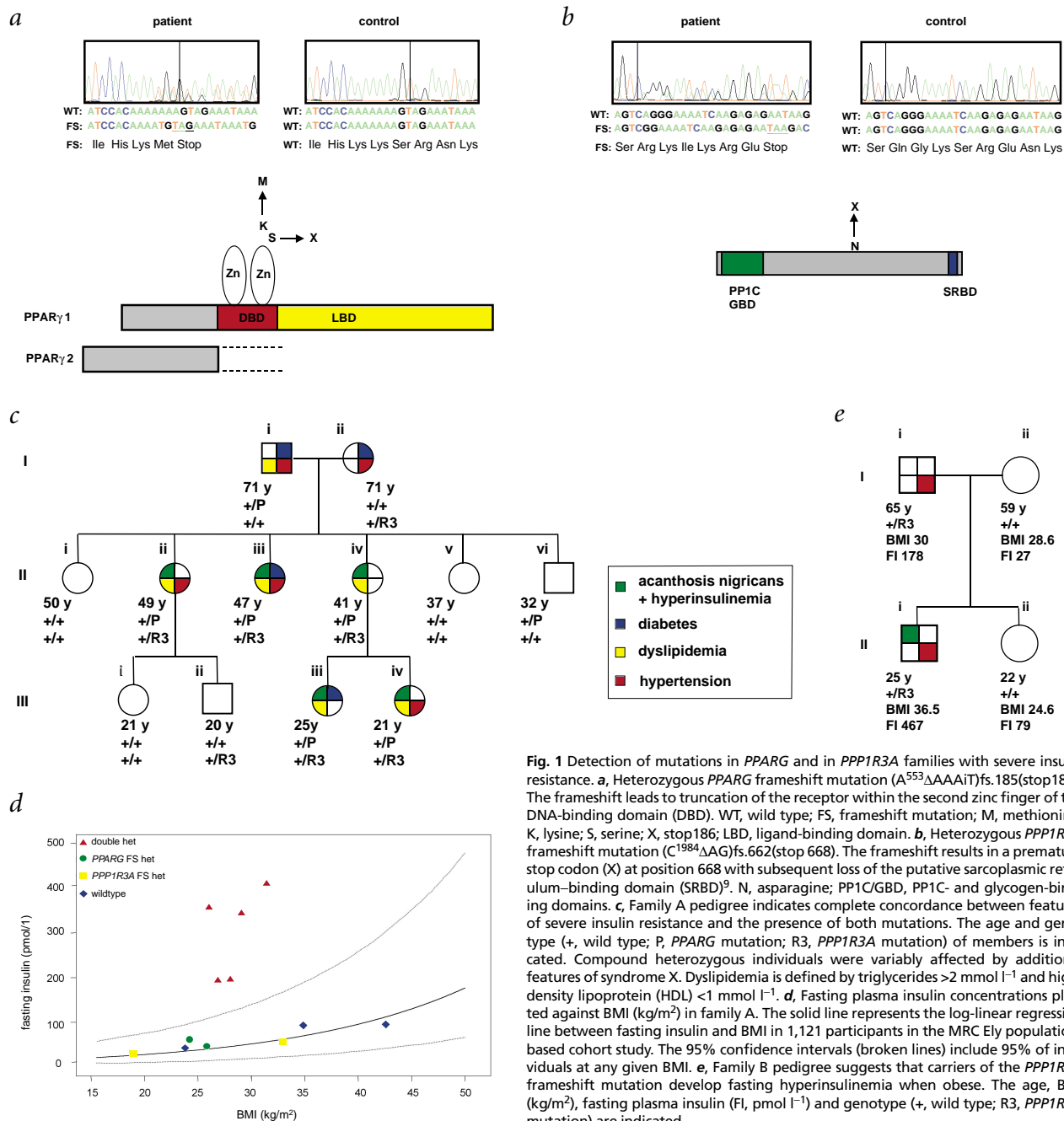


**Fig. 1** Detection of mutations in *PPARG* and *PPP1R3A* families with severe insulin resistance. **a**, Heterozygous *PPARG* frameshift mutation (A<sup>553</sup>ΔAAAiT)<sub>fs.185</sub>(stop186). The frameshift leads to truncation of the receptor within the second zinc finger of the DNA-binding domain (DBD). WT, wild type; FS, frameshift mutation; M, methionine; K, lysine; S, serine; X, stop186; LBD, ligand-binding domain. **b**, Heterozygous *PPP1R3A* frameshift mutation (C<sup>1984</sup>ΔAG)<sub>fs.662</sub>(stop 668). The frameshift results in a premature stop codon (X) at position 668 with subsequent loss of the putative sarcoplasmic reticulum-binding domain (SRBD)<sup>9</sup>. N, asparagine; PP1C/GBD, PP1C- and glycogen-binding domains. **c**, Family A pedigree indicates complete concordance between features of severe insulin resistance and the presence of both mutations. The age and genotype (+, wild type; P, *PPARG* mutation; R3, *PPP1R3A* mutation) of members is indicated. Compound heterozygous individuals were variably affected by additional features of syndrome X. Dyslipidemia is defined by triglycerides >2 mmol l<sup>-1</sup> and high-density lipoprotein (HDL) <1 mmol l<sup>-1</sup>. **d**, Fasting plasma insulin concentrations plotted against BMI (kg/m<sup>2</sup>) in family A. The solid line represents the log-linear regression line between fasting insulin and BMI in 1,121 participants in the MRC Ely population-based cohort study. The 95% confidence intervals (broken lines) include 95% of individuals at any given BMI. **e**, Family B pedigree suggests that carriers of the *PPP1R3A* frameshift mutation develop fasting hyperinsulinemia when obese. The age, BMI (kg/m<sup>2</sup>), fasting plasma insulin (FI, pmol l<sup>-1</sup>) and genotype (+, wild type; R3, *PPP1R3A* mutation) are indicated.



that quantitative decrements in PPAR $\gamma$  function have different metabolic implications for humans and mice.

The PPP1R3A protein is a key molecule in the regulation of glycogen metabolism. Insulin activates glycogen synthase, the rate-limiting enzyme in glycogen synthesis, by promoting its dephosphorylation through the inhibition of kinases (glycogen synthase kinase-3 and protein kinase-A) and the activation of protein phosphatase 1 (PP1)<sup>9</sup>. Insulin activates discrete pools of PP1 in the vicinity of glycogen by facilitating binding of the PP1 catalytic subunit (PP1C) to glycogen-targeting regulatory subunits<sup>9</sup>. These subunits serve as 'molecular scaffolds', bringing PP1C together with its substrates glycogen synthase and phosphorylase in a macromolecular complex, and in the process have significant effects on PP1C activity<sup>9</sup>.

The PPP1R3A regulatory subunit is specific to skeletal and cardiac muscle. The PPP1R3A frameshift mutation is predicted to truncate the protein prematurely (Fig. 1*b*), resulting in the loss of

its C-terminal sarcoplasmic reticulum-binding domain<sup>9</sup>. When transiently expressed in CHO cells, the frameshift-mutant vector produced a detectable protein of the expected reduced size (approximately 83 kD; Fig. 3*a*). In addition, the truncated protein interacted with PP1C with an efficiency similar to that of wildtype PPP1R3A (Fig. 3*b*). Confocal microscopy revealed different intracellular distributions of wildtype and mutant PPP1R3A. A significant fraction of wildtype PPP1R3A localized, as expected, to intracellular membranes, whereas mutant PPP1R3A was almost exclusively cytosolic (Fig. 3*c*).

Is the PPP1R3A frameshift mutation a plausible contributor to a state of insulin resistance? Mice rendered null for *Ppp1r3a* have major defects in muscle glycogen synthesis, although, somewhat unexpectedly, the effects of insulin on this process are maintained in such animals<sup>10</sup>. The PPP1R3A frameshift mutation in humans results in a major intracellular mislocalization of the truncated protein and is likely to have phenotypic effects distinct from those

**Table 1 • Clinical and biochemical characteristics of frameshift mutation carriers**

	Family A					Family B				Normal values		
	Compound heterozygous subjects		FS PPAR $\gamma$ mutant heterozygotes			FS PPP1R3A mutant heterozygotes						
Fig. 1 reference	lii	liiii	liiv	liiii	liiv	li	liiv	lii	liiii	lii	li	
Age	49	47	41	25	21	71	32	71	20	20	65	
Gender	F	F	F	F	F	M	M	F	M	M	M	
BMI (kg/m <sup>2</sup> )	26.8	26	28	31.4	29	24.2	25.8	32.9	18.9	36.5	30	
Blood pressure	190/ 110	140/ 80 <sup>a</sup>	130/ 84	130/ 70	150/ 110	170/ 90 <sup>a</sup>	125/ 90	170/ 105 <sup>a</sup>	105/ 69	135/ 82 <sup>a</sup>	172/ 93 <sup>a</sup>	
Measured/predicted body fat <sup>b</sup> (%)	84.3	63.5	83.7	46.8	79.4	n/a	75.2	n/a	n/a	n/a	n/a	100%
Glucose	5.6	6.4	4.4	9.2 <sup>c</sup>	3.9	12 <sup>c</sup>	4.6	4.5	5.2	4.4	6.2	3.5–6.3 mmol/l
Insulin	195	359	197	411	346	61	46	56	31	437	178	<80 pmol/l
Insulin sensitivity (HOMA; %) <sup>e</sup>	27	15	28	14	20	87	115	95	168	13	30	100%
TG	6.1	2.1 <sup>d</sup>	3.4	34.6 <sup>c</sup>	10.1	6.6	1.5	1.1	0.7	1.5	2.4	desirable <2.0 mmol/l
HDL	0.82	0.63 <sup>d</sup>	0.81	0.52	1.04	0.71	1.02	1.84	1.36	0.7	0.91	desirable >0.9 mmol/l
NEFA	1442	202 <sup>d</sup>	526	2532	867	1219	584	933	n/a	n/a	n/a	280–920 $\mu$ mol/l
Uric acid	0.31	0.24	0.23	0.23	0.28	0.35	0.31	0.23	0.32	0.17	0.44	0.15–0.35 mmol/l
Leptin	12.1	4.4	8.2	17.3	12.4	1.2	0.9	13.2	0.6	14.6	19.8	$\mu$ g/l
IMCL/creatinine ratio (soleus)	19.8	19.1	25.5	28.3	44.9	n/a	28.3	n/a	n/a	n/a	n/a	13.6 $\pm$ 6.6 <sup>f</sup>

All samples were obtained after an overnight fast. <sup>a</sup>Measurements affected by anti-hypertensive therapy. <sup>b</sup>Body fat was quantified by magnetic resonance imaging (MRI) as described previously<sup>27</sup>. Predicted body fat<sup>28</sup>: for women = (1.48  $\times$  BMI (kg/m<sup>2</sup>)) – 7.00; for men = (1.281  $\times$  BMI (kg/m<sup>2</sup>)) – 10.13. <sup>c</sup>Abnormalities detected at the time of screening. <sup>d</sup>Measurements affected by lipid-lowering therapy. <sup>e</sup>HOMA (homeostasis model assessment)<sup>29</sup> may be influenced by the diabetic status of some individuals. <sup>f</sup>IMCL reference values represent mean  $\pm$  s.d. of measurements from 76 control subjects (E.L. Thomas and J.D. Bell, unpublished observations). TG, triglycerides; HDL, high-density lipoprotein; NEFA, non-esterified fatty acids; IMCL, intramyocellular lipid.



the development of muscle insulin resistance in fat-specific *Glut4* knockout mice<sup>15</sup> recently provided *in vivo* evidence of such an interaction between fat and muscle.

The precise mechanism by which loss of a single *PPARG* allele might contribute to maladaptive metabolic cross-talk is not yet known. The generation of a mouse model is currently in progress and will help to reveal the details of such cross-talk. But deficiency of this key transcriptional regulator of adipocyte biology may alter plasma fatty-acid flux or adipokine concentrations<sup>16</sup>. Thus, it is notable that plasma leptin levels were below the 25<sup>th</sup> percentile of healthy BMI and sex-matched normal controls in all compound heterozygous individuals (see Web Table A online). In addition, the levels of intramyocellular lipids (IMCL) were higher in the soleus muscle of compound heterozygous individuals than in controls (mean  $\pm$  s.d. IMCL creatine ratio  $27.5 \pm 10.5$  as compared to  $13.6 \pm 6.6$ ,  $P < 0.05$ ). Levels of IMCL are correlated with whole-body and muscle-specific insulin sensitivity and are thought to reflect excessive delivery of non-esterified fatty acids from adipose stores to myocytes<sup>17</sup>. We hypothesize that in family B, carrying only the *PPP1R3A* mutation, the expanded fat mass of obesity produces the 'second hit' by altering adipose tissue function. This notion is supported by the marked effect of weight loss on fasting hyperinsulinemia in individual III of family B.

The *PPARG* frameshift mutation was not detected in 1,034 UK European individuals (517 diabetics and 517 controls). By contrast, the *PPP1R3A* frameshift mutation was found in two independent case-control studies in a total of 20/1,029 UK individuals with type 2 diabetes and 8/1,033 normoglycemic controls (weighted Mantel-Haenszel odds ratio 2.53; 95% confidence limits 1.06–6.70,  $P = 0.03$ ), indicating that this mutation may result in a predisposition to type 2 diabetes in the general UK population. Given the rarity of this mutation, further large multicenter population genetic studies are required to test this hypothesis.

These findings provide evidence that mutations that, when present alone, have at most subtle effects on different, metabolically relevant tissues can combine to result in extreme disturbances of human insulin action. There has been considerable debate about the relative roles of disturbances of carbohydrate or lipid metabolism in the development of insulin resistance, the metabolic syndrome and type 2 diabetes<sup>18</sup>. Our finding that a combination of modest primary defects in both processes can have significant consequences for insulin sensitivity emphasizes the need for an integrated approach to the search for etio-pathogenic pathways in common metabolic diseases.

## Methods

**Screening of *PPARG* and *PPP1R3A*.** Genomic DNA from subjects was randomly pre-amplified in a primer extension pre-amplification (PEP) reaction<sup>19</sup>. All coding exons and splice junctions of *PPARG* transcripts and *PPP1R3A* were amplified by PCR from PEP DNA with gene-specific primers (primer sequences are available upon request). We studied PCR products using single-stranded conformation polymorphism analysis and direct sequencing of all abnormal conformers<sup>20</sup>. We screened for the *PPP1R3A* frameshift mutation in participants in two independent, population-based, case-control studies in East Anglia, UK. The presence of type 2 diabetes was assumed if the onset of diabetes was after the age of 30 y and insulin therapy was not used in the first year after diagnosis. Controls were individually age- and gender-matched to each of the cases. We excluded controls that had glycated hemoglobin (HbA1c) levels  $>6.0\%$ . We did not detect the *PPARG* frameshift mutation in any individuals from the first population-based cohort.

**DNA-binding assays.** We assessed receptor binding to DNA in electrophoretic mobility supershift assays as described previously<sup>21</sup>, using <sup>35</sup>S-labeled, *in vitro* translated receptors quantified by SDS-PAGE

analysis, and a <sup>32</sup>P-labeled oligonucleotide duplex corresponding to the PPARE derived from the acyl-CoA oxidase gene<sup>22</sup>.

**Transactivation assays.** We transfected 293 EBNA cells in 24-well plates with 500 ng of (PPARE)<sub>3</sub>TKLUC<sup>23</sup> and 100 ng of receptor expression vector (wild type, frameshift mutants or empty vector pcDNA3) using the calcium phosphate method<sup>21</sup>. Luciferase values were normalized to  $\beta$ -galactosidase activity from the internal control plasmid Bos $\beta$ gal<sup>21</sup> and represent the mean  $\pm$  s.e.m. of at least three independent experiments, each carried out in triplicate.

**Immunofluorescence microscopy.** CHO cells were transiently transfected (Fugene) with N-terminal, HA-tagged expression vectors containing wildtype or mutated *PPP1R3A* (pACCMV.pKpA-HA-*PPP1R3A*, gift from P. Cohen<sup>24</sup>).

Cells were fixed in 3% paraformaldehyde/0.05% glutaraldehyde in 100 mM potassium HEPES/3 mM MgCl<sub>2</sub> buffer (pH 7.5) for 15 min, treated with 0.5% borohydride/PBS for 10 min, and then blocked and permeabilized in 1% BSA/0.1% saponin for 20 min. When permeabilizing cells before fixation, we incubated them for 5 min in 0.05% saponin in 80 mM potassium PIPES/5 mM EGTA/1 mM MgCl<sub>2</sub> (pH 6.8) at room temperature. Cells were labeled with a rat anti-HA (Boehringer; 1:100), followed by Texas Red goat anti-rat (Molecular Probes; 1:200). We collected confocal images using a Leica TCS SP system and processed them using Adobe Photoshop software (Adobe Systems).

**Clinical studies.** We obtained informed consent from all individuals involved in the study, and ethics committee approval from both the local (Cambridge) and regional ethics committees. We determined IMCL content as described previously<sup>25</sup> and measured plasma leptin concentration using an in-house, two-site immunoassay (see Web Note A online).

*Note: Supplementary information is available on the Nature Genetics website.*

## Acknowledgments

*This study drew upon the combined efforts of many individuals at Incyte Genomics Cambridge, to whom we extend our appreciation. We thank the patients and their families who participated in this study, P. Luzio for helpful discussion, V. Ibbotson for assistance with clinical investigations, K. Ong for HOMA analysis and I. Halsall for insulin and leptin measurements. D.B.S. is a Wellcome Trust Training Fellow, and S.O'R. and V.K.K.C. are supported by the Wellcome Trust. A.M. is funded by an Individual Marie Curie Fellowship. N.J.W., A.H.H., E.L.T. and J.D.B. are supported by the Medical Research Council.*

## Competing interests statement

*The authors declare that they have no competing financial interests.*

Received 19 February; accepted 16 May 2002.

- Barroso, I. *et al.* Dominant negative mutations in human PPAR $\gamma$  associated with severe insulin resistance, diabetes mellitus and hypertension. *Nature* **402**, 880–883 (1999).
- Rosen, E.D. & Spiegelman, B.M. Ppar $\gamma$ : a nuclear regulator of metabolism, differentiation, and cell growth. *J. Biol. Chem.* **276**, 37731–37734 (2001).
- Mukherjee, R. *et al.* Sensitization of diabetic and obese mice to insulin by retinoid X receptor agonists. *Nature* **386**, 407–410 (1997).
- Olefsky, J.M. Treatment of insulin resistance with peroxisome proliferator-activated receptor  $\gamma$  agonists. *J. Clin. Invest.* **106**, 467–472 (2000).
- Yamauchi, T. *et al.* Inhibition of RXR and PPAR $\gamma$  ameliorates diet-induced obesity and type 2 diabetes. *J. Clin. Invest.* **108**, 1001–1013 (2001).
- Kubota, N. *et al.* PPAR $\gamma$  mediates high-fat diet-induced adipocyte hypertrophy and insulin resistance. *Mol. Cell.* **4**, 597–609 (1999).
- Miles, P.D., Barak, Y., He, W., Evans, R.M. & Olefsky, J.M. Improved insulin-sensitivity in mice heterozygous for PPAR- $\gamma$  deficiency. *J. Clin. Invest.* **105**, 287–292 (2000).
- Bjorntorp, P. and Sjostrom, L. Carbohydrate storage in man: speculations and some quantitative considerations. *Metabolism* **27**, 1853–1865 (1978).
- Newgard, C.B., Brady, M.J., O'Doherty, R.M. & Saltiel, A.R. Organizing glucose disposal: emerging roles of the glycogen targeting subunits of protein phosphatase-1. *Diabetes* **49**, 1967–1977 (2000).
- Suzuki, Y. *et al.* Insulin control of glycogen metabolism in knockout mice lacking the muscle-specific phosphatase PP1G/RGL. *Mol. Cell. Biol.* **21**, 2683–2694 (2001).
- Nielsen, J.N. *et al.* Glycogen synthase localization and activity in rat skeletal muscle is strongly dependent on glycogen content. *J. Physiol.* **531**, 757–769 (2001).

12. Burghes, A.H., Vaessin, H.E. & de La Chapelle, A. Genetics. The land between Mendelian and multifactorial inheritance. *Science* **293**, 2213–2214 (2001).
13. Bruning, J.C. *et al.* Development of a novel polygenic model of NIDDM in mice heterozygous for IR and IRS-1 null alleles. *Cell* **88**, 561–572 (1997).
14. Birnbaum, M.J. Diabetes. Dialogue between muscle and fat. *Nature* **409**, 672–673 (2001).
15. Abel, E.D. *et al.* Adipose-selective targeting of the *GLUT4* gene impairs insulin action in muscle and liver. *Nature* **409**, 729–733 (2001).
16. Stepan, C.M. & Lazar, M.A. Resistin and obesity-associated insulin resistance. *Trends Endocrinol. Metab.* **13**, 18–23 (2002).
17. Kelley, D.E. & Goodpaster, B.H. Skeletal muscle triglyceride. An aspect of regional adiposity and insulin resistance. *Diabetes Care* **24**, 933–941 (2001).
18. McGarry, J.D. What if Minkowski had been ageusic? An alternative angle on diabetes. *Science* **258**, 766–770 (1992).
19. Zhang, L. *et al.* Whole genome amplification from a single cell: implications for genetic analysis. *Proc. Natl Acad. Sci. USA* **89**, 5847–5851 (1992).
20. Thorpe, K.L., Schafer, A.J., Genin, E., Trowsdale, J. & Beck, S. Detection of polymorphism in the *RING3* gene by high-throughput fluorescent SSCP analysis. *Immunogenetics* **49**, 256–265 (1999).
21. Collingwood, T.N., Adams, M., Tone, Y. & Chatterjee, V.K. Spectrum of transcriptional, dimerization, and dominant negative properties of twenty different mutant thyroid hormone  $\beta$ -receptors in thyroid hormone resistance syndrome. *Mol. Endocrinol.* **8**, 1262–1277 (1994).
22. Zamir, I., Zhang, J. & Lazar, M.A. Stoichiometric and steric principles governing repression by nuclear hormone receptors. *Genes Dev.* **11**, 835–846 (1997).
23. Forman, B.M. *et al.* 15-Deoxy- $\Delta$ 12, 14-prostaglandin J2 is a ligand for the adipocyte determination factor PPAR $\gamma$ . *Cell* **83**, 803–812 (1995).
24. Rasmussen, S.K. *et al.* Adenovirus-mediated expression of a naturally occurring Asp905Tyr variant of the glycogen-associated regulatory subunit of protein phosphatase-1 in L6 myotubes. *Diabetologia* **43**, 718–722 (2000).
25. Rico-Sanz, J. *et al.* Diversity in levels of intracellular total creatine and triglycerides in human skeletal muscles observed by (1)H-MRS. *J. Appl. Physiol.* **87**, 2068–2072 (1999).
26. Tang, P.M., Bondor, J.A., Swiderek, K.M. & DePaoli-Roach, A.A. Molecular cloning and expression of the regulatory (RG1) subunit of the glycogen-associated protein phosphatase. *J. Biol. Chem.* **266**, 15782–15789 (1991).
27. Thomas, E.L. *et al.* Magnetic resonance imaging of total body fat. *J. Appl. Physiol.* **85**, 1778–1785 (1998).
28. Black, D. *et al.* Obesity. A report of the Royal College of Physicians. *J. R. Coll. Physicians Lond.* **17**, 5–65 (1983).
29. Matthews, D.R. *et al.* Homeostasis model assessment: insulin resistance and  $\beta$ -cell function from fasting plasma glucose and insulin concentrations in man. *Diabetologia* **28**, 412–419 (1985).

## Digenic inheritance of severe insulin resistance in a human pedigree

D B Savage, M Agostini, I Barroso, M Gurnell, J Luan, A Meirhaeghe, A-H Harding, G Ihrke, O Rajanayagam, M A Soos, S George, D Berger, E L Thomas, J D Bell, K Meeran, R J Ross, A Vidal-Puig, N J Wareham, S O'Rahilly, V K K Chatterjee & A J Schafer

*Nature Genet.* 31, 379–384 (2002).

doi:10.1038/ng926

Owing to a copy-editing error that was implemented after the authors returned the corrected proofs, the term 'doubly heterozygous' was substituted with the term 'compound heterozygous' throughout the text and in Table 1. Similarly, 'double heterozygotes' was erroneously substituted with 'compound heterozygotes'. The full-text of the online Letter, including Table 1, has been corrected online. Per company policy, the PDF version has not been corrected; an erratum will be published in an upcoming issue. *Nature Genetics* sincerely regrets these errors.

## Supplemental data

### **Non-DNA binding, dominant-negative, human PPAR $\gamma$ mutations cause lipodystrophic insulin resistance**

**Maura Agostini, Erik Schoenmakers, Catherine Mitchell, Istvan Szatmari, David Savage, Aaron Smith, Odelia Rajanayagam, Robert Semple, Jian Luan, Louise Bath, Anthony Zalin, Mourad Labib, Sudhesh Kumar, Helen Simpson, Dirk Blom, David Marais, John Schwabe, Ines Barroso, Richard Trembath, Nicholas Wareham, Laszlo Nagy, Mark Gurnell, Stephen O’Rahilly, and Krishna Chatterjee**

## Supplemental experimental procedures

### **Case Histories of Subjects**

**Subject 1** (S1), presented at age 34yrs with oligomenorrhoea and subfertility, when dyslipidaemia was found. At age 41, partial lipodystrophy was noted; type 2 diabetes was diagnosed and diet-treated. She has developed severe three vessel coronary artery disease that was not alleviated by percutaneous revascularisation and is on triple antianginal therapy. She is heterozygous for a cysteine to arginine mutation at codon 114 (C114R) in PPAR $\gamma$ 1 and her mother and sister are genetically unaffected with normal biochemistry; her father (genotype unknown) died age 60yrs from a myocardial infarction.

**Subject 2** (S2), presented at age 35yrs with hypertension and syncopal episodes secondary to hyperinsulinaemia. Partial lipodystrophy and dyslipidaemia were noted and polycystic ovarian syndrome (PCOS) was diagnosed based on oligomenorrhoea and pelvic ultrasound appearances. At age 42, she developed type 2 diabetes which is diet controlled; although a non-smoker, she has developed single vessel coronary artery disease age 44yrs. She is heterozygous for a cysteine to tyrosine mutation at codon 131 (C131Y) of PPAR $\gamma$ 1. A genetically affected younger sister is insulin resistant and



dyslipidaemic (fasting insulin [FI] 168 pmol/L; triglycerides [TG] 8.6mmol/L, high density lipoprotein cholesterol [HDL-C] 1.0mmol/L), whereas an unaffected older sister is biochemically normal (FI 79 pmol/L; TG 0.8mmol/L, HDL-C 1.4mmol/L). Her genetically affected father was a long-term smoker and deceased from lung carcinoma.

**Subject 3 (S3)**, presented at age 19yrs with eruptive xanthomata secondary to severe hypertriglyceridaemia. Retrospectively, partial lipodystrophy was present since age 8, PCOS was diagnosed in her twenties and hypertension and acanthosis nigricans together with impaired glucose tolerance were noted age 29yrs. She is heterozygous for a cysteine to tryptophan mutation at codon 162 (C162W) in PPAR $\gamma$ 1. Significant hypertriglyceridaemia (TG 26mmol/L) has been diagnosed since age 49yrs in her genetically affected mother together with hypertension, type 2 diabetes and ischaemic heart disease age 52yrs; her genetically affected grandfather has type 2 diabetes and ischaemic heart disease.

**Subject 4 (S4)**, presented at age 8yrs with diabetes mellitus and partial lipodystrophy, acanthosis nigricans and severe hypertriglyceridaemia with eruptive xanthomata were noted; she is currently on metformin, pioglitazone and insulin therapy. She is heterozygous for a frameshift mutation predicting a premature stop mutation at codon 315 ([A<sup>935</sup> $\Delta$ C]fs.312[stop315]; FS315X) in PPAR $\gamma$ 1. Her mother is known to have developed type 2 diabetes aged 16 and possible hypertension but is deceased and of unknown genotype. Her maternal grandfather is genetically unaffected and family members are untraceable.

**Subject 5 (S5)**, presented at age 26yrs with gestational diabetes and hypertension and pregnancy was complicated by preeclampsia. Type 2 diabetes and hypertension persisted

post-partum and dyslipidaemia was noted subsequently leading to episodes of pancreatitis. Partial lipodystrophy and acanthosis nigricans were present. Treatment includes metformin, fenofibrate and insulin. She is heterozygous for a mutation changing arginine at codon 357 to a stop mutation (R357X). Her deceased mother, who was found to be genetically affected retrospectively, developed hypertension in her thirties, type 2 diabetes and dyslipidaemia (TG 4.9mmol/L, HDL-C 0.6mmol/L) in her forties and died suddenly from cardiovascular cause age 57.

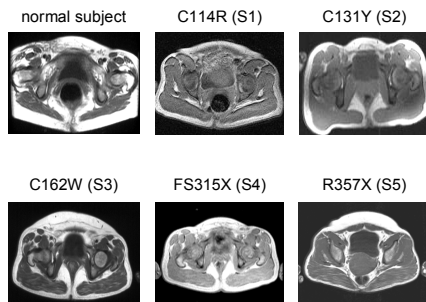


**Figure S1.** T1-weighted MRI scans at the level of the gluteal fat pad in PPAR $\gamma$  mutation carriers and a gender-matched healthy control subject. Note the striking diminution of the gluteal fat depot in all probands (S1-S5) with PPAR $\gamma$  mutations.

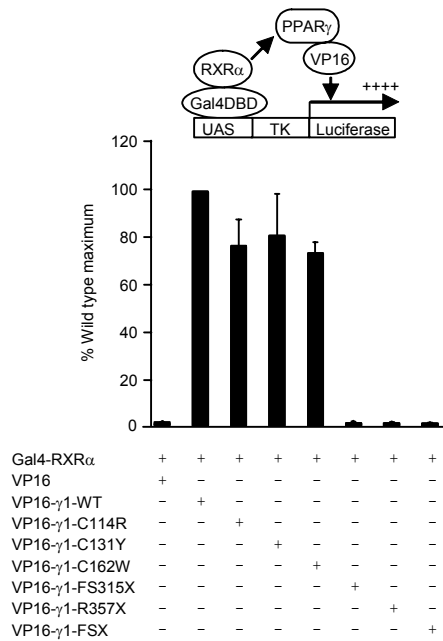


**Figure S2.** PPAR $\gamma$  mutants differ in their ability to interact with RXR. In a mammalian 2-hybrid assay, the DNA-binding domain mutants (C114R, C131Y and C162W) are recruited to RXR comparably to WT, whereas the FS315X, R357X and FSX truncation mutants, which lack an RXR interaction domain, exhibit negligible interaction. 293EBNA cells were transfected with 500ng of UASTKLUC reporter construct, 100ng of the internal control Bos- $\beta$ -gal, 50ng of Gal4DBD-RXR $\alpha$  and 50ng of expression vector encoding either VP16 alone or VP16-full length WT or mutant PPAR $\gamma$  fusions. Results are expressed as a percentage of the WT maximum response and represent the mean  $\pm$  s.e.m. of at least 3 independent experiments, each performed in triplicate.

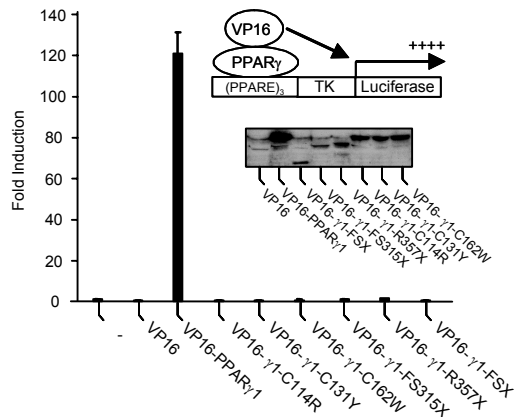


**Figure S3.** PPAR $\gamma$  mutants fail to bind to DNA. Chimaeric fusion proteins consisting of the VP16 activation domain linked to the N-terminus of full-length PPAR $\gamma$ 1 (WT or mutant) were co-expressed in 293EBNA cells with a PPARE-containing reporter gene [(PPARE) $_3$ TKLUC]. Interaction of WT VP16-PPAR $\gamma$  with (PPARE) $_3$ TKLUC markedly increased transactivation. In contrast, levels of reporter gene activity in cells expressing mutant chimaeras were similar to mock-transfected cells, suggesting no significant promoter interaction. 96-well plates of 293EBNA cells were transfected with 9ng of (PPARE) $_3$ TKLUC, 1.6ng of Bos- $\beta$ -gal, and 1.6ng of the respective VP16-PPAR $\gamma$ 1 chimaeras as shown. Inset,  $^{35}$ S-labeled *in vitro* translated wild type and mutant VP16-PPAR $\gamma$  fusion proteins. Results are expressed as fold induction relative to cells transfected with VP16 alone and represent the mean  $\pm$  s.e.m. of at least three independent experiments, each performed in triplicate.

# Non-DNA binding, dominant-negative, human PPAR $\gamma$ mutations cause lipodystrophic insulin resistance

Maura Agostini,<sup>1,12</sup> Erik Schoenmakers,<sup>1,12</sup> Catherine Mitchell,<sup>1</sup> Istvan Szatmari,<sup>3</sup> David Savage,<sup>2</sup> Aaron Smith,<sup>1</sup> Odelia Rajanayagam,<sup>1</sup> Robert Semple,<sup>2</sup> Jian'an Luan,<sup>4</sup> Louise Bath,<sup>5</sup> Anthony Zalin,<sup>6</sup> Mourad Labib,<sup>6</sup> Sudhesh Kumar,<sup>7</sup> Helen Simpson,<sup>1</sup> Dirk Blom,<sup>8</sup> David Marais,<sup>8</sup> John Schwabe,<sup>9</sup> Inês Barroso,<sup>10</sup> Richard Trembath,<sup>11</sup> Nicholas Wareham,<sup>4</sup> Laszlo Nagy,<sup>3</sup> Mark Gurnell,<sup>1</sup> Stephen O'Rahilly,<sup>1,2</sup> and Krishna Chatterjee<sup>1,\*</sup>

<sup>1</sup>Department of Medicine

<sup>2</sup>Department of Clinical Biochemistry

University of Cambridge, United Kingdom

<sup>3</sup>Department of Biochemistry and Molecular Biology, University of Debrecen, Hungary

<sup>4</sup>Medical Research Council Epidemiology Unit, Cambridge, United Kingdom

<sup>5</sup>Royal Hospital for Sick Children, Edinburgh, United Kingdom

<sup>6</sup>Wordsley Hospital, Stourbridge, United Kingdom

<sup>7</sup>Department of Medicine, University of Warwick, Coventry, United Kingdom

<sup>8</sup>Department of Internal Medicine, University of Cape Town, South Africa

<sup>9</sup>Medical Research Council, Laboratory of Molecular Biology, Cambridge, United Kingdom

<sup>10</sup>Metabolic Disease Group, Wellcome Trust Sanger Institute, Cambridgeshire, United Kingdom

<sup>11</sup>Department of Medical and Molecular Genetics, King's College, London, United Kingdom

<sup>12</sup>These authors contributed equally to this work.

\*Correspondence: kkc1@mole.bio.cam.ac.uk

## Summary

**PPAR $\gamma$  is essential for adipogenesis and metabolic homeostasis. We describe mutations in the DNA and ligand binding domains of human PPAR $\gamma$  in lipodystrophic, severe insulin resistance. These receptor mutants lack DNA binding and transcriptional activity but can translocate to the nucleus, interact with PPAR $\gamma$  coactivators and inhibit coexpressed wild-type receptor. Expression of PPAR $\gamma$  target genes is markedly attenuated in mutation-containing versus receptor haploinsufficient primary cells, indicating that such dominant-negative inhibition operates *in vivo*. Our observations suggest that these mutants restrict wild-type PPAR $\gamma$  action via a non-DNA binding, transcriptional interference mechanism, which may involve sequestration of functionally limiting coactivators.**

## Introduction

The nuclear receptor (NR) peroxisome proliferator-activated receptor  $\gamma$  (PPAR $\gamma$ ) is a ligand-inducible transcription factor that is essential for adipocyte differentiation (Tontonoz *et al.*, 1994b; Barak *et al.*, 1999; Rosen *et al.*, 1999). Alternative splicing and differential promoter usage generates two protein isoforms: PPAR $\gamma$ 2, expressed from a single  $\gamma$ 2 promoter, contains an additional 28 amino-terminal amino acids and is nearly adipose-specific; PPAR $\gamma$ 1, whose expression can be regulated by multiple ( $\gamma$ 1,  $\gamma$ 3,  $\gamma$ 4) promoters, is more ubiquitously distributed. In addition to adipogenesis, PPAR $\gamma$  also plays an important role in adipocyte lipid metabolism, regulating target genes (lipoprotein lipase, fatty-acid transport protein, aquaporin) that mediate triglyceride hydrolysis and fatty acid and glycerol uptake, together with genes (acylCoA synthetase, PEPCK, glycerol kinase) involved in fatty acid re-esterification and lipid storage (Lehrke and Lazar, 2005; Savage, 2005). The thiazolidinedione (TZD) class of antidiabetic agents are synthetic, high-affinity PPAR $\gamma$  ligands (Lehmann *et al.*, 1995) and putative endogenous activators include fatty acids, eicosanoids, and prostaglandin derivatives (Desvergne and Wahli, 1999) as well as undefined ligands produced during adipocyte differentiation (Tzamelis *et al.*, 2004).

The most common population genetic variant of PPAR $\gamma$  is a polymorphism replacing alanine for proline at codon 12 (Pro12Ala) in PPAR $\gamma$ 2, with a meta-analysis of association studies showing that the Pro allele confers a modest but significant increase in diabetes risk (Altshuler *et al.*, 2000). The discovery that PPAR $\gamma$  is a target for TZDs, which act by enhancing tissue insulin sensitivity, prompted screening of a cohort of subjects with severe insulin resistance, with identification of two missense PPAR $\gamma$  mutations (P467L, V290M) in unrelated cases (Barroso *et al.*, 1999). Functional studies showed that these mutant receptors retain DNA binding but exhibit significant impairment of transcriptional activation and coactivator recruitment in response to different ligands (Barroso *et al.*, 1999; Agostini *et al.*, 2004), due to the mutations destabilizing the carboxyterminal  $\alpha$  helix of PPAR $\gamma$  (Kallenberger *et al.*, 2003), which mediates these functions. Consonant with heterozygosity in affected subjects and dominant inheritance in one kindred, the P467L and V290M mutant receptors inhibited the transcriptional activity of wild-type (WT) PPAR $\gamma$  in a dominant-negative manner (Barroso *et al.*, 1999). Subsequently, two further heterozygous mutations in the ligand binding domain (LBD) of PPAR $\gamma$  (R425C; F388L) have been described, with recognition that in addition to insulin resistance the phenotype also includes a stereotyped pattern of partial

lipodystrophy (PLD) (Hegele et al., 2002; Agarwal and Garg, 2002; Savage et al., 2003).

Following this, we described several individuals who were heterozygous for a frameshift/premature stop codon mutation, ([A<sup>553</sup>ΔAAAI]fs.185[stop186]-hereafter abbreviated to FSX) in the DNA binding domain (DBD) of PPAR $\gamma$ , with this truncation mutant lacking DNA binding, transcriptional, and dominant-negative activity. Significantly, heterozygosity for the FSX mutation alone was not associated with insulin resistance, but individuals who were doubly heterozygous, with an additional defect in an unrelated gene encoding the muscle-specific regulatory subunit of protein phosphatase 1 (PPP1R3A), exhibited severe insulin resistance (Savage et al., 2002). Heterozygosity for a single nucleotide substitution in the promoter of human PPAR $\gamma$ 4 leading to its altered expression in vitro has been associated with PLD and insulin resistance in one family, but the authors did not exclude the possibility of interaction with a defect at a second genetic locus to produce this phenotype (Al-Shali et al., 2004).

Here, we describe the identification of five heterozygous human PPAR $\gamma$  mutations (C114R, C131Y, C162W, R357X, [A<sup>935</sup>ΔC]fs.312[stop315]-hereafter abbreviated to FS315X) not associated with a PPP1R3A gene defect, in unrelated cases of lipodystrophic insulin resistance and show that these mutants inhibit WT receptor action via a non-DNA binding, dominant-negative mechanism.

## Results and Discussion

### Heterozygous PPAR $\gamma$ mutations are associated with lipodystrophic insulin resistance

The case histories (see the [Supplemental Data](#) available with this article online) and characterization (Table 1) of index subjects (S1–S5) harboring PPAR $\gamma$  mutations indicate many of the features associated with previously described cases (Barroso et al., 1999; Hegele et al., 2002; Agarwal and Garg, 2002; Savage et al., 2003). All subjects showed marked fasting hyperinsulinaemia (Table 1) with acanthosis nigricans in a subset (S3, S4, S5), denoting severe insulin resistance; total body fat was reduced in all individuals, and imaging indicated a stereotyped pattern of partial lipodystrophy affecting gluteal (Figure S1) and peripheral limb depots; hepatic steatosis and marked dyslipidaemia (raised triglycerides, low high-density lipoprotein cholesterol [HDL-C]) with secondary complications (cutaneous eruptive xanthomata S3, S4; pancreatitis S5) were features of all cases; several individuals (S2, S3, S5) exhibited early-onset hypertension.

We sequenced the  $\gamma$ 4 promoter, coding exons and splice junctions of *PPARG* and identified heterozygous, missense mutations in the DBD (S1–S3), or premature stop mutations in the LBD (S4, S5) of the receptor in index cases. *PPARG* has also been sequenced by us in 215 additional subjects, comprising 93 patients from our severe insulin resistance cohort (Barroso et al., 1999), 48 CEPH individuals of European descent and 27 Europid, hyperinsulinaemic participants in the Ely study (Williams et al., 1995), and 47 controls from four different ethnic groups, or sequenced by others in 24 African and 23 CEPH European individuals (Seattle SNPs project, <http://pga.gs.washington.edu>), and other than the Pro12Ala polymorphism neither these or other mutations have been identified. We also sequenced *PPP1R3A* in each proband and identified no muta-

**Table 1.** Clinical, biochemical, and body composition details

Subject (gender)	S1 (F)	S2 (F)	S3 (F)	S4 (F)	S5 (F)
Mutation	C114R	C131Y	C162W	FS315X	R357X
Age (and at presentation, year)	41 (34)	42 (35)	31 (19)	13 (8)	35 (26)
BMI (kg/m <sup>2</sup> ) (nonobese < 30)	30.0	24.2	30.5	25.9	29.3
BP (mmHg) (< 130/85)	155/95	220/120	150/100*	125/65	125/80*
T2DM/IGT (age at diagnosis, yr)	T2DM (41)	T2DM (42)	IGT (29)	T2DM (8)	T2DM (26)
PCOS	Y	Y	Y	N/A	Y
Hepatic steatosis	Y	Y	Y	Y	Y
TG (mmol/L) (<1.7)	8.9*	4.5	5.0*	8.3*	34.8*
HDL-C (mmol/L) (>1.29)	0.47*	0.89	0.71*	0.72*	0.56*
FI (pmol/L) (<60)	310	174	220*	475*	170*
Predicted total body fat (%)	37.4	28.8	38.1	31.3	36.4
Measured total body fat (%)	26 <sup>-0.8</sup>	23 <sup>-1.2</sup>	nd	26 <sup>nd</sup>	21 <sup>-1.1</sup>
Measured lower limb fat (%)	20	17	nd	21	11
Measured truncal fat (%)	30	27	nd	31	28

BMI, body mass index; BP, blood pressure; T2DM, type 2 diabetes mellitus; IGT, impaired glucose tolerance; PCOS, polycystic ovarian syndrome; TG, triglycerides; HDL-C, high-density lipoprotein cholesterol; FI, fasting insulin; Predicted total body fat was calculated as follows (Black et al., 1983): males % fat = (1.281 × BMI) – 10.13; females % fat = (1.48 × BMI) – 7.00; measured total and depot-specific body fat were determined using dual-energy X-ray absorptiometry, with corresponding z scores for total body fat shown as superscript; Hepatic steatosis was diagnosed according to standard radiological criteria; F, female; healthy adult values where available are shown in parentheses; asterisk denotes patient studied on treatment; N/A, not applicable; nd, not determined.

tions or polymorphisms, excluding a second genetic defect at this locus as described previously (Savage et al., 2002).

Heterozygosity for PPAR $\gamma$  mutations in a parent and grandparent of S3 and a parent of S5 segregated with phenotype, constituting a dominant inheritance pattern in two families; one sibling of S2 with dyslipidaemia and insulin resistance was heterozygous for the PPAR $\gamma$  mutation whereas another genetically unaffected sibling was biochemically normal; the ascertainable family members of S1 were unaffected and normal and no relatives of S4 could be contacted (Figure 1B).

### PPAR $\gamma$ mutants fail to bind DNA and are transcriptionally inactive

Three missense mutations involve highly conserved cysteine residues within (C114R, C131Y, C162W) the DBD and two further nonsense (R357X) or frameshift/premature stop (FS315X) mutations truncate the receptor within the central part of its LBD (Figure 1A), predicting loss-of-function of the mutant proteins. We therefore characterised and compared the properties of these PPAR $\gamma$  mutants with the FSX mutant described previously (Savage et al., 2002).

The receptor mutants exhibited negligible transcriptional activity, lacking constitutive basal activity noted previously with WT PPAR $\gamma$  (Agostini et al., 2004; Zamir et al., 1997) as well as any response to rosiglitazone, a TZD receptor agonist (Figure 1C). Such complete loss of function was similar to the FSX mutant and might be anticipated with analogous truncation

mutants (FS315X, R357X) not possessing the transactivation (AF2) domain at the receptor carboxyterminus (Figure 1A) (Zamir et al., 1997; Wu et al., 2003), but the lack of function with DBD mutants (C114R, C131Y, C162W), prompted further investigation of their DNA binding properties.

PPAR $\gamma$  heterodimerizes with the retinoid X receptor (RXR) and this complex has been shown to bind a DNA response element (PPARE), consisting of a direct repeat (DR1) of the consensus sequence (AGGTCA) separated by a single nucleotide (Ijpenberg et al., 1997) and a recent study has suggested that the stringency of PPAR $\gamma$  binding to some response elements is relatively relaxed, not needing complete integrity of its DBD (Temple et al., 2005). A range of previously documented or predicted PPAREs from known target genes were therefore tested in electrophoretic mobility shift assays and both DBD and LBD truncation receptor mutants showed negligible heterodimeric binding (Figure 1D). To examine interaction of mutant receptors with RXR, we coexpressed VP16-full length PPAR $\gamma$  fusions with Gal4DBD-RXR in a mammalian two-hybrid assay. In keeping with preservation of the dimerization interface (Gampe et al., 2000) within their intact LBD (Figure 1A), the DBD mutants interacted readily whereas the FS315X, R357X, and FSX mutants lacking this interface failed to be recruited to Gal4-RXR (Figure S2). It was therefore conceivable that the DBD mutants could be recruited indirectly to a PPARE by binding RXR (Gampe et al., 2000), or conversely, that the LBD truncation mutants might bind a PPARE monomerically as has been documented with the thyroid hormone receptor (TR) (Lazar et al., 1991). However, unlike WT receptor, VP16-full length, mutant PPAR $\gamma$  fusions were unable to activate a PPARE-containing reporter gene (Figure S3), indicating that like FSX, these PPAR $\gamma$  mutants do not bind DNA directly or indirectly.

#### PPAR $\gamma$ mutants translocate to the nucleus and interact with cofactors

The intracellular localization of WT PPAR $\gamma$  is predominantly nuclear (Akiyama et al., 2002) and, analogous to steroid/thyroid hormone receptors, may be dependent on a putative nuclear localisation signal (NLS) located between its DBD and LBD (Figure 1A) (Guiochon-Mantel and Milgrom, 1993; Zhu et al., 1998). Studies of GFP-PPAR $\gamma$  fusions showed that, in keeping with preservation of the putative NLS, both DBD and LBD truncation mutants localized to the nucleus comparably to WT, whereas the FSX truncation mutant, which lacks this sequence, remained cytoplasmic similar to GFP alone (Figure 1E).

We next examined whether the PPAR $\gamma$  mutants might also retain the ability to interact with transcriptional coactivators. Steroid receptor coactivator-1 (SRC1/NCoA1) (Onate et al., 1995) and PPAR $\gamma$  binding protein/thyroid receptor-associated protein 220 (PBP/TRAP220) interact directly with the AF2 domain of PPAR $\gamma$ , with the latter cofactor being required for receptor-mediated adipogenesis (Zhu et al., 1996, 1997; Ge et al., 2002). Consistent with preservation of their AF2 domains, protein-protein interaction assays showed ligand-dependent binding of SRC1 or TRAP220 to the DBD mutants, but no specific interaction with FSX or LBD truncation mutants, which lack this region (Figure 1F). Conversely, we hypothesized that the PPAR $\gamma$  LBD truncation mutants would retain the ability to recruit coactivators, which can interact with receptor independently of its AF2 domain. PPAR $\gamma$  coactivator-1 (PGC1), which augments receptor action in fat cells (Puigserver and Spiegelman, 2003), can bind

PPAR $\gamma$  via its DBD and hinge region ( $\alpha\alpha$  128-229) (Puigserver et al., 1999); PDIP, isolated in a two hybrid assay using the DBD/hinge region of PPAR $\gamma$  (Tomaru et al., 2006), is a coactivator that also enhances PPAR $\alpha$  activity (Surapureddi et al., 2002). Both PGC1 and PDIP bound WT or FS315X and R357X LBD truncation mutants in protein-protein interaction assays, whereas the FSX mutant showed negligible interaction (Figure 1G).

#### PPAR $\gamma$ signaling is reduced in mutation-containing primary cells *ex vivo* or mutant-expressing cells *in vitro*

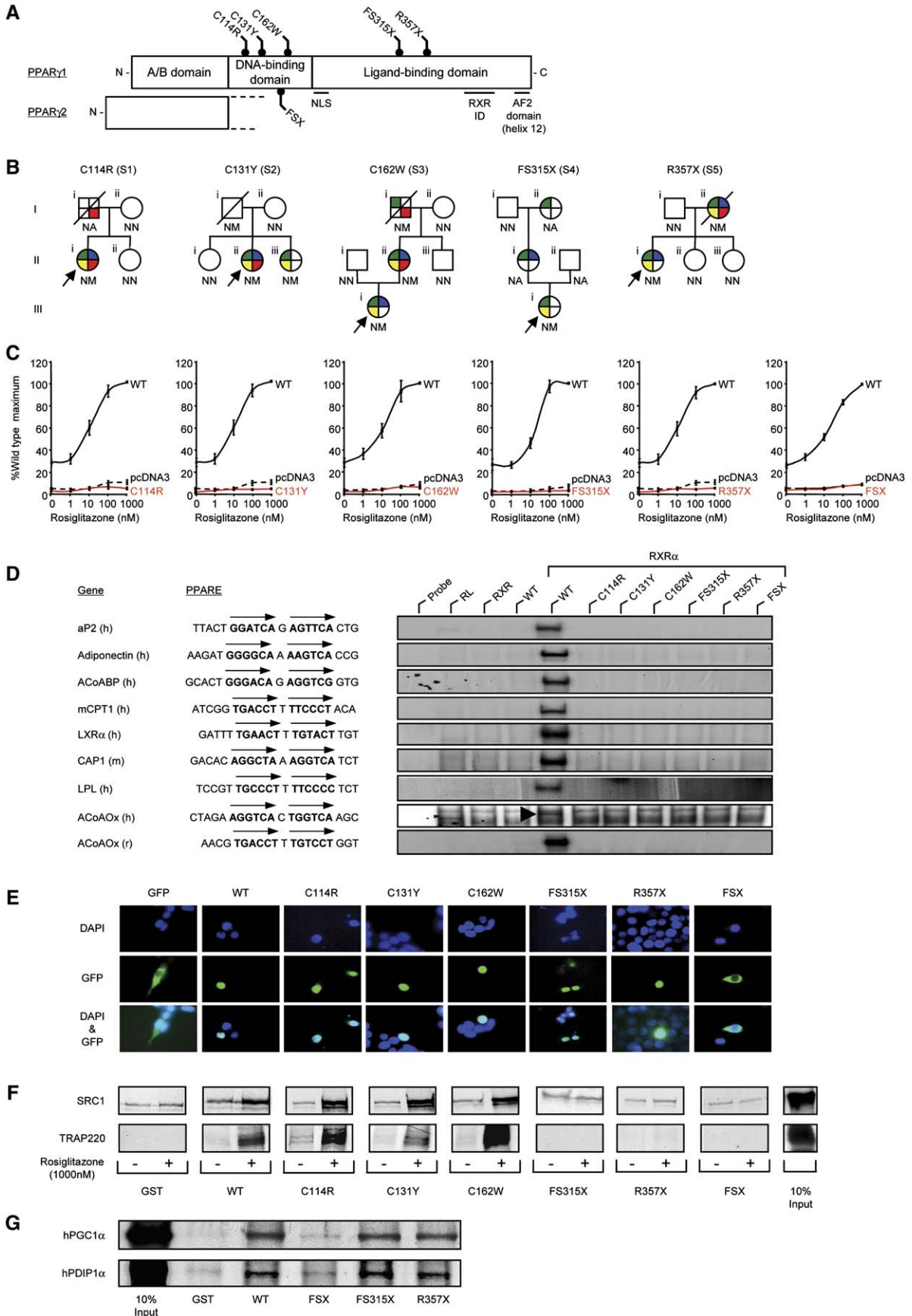
The observation that these PPAR $\gamma$  mutants translocate to the nucleus and interact with coactivators raised the possibility that they might interfere with WT receptor signaling. The murine adipocyte P2 (aP2) gene is a classical target of PPAR $\gamma$  action (Tontonoz et al., 1994a; Guan et al., 2005) and the human homolog (FABP4) is similarly responsive (Pelton et al., 1999). When coexpressed with WT PPAR $\gamma$  at equivalent levels in 3T3-L1 adipocytes, the DBD and LBD mutants blocked WT receptor mediated activation of the human aP2/FABP4 gene promoter comparably to an artificial, dominant-negative PPAR $\gamma$  mutant (AF2) described previously (Gurnell et al., 2000), whereas FSX lacked dominant-negative inhibitory activity (Figure 2A).

We wished to determine whether such divergent dominant-negative inhibition by these PPAR $\gamma$  mutants versus FSX might operate *in vivo*. PPAR $\gamma$  is highly expressed in immature dendritic cells (IDCs) derived from primary human blood monocytes and mediates marked receptor responsiveness, with strong ligand-dependent induction of aP2 expression in these cells (Szatmari et al., 2004). Induction of aP2/FABP4 expression in IDCs containing DBD or LBD PPAR $\gamma$  mutations was severely attenuated compared to responses in control cells from either normal individuals (WT) or from subjects (IR) with comparable insulin resistance without a PPAR $\gamma$  gene defect. Significantly, aP2 induction in FSX mutation-containing cells was comparable to responses from control subjects (Figure 2B). We examined other PPAR $\gamma$  target genes, identified from extensive microarray profiling of normal IDCs (I.S. and L.N., unpublished data) and found that responses to PPAR $\gamma$  agonist in DBD and LBD truncation mutation-containing cells were markedly attenuated whereas FSX mutation-containing cells exhibited responses that were either similar or only slightly reduced compared to WT cells (Figure 2C). PPAR $\gamma$  mRNA levels in control and mutation-containing primary cells were similar (data not shown), suggesting that differential responsiveness was not due to altered receptor expression. Furthermore, PPAR $\gamma$  mRNA from both WT and R357X alleles was expressed in mutation-containing IDCs (Figure 2D), indicating that the R357X transcript is not subject to nonsense-mediated decay (Culbertson, 1999) and both WT and R357X mutant PPAR $\gamma$  proteins were also expressed in these cells (Figure 2E).

Finally, we determined whether dominant-negative inhibition by a non-DNA binding PPAR $\gamma$  mutant could interfere with a receptor-mediated biological process. Compared to control, WT PPAR $\gamma$  or GFP adenovirus-transduced human preadipocyte cells, both cellular differentiation (Figure 3A) and aP2 gene expression (Figure 3B) in cells transduced with C114R mutant PPAR $\gamma$  adenovirus were significantly reduced.

#### Transcriptional interference via a non-DNA binding mechanism

We have shown previously that dominant-negative inhibition by PPAR $\gamma$  mutants (P467L, V290M), is mediated by repression of





target genes by DNA-bound mutant receptors, analogous to mechanisms of other mutant nuclear receptors (e.g., the v-erbA oncogene, TR $\beta$  mutants in Resistance to Thyroid Hormone, PZLF-RAR $\alpha$  fusion proteins in promyelocytic leukaemia) (Love et al., 2000). In contrast, the missense DBD and LBD truncation mutants identified here are unable to bind DNA, yet can inhibit WT PPAR $\gamma$  action, suggesting a different mechanism of transcriptional interference. Competition for shared cofactors by NRs was postulated to explain mutual antagonism of progesterone and estrogen receptor signaling (Meyer et al., 1989) and the subsequent observation that SRC1, a shared coactivator, could relieve such “squenching”, validated this hypothesis (Onate et al., 1995). Ligand-activated NRs have been shown to inhibit either their own function (Barettino et al., 1994) or that of heterologous receptors (Zhang et al., 1996) by limiting the availability of coactivators that are recruited to their transactivation domains. Our observations indicate that non-DNA binding, dominant-negative PPAR $\gamma$  mutants can recruit coactivators, suggesting an analogous cofactor sequestration mechanism for thereby restricting WT receptor function. Evidence suggests that similar mechanisms operate to inhibit PPAR signaling in other contexts: analogous to our natural DBD mutants, others have generated artificial, dominant-negative, PPAR $\gamma$  DBD mutants, which block either adipogenesis (Park et al., 2003) or neural stem cell differentiation (Wada et al., 2006);  $\gamma$ ORF4 is a newly identified human PPAR $\gamma$  splice variant with a truncated LBD ( $\alpha\alpha$ 273), which has dominant-negative activity and is selectively overexpressed in colorectal neoplasia (Sabatino et al., 2005); a dominant-negative PPAR $\alpha$  splice variant with a truncated LBD ( $\alpha\alpha$  174), is expressed in human tissues including liver (Gervois et al., 1999). Interestingly, heterozygous, non-DNA binding mutations in some nuclear receptors do not mediate a phenotype: mutations in the DBD of VDR only cause vitamin D resistance in the homozygous state (Malloy et al., 1999); a “knock-in” mutation in the DBD of murine TR $\beta$  does not produce thyroid hormone resistance (Shibusawa et al., 2003). Possibly due to its pivotal role in regulating transcription of genes mediating both adipocyte formation and function (Lehrke and Lazar, 2005), we suggest that PPAR $\gamma$  signaling may be particularly sensitive to interference via the postulated “squenching” mechanism, with deleterious metabolic consequences. A corollary of this may be that even modest enhancement of normal receptor activity in key tissues could be beneficial, supporting attempts to de-

velop partial or tissue-specific PPAR $\gamma$  agonists (Reginato et al., 1998; Rocchi et al., 2001; Berger et al., 2003).

## Experimental procedures

### Sequencing of PPAR $\gamma$ and PPP1R3A genes

The PPP1R3A (exons 1-4) and PPAR $\gamma$  (exons 1-6, B and promoter region of PPAR $\gamma$ 4) genes were amplified using specific primers (available upon request) and sequenced as described previously (Savage et al., 2002).

### Construction of PPAR $\gamma$ mutants and other vectors

Full length WT and mutant PPAR $\gamma$ 1 cDNAs were cloned in pGEX4T (Amersham Pharmacia Biotech), pCMX-VP16 (kind gift from R. Evans), pSG424 (Sadowski and Ptashne, 1989) and pEGFP-C1 (Clontech), to yield GST-PPAR $\gamma$ 1, VP16-PPAR $\gamma$ 1, Gal4DBD-PPAR $\gamma$  and GFP-PPAR $\gamma$ 1 fusions respectively.

### Electrophoretic mobility shift assays

Electrophoretic mobility shift assays (EMSA) were performed as described (Collingwood et al., 1994) with different natural PPAREs: aP2, derived by alignment of human and murine promoter sequences (Graves et al., 1992); Adiponectin (Iwaki et al., 2003); ACoABP (Helledie et al., 2002); mCPT1, (Mascaro et al., 1998); LXR $\alpha$ , (Laffitte et al., 2001); CAP1, (Baumann et al., 2000); LPL, (Schoonjans et al., 1996); ACoAOx, (Varanasi et al., 1996); ACoAOx (Zamir et al., 1997).

### Transfection assays

293EBNA cells, cultured in DMEM/10%FCS were transfected with Lipofectamine2000- or calcium phosphate-mediated in 96- or 24-well plates respectively and assayed for luciferase and  $\beta$ -galactosidase activity as described (Collingwood et al., 1994) following 36 hr with or without ligand. 3T3-L1 adipocyte cells were cultured and transfected with Lipofectamine2000 in 24-well plates as described above.

### Cellular localisation of EGFP-tagged mutants

293EBNA cells, grown on glass well slides were transfected using Lipofectamine 2000 with 1  $\mu$ g of EGFP-PPAR $\gamma$ 1 fusions, fixed with 4% paraformaldehyde, mounted using vectashield and fluorescence was visualized by digital microscopy.

### Peripheral blood monocyte purification and IDC culture

With ethical approval, monocytes were harvested from peripheral blood by Ficoll gradient centrifugation and immunomagnetic cell separation using anti-CD14-conjugated microbeads (VarioMACS; Miltenyi Biotec), resuspended in 6-well plates at a density of  $1.5 \times 10^6$  cells/ml and cultured in RPMI 1640 plus 10% FBS containing 800U/ml GM-CSF (Leucomax) and 500U/ml IL-4 (Peprotech) to generate IDCs as described (Sallusto and Lanzavecchia, 1994) with or without exposure to ligand for 24 hr.

**Figure 1.** Identification and characterization of loss-of-function mutations in human PPAR $\gamma$

- A)** Schematic representation of the three major domains of PPAR $\gamma$ , showing the locations of the five mutations (C114R, C131Y, C162W, FS315X, and R357X – PPAR $\gamma$ 1 nomenclature) and the previously reported FSX mutation. NLS, nuclear localisation signal; RXR ID, retinoid X receptor interaction domain; AF2, activation function 2 domain.
- B)** Family pedigrees showing genotypes (N, wild-type allele; M, mutant allele; NA, not available) and phenotypes (colored segments denote the presence of specific traits: green, type 2 diabetes mellitus/impaired glucose tolerance/hyperinsulinaemia; yellow, hypertriglyceridaemia; blue, hypertension; red, ischemic heart disease). Squares and circles represent male and female family members; slashed symbols denote deceased family members and arrows denote probands.
- C)** PPAR $\gamma$  mutants are unable to mediate ligand-dependent transactivation. 293EBNA cells were transfected with 100 ng of wild-type (WT), mutant, or empty (pcDNA3) expression vectors, together with 500 ng of (PPARE)<sub>3</sub>TKLUC reporter construct and 100 ng of Bos- $\beta$ -gal internal control plasmid, and increasing concentrations of rosiglitazone. Results are expressed as a percentage of the maximum activation with WT PPAR $\gamma$ 1 and represent the mean  $\pm$  SEM of at least three independent experiments in triplicate.
- D)** PPAR $\gamma$  mutants are unable to bind to DNA. EMSA with in vitro translated wild-type (WT) or mutant PPAR $\gamma$ 1 (C114R, C131Y, C162W, FS315X, R357X, or FSX) and RXR (C114R, muscle carnitine palmitoyl transferase 1; LXR $\alpha$ , liver X receptor  $\alpha$ ; CAP, cbl-associated protein; LPL, lipoprotein lipase, ACoAOx, acyl coenzyme A oxidase; h, human; m, mouse; r, rat; RL, reticulocyte lysate).
- E)** The C114R, C131Y, C162W, FS315X, and R357X mutants translocate to the nucleus whereas the FSX mutant remains cytoplasmic. 293EBNA cells were transfected as described. Top panels show DAPI-staining (blue) of nuclei, middle panels the cellular localisation of GFP-tagged receptors, and lower panels merged images.
- F)** The DBD PPAR $\gamma$  mutants recruit SRC1 and TRAP220 coactivators, whereas the FS315X, R357X, and FSX truncation mutants do not interact. GST alone or WT and mutant GST-PPAR $\gamma$  fusion proteins were tested with <sup>35</sup>S-labeled in vitro translated SRC1 (upper panel) or TRAP220 (lower panel) in the absence or presence of rosiglitazone. Coomassie-stained gels confirmed comparable protein loading (data not shown).
- G)** The LBD truncation mutants (FS315X, R357X) recruit PGC1 $\alpha$  and PDIP1 $\alpha$  coactivators, whereas the FSX mutant fails to interact. GST alone or WT and mutant GST-PPAR $\gamma$  fusion proteins were tested with <sup>35</sup>S-labeled in vitro translated human PGC1 $\alpha$  and human PDIP1 $\alpha$  in the absence of ligand. Coomassie-stained gels confirmed comparable protein loading (data not shown).

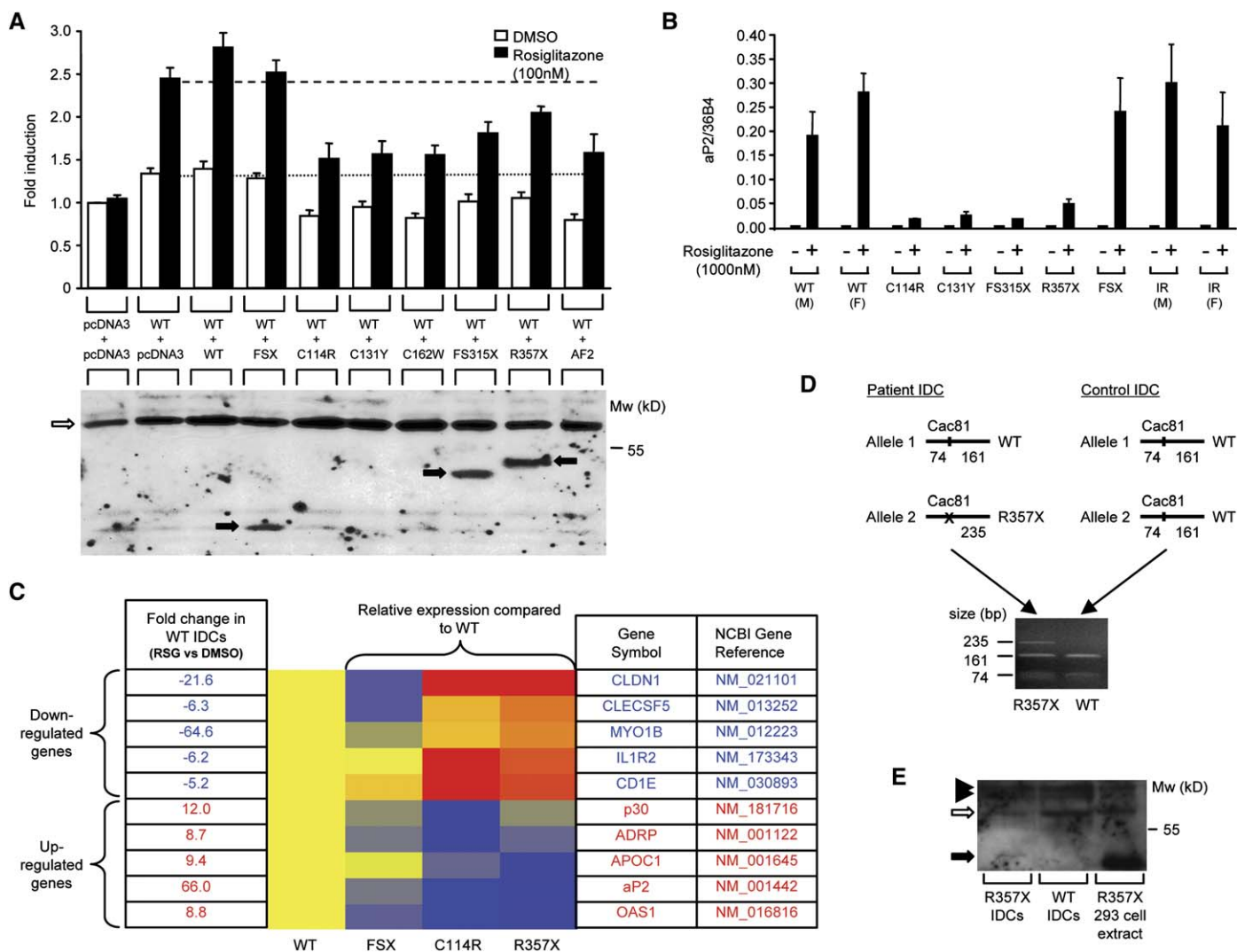


**Figure 2.** PPAR $\gamma$  mutants exhibit dominant-negative activity

**A** The C114R, C131Y, C162W, FS315X, and R357X PPAR $\gamma$  mutants inhibit transactivation by wild-type (WT) receptor, comparably to AF2, an artificial PPAR $\gamma$  mutant described previously, whereas the FSX mutant lacks dominant-negative activity (upper panel). 3T3-L1 cells were cotransfected with 33 ng of WT receptor plus an equal amount of either empty (pcDNA3) or WT or mutant expression vector, together with 265 ng of human aP2LUC reporter plasmid and 65 ng of the internal control plasmid Bos- $\beta$ -gal. The dotted and dashed lines denote transcriptional activity of WT receptor in the absence and presence of ligand respectively. Results are expressed as fold induction relative to empty vector (pcDNA3 + pcDNA3) and represent the mean  $\pm$  SEM of at least three independent experiments in triplicate. Expression of wild-type and mutant receptor proteins was confirmed by Western blotting (lower panel) and the positions of WT, C114R, C131Y, C162W, and AF2 PPAR $\gamma$  (open arrow) and FSX, FS315X and R357X truncation mutants (solid arrows) are indicated.

**B and C** Ligand-dependent regulation of PPAR $\gamma$  target genes in IDCs from subjects with the C114R, C131Y, FS315X, and R357X mutations, compared to responses in cells from normal (WT), severely insulin resistant (IR) subjects without mutations in PPAR $\gamma$  and cells with the FSX, haploinsufficient, mutation. Results represent the mean  $\pm$  SEM of more than three independent experiments in triplicate, except for cells with the FS315X mutation where a single representative experiment is shown. **(C)** Relative expression of several PPAR $\gamma$  target genes (5 downregulated and 5 upregulated) in WT and mutation-containing (FSX, C114R, R357X) IDCs, measured by qPCR using TLDA. Red indicates higher, and blue lower, levels of gene expression relative to rosiglitazone-treated (1000 nM) WT cells, whose responses are uniformly designated yellow. Fold changes in expression of each gene in rosiglitazone (RSG) versus vehicle (DMSO) treated WT cells are also listed.

**D and E** The R357X PPAR $\gamma$  mutant is expressed in IDCs. **(D)** PPAR $\gamma$  cDNA flanking the R357 codon was amplified by RT-PCR in IDCs from patient S5 and a control subject. Cac81 enzyme digestion of PCR products derived from the WT allele yields two fragments (161 and 74 bp), whereas abolition of this restriction site in the R357X mutant allele yields a larger 235 bp product. **(E)** Whole-cell lysates of WT and R357X mutant IDCs and 293EBNA cells transfected with R357X mutant were immunoprecipitated and Western blotted. The positions of WT PPAR $\gamma$  (open arrow), R357X (solid arrow), and nonspecific bands (solid arrowheads) are indicated.

**Quantitative real-time PCR analysis of gene expression**

100ng of total RNA from IDCs, isolated using TRIZOL (Invitrogen), was reverse transcribed and analyzed by Taqman quantitative real-time PCR (qPCR) as described (Szatmari et al., 2004). The sequences of primers and probes are available upon request.

Taqman qPCR low density arrays (TLDA) were used to quantify the expression of multiple target genes in IDCs, according to the manufacturer's instructions.

To obtain cDNA, RNA was reverse transcribed using a High Capacity cDNA Archive kit (Applied Biosystems). The following commercially available Taqman assays (Applied Biosystems) were used: ADRP/ADFP (Hs00605340\_m1), APOC1 (Hs00155790\_m1), CLDN1 (Hs00221623\_m1), aP2/FABP4 (Hs00609791\_m1), CLECSF5 (Hs00183780\_m1), CD1E (Hs00229421\_m1), MYO1B (Hs00362654\_m1), IL1R2 (Hs00174759\_m1), OAS1 (Hs00242943\_m1), p30 (Hs00396457\_m1), cyclophilinA/PPIA (Hs99999904\_m1). The comparative Ct method was used to quantify

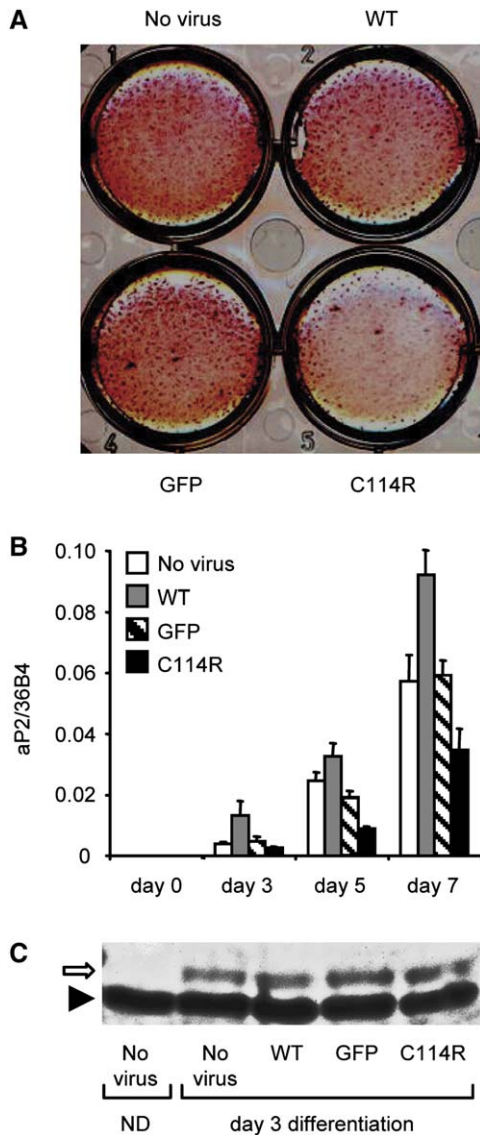


**Figure 3.** Adenoviral-mediated expression of the C114R PPAR $\gamma$  mutant inhibits human preadipocyte differentiation

Chub-S7 human preadipocyte cells were infected with comparable efficiency using recombinant adenoviruses expressing GFP, GFP-WT, or GFP-C114R mutant PPAR $\gamma$  and differentiated in the presence of rosiglitazone (100nM).

**A)** Fully differentiated Chub-S7 cells fixed and stained with oil red O.

**B)** aP2 expression quantitated by real-time qPCR at days 0, 3, 5, and 7 postdifferentiation with results representing the mean  $\pm$  SEM of at least three independent experiments in triplicate.

**C)** Western blotting of Chub-S7 cells at day 4 posttransduction with recombinant adenoviruses confirming comparable levels of total receptor expression. Nondifferentiated, (day 0) nontransduced, cell extracts (ND) are shown for comparison. The positions of PPAR $\gamma$  (open arrow) and nonspecific band (solid arrowhead) are indicated.

transcripts and normalize to cyclophilinA expression levels, which did not vary with ligand treatment. Thereafter, data were further normalized to expression levels in ligand-treated WT IDC samples using GeneSpring 7.2 software (Agilent).

#### RFLP analysis of PPAR $\gamma$ transcripts

PPAR $\gamma$  cDNAs were amplified from WT or R357X mutation-containing IDCs by RT-PCR using forward (CTCCTTGATGAATAAAGATGGGG) and reverse (ATGCTTCAATGGGCTTCACAT) primers, the PCR products were digested

with Cac8I enzyme (New England Biolabs) and analyzed by agarose gel electrophoresis.

#### Immunoprecipitation and Western blot analysis

IDCs, harvested from 200ml of peripheral blood, were lysed in RIPA buffer containing a protease inhibitor cocktail (Roche) and cell supernatants immunoprecipitated using a mouse monoclonal anti-PPAR $\gamma$  antibody (K8713, Perseus Proteomics) and analyzed by SDS-PAGE. Western blotting was carried out using a rabbit polyclonal anti-PPAR $\gamma$  antibody (H-100, Santa Cruz Biotechnology).

#### Adenovirus construction and expression

Recombinant type 5 adenoviruses (Ad5) expressing GFP alone or with either WT or C114R mutant PPAR $\gamma$ 1 were generated using the *AdEasy Vector System* (Quantum Biotechnologies, Montreal), amplified and purified as described (Gurnell et al., 2000). 6-well plates of Chub-S7 human preadipocyte cells were cultured and infected with  $2 \times 10^7$  pfu/well of recombinant virus 24 hr prior to differentiation in the presence of 100nM rosiglitazone as described (Darimont et al., 2003). Comparable infection efficiency was verified by fluorescence microscopy with subsequent qPCR analysis on days 0, 3, 5 and 7. Fully differentiated cells were fixed and stained with Oil Red-O as described (Adams et al., 1997).

#### Supplemental data

Supplemental Data include Supplemental Experimental Procedures and three figures and can be found with this article online at <http://www.cellmetabolism.org/cgi/content/full/4/4/303/DC1/>.

#### Acknowledgments

We would like to thank the Imaging Department (Royal Orthopaedic Hospital, Stanmore) for supplying control MRI data and Teturo Satoh (Gunma University) for providing PDIP1 $\alpha$  ahead of publication. This work was supported by the Wellcome Trust (V.K.K.C., S.O.R., L.N., I.B., D.B.S.) and the Medical Research Council (N.J.W., J.W.R.S.).

Received: May 16, 2006

Revised: September 1, 2006

Accepted: September 13, 2006

Published online: October 3, 2006

#### References

- Adams, M., Reginato, M.J., Shao, D., Lazar, M.A., and Chatterjee, V.K.K. (1997). Transcriptional activation by peroxisome proliferator-activated receptor  $\gamma$  is inhibited by phosphorylation at a consensus mitogen-activated protein kinase site. *J. Biol. Chem.* 272, 5128–5132.
- Agarwal, A.K., and Garg, A. (2002). A novel heterozygous mutation in peroxisome proliferator-activated receptor-gamma gene in a patient with familial partial lipodystrophy. *J. Clin. Endocrinol. Metab.* 87, 408–411.
- Agostini, M., Gurnell, M., Savage, D.B., Wood, E.M., Smith, A.G., Rajanayagam, O., Ganes, K.T., Levinson, S.H., Xu, H.E., Schwabe, J.W., et al. (2004). Tyrosine agonists reverse the molecular defects associated with dominant-negative mutations in human peroxisome proliferator-activated receptor gamma. *Endocrinology* 145, 1527–1538.
- Akiyama, T.E., Baumann, C.T., Sakai, S., Hager, G.L., and Gonzalez, F.J. (2002). Selective intranuclear redistribution of PPAR isoforms by RXR alpha. *Mol. Endocrinol.* 16, 707–721.
- Al-Shali, K., Cao, H., Knoers, N., Hermus, A.R., Tack, C.J., and Hegele, R.A. (2004). A single-base mutation in the peroxisome proliferator-activated receptor gamma4 promoter associated with altered in vitro expression and partial lipodystrophy. *J. Clin. Endocrinol. Metab.* 89, 5655–5660.
- Altshuler, D., Hirschhorn, J.N., Klannemark, M., Lindgren, C.M., Vohl, M.C., Nemesh, J., Lane, C.R., Schaffner, S.F., Bolck, S., Brewer, C., et al. (2000).

The common PPAR $\gamma$  Pro12Ala polymorphism is associated with decreased risk of type 2 diabetes. *Nat. Genet.* 26, 76–80.

Barak, Y., Nelson, M.C., Ong, E.S., Jones, Y.Z., Ruiz-Lozano, P., Chien, K.R., Koder, A., and Evans, R.M. (1999). PPAR $\gamma$  is required for placental, cardiac and adipose tissue development. *Mol. Cell* 4, 585–595.

Barettino, D., Vivanco Ruiz, M.D.M., and Stunnenberg, H.G. (1994). Characterization of the ligand-dependent transactivation domain of thyroid hormone receptor. *EMBO J.* 13, 3039–3049.

Barroso, I., Gurnell, M., Crowley, V.E.F., Agostini, M., Schwabe, J.W., Soos, M.A., Maslen, G.L.I., Williams, T.D.M., Lewis, H., Schafer, A.J., et al. (1999). Dominant negative mutations in human PPAR $\gamma$  are associated with severe insulin resistance, diabetes mellitus and hypertension. *Nature* 402, 880–883.

Baumann, C.A., Chokshi, N., Saltiel, A.R., and Ribon, V. (2000). Cloning and characterization of a functional peroxisome proliferator activator receptor-gamma-responsive element in the promoter of the CAP gene. *J. Biol. Chem.* 275, 9131–9135.

Berger, J.P., Petro, A.E., Macnaul, K.L., Kelly, L.J., Zhang, B.B., Richards, K., Elbrecht, A., Johnson, B.A., Zhou, G., Doebber, T.W., et al. (2003). Distinct properties and advantages of a novel peroxisome proliferator-activated protein [gamma] selective modulator. *Mol. Endocrinol.* 17, 662–676.

Black, D., James, W.P.T., Besser, G.M., Brock, C.G.D., Craddock, D., Garrow, J.S., Hockaday, T.D.R., Lewis, B., Pilkington, T.R.E., Silverstone, J.T., et al. (1983). Obesity: A report of the College of Physicians. *J. Roy. Coll. Phys. London* 17, 5–65.

Collingwood, T.N., Adams, M., Tone, Y., and Chatterjee, V.K.K. (1994). Spectrum of transcriptional dimerization and dominant negative properties of twenty different mutant thyroid hormone  $\beta$  receptors in thyroid hormone resistance syndrome. *Mol. Endocrinol.* 8, 1262–1277.

Culbertson, M.R. (1999). RNA surveillance. Unforeseen consequences for gene expression, inherited genetic disorders and cancer. *Trends Genet.* 15, 74–80.

Darimont, C., Zbinden, I., Avanti, O., Leone-Vautravers, P., Giusti, V., Burckhardt, P., Pfeifer, A.M., and Mace, K. (2003). Reconstitution of telomerase activity combined with HPV-E7 expression allow human preadipocytes to preserve their differentiation capacity after immortalization. *Cell Death Differ.* 10, 1025–1031.

Desvergne, B., and Wahli, W. (1999). Peroxisome proliferator-activated receptors: nuclear control of metabolism. *Endocr. Rev.* 20, 649–688.

Gampe, J.R.T., Montana, V.G., Lambert, M.H., Miller, A.B., Bledsoe, R.K., Milburn, M.V., Kliewer, S.A., Willson, T.M., and Xu, H.E. (2000). Asymmetry in the PPAR $\gamma$ /RXR $\alpha$  crystal structure reveals the molecular basis of heterodimerization among nuclear receptors. *Mol. Cell* 5, 545–555.

Ge, K., Guermah, M., Yuan, C.X., Ito, M., Wallberg, A.E., Spiegelman, B.M., and Roeder, R.G. (2002). Transcription coactivator TRAP220 is required for PPAR gamma 2-stimulated adipogenesis. *Nature* 417, 563–567.

Gervois, P., Torra, I.P., Chinetti, G., Grotzinger, T., Dubois, G., Fruchart, J.C., Fruchart-Najib, J., Leitersdorf, E., and Staels, B. (1999). A truncated human peroxisome proliferator-activated receptor alpha splice variant with dominant negative activity. *Mol. Endocrinol.* 13, 1535–1549.

Graves, R.A., Tontonoz, P., Platt, K.A., Ross, S.R., and Spiegelman, B.M. (1992). Identification of a fat cell enhancer: analysis of requirements for adipose tissue-specific gene expression. *J. Cell. Biochem.* 49, 219–224.

Guan, H.P., Ishizuka, T., Chui, P.C., Lehrke, M., and Lazar, M.A. (2005). Corepressors selectively control the transcriptional activity of PPAR $\gamma$  in adipocytes. *Genes Dev.* 19, 453–461.

Guiochon-Mantel, A., and Milgrom, E. (1993). Cytoplasmic-nuclear trafficking of steroid hormone receptors. *Tr Endocrinol Metab* 10, 322–328.

Gurnell, M., Wentworth, J.M., Agostini, M., Adams, M., Collingwood, T.N., Provenzano, C., Browne, P.O., Rajanayagam, O., Burris, T.P., Schwabe, J.W., et al. (2000). A dominant negative Peroxisome Proliferator-activated Receptor  $\gamma$  (PPAR $\gamma$ ) mutant is a constitutive repressor and inhibits PPAR $\gamma$ -mediated adipogenesis. *J. Biol. Chem.* 275, 5754–5759.

Hegele, R.A., Cao, H., Frankowski, C., Mathews, S.T., and Leff, T. (2002). PPAR $\gamma$  F388L, a transactivation-deficient mutant, in familial partial lipodystrophy. *Diabetes* 51, 3586–3590.

Helledie, T., Grontved, L., Jensen, S.S., Kiilerich, P., Rietveld, L., Albrechtsen, T., Boysen, M.S., Nohr, J., Larsen, L.K., Fleckner, J., et al. (2002). The gene encoding the Acyl-CoA-binding protein is activated by peroxisome proliferator-activated receptor gamma through an intronic response element functionally conserved between humans and rodents. *J. Biol. Chem.* 277, 26821–26830.

Ijpenberg, A., Jeannin, E., Wahli, W., and Desvergne, B. (1997). Polarity and specific sequence requirements of peroxisome proliferator-activated receptor (PPAR)/retinoid X receptor heterodimer binding to DNA. A functional analysis of the malic enzyme gene PPAR response element. *J. Biol. Chem.* 272, 20108–20117.

Iwaki, M., Matsuda, M., Maeda, N., Funahashi, T., Matsuzawa, Y., Makishima, M., and Shimomura, I. (2003). Induction of adiponectin, a fat-derived antidiabetic and antiatherogenic factor, by nuclear receptors. *Diabetes* 52, 1655–1663.

Kallenberger, B.C., Love, J.D., Chatterjee, V.K., and Schwabe, J.W. (2003). A dynamic mechanism of nuclear receptor activation and its perturbation in a human disease. *Nat. Struct. Biol.* 10, 136–140.

Laffitte, B.A., Joseph, S.B., Walczak, R., Pei, L., Wilpitz, D.C., Collins, J.L., and Tontonoz, P. (2001). Autoregulation of the human liver X receptor alpha promoter. *Mol. Cell. Biol.* 21, 7558–7568.

Lazar, M.A., Berrodrin, T.J., and Harding, H.P. (1991). Differential DNA binding by monomeric, homodimeric, and potentially heteromeric forms of the thyroid hormone receptor. *Mol. Cell. Biol.* 11, 5005–5015.

Lehmann, J.M., Moore, L.B., Smith-Oliver, T.A., Wilkison, W.O., Willson, T.M., and Kliewer, S.A. (1995). An antidiabetic thiazolidinedione is a high affinity ligand for peroxisome proliferator-activated receptor  $\gamma$  (PPAR $\gamma$ ). *J. Biol. Chem.* 270, 12953–12956.

Lehrke, M., and Lazar, M.A. (2005). The many faces of PPAR $\gamma$ . *Cell* 123, 993–999.

Love, J.D., Gooch, J.T., Nagy, L., Chatterjee, V.K.K., and Schwabe, J.W.R. (2000). Transcriptional repression by nuclear receptors: mechanisms and role in disease. *Biochem. Soc. Trans.* 28, 390–396.

Malloy, P.J., Pike, J.W., and Feldman, D. (1999). The vitamin D receptor and the syndrome of hereditary 1,25-dihydroxyvitamin D-resistant rickets. *Endocr. Rev.* 20, 156–188.

Mascaro, C., Acosta, E., Ortiz, J.A., Marrero, P.F., Heggardt, F.G., and Haro, D. (1998). Control of human muscle-type carnitine palmitoyltransferase I gene transcription by peroxisome proliferator-activated receptor. *J. Biol. Chem.* 273, 8560–8563.

Meyer, M.E., Gronemeyer, H., Turcotte, B., Bocquel, M.T., Tasset, D., and Chambon, P. (1989). Steroid hormone receptors compete for factors that mediate their enhancer function. *Cell* 57, 433–442.

Onate, S.A., Tsai, S.Y., Tsai, M.-J., and O'Malley, B.W. (1995). Sequence and characterization of a coactivator for the steroid hormone receptor superfamily. *Science* 270, 1354–1357.

Park, Y., Freedman, B.D., Lee, E.J., Park, S., and Jameson, J.L. (2003). A dominant negative PPAR $\gamma$  mutant shows altered cofactor recruitment and inhibits adipogenesis in 3T3-L1 cells. *Diabetologia* 46, 365–377.

Pelton, P.D., Zhou, L., Demarest, K.T., and Burris, T.P. (1999). PPAR $\gamma$  activation induces the expression of the adipocyte fatty acid binding protein gene in human monocytes. *Biochem. Biophys. Res. Commun.* 261, 456–458.

Puigserver, P., Adelmant, G., Wu, Z., Fan, M., Xu, J., O'Malley, B., and Spiegelman, B.M. (1999). Activation of PPAR $\gamma$  coactivator-1 through transcription factor docking. *Science* 286, 1368–1371.

Puigserver, P., and Spiegelman, B.M. (2003). Peroxisome proliferator-activated receptor-gamma coactivator 1 alpha (PGC-1 alpha): transcriptional coactivator and metabolic regulator. *Endocr. Rev.* 24, 78–90.

- Reginato, M.J., Bailey, S.T., Krakow, S.L., Minami, C., Ishii, S., Tanaka, H., and Lazar, M.A. (1998). A potent antidiabetic thiazolidinedione with unique peroxisome proliferator-activated receptor  $\gamma$ -activating properties. *J. Biol. Chem.* **273**, 32679–32684.
- Rocchi, S., Picard, F., Vamecq, J., Gelman, L., Potier, N., Zeyer, D., Dubuquoy, L., Bac, P., Champy, M.F., Plunket, K.D., et al. (2001). A unique PPAR-gamma ligand with potent insulin-sensitizing yet weak adipogenic activity. *Mol. Cell* **8**, 737–747.
- Rosen, E.D., Sarraf, P., Troy, A.E., Bradwin, G., Moore, K., Milstone, D.S., Spiegelman, B.M., and Mortensen, R.M. (1999). PPAR gamma is required for the differentiation of adipose tissue in vivo and in vitro. *Mol. Cell* **4**, 611–617.
- Sabatino, L., Casamassimi, A., Peluso, G., Barone, M.V., Capaccio, D., Migliore, C., Bonelli, P., Pedicini, A., Febbraro, A., Ciccociola, A., et al. (2005). A novel peroxisome proliferator-activated receptor gamma isoform with dominant negative activity generated by alternative splicing. *J. Biol. Chem.* **280**, 26517–26525.
- Sadowski, I., and Ptashne, M. (1989). A vector for expressing GAL4(1-147) fusions in mammalian cells. *Nucleic Acids Res.* **17**, 7539.
- Sallusto, F., and Lanzavecchia, A. (1994). Efficient presentation of soluble antigen by cultured human dendritic cells is maintained by granulocyte/macrophage colony-stimulating factor plus interleukin 4 and downregulated by tumor necrosis factor alpha. *J. Exp. Med.* **179**, 1109–1118.
- Savage, D.B. (2005). PPARgamma as a metabolic regulator: insights from genomics and pharmacology. *Expert Rev. Mol. Med.* **2005**, 1–16.
- Savage, D.B., Agostini, M., Barroso, I., Gurnell, M., Luan, J., Meirhaeghe, A., Harding, A.H., Ihrke, G., Rajanayagam, O., Soos, M.A., et al. (2002). Digenic inheritance of severe insulin resistance in a human pedigree. *Nat. Genet.* **31**, 379–384.
- Savage, D.B., Tan, G.D., Acerini, C.L., Jebb, S.A., Agostini, M., Gurnell, M., Williams, R.L., Umpleby, A.M., Thomas, E.L., Bell, J.D., et al. (2003). Human metabolic syndrome resulting from dominant-negative mutations in the nuclear receptor peroxisome proliferator-activated receptor-gamma. *Diabetes* **52**, 910–917.
- Schoonjans, K., Staels, B., and Auwerx, J. (1996). Role of the peroxisome proliferator-activated receptor (PPAR) in mediating the effects of fibrates and fatty acids on gene expression. *J. Lipid Res.* **37**, 907–925.
- Shibusawa, N., Hashimoto, K., Nikrodhanond, A.A., Liberman, M.C., Applebury, M.L., Liao, X.H., Robbins, J.T., Refetoff, S., Cohen, R.N., and Wondisford, F.E. (2003). Thyroid hormone action in the absence of thyroid hormone receptor DNA-binding in vivo. *J. Clin. Invest.* **112**, 588–597.
- Surapureddi, S., Yu, S., Bu, H., Hashimoto, T., Yeldandi, A.V., Kashireddy, P., Cherkaoui-Malki, M., Qi, C., Zhu, Y.J., Rao, M.S., et al. (2002). Identification of a transcriptionally active peroxisome proliferator-activated receptor alpha-interacting cofactor complex in rat liver and characterization of PRIC285 as a coactivator. *Proc. Natl. Acad. Sci. USA* **99**, 11836–11841.
- Szatmari, I., Gogolak, P., Im, J.S., Dezso, B., Rajnavolgyi, E., and Nagy, L. (2004). Activation of PPARgamma specifies a dendritic cell subtype capable of enhanced induction of iNKT cell expansion. *Immunity* **21**, 95–106.
- Temple, K.A., Cohen, R.N., Wondisford, S.R., Yu, C., Deplewski, D., and Wondisford, F.E. (2005). An intact DNA-binding domain is not required for peroxisome proliferator-activated receptor gamma (PPARgamma) binding and activation on some PPAR response elements. *J. Biol. Chem.* **280**, 3529–3540.
- Tomaru, T., Satoh, T., Yoshino, S., Ishizuka, T., Hashimoto, K., Monden, T., Yamada, M., and Mori, M. (2006). Isolation and characterization of a transcriptional cofactor and its novel isoform that bind the deoxyribonucleic acid-binding domain of peroxisome proliferator-activated receptor-gamma. *Endocrinology* **147**, 377–388.
- Tontonoz, P., Hu, E., Graves, R.A., Budavari, A.I., and Spiegelman, B.M. (1994a). mPPAR $\gamma$ 2: tissue-specific regulator of an adipocyte enhancer. *Genes Dev.* **8**, 1224–1234.
- Tontonoz, P., Hu, E., and Spiegelman, B.M. (1994b). Stimulation of adipogenesis in fibroblasts by PPAR $\gamma$ 2, a lipid-activated transcription factor. *Cell* **79**, 1147–1156.
- Tzamelis, I., Fang, H., Ollero, M., Shi, H., Hamm, J.K., Kievit, P., Hollenberg, A.N., and Flier, J.S. (2004). Regulated production of a peroxisome proliferator-activated receptor-gamma ligand during an early phase of adipocyte differentiation in 3T3-L1 adipocytes. *J. Biol. Chem.* **279**, 36093–36102.
- Varanasi, U., Chu, R., Huang, Q., Castellon, R., Yeldandi, A.V., and Reddy, J.K. (1996). Identification of a peroxisome proliferator-responsive element upstream of the human peroxisomal fatty acyl coenzyme A oxidase gene. *J. Biol. Chem.* **271**, 2147–2155.
- Wada, K., Nakajima, A., Katayama, K., Kudo, C., Shibuya, A., Kubota, N., Terauchi, Y., Tachibana, M., Miyoshi, H., Kamisaki, Y., et al. (2006). Peroxisome proliferator-activated receptor gamma-mediated regulation of neural stem cell proliferation and differentiation. *J. Biol. Chem.* **281**, 12673–12681.
- Williams, D.R., Wareham, N.J., Brown, D.C., Byrne, C.D., Clark, P.M., Cox, B.D., Cox, L.J., Day, N.E., Hales, C.N., Palmer, C.R., et al. (1995). Undiagnosed glucose intolerance in the community: The Isle of Ely Diabetes Project. *Diabet. Med.* **12**, 30–35.
- Wu, Y., Chin, W.W., Wang, Y., and Burris, T.P. (2003). Ligand and coactivator identity determines the requirement of the charge clamp for coactivation of the peroxisome proliferator-activated receptor gamma. *J. Biol. Chem.* **278**, 8637–8644.
- Zamir, I., Zhang, J., and Lazar, M.A. (1997). Stoichiometric and steric principles governing repression by nuclear hormone receptors. *Genes Dev.* **11**, 835–846.
- Zhang, X., Jeyakumar, M., and Bagchi, M.K. (1996). Ligand-dependent cross-talk between steroid and thyroid hormone receptors. Evidence for common transcriptional coactivator(s). *J. Biol. Chem.* **271**, 14825–14833.
- Zhu, X.G., Hanover, J.A., Hager, G.L., and Cheng, S.Y. (1998). Hormone-induced translocation of thyroid hormone receptors in living cells visualized using a receptor green fluorescent protein chimera. *J. Biol. Chem.* **273**, 27058–27063.
- Zhu, Y., Qi, C., Calandra, C., Rao, M.S., and Reddy, J.K. (1996). Cloning and identification of mouse steroid receptor coactivator-1 (mSRC-1), as a coactivator of peroxisome proliferator-activated receptor gamma. *Gene Expr.* **6**, 185–195.
- Zhu, Y., Qi, C., Jain, S., Rao, M.S., and Reddy, J.K. (1997). Isolation and characterization of PBP, a protein that interacts with peroxisome proliferator-activated receptor. *J. Biol. Chem.* **272**, 25500–25506.